Doctoral Thesis
Madrid, Spain 2014

Unit Commitment

Computational Performance, System Representation and Wind Uncertainty Management

Germán Andrés Morales-España

Doctoral Thesis supervisors:

Prof.dr. Andrés Ramos,	Universidad Pontificia Comillas, director
Dr. Javier García-González,	Universidad Pontificia Comillas, co-director
Prof.dr.ir. Lennart Söder,	Kungliga Tekniska Högskolan, supervisor
Prof.dr.ir. Paulien M. Herder,	Technische Universiteit Delft, promotor

Members of the Examination Committee:

Prof.dr.ir. Francisco J. Prieto,	Universidad Carlos III de Madrid, chairman
Dr. Mohammad R. Hesamzadeh,	Kungliga Tekniska Högskolan
Dr. Efraim Centeno,	Universidad Pontificia Comillas
Dr.ir. Laurens J. de Vries,	Technische Universiteit Delft
Prof.dr.ir. Benjamin F. Hobbs,	Johns Hopkins University

This research was funded by the European Commission through the Erasmus Mundus Joint Doctorate Program, and also partially supported by the Institute for Research in Technology at Universidad Pontificia Comillas and the Cátedra Iberdrola de Energía e Innovación.

TRITA-EE 2014:041
ISSN 1653-5146
ISBN 978-84-697-1230-6

Printed in Spain

Unit Commitment

Computational Performance, System Representation and Wind Uncertainty Management

PROEFSCHRIFT

ter verkrijging van de graad van doctor
aan de Technische Universiteit Delft,
op gezag van de Rector Magnificus prof. ir. K.C.A.M. Luyben,
voorzitter van het College voor Promoties,
in het openbaar te verdedigen
op woensdag 8 oktober 2014 om 13:00 uur

door

Germán Andrés MORALES-ESPAÑA

geboren te Florencia, Colombia
in 1982

Dit proefschrift is goedgekeurd door de promotoren:

Prof.dr. Andrés Ramos,	Universidad Pontificia Comillas, director
Dr. Javier García-González,	Universidad Pontificia Comillas, co-director
Prof.dr.ir. Lennart Söder,	Kungliga Tekniska Högskolan, supervisor
Prof.dr.ir. Paulien M. Herder,	Technische Universiteit Delft, promotor

Samenstelling promotiecommissie:

Prof.dr.ir. Francisco J. Prieto,	Universidad Carlos III de Madrid, voorzitter
Dr. Mohammad R. Hesamzadeh,	Kungliga Tekniska Högskolan
Dr. Efraim Centeno,	Universidad Pontificia Comillas
Dr.ir. Laurens J. de Vries,	Technische Universiteit Delft
Prof.dr.ir. Benjamin F. Hobbs,	Johns Hopkins University

ISBN 978-84-697-1230-6

Printed in Spain

SETS Joint Doctorate

The Erasmus Mundus Joint Doctorate in **Sustainable Energy Technologies and Strategies**, SETS Joint Doctorate, is an international programme run by six institutions in cooperation:

- Comillas Pontifical University, Madrid, Spain
- Delft University of Technology, Delft, the Netherlands
- Florence School of Regulation, Florence, Italy
- Johns Hopkins University, Baltimore, USA
- KTH Royal Institute of Technology, Stockholm, Sweden
- University Paris-Sud 11, Paris, France

The Doctoral Degrees issued upon completion of the programme are issued by Comillas Pontifical University, Delft University of Technology, and KTH Royal Institute of Technology.

The Degree Certificates are giving reference to the joint programme. The doctoral candidates are jointly supervised, and must pass a joint examination procedure set up by the three institutions issuing the degrees.

This Thesis is a part of the examination for the doctoral degree.

The invested degrees are official in Spain, the Netherlands and Sweden respectively.

SETS Joint Doctorate was awarded the Erasmus Mundus **excellence label** by the European Commission in year 2010, and the European Commission's **Education, Audiovisual and Culture Executive Agency**, EACEA, has supported the funding of this programme.

The EACEA is not to be held responsible for contents of the Thesis.

A Sandra Kemperman
por estar a mi lado y ser mi apoyo,
gracias por darme la estabilidad mental
que hizo posible esta tesis

Summary

In recent years, high penetration of variable generating sources, such as wind power, has challenged independent system operators (ISO) in keeping a cheap and reliable power system operation. Any deviation between expected and real wind production must be absorbed by the power system resources (reserves), which must be available and ready to be deployed in real time. To guarantee this resource availability, the system resources must be committed in advance, usually the day-ahead, by solving the so-called unit commitment (UC) problem. If the quantity of committed resources is extremely low, there will be devastating and costly consequences in the system, such as significant load shedding. On the other hand, if this quantity is extremely high, the system operation will be excessively expensive, mainly because facilities will not be fully exploited.

This thesis proposes computationally efficient models for optimal day-ahead planning in (thermal) power systems to adequately face the stochastic nature of wind production in the real-time system operation. The models can support ISOs to face the new challenges in short-term planning as uncertainty increases dramatically due to the integration of variable generating resources. This thesis then tackles the UC problem in the following aspects:

- *Power system representation*: This thesis identifies drawbacks of the traditional energy-block scheduling approach, which make it unable to adequately prepare the power system to face deterministic and perfectly known events. To overcome those drawbacks, we propose the ramp-based scheduling approach that more accurately describes the system operation, thus better exploiting the system flexibility.
- *UC computational performance*: Developing more accurate models would be pointless if these models considerably increase the computational burden of the UC problem, which is already a complex integer and non-convex problem. We then devise simultaneously tight and compact formulations under the mixed-integer programming (MIP) approach. This simultaneous characteristic reinforces the convergence speed by reducing the search space (tightness) and simultaneously increasing the searching speed (compactness) with which solvers explore that reduced space.
- *Uncertainty management in UC*: By putting together the improvements in the previous two aspects, this thesis contributes to a better management of wind uncertainty in UC, even though these two aspects are in conflict and improving one often means harming the other. If compared with a traditional energy-block UC model under the stochastic (deterministic) paradigm, a stochastic (deterministic) ramp-based UC model: 1) leads to more economic operation, due to a better and more detailed system representation, while 2) being solved significantly faster, because the core of the model is built upon simultaneously tight and compact MIP formulations.
- To further improve the uncertainty management in the proposed ramp-based UC, we extend the formulation to a network-constrained UC with robust reserve modelling. Based on robust optimization insights, the UC solution guarantees feasibility for any realization of the uncertain wind production, within the considered uncertainty ranges. This final model remains as a pure linear MIP problem whose size does not depend on the uncertainty representation, thus avoiding the inherent computational complications of the stochastic and robust UCs commonly found in the literature.

Dissertation

This doctoral thesis includes an analysis of the unit commitment (UC) problem with emphasis on three different aspects: computational performance, power system representation and wind uncertainty management. This thesis is based on the work of the following (JCR) journal papers [53, 91, 95, 97, 99, 100] which are included at the end of this document (labelled Article I–VI) and listed as follows. The list of papers is separated on the different aspects of the thesis, but some of the papers fit in more than one. Further details of the thesis structure and roadmap are given in section 1.3.

Power System Representation

Article I G. Morales-España, J. M. Latorre, and A. Ramos, "Tight and compact MILP formulation of start-up and shut-down ramping in unit commitment," *IEEE Transactions on Power Systems*, vol. 28, no. 2, pp. 1288–1296. May 2013.

Article II G. Morales-España, A. Ramos, and J. García-González, "An MIP Formulation for Joint Market-Clearing of Energy and Reserves Based on Ramp Scheduling," *IEEE Transactions on Power Systems*, vol. 29, no. 1, pp. 476–488, Jan. 2014.

UC Computational Performance

Article III G. Morales-España, J. M. Latorre, and A. Ramos, "Tight and compact MILP formulation for the thermal unit commitment problem," *IEEE Transactions on Power Systems*, vol. 28, no. 4, pp. 4897–4908. Nov. 2013.

Article IV C. Gentile, G. Morales-España, and A. Ramos, "A Tight MIP Formulation of the Unit Commitment Problem with Start-up and Shut-down Constraints," *Computers & Operations Research*, paper under review.

Article V G. Morales-Espana, C. Gentile, and A. Ramos, "Tight MIP Formulations of the Power-Based Unit Commitment Problem," *Optimization Letters*, 2014, paper under review (Manuscript ID: OPTL-S-14-00348).

Wind Uncertainty Management

Article VI G. Morales-Espana, R. Baldick, J. García-González, and A. Ramos, "Robust Reserve Modelling for Wind Power Integration in Ramp-Based Unit Commitment," *IEEE Transactions on Power Systems*, 2014, paper under review.

The following two working papers are also result of this PhD research:

Article VII "Comparison of Energy-Block and Ramp-Based Scheduling Approaches," Targeted Journal: *IEEE Transactions on Power Systems*. See chapter 3.

Article VIII "The Worst-case Wind Scenario for Adaptive Robust Unit Commitment Problems," Targeted Journal: *IEEE Transactions on Power Systems*. See Appendix A.

Apart from this, during my four years as a PhD student I presented the relevant results in several conferences [87–90, 92–94, 98, 114, 115] and I also co-authored three other (JCR) journal papers [85, 96, 122].

Contents

List of Acronyms

AGC	Automatic Generation Control
ARO	Adaptive Robust Optimization
CE	Continental Europe
DAM	Day-Ahead Market
DRUC	Day-Ahead Reliability Unit Commitment
ED	Economic dispatch
HRUC	Hourly Reliability Unit Commitment
IP	Integer Programming
ISO	Independent System Operator
LFC	Load Frequency Control
LHS	Latin hypercube sampling
LP	Linear Programming
MIP	Mixed-Integer (linear) Programming
RTM	Real-Time Markets
RUC	Reliability Unit Commitment
SO	Stochastic Optimization
SRO	Static Robust Optimization
UC	Unit Commitment

1. Introduction

Contents

This Chapter introduces the context of this thesis, defines its main objectives, and presents the structure of the document.

1.1. Context

Renewable energy plays a key role in tackling the challenges of global warming. The electricity sector, which significantly contributes to greenhouse emissions, has been shifting toward a stronger presence of renewable energy sources. Wind power production is the leading renewable technology in the electricity sector and it has been firmly penetrating current power systems worldwide[1]. This is mainly due to technological maturity, zero emissions, costless fuel resource and widespread availability.

Wind electricity production cannot be dispatched in a traditional manner because of its inherent randomness caused by the intrinsic chaotic nature of weather. Wind is considered an intermittent resource due to its limited-controllable variability and uncertainty. As a result, wind generation constitutes a source of uncertainty in the planning and operation of power systems. Power systems can accommodate some amount of intermittent generation with the current planning and operation practices. However, high penetration levels of intermittent generation considerably alter the usual system conditions which may endanger the security of the energy supply. Therefore, new procedures to plan and operate power systems are required in order to deal with high penetration levels of intermittent generation, while maintaining the security and reliability of the bulk power system [63, 104].

[1] In some power systems, hydropower is the leading renewable technology; however, its availability is not as widespread as wind.

The wind (un)predictability affects the power systems in different ways depending on the time span. For example:

1. In long-term (years to decades) planning, the adequacy of the system is affected because wind predictability influences the investments in generation capacity and thus the transmission (expansion) network capacity. The firm capacity of the system is the main factor that determines the adequacy level of the system. Wind power has been considered as an energy source rather than a capacity source [83], and the capacity credit of wind power plants is directly affected by its (un)predictability [3].
2. In medium-term (months to years) planning, the adequacy of the system is also affected because wind power predictability influences the management, coordination and maintenance of components in power systems [148].
3. In short term (hours to days) planning, the security of the power system is affected. The variability and uncertainty of wind power output is managed in short term scheduling, hence wind predictability influences the decision of which generating units need to be committed to provide the energy and the extra capacity (reserves) available to respond to unforeseen wind production changes [126].
4. In real-time (seconds to minutes) operation, the security of the power system is directly affected. In real time, a perfect balance between supply and demand is always required to prevent the power system from collapsing. To avoid devastating and costly consequences, any deviation between expected and real wind production must be absorbed by the power system resources (reserves), which must be available in real time.

To adequately face real-time wind uncertainty, enough system resources must be available and ready to be deployed. To guarantee this availability for real-time operations, these system resources must be scheduled and committed in advance, because a significant part of them may take few hours (or even days) to be brought online [128]. The day-ahead Unit Commitment (UC) is the short-term planning process that is commonly used to commit resources at minimum cost, while operating the system and units within secure technical limits [60, 123]. These resources must be enough to face expected (e.g., forecasted demand) and unexpected (e.g., unforeseen wind) events.

On the one hand, if the quantity of committed resources is extremely low, there will be devastating and costly consequences in the system, such as significant load shedding or startup of expensive fast-start units. For example, large industrial and commercial electricity consumers were disconnected in Texas in February 2008 [41, 79], due to an unexpected ramp-down of 1700 MW of wind generation that occurred within three hours. On the other hand, if the quantity of committed resources is extremely high, the system operation will be excessively expensive, mainly because facilities will not be fully exploited, and there may also be an excessive curtailment of wind power that would lead to high fuel costs [31, 101].

This thesis focuses on the short-term planning problem in thermal power systems, specifically on optimally preparing the power system, through day-ahead planning, to face the stochastic nature of wind production in the real-time operation. This can be done by committing an optimal amount of system resources through a network-constrained UC[2], using uncertainty-oriented optimization paradigms such as stochastic or robust optimization [12, 48, 112]. To achieve this, the thesis tackles the UC problem in three different aspects: power system representation, the UC computational performance, and wind uncertainty management, see Figure 1.1.

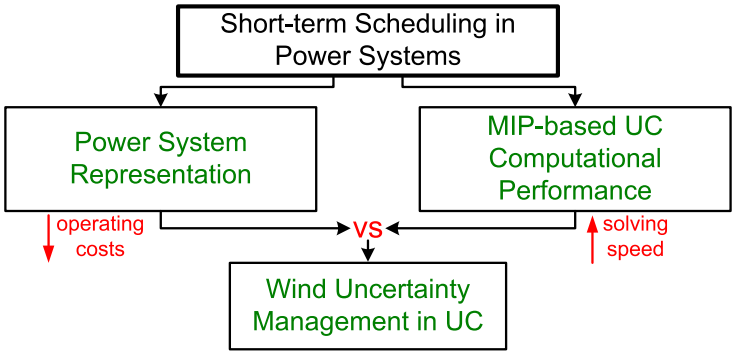

Figure 1.1.: Thesis Structure

First, for the *power system representation*, we start by questioning the standard UC formulations found in the literature. In particular, we investigate if current UC approaches effectively deal with completely known (certain) events. All predictable events must be directly included in the scheduling stage; otherwise, the actual system flexibility is not exploited adequately, and this can even endanger the power system security. We show that the traditional energy-block scheduling approach is unable to adequately prepare the power system to face perfectly known system conditions. This thesis then proposes the ramp-based scheduling approach to overcome the drawbacks of the traditional energy-block approach. The following example illustrates one of the main reasons why a change of scheduling approach is required. Figure 1.2 shows two power demand profiles that present the same energy profile. Notice that the two power profiles present very different ramp requirements, even though the hourly energy requirements are identical. For example: 1) between hours 8 and 10, the ramp requirement of one power demand profile is twice the other; and 2) during hours 6-7 and 10-11, the ramp requirement is 0 for the power demand profile D2 and 250 MW/h for D1.

One energy profile has infinite potential power profiles; therefore, even though the traditional energy-block approach could provide a given energy profile, it cannot guarantee that all possible resulting power profiles can be supplied. Moreover, the proposed ramp-based approach schedules one power profile which has a unique energy profile, thus satisfying both the ramp and energy demand requirements.

[2]Network-constrained UC refers to a UC that includes network constraints, that is, the UC also solves an optimal power flow problem respecting all transmission capacity limits [123].

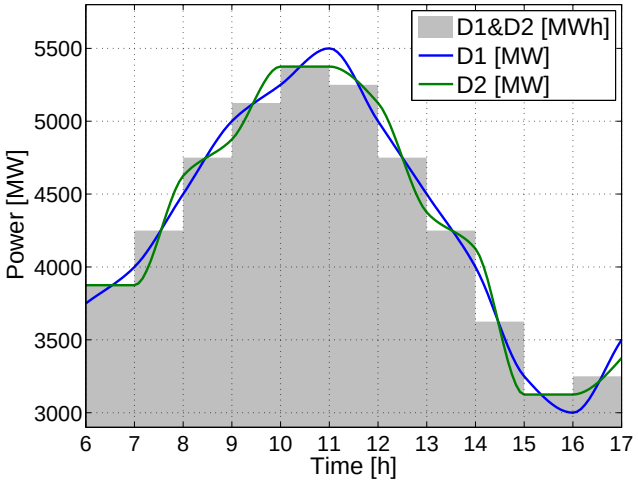

Figure 1.2.: Two power demand profiles D1 and D2 with the same energy profile

Second, special attention must be paid to *computational burden of UC* problems. Developing more accurate models would be pointless if the models cannot be solved efficiently enough[3] in the first place. The UC problem is an integer and non-convex problem which is difficult to solve efficiently, especially for large-scale problems. Mixed-integer (linear) programming (MIP) has become a very popular approach to solve UC problems due to significant improvements in MIP solvers over the last two decades [69]. Despite this significant breakthrough in MIP solving, the time required to solve UC problems continues to be a critical limitation that restricts their size and scope. Therefore, we devise computationally efficient MIP models, by developing simultaneously "tight" and "compact" formulations so they present a much lower computational burden compared with UC formulations commonly found in the literature.

By improving either of the two previous aspects in the UC, an uncertainty-oriented UC is indirectly improved. For example, a stochastic UC including a better (more realistic and acurate) system representation will lead to a more economic operation; and UCs with lower computational burden leads to faster stochastic UCs. However, these two aspects are in conflict and improving one often means harming the other. That is, a more accurate UC usually implies increasing its computational burden. On the other hand, simplifications are usually needed (e.g., removing network constraints) to obtain faster UCs.

Finally, to improve the *uncertainty management in UC,* we put together the developments in the previous two aspects (which were achieved in this thesis). Therefore, we develop new deterministic and stochastic UC formulations, whose objective is to lower operating costs while being solved significantly faster when compared with

[3]A model is considered to be solved efficiently enough (or within rational time) if it can be solved within the required time using the available computing power. For example, if a UC needs to be carried out every hour, then the UC is required to be solved in much less than an hour.

traditional UC models. In addition, based on robust optimization insights and taking into account the wind generation flexibility, i.e., curtailment, we propose a network-constrained UC formulation with robust reserve modelling. Similarly to the stochastic and robust approaches, the proposed network-constrained UC formulation seeks to provide commitment (first-stage) decisions that give flexibility to the power system to face wind uncertainty. This flexibility is provided by units and wind dispatch (second-stage). This final proposed model remains as a pure linear MIP problem, whose size does not depend on the uncertainty wind representation, unlike stochastic UCs whose size directly depends on of the quantity of scenarios considered. In comparison, the traditional robust UCs available in the literature requires solving an MIP together with a bilinear program, making the final problem considerably more complex to solve than a pure linear MIP.

In summary, this thesis proposes computationally efficient tools to optimally commit the required power-system resources to face wind uncertainty in real time, hence allowing power systems to deal with high penetration levels of wind production in an efficient manner. These tools can support ISOs to face the new challenges in day-ahead planning as uncertainty increases dramatically due to the integration of variable and uncertain generation resources, such as wind and solar power.

1.2. Objectives

1.2.1. Main Objective

The main objective of this research is to propose computationally efficient models for day-ahead planning in power systems to adequately prepare the system to face the stochastic nature of wind production in the real-time operation.

1.2.2. Specific Objectives

The main objective can be broken down in the following specific objectives:

Obj1. To develop new day-ahead UC formulations that are able to describe more accurately the system's real-time operation.

Obj2. To devise computationally efficient UC formulations under the MIP approach, by identifying and taking into account the key features that affects the computational burden of MIP formulations.

Obj3. To propose network-constrained UC formulations to optimally schedule generating resources to deal with the stochastic nature of wind production.

1.3. Thesis Outline

This section presents the roadmap of the thesis. This roadmap or outline is based on a partition into three parts, one part for each specific objective. The thesis is mainly based on a collection of papers. We separate the papers on the different parts, but some of the following papers fit in more than one, as shown in Figure 1.3.

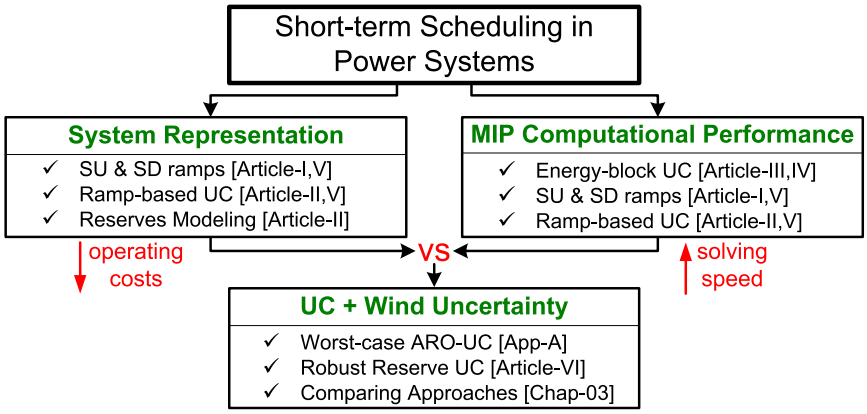

Figure 1.3.: Contributions of this thesis (ARO: Adaptive Robust Optimization; and SU & SD: startup and shutdown)

The structure of this thesis is then described as follows:

Chapter II: This chapter provides a basic background to the thesis area. We give a short introduction of the short-term planning and operating process in the electricity sector. Next, we discuss the capabilities of current power system operating practices to deal with perfectly known system conditions. That is, are the current scheduling practices able to cope with completely known events? Since MIP is the leading approach to solve UC problems, we then introduce the key aspects that define the performance of MIP formulations. Finally, we shortly describe the main optimization paradigms that have been applied to UCs to deal with wind uncertainty.

Power System Representation

Article I: This paper presents an MIP formulation of startup and shutdown power trajectories of thermal units. Multiple startup power-trajectories and costs are modelled according to how long the unit has been offline. The proposed formulation significantly reduces the computational burden in comparison with others commonly found in the literature. This is because the formulation is 1) tighter, i.e., the relaxed solution is nearer to the optimal integer solution; and 2) more compact, i.e., it needs fewer constraints, variables and nonzero elements in the constraint matrix. For illustration, the self-unit commitment

problem faced by a thermal unit is employed. We provide computational results comparing the proposed formulation with others found in the literature.

Article II: In this paper, we propose the ramp-based UC scheduling approach, which draws a clear distinction between power and energy. Demand and generation are modelled as hourly piecewise-linear functions representing their instantaneous power trajectories. The schedule of generating units' output is no longer a stepwise function, but a smoother function that respects all ramp constraints. The formulation represents in detail the operating reserves (online and offline), their time deployment limits (e.g., 15 min), their potential substitution, and their limits according to the actual ramp schedule. The startup and shutdown power trajectories presented in Article I are also included in the ramp-based UC model, thus obtaining a more efficient scheduling of ramp, energy and reserves. The model is formulated as an MIP problem, and is tested with a 10-unit and 100-unit system in which its computational performance is compared with a traditional UC formulation.

UC Computational Performance

Article III: This paper presents an MIP reformulation of the traditional energy-block UC problem. The proposed formulation is simultaneously tight and compact. The tighter characteristic reduces the search space and the more compact characteristic increases the searching speed with which solvers explore that reduced space. Therefore, as a natural consequence, the proposed formulation significantly reduces the computational burden in comparison with analogous MIP-based UC formulations. We provide computational results comparing the proposed formulation with two others which have been recognized as computationally efficient in the literature. The experiments are carried out on 40 different power system mixes and sizes, running from 28 to 1870 generating units.

Article IV: This paper further improves the work in Article III by providing the convex hull description for the following basic operating constraints of a single generation unit energy-block UC problems: 1) generation limits, 2) startup and shutdown capabilities, and 3) minimum up and down times. Although the model does not consider some crucial constraints, such as ramping, the proposed constraints can be used as the core of any energy-block UC formulation, thus tightening the final UC model. We provide evidence that dramatic improvements in computational time are obtained by solving a self-UC problem for different case studies.

Article V: This paper is an extension of the MIP model of a single unit operation under the ramp-based scheduling approach presented in Article II. This paper provides the convex hull description for the basic operation of slow- and quick-start units in ramp-based UC problems. The basic operating constraints that

are modelled for both types of units are: 1) generation limits and 2) minimum up and down times. Apart from this, the startup and shutdown processes are also included, by using 3) startup and shutdown power trajectories for slow-start units, and 4) startup and shutdown ramps for quick-start units. The proposed constraints can be used as the core of any ramp-based UC formulation, thus tightening the final MIP problem. We provide evidence that dramatic improvements in computational time are obtained by solving a self-UC problem for different case studies.

Wind Uncertainty Management

Article VI: This paper proposes a robust reserve-based network-constrained UC formulation as an alternative to traditional robust and stochastic UC formulations under wind generation uncertainty. The formulation draws a clear distinction between power-capacity and ramp-capability reserves to deal with wind production uncertainty. These power and ramp requirements can be obtained from wind forecast information. Using the solution of the worst-case wind scenario (see Appendix A) the formulation guarantees feasibility for any realization of the wind uncertainty. The model is formulated under the ramp-based scheduling approach (Article II), this allows a correct representation of unit's ramp schedule which define their ramp availability for reserves. The core of the proposed MIP formulation is built upon 1) the convex hull description of slow- and quick-start units (Article V), and 2) the tight and compact formulation for multiple startup power-trajectories and costs (Article I), thus taking advantage of their mathematical properties. Furthermore, the proposed formulation significantly decreases operation costs if compared to traditional deterministic and stochastic UC formulations while simultaneously lowering the computational burden. The operation cost comparison is made through 5-min economic dispatch simulation under hundreds of out-of-sample wind-power scenarios.

Chapter III: This chapter presents case studies where the traditional energy-block scheduling approach is compared with the ramp-based one proposed in this thesis. We compare the different commitment policies using a 5-min economic dispatch simulation. We assess the performance of the two approaches under certain and uncertain events. To observe how the approaches deal with certainty, we compare the two approaches using completely known demand profiles. To assess the performance of the two approaches under uncertainty, the two scheduling approaches are implemented under different uncertainty-oriented optimization paradigms (e.g., deterministic, stochastic) and they are compared through an out-of-sample evaluation stage.

Chapter IV: In this, the last chapter of the thesis, conclusions are drawn and guidelines for future work are outlined.

2. Background

Contents

This chapter presents the basic theoretical background of the thesis research topics. We first provide an overview of the short-term planning process in the electricity sector. Next, we discuss the capabilities of current power system operating practices to deal with perfectly known system conditions. We then introduce the key aspects that define the performance of MIP formulations. Last, we shortly describe the main optimization paradigms that have been applied to UCs to deal with wind uncertainty.

2.1. Short-Term Planning in the Electricity Sector

In recent years, large-scale integration of wind generation in power systems has challenged system operators in keeping a reliable power system operation, due to the unpredictable and highly variable pattern of wind. Uncertainty in power system operations is commonly classified in discrete and continuous disturbances. Discrete

disturbances are mainly due to transmission and generation outages. Continuous disturbances mostly result from stochastic fluctuations in electricity demand and renewable energy sources, such as wind and solar energy production.

The appearance of these disturbances in real-time operation results in an imbalance between supply and demand. A perfect balance between supply and demand is always required in real time to prevent the power system from collapsing. Any imbalance must be absorbed by the power system resources (reserves), which must be available and ready to be deployed in real time. To guarantee this availability, the system resources must be committed in advance, usually the day-ahead, by solving the so-called unit commitment (UC) problem.

In many electricity markets, the market operator or Independent System Operator (ISO) is in charge of performing the market clearing in order to determine the set of accepted bids (supply and demand), and the prices to be used in the resulting economic transactions. The electricity market is usually structured as day-ahead markets (DAM) and a sequence of real-time markets (RTM), or intra-day markets. There are many electricity markets, such as those in USA, where the DAM is based on UC formulations, then commitment decisions and market clearing prices for the next 24 hours are computed by solving an UC problem. The objective of this UC is to make the unit's on/off (commitment) decisions to ensure that enough units are online to meet the demand at minimum cost. In RTM, the clearing prices and quantities are commonly obtained by using an optimal economic dispatch (ED). The objective of the ED is to optimally manage the online units to meet demand at minimum cost. The market settlement is usually based on deviations between DAM and RTM [136]. As stated in chapter 1, this thesis is focused on scheduling quantities, and the problem of determining the prices that will allow generators to recover their non-convex costs is beyond the scope of this work.

Although DAM and RTM are the market-driven practices in power systems to meet demand at minimum cost, there are other planning and operating practices that are carried out to maintain the reliability of the system. Figure 2.1 shows common short-term planning and operating practices in power systems. The specific time schedules shown in Figure 2.1 are those followed by the ISO of Texas ERCOT [43–45], other ISOs follow similar schedules [20, 116, 117]. The ISO commonly performs a reliability unit commitment (RUC) to ensure the system reliability[1]. Most ISOs perform the RUC after the DAM, day-ahead RUC (DRUC), and at least once every hour, hourly RUC (HRUC) [20, 43]. The DRUC checks if the DAM committed enough resources in the right location to reliably serve the forecasted load taking into account wind uncertainty [43, 136]. As a result of DRUC, the ISO may change the commitment schedule of DAM to ensure that enough system resources are committed to serve the expected wind and load. Similarly, the rolling HRUC is

[1]Reliability or residual UC (RUC) is used to ensure that enough resource capacity, in addition to ancillary service capacity, is committed in the right locations to reliably serve the forecasted net load [25, 43, 47].

performed with updated demand and wind power forecasts to provide more accurate information, thus permanently checking and ensuring that enough resources are available to face demand and wind uncertainties in real time.

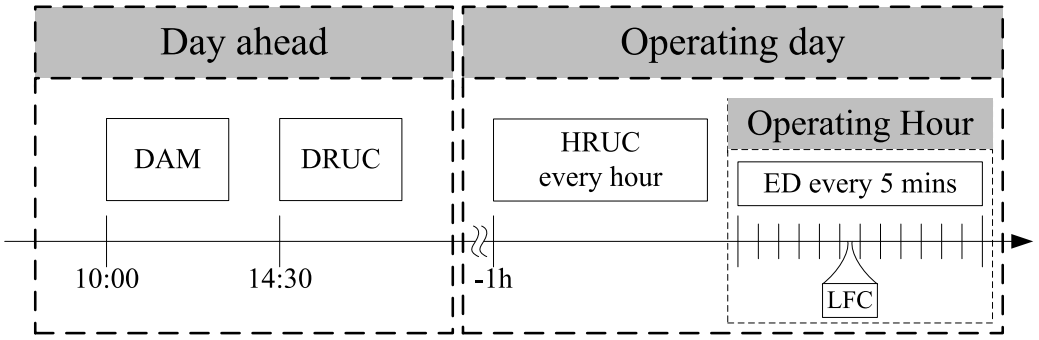

Figure 2.1.: Short-term planning and operating practices in power systems.

Apart from the day-ahead (DAM and DRUC) and hourly scheduling practices (HRUC) the ED is usually executed every 5 minutes to economically dispatch the units. Finally, in even shorter time frames, a load frequency control (LFC) keeps the supply and load balance in real time, by maintaining the system frequency on its nominal value through control strategies without cost optimization functions [37, 106]. These control strategies are usually composed 1) by an Automatic Generation Control (AGC), whose response is between seconds and minutes; and 2) by a primary frequency control, whose response is within few seconds. The former control mainly responds to smooth changes and the latter to more sudden changes of frequency.

It is important to highlight that the ED and LFC are the strategies that finally matches demand and supply. However, they only manage the committed resources that are available in real time. If there are not enough resources available, the ISO needs to take expensive emergency actions to maintain system security and avoid devastating consequences (e.g. blackout). These emergency actions include dispatching fast-start units, voltage reduction, or load shedding [37, 106]. To avoid these emergency actions, ISOs frequently monitor the system condition by using rolling DRUC and HRUC, thus ensuring that enough system resources are always committed to face unexpected events in real time.

2.1.1. Generic Formulation of the UC Problem

Efficient resource scheduling is necessary in power systems to achieve an economical and reliable energy production and system operation, either under centralized or competitive environments. This can be achieved by solving the UC problem, as discussed above.

The UC main objective is to meet demand at minimum cost while operating the system and units within secure technical limits [61, 111, 127, 149]. Here, we present a compact matrix formulation:

$$\begin{aligned}
\min_{\boldsymbol{x},\boldsymbol{p},\boldsymbol{w}} \quad & \left(\mathbf{b}^\top \boldsymbol{x} + \mathbf{c}^\top \boldsymbol{p} + \mathbf{d}^\top \boldsymbol{w}\right) \\
\text{s.t.} \quad & \mathbf{F}\boldsymbol{x} \leq \mathbf{f},\ \boldsymbol{x} \text{ is binary} && (2.1)\\
& \mathbf{H}\boldsymbol{p} + \mathbf{J}\boldsymbol{w} \leq \mathbf{h} && (2.2)\\
& \mathbf{A}\boldsymbol{x} + \mathbf{B}\boldsymbol{p} + \mathbf{C}\boldsymbol{w} \leq \mathbf{g} && (2.3)\\
& \boldsymbol{w} \leq \mathbf{W} && (2.4)
\end{aligned}$$

where $\boldsymbol{x}, \boldsymbol{p}$ and $\boldsymbol{w}$ are decision variables. The binary variable $\boldsymbol{x}$ is a vector of commitment related decisions (e.g., on/off and startup/shutdown) of each generation unit for each time interval over the planning horizon. The continuous variable $\boldsymbol{p}$ is a vector of each unit dispatch decision for each time interval. The continuous variable $\boldsymbol{w}$ is a vector of wind dispatch decision for each time interval at each node where wind is injected.

The objective function is to minimize the sum of the commitment cost $\mathbf{b}^\top \boldsymbol{x}$ (including non-load, start-up and shut-down costs), dispatch cost $\mathbf{c}^\top \boldsymbol{p}$ and wind dispatch cost $\mathbf{d}^\top \boldsymbol{w}$ over the planning horizon. Wind dispatch cost is usually considered to be zero. However, the parameter $\mathbf{d}$ is explicitly included to consider the possibility where this cost is different than zero (in some power systems, this cost can even be negative reflecting opportunity costs, e.g., -40 $/MWh in ERCOT [7])

Constraint (Equation 2.1) involves only commitment-related variables, e.g., minimum up and down times, startup and shutdown constraints, variable startup costs. Constraint (Equation 2.2) contains dispatch-related constraints, e.g., energy balance (equality can always be written as two opposite inequalities), reserve requirements, transmission limits, ramping constraints. Constraint (Equation 2.3) couples the commitment and dispatch decisions. e.g., minimum and maximum generation capacity constraints. Constraint (Equation 2.4) empathizes that wind dispatch cannot exceed its forecasted values $\mathbf{W}$. The reader is referred to [61], Morales-Espana et al. [91, 99] and Appendix B for more detailed UC formulations.

2.2. Power System Representation: Dealing with Certainty

This section illustrates how the traditional energy-block scheduling approach is unable to adequately prepare the power system to face perfectly known system conditions. This section is mainly based on the work in Morales-Espana et al. [88].

2.2.1. Energy-Block: Scheduling vs. Real-time-operation

An inherent problem of markets that are physically cleared on an hourly (or half-hourly) basis is that they make an (stepwise) hourly energy balance between supply and demand rather than matching the instantaneous generating power profiles with the power demand profile. In these kind of markets, such as those in Europe [116, 117], generators are penalized if they deviate from their hourly energy schedule. Therefore, units operate by trying to match their power profile with the stepwise energy blocks [34, 39, 49, 71, 107, 138]. This stepwise behaviour creates large generation gradients at the beginning and at the end of every trading hour, causing large frequency deviations during these time intervals [34, 103].

Figure 2.2 shows a power demand curve[2] and the hourly energy blocks which are needed to satisfy that hourly energy demand. Assuming that the stepwise energy profile can be exactly reproduced by the generation side, there is still an imbalance between generation and demand, see the lower part of Figure 2.2. Since generation and load must be always in balance, the resulting imbalances are compensated by the operating reserves.

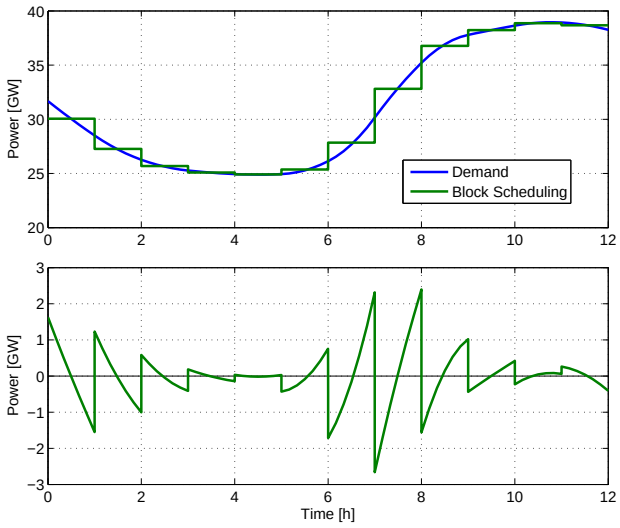

Figure 2.2.: Upper figure shows a power demand profile and its energy-block schedule. Lower figure shows the power deviation between them.

Note that the example presented in Figure 2.2 does not have any uncertain event and yet there is a significant amount of reserves that is needed to balance generation and load all the time. Power reserves are a costly commodity but needed to provide security to the power system under unforeseen events [71]. Furthermore, the worst consequence to the power system, is the high frequency deviation due to significant generating gradients caused by generators in order to follow their scheduled energy

[2]The demand curve corresponds to the real demand in the Spanish power system at 17/01/2012 www.ree.es

blocks. Such frequency deviations have been observed in the Continental Europe (CE) power system, see in Figure 2.3.

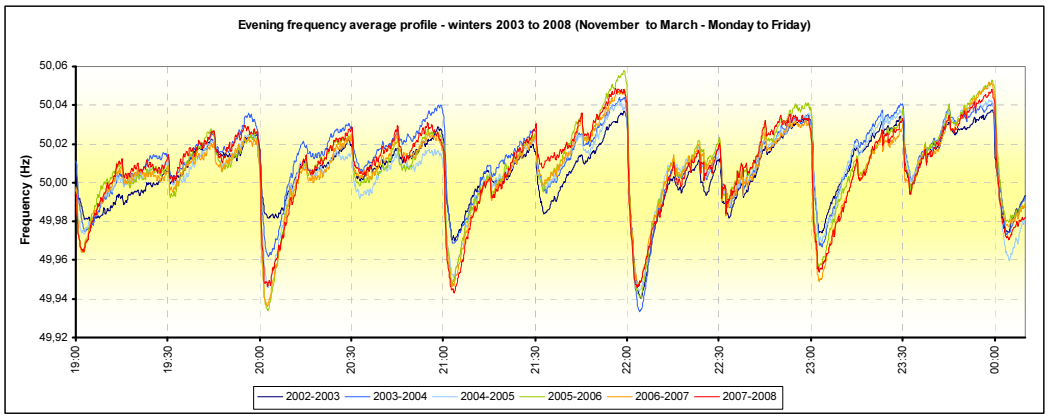

Figure 2.3.: Average frequency profiles of the CE grid, winters 2003 to 2008 (November to March - Monday to Friday). Source: [34]

Stable power systems are designed to operate within a small deviation from the nominal frequency. CE system, for example, must operate between 50Hz±50mHz. A generation outage of 1300 MW will usually lead to a frequency drop around 50 mHz [34]. Figure 2.3 shows the evening average frequency profiles of the CE grid for the years 2003 to 2008. Evidently, the CE system is operating outside the secure limits, and this happens many times every day, for around 10 minutes every hour. These frequency deviations also arise due to large schedule steps at certain half hour shifts [39]. The frequency swings due to market behaviour have been reported in different power grids, for example the USA [103] and Nordic countries [107].

The severity of these events can be observed as follows: In 2010, if the market induced imbalances did not occur, the probability for the CE system to black out[3] would be less than once in 190 years compared to once in 19.3 years with the real frequency data [36]. That is, the market-induced imbalances have increased the probability to black by 10 times. These frequency swings have been increasing with time [34, 40, 71]. In 2012, the peak-to-peak values went up to 150 mHz [40]

2.2.1.1. Consequences

As a consequence, even in the absence of uncertainty, the energy-block-based market operation endangers the system security and increases the operation costs, because a significant quantity of operating reserves need to be deployed in real time to maintain the supply-demand balance. The reports [34, 36, 38, 39, 103] present

[3]This would happen if the CE system runs out of Frequency Containment Reserve (FCR) (3000 MW), which is also commonly known as primary reserve [38] and it is based on primary frequency control [37, 105]

detailed consequences of the frequency swings. We summarize and classify them as follows:

Operational risks

- Insufficient primary reserve leaves the power system unprotected to face generation and demand outages. This endangers the security supply.
- Frequency oscillations can lead into uncontrollable operational situation, which may cause the loss of generation or demand units. This may cause a snowball effect leading to a blackout.
- Power flow variations cause overload which may lead to tripping in systems operating close to their limits. As the previous consequence, this may also lead to a blackout.

Economic impact

- Unnecessary use of primary reserves, which is repeatedly used during a day, results in higher power plant stress. This has a direct impact on the lifetime of the units and inevitably increases the cost of providing this reserve. Besides, more primary reserve must be scheduled for not leaving the system unprotected during the inter-hour periods.
- Unnecessary use of secondary reserves, which are needed to restore the primary reserves, hence increasing the operation costs of the system. In addition, more reserves must then be scheduled to deal with this issue. For example, the costs associated to the overuse of secondary reserves due to the block scheduled in Spain in 2010 was calculated on 17.5 millions of Euros[4] [33].
- Generators following the stepwise energy profiles and also providing reserves present a high ramp use during the changing hours, for around 10 minutes, and thus decreasing their possibility to provide reserves [118].

2.2.1.2. Actions to take

Many measures have been proposed to diminish the previously mentioned consequences [33, 34, 39, 40, 49, 71, 103, 107, 138], from an extremely centralized point of view, e.g. unilateral control of the generation output by ISOs; to very decentralized one, e.g. generation unit must incorporate the ramping costs then avoiding sudden output changes. Here, we summarize some of the outstanding measures.

[4]Egido et al. [33] presented that savings of about 14.5 millions of Euros, for Spain in 2010, could have been obtained by changing the dispatch of units to a half an hour basis and following piecewise power patterns even thought the scheduling was stepwise-based.

- Implement shorter trading periods. The shorter the periods, the smaller the impact on frequency. This is because the resulting energy blocks will be more similar to the smoother continuous demand profile. This will inevitably increase transaction costs.
- Imposing maximum ramp rates on generators during short time periods (minutes). That way, their power profiles will be smoother. This measure constrains the freedom and technical flexibility of generators.
- Dispatching with smooth profiles although the scheduling is made in hourly blocks. This measure is similar to the previous one, with the difference that a constant ramp rate must be followed during the operation stage. The main disadvantage of this solution is that once the energy blocks are fixed, the plausible power profiles of generators may oscillate, besides generators not having the incentives to do so. This problem can be diminished by considering shorter trading periods.

All these measures to diminish these deterministic frequency deviations keep the energy-block paradigm. As proposed in Morales-Espana et al. [88], a change to a ramp-scheduling paradigm (Article II) might deal with this problem. In other words, changing the stepwise energy schedule for a piecewise power schedule. Even though the energy profiles of the two scheduling types are identical, the resulting power profile of the ramp-scheduling will be very similar to the smooth demand profile; therefore, decreasing the impact on the operating reserves.

Under the ramp-scheduling approach, the units should be penalized if they deviate from their ramp schedule[5], instead of penalizing any deviation from the stepwise energy profile. This will then give units the incentive to follow the smooth power demand profile instead of the stepwise energy profile. Figure 2.4 shows the imbalance differences between the hourly energy-block vs. the ramp-scheduling profiles, assuming that units perfectly follow their schedule. For this example, the ramp-based schedule decreases the need of reserves (energy needed to compensate the imbalances) by more than 80%, and also diminishes dramatically the sudden generation changes, thus avoiding the unnecessary high frequency deviations that risk the power system security.

2.2.2. Infeasible Power Delivery

Conventional UC formulations fail to deal with ramp capabilities appropriately. Inefficient ramp management arises from applying ramp-constraints to energy levels

[5]Although the market follows hourly trading periods, measurements for shorter periods are needed to follow the units' ramp, and thus being able to penalize them if deviate from their ramp schedule. For example, energy measurements every few minutes (around 5-10) would be enough to follow the ramp profiles. Actually, these measurements are currently available and needed by the secondary reserve control to work adequately (AGC uses continuous measurements around each 10 seconds [35]).

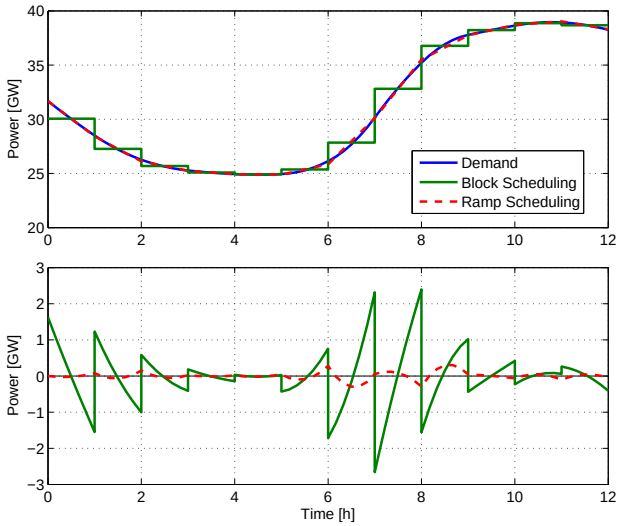

Figure 2.4.: Energy-blocks vs. ramp scheduling and their impact on reserves. Upper figure shows a power demand profile and its energy-block/ramp-based schedules. Lower figure shows the power deviation between the schedules and the demand.

or (hourly) averaged generation levels, which is a standard practice in traditional UC models [28, 51, 60, 123]. As a result, energy schedules may not be feasible [57].

To illustrate this problem, consider the following scheduling example for one generating unit. This example assumes that the minimum and maximum generation outputs of the unit are 100 MW and 300 MW, respectively, and that the maximum ramp rate is 200 MW/h. As shown in Figure 2.5a, if the unit ramps up at its maximum capability and has been producing 100 MW during the first hour, then the expected hourly energy level for the second hour will be 300 MWh. This would be a natural energy schedule resulting from the traditional UC formulations, which are based on the energy scheduling approach. However, the unit is just physically capable of reaching its maximum output at the end of the second hour due to its limited ramp rate, as shown in Figure 2.5b. Consequently, the solution obtained in Figure 2.5a is not feasible. In fact, the unit requires an infinite ramping capability to be able to reproduce the energy schedule presented in Figure 2.5a. Note that representing the generation in a stepwise fashion (energy blocks) may lead to misleading estimations of a system's ramp availability. This in turn could leave the system unprepared to face real-time uncertainties [99]. There are plenty of examples reported in the literature showing that the resulting schedule of the traditional UC, based on energy schedules, may not be feasible, see for example [57, 58] and Morales-Espana et al. [88, 99].

Although Guan et al. [56], [57] proved that delivering the energy schedule obtained from these energy-block formulations may not be feasible, insufficient attention has been paid to this issue. Formulations drawing a clear distinction between power and

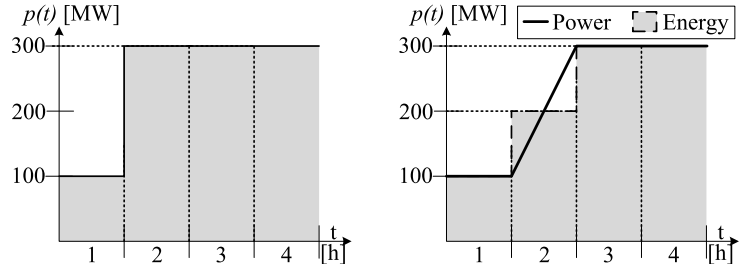

(a) Traditional Energy Schedule **(b)** Actual Deployment

Figure 2.5.: Scheduling vs. Deployment

energy have been proposed, guaranteeing that stepwise energy schedules can be realized [26, 52, 58, 144, 150]. Guan et al. [58] proposes a smooth nonlinear programming problem which does not take into account discrete decisions (e.g. commitment). Wu et al. [144] presents a formulation with feasible energy delivery constraints, which is further extended in Yang et al. [150], where a sub-hourly UC is formulated. The work in [26, 52] use power profiles to guarantee that the scheduled energy can be provided. These formulations are focused on feasible energy schedules rather than on matching generation and demand power profiles. In fact, these formulations supply hourly energy demand with power profiles that vary from stepwise [150] to oscillating power trajectories [26, 52, 118], which are far from matching the instantaneous power demand forecast. This indiscriminate use of ramping resources from the scheduling stage does not permit the effective management of the system ramp capabilities to face real-time uncertainties.

2.2.3. Startup and Shutdown Power Trajectories

Conventional UC formulations assume that units start/end their production at their minimum output [60, 111, 143, 149]. Ignoring the inherent startup and shutdown power trajectories of generating units is a common simplification that is being used for the sake of saving computational effort in solving the UC problem. However, this implies ignoring the energy production during the startup and shutdown processes which is inevitably present in the real-time operation. Consequently, there is an increasing amount of energy that is not being allocated by day-ahead scheduling approaches because, first, units provide energy (and ramp) during the startup and shutdown processes, affecting the total load balance; and second, thermal units are being shut down and started up more often due to the increasing penetration of variable generation [130].

To observe the impact of ignoring the inherent startup and shutdown trajectories of generating units, consider the following illustrative example. Figure 2.6 shows the scheduling (Figure 2.6a) and actual real-time operation (Figure 2.6b) stages of two power generating units, where the objective is to meet a required demand

(see solid line in Figure 2.6) and at least 50 MW of up and down reserves. The two units are identical and their technical characteristics are: 1) 100 MW of minimum output, 2) 300 MW of maximum output, 3) 100 MW/h as maximum up/down ramping capability, and 4) 2 hours are needed to achieve the minimum output after the unit is synchronized to the system (see the startup power trajectory of unit G2 in Figure 2.6b). Figure 2.6 shows that, from the scheduling stage, the demand is satisfied with the instant power at the end of each period, but the energy cannot be completely satisfied due to the discontinuities introduced by the startup process of G2, which was ignored in this scheduling stage.

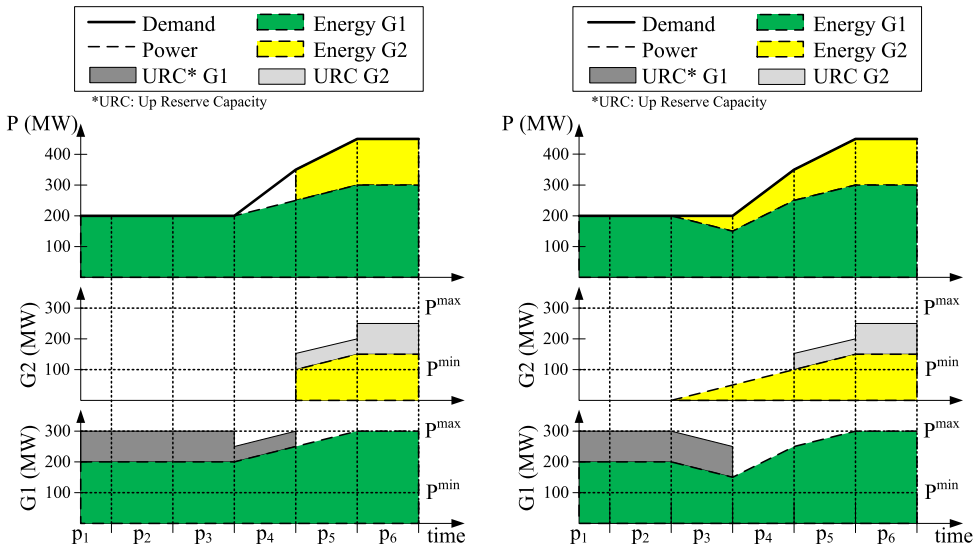

(a) Generation scheduling **(b)** Actual real-time operation

Figure 2.6.: Scheduling vs. real-time operation example. From the bottom to the top, power output of unit G1, power output of unit G2, and power output of G1 and G2 matching the electric demand.

Figure 2.6a shows the UC scheduling for two generating units, ignoring the startup and shutdown power trajectories. From this scheduling stage, the total up reserve capacity of the power system that is expected to be available is: 50 MW for periods p_4 and p_5, and 100 MW for the others, see Figure 2.6a. Similarly, the expected down reserve available is 100 MW for periods p_1 to p_4 and 150 MW for p_5 and p_6: 100 MW that G1 can provide all the time and 50 MW that G2 can provide for periods p_5 and p_6.

Let us observe what would happen in the real-time operation stage, where the commitment decisions are fixed and the units are dispatched to match the actual demand. From the scheduling stage, unit G2 must start to operate at its minimum output at the end of p_4, then, the unit must be synchronized to the system from the

end of p_2 due to its inherent startup process. Hence, in order to match generation and load all the time, unit G1 has to change its scheduled output, by using down reserves, and thus accommodate the startup power trajectory of G2, as shown in Figure 2.6b. Two important situations can be observed:

1. The down reserves were used (in p_3 and p_4), even though this was not expected from the scheduling stage.
2. The system ran out of up reserves for period p_4, because G1 needs to ramp up at its maximum capability to accommodate the startup power trajectory of G2.

As a result, in order to maintain the balance between supply and demand, there is an inefficient deployment of resources in real-time operations in order to accommodate the inherent units' startup and shutdown power trajectories, which were ignored in the scheduling stage. This inefficient use of resources is unnecessary and can be easily avoided by including the units' startup and shutdown trajectories in the scheduling stage, thus obtaining better commitment decisions, as shown in Figure 2.7. Furthermore, as discussed in Morales-Espana et al. [100], ignoring these power trajectories can significantly change commitment decisions, which in turn increases operating costs.

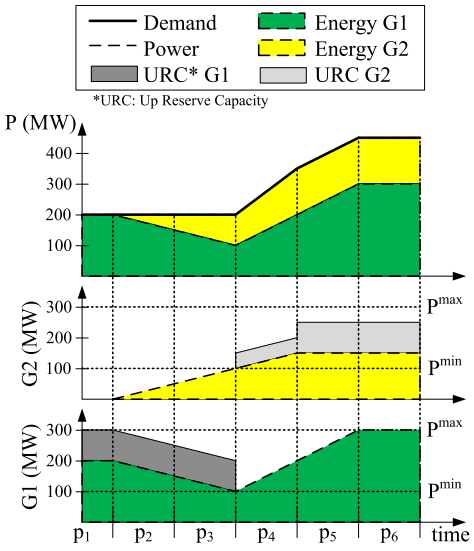

Figure 2.7.: Units' schedule including their startup and shutdown power trajectories

Although some recent works are aware of the importance of including the startup and shutdown processes in UC problems [26, 42, 52, 82] and there are models available in the literature [6, 125, 133], these power trajectories continue being ignored because the resulting model would considerably increase the complexity of the UC problem and hence its computational intensity.

An adequate day-ahead schedule not only must take into account these startup and shutdown power trajectories, but also must optimally schedule them to avoid the aforementioned drawbacks.

2.3. Performance of MIP Formulations

Mixed-integer (linear) programming (MIP) has become a very popular approach to solving UC problems due to significant improvements in off-the-shelf MIP solvers, based on the branch-and-cut algorithm. The combination of pure algorithmic speedup and the progress in computer machinery has meant that solving MIPs has become 100 million times faster over the last 20 years [69]. Recently, the world's largest competitive wholesale market, PJM, changed from Lagrangian Relaxation to MIP to tackle its UC-based scheduling problems [46, 110]. There is extensive literature comparing the pros and cons of MIP with its competitors, see for example [61] and [72].

Despite the significant improvements in MIP solving, the time required to solve UC problems continues to be a critical limitation that restricts the size and scope of UC models. Nevertheless, improving an MIP formulation can dramatically reduce its computational burden and so allow the implementation of more advanced and computationally demanding problems, such as stochastic formulations [22, 23, 112], accurate modelling of different types of (online and offline) reserves Morales-Espana et al. [99], transmission switching [59], or detailed modelling of combined-cycle generating units [24, 72, 74, 78].

2.3.1. Good and Ideal MIP formulations

Figure 2.8 shows three different linear programming (LP) formulations (LP1, LP2 and LP3) of the same integer programming (IP) problem. Geometrically we can observe that there is actually an infinite number of LP formulations for the same integer problem, so the next question that could be raised: which of these formulations is the most computationally efficient?

Formulation LP3 (solid line in Figure 2.8) is *ideal*, because each vertex is an integer so the optimal LP solution (which lies in a vertex) is optimal for the corresponding IP. In general, for every MIP problem there is only one ideal formulation called *convex hull*, defined as the smallest convex feasible region containing all the feasible integer points [142]. Each vertex of this unique formulation is a point satisfying the integrality constraints, hence it allows solving the IP (non-convex) problem as an LP (convex-problem).

Unfortunately, in many practical problems there is an enormous number of inequalities needed to describe the convex hull, and the effort required to obtain them

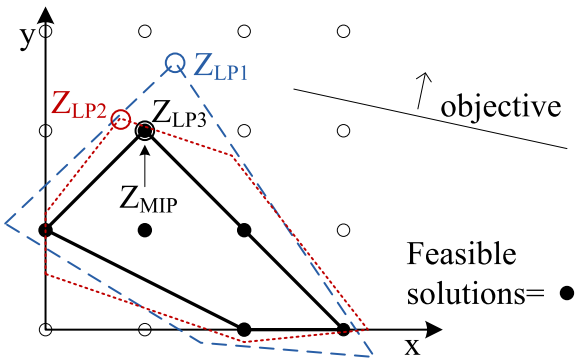

Figure 2.8.: The ideal MIP formulation

outweighs the computation needed to solve the original formulation of the MIP problem [139, 142]. Furthermore, there is usually no simple characterization of these inequalities.

For an MIP problem, however, it is possible to tighten the feasible region of the relaxed LP problem, consequently obtaining dramatic improvements in computation [102, 139, 140, 142]. An MIP formulation can be considerably tightened by providing the convex hull (or tight) description of some set of constraints. Even though other constraints in the problem might add some fractional vertices, this LP solution should be nearer to the IP optimal solution than would be the original model, hence faster to find by branch-and-cut solvers [139, 142].

Therefore, given two formulations F1 and F2 for the same MIP problem, the tighter (nearer to the convex hull) one would be more computationally efficient. If the feasible region of F1 is contained inside the feasible region of F2, then F1 is a tighter formulation than F2, and thus the lower bound (in a minimization problem) provided by the LP relaxation of F1 is always greater than or equal to that provided by F2 [75, 142]. That is, F1 provides stronger lower bounds and the optimal solution of its LP relaxation is nearer to the optimal integer solution.

2.3.2. Tightness vs. Compactness

Apart from the tightness, the computational performance of an MIP formulation is also influenced by its compactness (quantity of data to process when solving the problem). The compactness of an MIP formulation refers to its size. Although, the number of constraints is considered to be the best simple predictor of the LP models' difficulty [18, 139], the number of nonzeros also has a significant impact on solution times [16]. Therefore, formulation F1 is considered more compact than F2 if F1 presents simultaneously fewer constraints and nonzeros than F2.

The branch-and-cut algorithm solves MIP problems by solving a sequence of LP relaxations. The LP relaxation of a MIP problem is obtained by relaxing its integrality requirements. During the solving process (branching), upper bounds (feasible

integer solutions) and lower bounds (LP relaxations) are computed. The quality of a feasible integer solution is measured with the optimality tolerance, which is the difference between upper and lower bounds. In order to reduce this difference, upper bounds are decreased by finding better integer solutions (e.g. by using heuristics) and lower bounds are increased by strengthening the LP relaxation (e.g. by adding cutting planes) [16]. Providing an MIP formulation with strong lower bounds (LP relaxation near to the optimal integer solution) can dramatically reduce the length of the search for optimality [102, 132, 139, 142]. In addition, strong lower bounds effectively guide the search for better upper bounds (i.e. heuristics explore the neighbourhood of the LP relaxation to find potentially better integer solutions).

In short, the tightness of an MIP formulation defines the search space (relaxed feasible region) that the solver needs to explore in order to find the (optimal integer) solution. On the other hand, the compactness of an MIP formulation refers to its size and defines the searching speed that the solver takes to find the optimal solution, since during the process many LP relaxations are repeatedly solved.

Off-the-shelf MIP solvers fully exploit tightening and compacting strategies. Even though solvers' breakthrough is due to the synergy between different strategies (e.g. heuristics, cuts, node presolve), introducing cutting planes has been recognized as the most effective strategy, followed by root presolve [16, 17, 19, 119]. The former strategy dynamically tightens the formulation around the integer feasible solution point. The latter makes the initial problem formulation more compact (by removing redundant variables and constraints) and also tighter (by strengthening constraints and variable bounds).

Research on improving MIP formulations is usually focused on tightening rather than on compacting. An MIP formulation is typically tightened by adding a huge number of constraints, which increases the problem size [64, 109]. Although this tightening reduces the search space, solvers may take more time exploring it because they are now required to repeatedly solve larger LPs. Consequently, when a formulation is tightened while significantly affecting its compactness, a more compact and less tight formulation may be solved faster, because the solver is able to explore the larger feasible region more rapidly [64]. On the other hand, compact formulations usually provide weak (not strong) lower bounds.

In conclusion, creating tight or compact computationally efficient formulations is a non trivial task because the obvious formulations are very weak (not tight) or very large, and trying to improve the tightness (compactness) usually means harming the compactness (tightness).

2.3.3. Improving UC formulations

Improving MIP formulations, especially the tightness, has been widely researched. In fact, all the cutting plane theory, which has meant the breakthrough in MIP solving, is about tightening the formulations [16, 17, 69, 140, 140, 141]. In the

case of UC problems, there have been efforts affecting single sets of constraints [48, 70, 109, 113]. Lee et al. [70] and Rajan and Takriti [113] describe the convex hull of the minimum up/down time constraints for the 1-binary (only modelling commitment binary variables) and 3-binary format (modelling commitment, startup and shutdown binary variables), respectively. Although both formulations are ideal in terms of tightness, the formulation in [113] is considerably more compact which results in a much lower computational burden.

Apart from convex hulls, some contributions seek to find stronger MIP formulations. Frangioni et al. [48] proposes a tighter linear approximation for quadratic generation costs; Ostrowski et al. [109] presents a new class of valid inequalities (cuts) to tighten ramping constraints.

2.4. Modelling Wind Uncertainty

The high penetration of uncertain generation sources, such as wind and solar power, in power systems have posed new challenges to the UC process. The deviation between expected and real wind production must be absorbed by the power system resources (reserves), which must be available and ready to be deployed in real time. To guarantee that enough system resources are available to face real-time uncertainty, the system resources must be committed in advance, usually the day-ahead, by solving the so-called UC problem. It is imperative for ISOs to have an adequate methodology to schedule an efficient amount of system resources (reserves) to face the increasing amount of real-time uncertainty.

The short-term decision process for power systems operations (see section 2.1) is conceptually a two-stage problem [143]. In the first-stage, the unit commitment decision takes places hours to days ahead of the actual operation, where units are committed to meet an expected power demand for each hour, based on the units' costs and constraints. In the second-stage, after the uncertainty (e.g. wind) has been realized, the power outputs of committed units are decided to meet the real-time load. These dispatch decisions take place between minutes to seconds ahead of the time implementation.

Let us consider the second-stage of the UC optimization problem (Equation 2.1)-(Equation 2.4), which is obtained by fixing the first-stage variable $\boldsymbol{x}$:

$$\begin{aligned} \min_{\boldsymbol{p},\boldsymbol{w}} \quad & \mathbf{c}^\top \boldsymbol{p} + \mathbf{d}^\top \boldsymbol{w} \\ \text{s.t.} \quad & \mathbf{H}\boldsymbol{p} + \mathbf{J}\boldsymbol{w} \leq \mathbf{h} && (2.5) \\ & \mathbf{B}\boldsymbol{p} + \mathbf{C}\boldsymbol{w} \leq \tilde{\mathbf{g}} && (2.6) \\ & \boldsymbol{w} \leq \mathbf{W} && (2.7) \end{aligned}$$

where $\tilde{\mathbf{g}} = \mathbf{g} - \mathbf{A}\boldsymbol{x}$.

The optimal solution of this LP problem will always be at a vertex of the feasible region, because the objective function is linear and the feasible region is convex. Therefore, the optimal solution is always at the very boundary of the feasible region, which is also the boundary of feasibility. This solution is then by nature not designed to be robust against perturbations in the feasible region.

In fact, Ben-Tal and Nemirovski [9],[10] reported that for many real LP problems, the optimal solutions presented more than 50% violations of some of the constraints due to small perturbations (0.01%) of uncertain data. These "optimal" solutions become meaningless, especially if the constraints of the optimization problem are hard constraints that cannot be violated. Similarly, under the stochastic paradigm, it has been observed that using a single deterministic value (usually the mean value) instead of uncertain parameters lead to very poor solutions (see, e.g., [15, 124]).

A reasonable strategy to overcome this problem is then to find a solution away from the boundary (of feasibility), sacrificing optimality for some robustness. This can be achieved by modifying the optimization problem to somehow consider a given level of uncertainty. There are different strategies for modelling uncertainty in optimization problems. These strategies define how much and where to move in the interior of the feasible region.

For the case of the UC problem, there are mainly three different paradigms for modelling uncertainty: deterministic, stochastic and robust. In the deterministic paradigm, reserve levels must be given and they define how much the solution must be away from the boundary of some constraints (usually the units' generation limits). The other two paradigms rely on uncertainty-oriented optimization techniques, stochastic and robust programming, and they optimize the reserve levels endogenously. In order to ensure feasibility, the stochastic and robust paradigms may move the solution away from the boundary of all constraints if necessary.

The following three subsections provide an overview of all three paradigms. For other methodologies, like chance-constrained optimization, the reader is referred to [128] and references therein.

2.4.1. Deterministic Paradigm

The deterministic paradigm has been the most common practice used for dealing with uncertainty in the power industry, and it has been widely studied in the UC literature, see for example [60, 123], Morales-Espana et al. [91, 99] and references therein. A deterministic UC solves the problem (Equation 2.1)-(Equation 2.4), thus committing and dispatching generating units to meet a deterministic expected load. The uncertainty is handled by including (capacity) reserve constraints that impose given reserve levels, e.g., the total capacity of committed units exceed the forecasted load.

The reserve sizing is usually based on deterministic rule-of-thumb criteria. A common practice is to determine the level of reserve to cover the loss of the largest

generator, known as the $N-1$ criterion, or a fraction of the hourly demand [116]. To consider different sources of uncertainty, the $N-1$ criterion is commonly mixed with a number of standard deviations of the error in uncertainty introduced by load and wind. Some ISOs require enough power reserves to cover at least three times the standard deviation of the net-load (forecast load minus forecast wind generation) error prediction [54, 62]. Although probabilistic methods have been proposed to size the level of reserves [2, 5, 32, 81, 108], the deterministic rule-of-thumb criteria are still very popular in the electricity sector due to their simplicity.

The deterministic paradigm remains the most common paradigm in the power industry, because it is easy to implement in practice. However, the deterministic paradigm usually leads to an over-scheduling of resources resulting in an economically inefficient way to handle uncertainty, especially when the reserve sizing is determined by rule-of-thumb rules. This can be illustrated with the following example. Suppose that an ISO wants to schedule enough reserves to cope with the uncertainty range of a wind farm. This uncertainty range is between 100 and 200 MW, hence 100 MW of reserves (up and down together) is then required. Now, suppose that the wind farm is only connected to a power line with transmission capacity of 75 MW, then a maximum wind production of 75 MW can be dispatched, regardless of the possible realization of uncertainty. Consequently, the actual reserve requirement is zero due to the transmission limit.

Although for this illustrative example it was easy to readjust the reserve levels, real power systems are considerably more complex and it is not possible to perform this reserve adjustment a priori. Furthermore, since a deterministic UC only considers one expected deterministic condition, even with enough reserve levels, the power system may not be able to deploy the reserves if the real-time condition deviates significantly from the expected value. This has been confirmed by ISO's operational experience [84] as well as by numerical simulations shown in [12], [95] and chapter 3.

Uncertainty-oriented optimization methods, such as stochastic and robust programming, seek to overcome these weaknesses, as described in the following sections.

2.4.2. Stochastic Paradigm

Stochastic optimization has gained substantial popularity for UC optimization under parameter uncertainty. In the stochastic optimization approach, different (stochastic) conditions can be considered through an explicit description of scenarios and their associated probability [112, 121, 124].

Here, we provide an overview of the generic two-stage stochastic UC problem. Much work has been done in various aspects of stochastic optimization. The reader is referred to [15, 68, 124] and references therein for a more comprehensive picture of stochastic optimization (including multi-stage stochastic problems).

In the two-stage stochastic problem, the uncertainty is realized after the first-stage decisions must be implemented, but before the implementation of the second-stage

decisions. Thus, the second-stage decisions are the actions implemented to face the unexpected realization of the uncertainty.

The two-stage UC problem (Equation 2.1)-(Equation 2.4) under the stochastic paradigm, only considering wind uncertainty, can be represented as follows:

$$\min_{\boldsymbol{x},\boldsymbol{p}_{\boldsymbol{\varsigma}},\boldsymbol{w}_{\boldsymbol{\varsigma}}} \quad \left(\mathbf{b}^{\top}\boldsymbol{x} + \mathbb{E}\left[\mathbf{c}^{\top}\boldsymbol{p}_{\boldsymbol{\varsigma}} + \mathbf{d}^{\top}\boldsymbol{w}_{\boldsymbol{\varsigma}}\right]\right)$$

$$\text{s.t.} \quad \mathbf{F}\boldsymbol{x} \leq \mathbf{f}, \ \boldsymbol{x} \text{ is binary} \tag{2.8}$$

$$\mathbf{H}\boldsymbol{p}_{\boldsymbol{\varsigma}} + \mathbf{J}\boldsymbol{w}_{\boldsymbol{\varsigma}} \leq \mathbf{h}, \quad \forall \boldsymbol{\varsigma} \in \mathcal{Z} \tag{2.9}$$

$$\mathbf{A}\boldsymbol{x} + \mathbf{B}\boldsymbol{p}_{\boldsymbol{\varsigma}} + \mathbf{C}\boldsymbol{w}_{\boldsymbol{\varsigma}} \leq \mathbf{g}, \quad \forall \boldsymbol{\varsigma} \in \mathcal{Z} \tag{2.10}$$

$$\boldsymbol{w}_{\boldsymbol{\varsigma}} \leq \mathbf{W}_{\boldsymbol{\varsigma}}, \quad \forall \boldsymbol{\varsigma} \in \mathcal{Z} \tag{2.11}$$

where the objective is usually to minimize the expected generation cost considering the occurrence probability of each scenario. The variables $\boldsymbol{x}$ represent the first-stage decisions, $\boldsymbol{p}_{\boldsymbol{\varsigma}}$ and $\boldsymbol{w}_{\boldsymbol{\varsigma}}$ the second-stage decisions, $\mathbf{W}_{\boldsymbol{\varsigma}}$ the uncertain wind realization for scenario ς, and $\mathcal{Z}$ the set of scenarios. The operating constraints involving the second-stage variables (Equation 2.9)-(Equation 2.11) are enforced for all scenarios.

Much research along the stochastic UC has been done. Takriti et al. [129] proposes one of the first UC under the stochastic paradigm, where uncertain demand was considered. Bouffard et al. [22],[23] introduces uncertain generation outages. Wu et al. [145] models outages of generation units and transmission lines as well as uncertain demand. Ruiz et al. [120] also incorporates two different sources of uncertainty, generation unreliability and deviations from the load forecast. Some other works have focused on modelling wind generation uncertainty, see for example [21, 86, 112, 131, 134].

Although the stochastic paradigm overcomes the main drawbacks of the deterministic paradigm, it presents however some practical limitations: 1) a large number of scenario samples is required to obtain robust solutions (i.e. feasible solutions for any wind uncertainty realization), which results in a computationally intensive problem (often intractable); and 2) it may be difficult to obtain an accurate probability distribution of the uncertainty, this could considerably affect the efficiency of the final decisions [14].

2.4.3. Robust Paradigm

Here we present the two-stage adaptive robust UC problem. For adaptive-multistage and static robust problems as well as details about different uncertainty sets, the reader is referred to [10, 14, 27] and references therein.

The two-stage adaptive UC problem, only considering wind uncertainty, can be

represented as follows:

$$\min_{\boldsymbol{x}} \quad \left(\mathbf{b}^{\top}\boldsymbol{x} + \max_{\boldsymbol{\xi}\in\Xi} \min_{\boldsymbol{p}(\cdot)} \left(\mathbf{c}^{\top}\boldsymbol{p}\left(\boldsymbol{\xi}\right) + \mathbf{d}^{\top}\boldsymbol{w}\right)\right)$$

$$\text{s.t.} \quad \mathbf{F}\boldsymbol{x} \leq \mathbf{f},\ \boldsymbol{x} \text{ is binary} \tag{2.12}$$

$$\mathbf{H}\boldsymbol{p}\left(\boldsymbol{\xi}\right) + \mathbf{J}\boldsymbol{w} \leq \mathbf{h}, \quad \forall \boldsymbol{\xi} \in \Xi \tag{2.13}$$

$$\mathbf{A}\boldsymbol{x} + \mathbf{B}\boldsymbol{p}\left(\boldsymbol{\xi}\right) + \mathbf{C}\boldsymbol{w} \leq \mathbf{g}, \quad \forall \boldsymbol{\xi} \in \Xi \tag{2.14}$$

$$\boldsymbol{w} = \boldsymbol{\xi}, \quad \forall \boldsymbol{\xi} \in \Xi \tag{2.15}$$

where the objective function is to minimize the sum of commitment cost $\mathbf{b}^{\top}\boldsymbol{x}$ and worst-case dispatch cost (max-min expression) $\max_{\boldsymbol{\xi}\in\Xi} \min_{\boldsymbol{p}} \left(\mathbf{c}^{\top}\boldsymbol{p} + \mathbf{d}^{\top}\boldsymbol{w}\right)$ over the planning horizon. Notice that max-min form for the worst-case dispatch cost seeks to minimize the economic dispatch cost for a fixed commitment $\boldsymbol{x}$ and wind nodal injection $\boldsymbol{\xi}$, which is then maximized under the uncertainty set Ξ.

Note that only the right hand side of (Equation 2.15) have an explicit dependence on the uncertain parameter $\boldsymbol{\xi}$ (equal to $\boldsymbol{w}$), while the vectors $\mathbf{b}, \mathbf{c}, \mathbf{d}, \mathbf{f}, \mathbf{g}$, and $\mathbf{h}$ together with matrices $\mathbf{A}, \mathbf{B}, \mathbf{C}, \mathbf{F}, \mathbf{H}$ and $\mathbf{J}$ are taken to be deterministically and exactly known. On the other hand, the second-stage variables $\boldsymbol{p}\left(\boldsymbol{\xi}\right)$ are a function of the uncertain parameter $\boldsymbol{\xi}$, hence fully adaptive to any uncertain realization of the uncertainty.

The robust paradigm is attractive in several aspects 1) it requires moderate information about the underlying uncertainty, such as the mean and the range of the uncertain data; and 2) it immunizes the solution against all realizations of the uncertain data within a deterministic uncertainty range. There have been recent works addressing wind uncertainty in the adaptive robust UC problem [12, 65, 151, 152]. Bertsimas et al. [12] presents a two-stage adaptive UC, where wind uncertainty is modelled as a continuous bounded range (polyhedral uncertainty set). Zhao et al. [152] takes into account demand-response and wind uncertainties simultaneously. Zhao and Guan [151] mixes robust and stochastic optimization with the objective to achieve lower expected total costs while ensuring the system robustness. Hu et al. [65] elaborates an uncertainty set that takes into account the correlation between wind and demand.

Although the robust paradigm partly overcomes the disadvantages of the stochastic paradigm, it presents two main drawbacks, one related with its computational intensity and the other with its over-conservatism. The computational burden of adaptive robust UC does not depend on the number of scenarios, but it requires solving an MIP problem together with a bilinear program to obtain the worst-case scenario [12, 151–153]. This problem is considerably more complex to solve than a pure MIP, requiring ad-hoc solving strategies [12, 151], and only local optimum is guaranteed, in contrast with the boundedly close to global optimum that is guaranteed by the MIP.

The over-conservatism in the robust paradigm is a natural consequence of protecting

the solution against each uncertainty realization within the uncertainty set, regardless of its probability. The solution is especially protected against the worst case scenario which may be fictitious and very unlikely to occur. To deal with the over-conservatism, parameters (like the budget-of-uncertainty [13]) are introduced in the optimization problem to control the level of conservatism of the robust solution [12, 65, 151, 152]. However, tuning these parameters is a far from trivial task [128] and highly dependent on the specific study case [12, 151].

In addition, and to the best of our knowledge, all the work introducing wind uncertainty into adaptive robust UCs does not allow wind to have any flexibility because (Equation 2.15) imposes that $\boldsymbol{w}$ takes a fixed wind realization. However, wind has some flexibility because it can be curtailed. Therefore, what is uncertain is not the wind production range but rather the upper bound of the possible wind dispatch.

2.5. Conclusions

The traditional energy-block scheduling approach is unable to adequately prepare the power system to face perfectly known system conditions. We identified three main drawbacks of the traditional energy-block scheduling approach that lead to an unnecessary and inefficient use of system resources (reserves) and can even compromise the power system security. These drawbacks can be overcome 1) by scheduling the power generation in a piecewise-linear fashion to follow a forecasted smooth power demand profile; 2) by modelling the ramp constraints, in UCs, based on power production instead of energy, then respecting all ramping constraints; and 3) by explicitly scheduling the intrinsic startup and shutdown power trajectories of generating units, i.e., introducing these constraints in the UC formulations. Consequently, it is imperative to develop more adequate and accurate models.

Developing more accurate models would be pointless if the models cannot be solved efficiently enough in the first place. The UC problem is an integer and non-convex problem which is difficult to solve efficiently, especially for large-scale problems. Mixed-integer (linear) programming (MIP) has become a very popular approach to solve UC problems due to significant improvements in MIP solvers over the last two decades. Despite this significant breakthrough, the time required to solve UC problems continues to be a critical limitation that restricts its size and scope. This chapter identified the key features that affects the computational burden of MIP formulations: the tightness and compactness. Therefore, to develop computationally efficient MIP models, it is neccesary to devise tight and preferably simultaneously compact MIP formulations. This is, however, a non trivial task because the obvious formulations are very weak (not tight) or very large, and trying to improve the tightness (compactness) usually means harming the compactness (tightness).

UC formulations can be further extended to deal with uncertainty. This chapter also gave an overview of the the three main paradigms used to deal with wind uncertainty

in UC problems: deterministic, stochastic and robust. The deterministic paradigm, based on reserve levels, is the most common in the power industry because it is easy to implement in practice and it is not as computationally intensive as the other paradigms. However, the deterministic paradigm usually leads to an over-scheduling of resources resulting in an economically inefficient way to handle uncertainty. Furthermore, a deterministic UC only considers one expected deterministic condition, even with enough reserve levels, the power system may not be able to deploy the reserves if the real-time condition deviates significantly from the expected value.

Uncertainty-oriented optimization methods, such as stochastic and robust programming, seek to overcome the weaknesses of the deterministic paradigm. However, there is a price to pay in order to better tackle uncertainty:

- The stochastic approach presents some practical limitations: 1) a large number of scenario samples is required to obtain robust solutions, which results in a computationally intensive problem (often intractable); and 2) it may be difficult to obtain an accurate probability distribution of the uncertainty.
- Although the robust paradigm partly overcomes the disadvantages of the stochastic one, it presents two main drawbacks: 1) it requires solving an MIP problem together with a bilinear program to obtain the worst-case scenario, this problem is considerably more complex to solve than a pure MIP. 2) The over-conservatism in the robust paradigm is a natural consequence of protecting the solution against each uncertainty realization within the uncertainty set, regardless of its probability. The solution is especially protected against the worst-case scenario which may be fictitious and very unlikely to occur.

3. Comparison of Energy-Block and Ramp-Based Scheduling Approaches

Contents

This Chapter presents a comparison between the traditional energy-block scheduling approach and the ramp-based scheduling approach proposed in this thesis. In the first section, we introduce the two approaches and the models used to represent them, and we also present the power system used to perform the comparisons. Then, we describe the procedure used to assess their performance. The last two sections analyse the cases where scheduling is performed under certain and uncertain system conditions, where the latter only considers wind uncertainty.

3.1. UC approaches and Power System

3.1.1. UC approaches

Two different network-constrained scheduling approaches are implemented. The traditional energy-block approach, labelled as *EnSch*, and the ramp-based scheduling approach, labelled as *RmpSch*. All models are implemented as MIP formulations.

Conventional *EnSch* UC seek to provide an energy demand profile at minimum cost. The energy demand is represented using energy levels, hourly averaged generation, in a stepwise fashion. All constraints involving generation levels, e.g., ramp-constraints, are applied to these energy levels. For this study, we use the MIP-based network-constrained unit commitment (UC) formulation in [47] to represent *EnSch*, which is quite standard in the UC literature [51, 60, 109, 123].

The *RmpSch* approach proposed in [99], draws a clear distinction between power and energy. Demand and generation are modelled as hourly piecewise-linear functions representing their instantaneous power trajectories. The schedule of generating unit output is no longer a stepwise function, but a smoother function that respects all ramp constraints. In addition, *RmpSch* also includes the inherent startup and shutdown power trajectories of generating units, thus avoiding power discontinuities in the scheduling stage. The network-constrained formulation used in this study is the MIP-based UC proposed in [99] (see Appendix B), which core is built upon the convex hull formulation in [97].

3.1.2. Power System

To evaluate the performance of different network-constrained UC approaches, we use the modified IEEE 118-bus test system described in Appendix C for a time span of 24 hours. The system has 118 buses; 186 transmission lines; 54 thermal units; 91 loads, with average and maximum levels of 3991 MW and 5592 MW, respectively; and three wind units, with aggregated average and maximum production of 867 MW and 1333 MW, respectively, for the nominal wind case (see Figure 3.3).

All tests were carried out using CPLEX 12.6 [1] on an Intel-i7 (64-bit) 3.4-GHz personal computer with 16 GB of RAM memory. The problems are solved until they hit a time limit of 24 hours or until they reach an optimality tolerance of 0.05%.

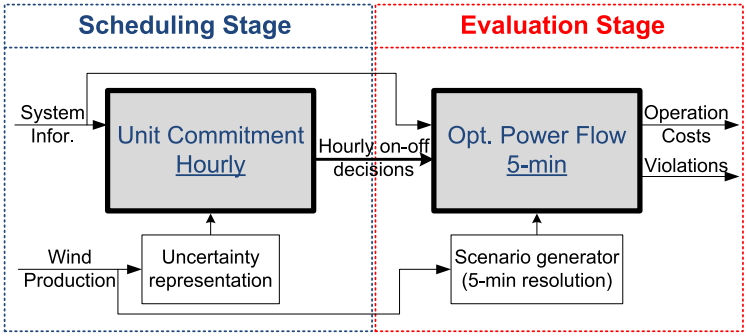

Figure 3.1.: Scheduling and Evaluation Stages

3.2. UC Approach Analysis

3.2.1. Scheduling and Evaluation Stages

To compare the performance of the different network-constrained UC approaches, we make a clear difference between the scheduling stage and the evaluation stage. Here, we analyse the cases where scheduling is performed to deal with certain and uncertain system conditions, where the latter only considers wind uncertainty. The computational experiments proceed as follows, see Figure 3.1.

1. Scheduling stage: solve the different network-constrained UC models and obtain the hourly commitment policy (first-stage decisions), using a small representative number of wind scenarios for the wind units.

2. Out-of-sample evaluation stage: for each commitment policy, solve a 5-min network-constrained economic dispatch problem repetitively for a large set of new wind scenarios in order to obtain an accurate estimate of the expected performance of each UC policy.

In order to mimic the high costs due to corrective actions in real time operations, we introduce penalty costs for the violation of some constraints in the 5-min economic dispatch. The penalty costs are set to 10000 \$/MWh and 5000 \$/MWh for demand-balance and transmission-limits violations, respectively, as suggested in [47] (similarly to [12, 151]). These penalty costs represent the expensive real-time corrective actions that an independent system operator (ISO) needs to take in the event that the actual system condition significantly deviates from the expected condition, such as dispatching fast-start units, voltage reduction or load shedding.

To represent the degree of flexibility that generating units have during the statup and shutdown time, the 5-min simulation allows the units to shutdown and startup around ± 30 min from the exact hourly commitment that resulted from the day-ahead UC. This flexibility is introduced to mimic real-time operation actions which occur in real power systems with 5-min real-time markets [80].

The 5-min network-constrained economic dispatch (ED) model used for the evaluation stage is an approximation of a more complex architecture of real-time markets [29, 45]. Figure 3.2 shows how the generation is generally dispatched in 5-min real-time markets. A snapshot of the power system state is taken 1 min prior to the beginning of the 5-min balancing interval. Next, an ED is used to match the expected demand for the next 5 min, thus obtaining the base point of all generating units. Generation must ramp from the previous to the next base point in 4-min and stay at the new base point for 1 min, where the new snapshot of the system is taken and the next ED is solved. For the sake of simplicity, in the simulation stage, the generating units are dispatched to ramp linearly from one base point to the next, see dashed line in Figure 3.2. The 5-min network-constrained economic dispatch model is then based on [99] (see Appendix B).

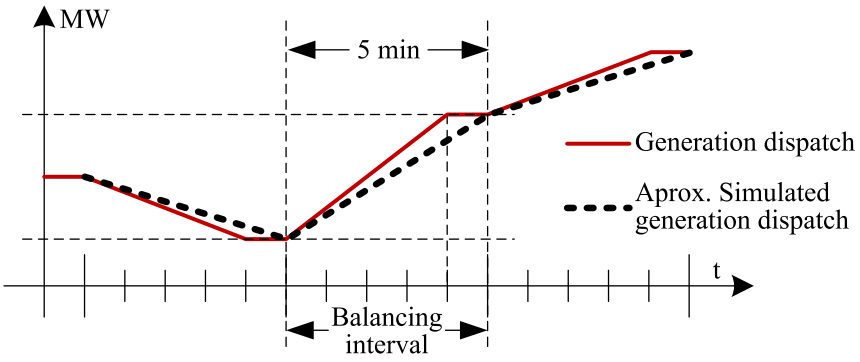

Figure 3.2.: Simulated generation dispatch

To generate scenarios for the uncertain wind power production, we use Latin Hypercube Sampling (LHS). We assume that the wind production follows a multivariate normal distribution with predicted nominal value and volatility matrix [151]. The idea in applying LHS is to optimally distribute the samples to explore the whole area in the experimental region, avoiding the creation of scenarios that are too similar (clusters) [55].

3.2.2. Performance Metrics

We assess the performance of the UC scheduling approaches in eight aspects, two related with the scheduling stage and six with the evaluation stage. These aspects are described as follows.

Scheduling stage: 1) the fixed production costs (FxdCost [k$]), including non-load, startup and shutdown costs; and 2) the number of startups (# SU). These two aspects indicate the commitment decisions that were needed by each approach to prepare the system to deal with the given wind uncertainty.

Evaluation stage: 3) the average dispatch costs (Average [k$]), indicates the economic efficiency of the UC decision; 4) the volatility of these costs represented by

the standard deviation of dispatch costs (Std [k$]), which indicates the reliability of the real-time dispatch operation under the UC decision; 5) the dispatch cost of the worst-case scenario (Worst [k$]), indicates how robust the UC decision is against the worst-case scenario (from the full set of out-of-sample scenarios); 6) number of scenarios where there were violations in either demand-balance or transmission-limits constraints (# Sc); 7) total number of these violations (# Tot); and 8) total accumulated energy that could not be accommodated, demand-balance violations (MWh). The last three aspects also indicate how robust the UC decision is against different wind scenarios.

3.3. Dealing with "Certainty"

Before assessing the performance of the different network-constrained UC approaches under uncertainty, we evaluate them under completely known and expected system conditions. For this case study, then, wind is not considered and the objective is to find the cheapest schedule for two deterministic and completely known power demand profiles. We assume that the power demand profiles are perfectly known and that no uncertain events will happen. Therefore, there should be no need for operating reserves and hence they are taken into account (i.e., they are set to zero). Although this situation is hypothetical, it helps to evaluate and compare the two scheduling approaches.

Table 3.1 shows the two power demand profiles D1 and D2, which present the same energy profile (D^E in Table 3.1) but different ramp requirements.

Table 3.1.: Power and Energy Demand Profiles

Hour	**0**	**1**	**2**	**3**	**4**	**5**	**6**	**7**	**8**	**9**	**10**	**11**	**12**
D1*	1500	1750	2250	2750	3000	3500	3750	4000	4500	5000	5250	5500	5000
D2*	1625	1625	2375	2625	3125	3375	3875	3875	4625	4875	5375	5375	5125
$D^{E\dagger}$	1625	1625	2000	2500	2875	3250	3625	3875	4250	4750	5125	5375	5250

Hour	**13**	**14**	**15**	**16**	**17**	**18**	**19**	**20**	**21**	**22**	**23**	**24**
D1*	4500	4000	3250	3000	3500	4000	5000	4500	3500	2500	2000	1500
D2*	4375	4125	3125	3125	3375	4125	4875	4625	3375	2625	1875	1625
$D^{E\dagger}$	4750	4250	3625	3125	3250	3750	4500	4750	4000	3000	2250	1750

*Power [MW] at the end of the hour †Total Energy [MWh] for the hour

Table 3.2 shows the optimal solutions found by *RmpSch* and *EnSch* to supply D1 and D2. The optimal schedules obtained by each approach for all 54 generating units are listed in Appendix D. Note in Table 3.2 that *EnSch* provides the same optimal scheduling solution for D1 and D2 because they present the same energy profile. On the other hand, *RmpSch* provides different optimal scheduling for D1 and D2, although both scheduling solutions satisfy the same total energy demand. Notice that the FxdCost of *RmpSch* are higher than those of *EnSch*, because: 1)

RmpSch needs to satisfy both specific power and energy profiles, unlike *EnSch* which just seeks to satisfy an energy profile at minimum cost; and 2) *EnSch* overestimates the units' ramp capability, that is, *EnSch* may produce energy schedules requiring fewer units than are actually needed (this is one reason why these energy schedules are usually infeasible [99]).

Table 3.2.: Scheduling results for the different approaches for demand D1 and D2

Approach	Demand	FxdCost [k$]	Dispatch [k$]	# SU
RmpSch	D1	51.352	901.908	16
	D2	49.618	907.425	19
EnSch	D1 & D2	34.724	930.185	11

Table 3.3 and Table 3.4 show the ramp requirements of the power demand profiles D1 and D2, respectively, and the ramp that was scheduled for both scheduling approaches. The ramp requirements can be easily calculated from the power demand D_t as $D_t - D_{t-1}$. The ramp schedule of every approach is calculated as the total ramp available of all committed units. The positive and negative values refer to upward and downward ramps, respectively. Numbers between parenthesis stand for the cases where the scheduled ramp of *RmpSch* or *EnSch* is lower than the required ramp imposed by the demand.

We can observe that *RmpSch* always schedule enough ramp capabilities to supply the ramp demand. On the other hand, the *EnSch* schedule does not provide enough ramp resources for three periods for the case of D1, see Table 3.3, and for two periods for the case of D2, see Table 3.4. This is because *EnSch* presents the same ramp schedule for D1 and D2, because they have the same energy profile. One power profile has a unique energy profile and hence satisfying a power profile automatically satisfies the energy profile. However, one energy profile has infinite possible power profiles [57, 99, 118]; therefore, even though *EnSch* could provide a given energy profile, it cannot guarantee that all possible resulting power profiles can be supplied [88, 99].

Table 3.3.: Ramp Profiles for demand D1 (MW/h)

Hour	**1**	**2**	**3**	**4**	**5**	**6**	**7**	**8**	**9**	**10**	**11**	**12**
D1*	250	500	500	250	500	250	250	500	500	250	250	-500
RmpSch†	935.6	960.6	552.5	696.75	981.75	994.25	1006.75	1033	1103	1138	1138	-1138
EnSch†	1045.6	727.5	900.5	923	1058	1058	1083	1083	1098	1098	1098	-1098
Hour	**13**	**14**	**15**	**16**	**17**	**18**	**19**	**20**	**21**	**22**	**23**	**24**
D1*	-500	-500	-750	-250	500	500	1000	-500	-1000	-1000	-500	-500
RmpSch†	-1138	-1143	-1128	-1078	1078	1078	1078	-1078	-1088	-1063	-983	-808
EnSch†	-1098	-1108	-1073	-998	998	998	(998)	-998	(-998)	(-983)	-983	-958

* Ramp Requirement †Ramp Available

Table 3.4.: Ramp Profiles for demand D2 (MW/h)

Hour	**1**	**2**	**3**	**4**	**5**	**6**	**7**	**8**	**9**	**10**	**11**	**12**
D2*	0	750	250	500	250	500	0	750	250	500	0	-250
RmpSch†	1045.6	1070.6	612.5	763	1010.5	1029.3	1041.8	1081.8	1089.3	1138	1138	-1138
EnSch†	1045.6	(727.5)	900.5	923	1058	1058	1083	1083	1098	1098	1098	-1098
Hour	**13**	**14**	**15**	**16**	**17**	**18**	**19**	**20**	**21**	**22**	**23**	**24**
D2*	-750	-250	-1000	0	250	750	750	-250	-1250	-750	-750	-250
RmpSch†	-1143	-1118	-1118	1130.5	1130.5	1145.5	1130.5	-1213	-1258	-1038	-933	-758
EnSch†	-1098	-1108	-1073	998	998	998	998	-998	(-998)	-983	-983	-958

* Ramp Requirement †Ramp Available

Table 3.5 shows the results from the evaluation stage for the different approaches, where once the commitment decisions are obtained, the deterministic demand must be supplied through a 5-min economic dispatch, as described in subsection 3.2.1. The ramp-based scheduling approach *RmpSch* was able to supply both demand profiles without incurring any constraint violation. In fact, the dispatch cost in the evaluation stage is lower than that in the scheduling stage (see Table 3.2). This is because the 5-min optimal dispatch provides more flexibility than the 1-hour dispatch used in the scheduling stage.

Table 3.5.: Evaluation Stage: 5-min economic dispatch

Approach	Demand	Dispatch Costs [k$]	Violations	
			# Tot	MWh
RmpSch	D1	899.641	0	0
	D2	905.472	0	0
EnSch	D1	1501.029	47	58.189
	D2	2036.099	22	111.599

On the other hand, the traditional energy-block scheduling approach *EnSch* could not satisfy any of the demand profiles. The high dispatch costs are due to violations of the demand-balance constraint (58 MWh and 111 MWh for D1 and D2, respectively). These demand violations are mainly due to ramp scarcity, infeasible energy delivery, capacity scarcity, and deterministic unplanned events:

1. *Ramp Scarcity*: As discussed above, planning one unique energy profile does not guarantee that the system can satisfy the potential infinite power profiles.
2. *Infeasible Energy Delivery*: Applying ramp-constraints to energy levels or (hourly) averaged generation levels, instead of power, results in energy schedules that are not feasible [57]. That is, the energy-block schedule approach does not guarantee that the commitment decisions can actually provide the resulting energy schedule, as widely reported in the literature, see for example [57, 58, 88, 99, 144, 150].

3. *Capacity Scarcity*: The demand peak of D1 is 5500 MW and occurs at the end of hour 11. Note that *EnSch* scheduled 21 units for this hour (see Table D.5 and Table D.6 in Appendix D) having a total production capacity of 5390 MW. This is in contrast to *RmpSch*, which committed 24 units, for a total capacity of 5690 MW, at hour 11 (see Table D.1 and Table D.2 in Appendix D) to satisfy the peak demand of D1. This capacity scarcity event has been also reported in [99], and they appear because the maximum power in one period is always greater than or equal to the energy level for that period (because the energy is the average power), as shown in Figure 1.2 in chapter 1. Therefore, modelling only energy levels ignores the possible power peaks.

4. *Deterministic Unplanned Events*: The traditional energy-based scheduling approach usually ignores the intrinsic startup and shutdown power trajectories of thermal units. Consequently, there may be a significant amount of energy that is not being allocated, affecting the total load balance. As a result, there is an unplanned and inefficient deployment of resources in real time that is required to accommodate these power trajectories [88].

3.4. Dealing with Uncertainty

This section compares the performance of five different UC formulations that deal with uncertainty: four resulting from applying the deterministic and stochastic paradigms to both *EnSch* and *RmpSch* approaches, and one from the robust modelling of reserves under the *RmpSch* approach [95].

To compare the performance of the different network-constrained UC approaches, we implement the scheduling and the evaluation stages described in section 3.2:

1. Scheduling stage: solve the different network-constrained UC models and obtain the hourly commitment policy (first-stage decisions), using 20 wind scenarios for each of the three wind units presented in Table C.6, Table C.7 and Table C.8 in Appendix C. Figure 3.3 shows the aggregated wind production of these wind scenarios.

2. Out-of-sample evaluation stage: for each commitment policy, solve a 5-min network-constrained ED problem repetitively for a set of 200 new wind scenarios in order to obtain an accurate estimate of the expected performance of each UC policy. It is important to highlight that more than the 20% of these out-of-sample scenarios fall outside (in at least one hour) the uncertainty bounds shown in Figure 3.3.

We assume that the 20 scenarios of the scheduling stage (see Figure 3.3) are the only information available to obtain the commitment decisions. Therefore, we use these data to describe the different wind uncertainty representation required by the different optimization paradigms. The deterministic paradigm (Det) uses the

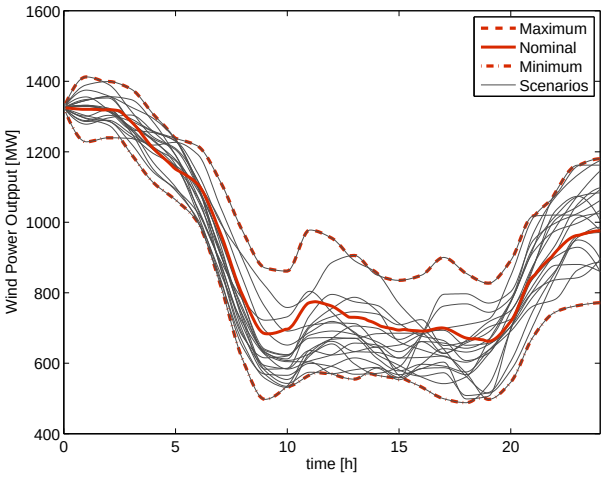

Figure 3.3.: Representation of wind uncertainty over time, 20 scenarios and envelopes

nominal wind production and two hourly reserves, upwards and downwards which are defined as the nominal wind production minus the minimum wind envelope and the maximum wind envelope minus the nominal wind production, respectively (see Figure 3.3). The stochastic paradigm (Stch) uses all 20 scenarios. Finally, the robust (Rob) paradigm uses the nominal wind production together with minimum and maximum envelopes of power-capacity and ramp-capability, which are obtained from this set of 20 scenarios.

3.4.1. Out-of-sample Evaluation

Table 3.6 compares the performance of the different UC approaches under different optimization paradigms. This comparison is made through 200 out-of sample wind scenarios, as described above. From the scheduling stage, we can observe that the deterministic paradigm, for both scheduling approaches, commits the largest quantity of resources (higher FxdCost), because this is the only approach that cannot readjust (optimize) the given level of reserves by considering wind curtailment. That is, the reserve requirements for the deterministic paradigm results in a larger quantity of committed resources. For the *RmpSch* approach, Rob presents lower FxdCost than Stch, but Rob started two more units. This difference is because Rob schedule more flexible units (higher ramps) which usually present lower fixed cost but higher variable cost. This difference also indicates that the uncertainty information required by these two paradigms leads to different commitment strategies, where Rob seeks to guarantee feasibility to the given uncertainty ranges, and Stch seeks to minimize the expected costs of the given scenarios.

From the evaluation stage in Table 3.6, we can observe the following:

1. Stch vs. Det: Despite the scheduling approach used, Stch presents signific-

Table 3.6.: Comparison Between the Deterministic, Stochastic and Proposed Robust Paradigms Under 200 Out-of-Sample Wind Scenarios

		Scheduling Hourly		Evaluation: 5-min Economic Dispatch					
				Dispatch Costs [k$]			Violations		
		FxdCost [k$]	# SU	Average	Std	Worst	# Sc	# Tot	MWh
EnSch	Det	33.977	10	1223.191	509.703	4818.712	200	2089	8630.74
	Stch	33.728	10	1051.266	147.652	2568.092	200	1159	5187.56
RmpSch	Det	55.492	16	795.559	148.442	2234.517	29	252	594.13
	Stch	54.765	12	784.030	124.964	2192.011	13	126	392.25
	Rob	51.986	14	769.072	14.520	812.844	0	0	0

antly lower Average, Std and Worst-case dispatch costs than Det. This clearly shows the advantages of the stochastic paradigm over the deterministic one, as expected.

2. Robustness of Det: Det committed the largest quantity of resources, but it is the least robust despite the scheduling approach. This is mainly because, under the deterministic paradigm, most of the constraints, e.g., the network constraints, are only modelled for the nominal case and this cannot guarantee that the committed reserves can be deployed through the network. This is in contrast to Rob and Stch, where generating units are committed taking into account that power must (and can) be delivered to specific places in the network where the uncertainty appears. In short, since Det only considers one expected deterministic condition, even with enough reserve levels, the power system may not be able to deploy the reserves if the real-time condition deviates significantly from the expected value. This has been confirmed by ISO's operational experience [84] as well as by numerical simulations shown here and in [12, 95].

3. Det-*RmpSch* vs. Stch-*EnSch*: The Average and Worst-case dispatch cost of Stch-*EnSch* are around 32% and 15% higher than Det-*RmpSch*, respectively. This cost difference is mainly due to the penalty costs of the energy-balance constraint violations. For Stch-*EnSch*, the total number of violations and the total energy that could not be accommodated is more than 4.5 and 8.7 times higher than Det-*RmpSch*, respectively. This very surprising efficiency that the deterministic *RmpSch* exhibits over the stochastic *EnSch* is due to the adequate system representation of the *RmpSch* approach (see section 3.3). It would be misleading to expect that the stochastic *EnSch* would produce much better results dealing with uncertainty when, actually, this traditional *EnSch* approach is not even able to adequately deal with certainty, as widely discussed in section 3.3 and section 2.2.

4. Stch-*RmpSch* vs. Rob-*RmpSch*: The Average dispatch cost of Stch-*RmpSch* is around 2% higher than Rob-*RmpSch*. The Std and Worst-case dispatch

costs for Stch-*RmpSch* are more than 8.6 and 2.6 times higher, respectively. These significant costs differences is because Stch-*RmpSch* incurred in some constraint violations, unlike Rob-*RmpSch*.

In summary, for this case study, the *RmpSch* approach outperforms *EnSch* due to an adequate system representation. Furthermore, a deterministic formulation using this adequate system representation can outperform a stochastic formulation that uses an "inadequate" representation. In addition, the performance of the Det-*RmpSch* can be further improved by dealing with uncertainty under Stch and Rob paradigms.

3.4.2. In-sample Evaluation

To observe the performance of the Rob and Det paradigms compared with a "perfect" Stch paradigm, we carried out the 5-min economic-dispatch evaluation stage using the same (in-sample) scenarios that were used by the Stch formulations in the scheduling stage.

Table 3.7 shows the performance of the different UC approaches under the 20 (in-sample) scheduling scenarios. In general the results follow the same behaviour of those found in the out-of-sample evaluation presented in subsection 3.4.1, hence similar conclusions can be drawn. However, in this specific in-sample case, the Average and Worst-case dispatch costs of Stch-*Rmp* are slightly lower than Rob-*Rmp* (around 0.6 and 0.5%, respectively), because 1) Stch-*Rmp* did not present any constraint violation in the evaluation stage, and 2) Stch-*Rmp* is the optimal schedule for the 20 in-sample wind scenarios, unlike Rob-*Rmp* that optimizes over a nominal scenario.

Table 3.7.: Comparison Between the Deterministic, Stochastic and Proposed Robust Paradigms Under the 20 In-Sample Wind Scenarios

		Scheduling Hourly		Evaluation: 5-min Economic Dispatch					
				Dispatch Costs [k$]			Violations		
		FxdCost [k$]	# SU	Average	Std	Worst	# Sc	# Tot	MWh
EnSch	Det	33.977	10	1165.768	385.561	2501.214	20	162	750.21
	Stch	33.728	10	1027.414	18.267	1088.448	20	108	471.14
RmpSch	Det	55.492	16	770.707	29.597	887.280	2	15	9.6
	Stch	54.765	12	764.406	12.879	790.333	0	0	0
	Rob	51.986	14	769.037	12.517	794.039	0	0	0

3.5. Computational Performance

3.5.1. *EnSch* vs. *RmpSch*

Table 3.8 shows a comparison of problem size between the different models. The deterministic and stochastic models based on the *EnSch* approach present a larger number of constraints and nonzero elements than the models based on the *RmpSch* approach, even though *RmpSch* models the units' shutdown and variable-startup power trajectories, unlike *EnSch*. This is because *RmpSch* is built upon tight and compact formulations [97, 100]. However, *RmpSch* presents a larger number of continuous and binary variables, where the extra binary variables are used to model the variable startup costs, depending on how long the units have been offline [100]. Notice that, actually, both formulations *EnSch* and *RmpSch* only require the commitment variables to be defined as binary, because the other variables (e.g., startup and shutdown) take binary variables even if they are defined as continuous. This is widely discussed in [109] and specially in [91]. Note however that both references claimed that it is convenient to define these variables as binary to fully exploit the solver's strategies.

Table 3.8.: Problem Size of The Different Approaches

		Constraints	Nonzero elements	Continuous variables	Binary variables
EnSch	Det	33969	467329	9720	3888
	Stch	217689	5559883	117936	3888
RmpSch	Det	18093	315424	11016	6376
	Stch	199221	5497707	143856	6376
	Rob	36141	1074712	21096	6520

It is interesting to highlight the difference between Rob-*RmpSch* and Det-*EnSch*. Regarding the number of constraints, Rob-*RmpSch* is larger, but it is around twice the size of Det-*EnSch* in terms of nonzero elements, continuous and binary variables. This is an insignificant problem-size increase considering the fact that Rob-*RmpSch* includes the inherent startup and shutdown power trajectories of generating units, and a robust modelling of power-capacity and ramp-capability reserves (in comparison, Det-*EnSch* only models power-capacity reserves in a very simplistic fashion [47]).

Although the size of an MIP formulation influence its computational burden, the tradeoff between the problem size (compactness) and tightness is what finally defines the computational performance [91, 139, 141], as detailed in subsection 2.3.2 in

chapter 2. The tightness of an MIP formulation defines the search space (relaxed feasible region) that the solver needs to explore in order to find the (optimal integer) solution. The tightness of an MIP formulation can be measured with the integrality gap [91, 109, 139], which is defined as the relative distance between the relaxed and integer solutions. Although the integrality gap of the two formulations which are not modelling exactly the same problem should not be directly compared, these gaps provide an indication of the strength of each formulation.

Table 3.9 shows the computational performance of the different models. *RmpSch* formulations are tighter than *EnSch* formulations, and the integrality gaps of *RmpSch* are around half the ones of *EnSch*. This roughly means that before starting the branch-and-cut process to find the integer solution, *RmpSch* is already half way nearer than *EnSch*. Consequently, *RmpSch* formulations find the integer optimal solutions considerably faster than *EnSch* (within the required optimality tolerance).

Table 3.9.: Computational Burden of The Different Approaches

		Integrality Gap [%]	MIP* Time [s]	LP Time [s]	Nodes explored
EnSch	Det	1.205	766.2	1.86	60756
	Stch	1.267	(0.22%)	246.76	79192
RmpSch	Det	0.721	8.75	0.67	29
	Stch	0.737	867.88	38.13	819
	Rob	0.416	90.45	16.77	250

*(·)shows the final optimality tolerance if the time limit is reached

Although all models deal with uncertainty, the problem size and computational burden of those under the stochastic paradigm directly depend on the quantity of scenarios modelled.

Finally, it is interesting to note that Rob-*RmpSch* is almost an order of magnitude faster (around 8.5x) than Det-*EnSch*, and Rob-*RmpSch* solved the MIP problem above 2.7 faster than the time required by Stch-*EnSch* to solve the LP relaxation.

3.5.2. Tight and Compact *EnSch*

As described in section 3.1, the mathematical formulation in [47] was used in this study to represent *EnSch*, because this formulation is quite standard in the UC literature [51, 60, 109, 123]. However, this thesis proposes a tight and compact formulation for *EnSch*, see Article III.

Table 3.10 and Table 3.11 shows the problem size and computational performance of this tight and compact formulation, labelled as *TCEnSch*. The formulation

TCEnSch is above two orders of magnitude faster than *EnSch*. Furthermore, the stochastic version of *TCEnSch* solved the MIP problem around 1.2x faster than the time required by the Stch-*EnSch* to solve the LP relaxation.

Table 3.10.: Problem Size of The Different Approaches

		Constraints	Nonzero elements	Continuous variables	Binary variables
TCEnSch	Det	17199	536359	8424	6390
	Stch	182367	9994075	116640	6390

Table 3.11.: Computational Burden of The Different Approaches

		Integrality Gap [%]	MIP Time [s]	LP Time [s]	Nodes explored
TCEnSch	Det	0.504	4.54	0.34	121
	Stch	0.577	206.47	22.03	100

A detailed comparison between formulations *TCEnSch* and *EmSch* can be found in Article III (where these formulations are labelled as *P2* and *3bin*, respectively). Here, it is important to highlight that building more elaborated models, such as *RmpSch*, upon tight and compact formulations [53, 91, 97, 100] lead to computationally efficient models.

3.6. Conclusions

In this chapter, we presented numerical results comparing the performance of two different network-constrained scheduling approaches: the traditional energy-block approach and the ramp-based scheduling approach proposed in this thesis. The comparison is carried out under certain and uncertain system conditions, where the latter only considers wind uncertainty. Numerical results reflected that the consequences of theoretical problems of the traditional energy-block scheduling approach. The ramp-based scheduling approach outperformed the traditional energy-block approach due to an adequate system representation; hence to efficiently deal with uncertainty, it is imperative to adequately deal with certainty. Furthermore,

numerical results showed that a deterministic formulation using this adequate system representation can outperform a stochastic formulation that uses an "inadequate" representation. In addition, the performance of the deterministic ramp-based scheduling approach was further improved by dealing with uncertainty under stochastic and robust paradigms.

4. Conclusions, Contributions and Future Work

Contents

In this last chapter of the thesis, the main conclusions are drawn, the most relevant contributions are presented, and some guidelines for future work are outlined.

4.1. Conclusions

This thesis proposes computationally efficient models for day-ahead planning in thermal power systems to adequately face the stochastic nature of wind production in the real-time system operation. These models can support ISOs to face the new challenges in day-ahead planning as uncertainty increases dramatically due to the integration of variable and uncertain generation resources, such as wind and solar power.

The following subsections expose the conclusions in three parts: power system representation, UC computational performance, and wind uncertainty management. A

list of specific contributions for each of these parts can be found in section 4.2 in chapter 1.

4.1.1. Power System Representation

Even in the absence of uncertainty, current day-ahead scheduling practices do not exploit the real flexibility of power systems, this increases operation costs and may even endanger the power system security. In this thesis, we have identified four main drawbacks of current energy-block scheduling practices that lead to an unnecessary and inefficient use of system resources (reserves):

1. In markets that are physically cleared on an hourly (or half-hourly) basis, such as those in Europe, generators are penalized if they deviate from their hourly energy schedule. In practice, units operate by trying to match their power profile with the stepwise energy blocks. This stepwise behaviour creates large generation gradients at the beginning and at the end of every trading hour, causing large frequency deviations during these time intervals.
2. In the traditional energy-block UC formulations, generation production levels are taken as stepwise energy blocks and ramp constraints are then applied to the inter-hour changes between these energy blocks. Although it has been proven that the energy delivery obtained from these energy-block formulations may not be feasible, insufficient attention has been paid to this issue in the literature. Consequently, generating units cannot follow their scheduled power profile causing an overuse of other system resources to supply the demand.
3. Traditional UC formulations do not consider the intrinsic startup and shutdown power trajectories of thermal units. Ignoring these trajectories at the scheduling stage inevitably leads to an unnecessary deployment of resources in real-time, which are needed to accommodate the energy produced by the units during their startup and shutdown processes. Although some recent works are aware of this problem, these power trajectories continue being ignored mainly because the resulting model would considerably increase the complexity of the problem and hence its computational intensity.
4. Traditional short-term scheduling approaches seek to supply an energy-block (stepwise) demand profile. One energy profile has infinite possible power profiles; therefore, even though the traditional energy-block scheduling approach could provide a given energy profile, it cannot guarantee that the final profile can be supplied.

To overcome all these drawbacks and to better exploit the power system flexibility, this thesis proposes the ramp-based scheduling approach. Demand and generation are modelled as hourly piecewise-linear functions representing their instantaneous power trajectories. The schedule of generating units output is no longer a stepwise function, but a smoother function that respects all ramp constraints. As a consequence:

- The first two drawbacks are then overcome by scheduling the power generation in a piecewise-linear fashion to follow a forecasted smooth power demand profile.
- The third drawback is tackled by explicitly scheduling the startup and shutdown power trajectories of generating units. That is, these trajectories are included in the ramp-based UC formulation.
- The last drawback is overcome by directly scheduling a power profile, which automatically satisfies the energy profile (since one power profile only has an unique energy profile).

4.1.2. UC Computational Performance

Developing more accurate models would be pointless if the models cannot be solved within rational time[1]. The UC problem is an integer and non-convex problem which is difficult to solve efficiently, especially for large-scale problems. Mixed-integer (linear) programming (MIP) has become a very popular approach to solve UC problems due to significant improvements in MIP solvers over the last two decades. Despite this significant breakthrough in MIP solving, the time required to solve UC problems continues to be a critical limitation that restricts its size and scope.

This thesis identifies and takes into account the key features that affects the computational burden of MIP formulations. These key features are the tightness and the compactness: the tightness of an MIP problem defines the search space that the solver needs to explore in order to find the optimal (integer) solution; the compactness of an MIP problem refers to its size and defines the searching speed that the solver takes to find the optimal solution. Creating tight or compact computationally efficient formulations is a nontrivial task because the obvious formulations are very weak (not tight) or very large, and trying to improve the tightness (compactness) usually means harming the compactness (tightness).

Although much work has been done in developing tight generic constraints, especially to improve MIP solvers, little has been done in improving the computational burden of UC formulations. This thesis also contributes to improving the performance of MIP-based UC formulations. We provide the convex hulls descriptions for the basic operating constraints (without ramp constraints) of slow- and quick-start units, for both the energy-block and ramp-based scheduling approaches. Using these convex hulls as the core of energy-block or ramp-based UC models lead to simultaneously tight and compact MIP formulations. This simultaneous characteristic reinforces the convergence speed by reducing the search space (tightness) and at the same

[1] As stated in chapter 1, a model is considered to be solved within rational time (or efficiently enough) if it can be solved within the required time using the available computing power. For example, if an UC needs to be carried out every hour, then the UC is required to be solved in much less than an hour.

time by increasing the searching speed (compactness) with which solvers explore that reduced space.

As a consequence, although the proposed ramp-based UC model contains more detailed features than a traditional energy-block UC model, it solves significantly faster, because it is based on tight and compact MIP formulations.

4.1.3. Wind Uncertainty Management

Introducing uncertainty management to a given UC model inevitably increases its computational burden. There are three main paradigms to deal with wind uncertainty in UC:

1. The deterministic paradigm, based on reserve levels, is the most common practice in the power industry nowadays, because it is simple and presents a low computational burden. However, it is one of the least robust paradigms and it usually needs an over-dimension of reserve requirements to improve its robustness, this over-dimension increases operating costs. Furthermore, since a deterministic UC only considers one expected deterministic condition, even with enough reserve levels, the power system may not be able to deploy the reserves if the real-time condition deviates significantly from the expected value.
2. The stochastic paradigm overcomes the disadvantages of the deterministic paradigm. Unfortunately, there is a "price to pay" for this. The stochastic paradigm presents some practical limitations: 1) it may be difficult to obtain an accurate probability distribution of the uncertainty; and 2) a large number of scenarios is required to obtain robust solutions, which results in a computationally intensive problem (often intractable). Therefore, many simplifications are usually employed to make the problem tractable, e.g., fewer scenarios are considered and many crucial constraints (e.g., network constraints) are usually neglected.
3. The robust optimization paradigm partly overcomes these disadvantages 1) by requiring moderate information about the underlying uncertainty, such as the mean and the range of the uncertain data; and 2) by immunizing the solution against all realizations of the data within the uncertainty range. However, this paradigm may be too conservative, since the objective function is to minimize the worst-case cost scenario, which may be fictitious and never be realized in practice. Although a robust UC may not be as computationally intensive as a stochastic one, it requires solving an MIP problem together with a bilinear problem. This is considerably more complex to solve than a pure MIP, requiring ad-hoc solving strategies, and only local optimum is guaranteed.

Although the main objective of this thesis is wind uncertainty management in UC models, we first focused on dealing adequately with certainty (power system representation) and the UC computational performance. These two aspects are in conflict

and improving one usually means harming the other. By putting together improvements in the previous two aspects, this thesis contributes to a better management of wind uncertainty in UC. Therefore, as a natural consequence, if compared with a traditional energy-block UC model under the stochastic (deterministic) paradigm, a stochastic (deterministic) ramp-based UC model 1) leads to more economic operation, due to a better and more detailed system representation, while 2) being solved significantly faster, because the core of the model is built upon simultaneously tight and compact MIP formulations.

This thesis also proposes a methodology to assess the performance of a given UC solution, which helps to perform comparisons between different commitment strategies. We then make a clear difference between the scheduling stage and the evaluation stage, where the commitment decisions obtained from the scheduling stage, are evaluated using a 5-min optimal dispatch simulation. This evaluation stage mimics the actual real-time system operation where generating units are dispatched to supply the demand every instant. To the best of our knowledge, there are previous works that only uses hourly simulation as evaluation procedure. In this thesis, we propose to increase the granularity of the simulation stage up to 5 min in order to mimic the actual real-time system operation (where generating units are dispatched to supply the demand at every instant). Consequently, as shown in the different case studies, this 5-min evaluation stage helped to unveil drawbacks of traditional energy-block UC approaches, which are not possible to be identified by using 1-hour period simulation.

In addition, based on robust optimization insights and taking into account the wind generation flexibility (i.e., curtailment), we propose a network-constrained UC formulation with robust reserve modelling, which main characteristics as listed as follows:

- The model is formulated under the ramp-based scheduling approach and built upon thigh and compact MIP formulations, hence taking complete advantage of putting together the improvements in these two aspects (power system representation and UC computational performance).
- To guarantee that the UC solution is feasible for any realization of the uncertain wind production within the considered uncertainty ranges, the model includes the worst-case wind power scenario provided by the adaptive robust optimization problem. We show that by allowing wind curtailment, the worst-case scenario can be obtained a priori, and thus the robust UC becomes a single-scenario UC. That is, the final proposed model remains as a pure MIP problem.
- To correctly represent wind uncertainty, the model distinguishes between power-capacity and ramp-capability reserve requirements. This is aligned with a current trend of defining new products in electricity markets to increase its flexibility in real-time operation.
- The final UC model remains as a pure MIP problem, which size does not

depend on the uncertainty wind representation. Therefore, overcoming the computational drawbacks of both the robust and stochastic UCs commonly found in the literature.

If compared with the traditional deterministic and stochastic UCs through out-of-sample simulation, the proposed UC significantly decreases operation costs while simultaneously lowering the computational burden. Furthermore, it presents similar optimal solutions when compared to a "perfect" stochastic ramp-based UC (evaluation made through an in-sample simulation).

In summary, before trying to tackle uncertainty, we must be able to deal adequately with certainty. In this way, and at least in the cases analysed in this thesis, we can conclude the following:

1. An adequate deterministic UC can outperform an inadequate stochastic one.
2. An adequate stochastic UC certainly outperforms an inadequate stochastic one.
3. An adequate robust reserve-based UC overcomes the disadvantages of an adequate stochastic UC.

4.2. Scientific Contributions

To summarize, the main contributions of the work presented in this thesis are the following ones, which are classified in three main areas, as shown in Figure 4.1.

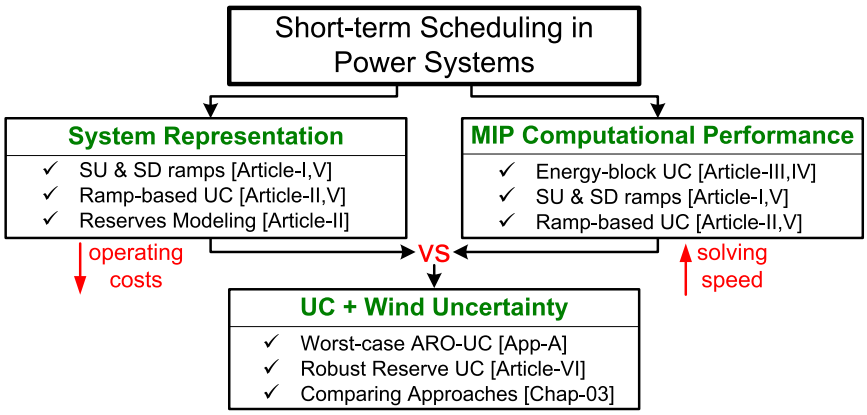

Figure 4.1.: Contributions of this thesis (ARO: Adaptive Robust Optimization; and SU & SD: startup and shutdown)

4.2.1. Power System Representation

1. A model of startup and shutdown power trajectories of generating units (Article I).

2. A ramp-based scheduling approach (Article II), which schedules piecewise power profiles instead of the traditional stepwise energy blocks.
3. Ramp-based models for slow- and quick-start units (Article V), including different operating reserves (online and offline) and their time deployment limits, e.g., 15 min, (section II-B and II-C in Article II).

4.2.2. UC Computational Performance

1. Convex hull of the energy-block scheduling approach for quick-start units (Article IV). To model slow-start units, the startup and shutdown energy trajectories presented in Article V (see equation (10) in section 3.2) can be added to the convex hull in Article IV where the resulting enlarged formulation is still a convex hull. This is because the startup and shutdown energy trajectories in Article V are equalities that add new variables, so they do not add any fractional vertex to the previous formulation (see Lemma 7 in Article IV). Using these convex hulls as the core of any energy-block UC formulation yields simultaneously tight and compact formulations, as presented in Article III.
2. Convex hull of the proposed ramp-based scheduling approach for both slow- and quick-start units (Article V). When used as the core of any UC problem modelling startup and shutdown power trajectories, the proposed model considerably outperforms other analogous formulations (section II-B in Article I). If compared with simpler energy-block UC formulations commonly found in the literature, which do not include these startup and shutdown power trajectories, the proposed model still reduces the computational burden (section II-C in Article II, section 5 in Article V, and section 3.5 in chapter 3).
3. Tight and compact MIP formulation for variable startup costs (section II-A-2 in Article III), according to how long a unit has been offline. This formulation allows a straightforward introduction of different startup power trajectories into UC models (section II-A-5 in Article II, and section II-A-7 in Article I).

4.2.3. Wind uncertainty Management

1. Using the ramp-based approach, we produce deterministic and stochastic UC formulations to deal with wind uncertainty. If compared with traditional energy-block UCs commonly found in the literature, the proposed ramp-based formulations: 1) lower operating costs due to a better system representation; while 2) being solved significantly faster, because the models are built upon tight and compact MIP formulations (Article VI and chapter 3).
2. A linear MIP formulation for the worst-case wind power scenario for adaptive robust UC problems (Appendix A).

3. A robust network-constrained UC formulation based on the ramp-based scheduling approach (Article VI). The model distinguishes between power-capacity and ramp-capability reserve requirements to correctly represent wind uncertainty (Article VI). In addition, by including the worst-case wind scenario (Appendix A), the formulation ensures feasibility for any wind uncertainty realization. If compared with a traditional energy-block stochastic UC, the proposed approach lowers operating costs while being solved significantly faster (chapter 3).
4. To assess the performance of the different UC approaches, this thesis also proposes to make a clear difference between the scheduling and the evaluation stages (Section III-A in Article VI and section 3.2 in chapter 3). The commitment decisions, obtained from the scheduling stage, are evaluated through a 5-min optimal dispatch simulation. To the best of our knowledge, there are works that uses hourly simulation as evaluation stage, but not a more detailed 5-min simulation to mimic the actual real-time system operation (where generating units are dispatched to supply the demand at every instant). Consequently, this evaluation stage helped to unveil drawbacks of traditional energy-block UC approaches, which are not possible to be identified by just using an hourly simulation.

4.3. Future Work

The main work presented in this thesis is a novel scheduling approach to better represent and exploit the power system flexibility. This opens many new questions and possible steps for further research, some of which are listed below:

4.3.1. Power system representation

The proposed ramp-based scheduling approach implies that all technologies that provide (or consume) power must be modelled using piecewise power trajectories, instead of the traditional stepwise energy blocks. This thesis has only modelled thermal units. Although many technologies can be formulated in a similar way, they must be carefully modelled respecting all their technical characteristics. Therefore, all technologies that have been already modelled using the traditional energy-block approach should now be modelled under the ramp-based scheduling approach, making a clear distinction between their power and energy production levels.

Some of the technologies that need to be modelled following the ramp-based scheduling approach, which were not included in this thesis, are: 1) hydropower plants, with and without pumped storage; 2) plug-in electric vehicles; and 3) multi-mode combined-cycle units (which present different operating modes or states with different technical parameters).

There are also some specific set of constraints that may apply to different technologies and should be remodelled under the ramp-scheduling approach, such as dynamic ramping[2].

4.3.2. UC computational performance

The UC problem involves binary variables by definition. Therefore, it will always be challenging to build MIP-based computationally efficient models. Therefore, much research is needed in developing "tight" and, if possible, simultaneously "compact" models so they can be solved within rational time.

The previous section mentioned some of the models that need to be formulated under the ramp-based scheduling approach, these models should be carefully crafted to achieve tight and compact MIP formulations. This can be done with the help of specialized computational software (e.g., PORTA [30]).

Some models, which are already available in the literature, require further improvements, for example:

1. Further tightening the complete UC models under the deterministic, stochastic and robust paradigms. For example, proposing the convex hull or tighter formulations for a single unit taking into account the ramping constraints.
2. Developing compact stochastic UCs without loosing accuracy in the solution. That is, identify or develop dominating constraints that allows removing possible redundant constraints, especially when introducing network constraints.
3. Proposing tight and compact MIP formulations for cumbersome (energy-based) UC problems that involve many binary variables, e.g., dynamic ramping, multi-mode combined-cycle units.

4.3.3. Uncertainty Management

As widely discussed in this thesis, any improvement in either of the two previous fields will naturally yield to UC models that can better deal with uncertainty. On the one hand, by better representing the power system, lower operating costs will be expected when dealing with uncertainty, since the deterministic and completely known events will be optimally scheduled. On the other hand, by improving the computational performance of UC models, stochastic and robust UCs will be solved faster then less simplifications will be needed.

This thesis proposes a linear MIP formulation for the worst-case adaptive-robust UC problem. Although this worst-case scenario ensures feasibility, further research

[2]Dynamic ramping refers to the unit's variable ramp capability, which numerical value depends on the unit's production level.

is needed to obtain deterministic formulations that control the level of conservatism of the adaptive-robust optimal solution, avoiding the bilinear problem and its associated disadvantages.

This thesis focused on dealing with wind uncertainty and introducing of any source of uncertainty that can be curtailed is straightforward, but other sources of uncertainty should be included in the future, such as demand-response, hydro inflows, generators and line outages. Furthermore, possible correlations (e.g. temporal and spacial correlations) should also be considered.

We proposed a deterministic ramp-based approach that includes different types of reserves depending on their time-deployment requirements (e.g., 15 mins, 30 mins). The robust reserve-based approach proposed in this thesis can be further extended to consider these different time-dependent reserves, thus dealing simultaneously with inter- and intra-hourly wind power fluctuations (which have different stochastic characteristics).

4.3.4. Analysis of Case Studies

One of the main objectives of this thesis was to propose new formulations to deal with wind uncertainty. The case studies were carried out for illustrative purposes; they were not based on real power systems, but rather based on benchmark study cases widely used in the UC literature. Much more work can be done in this vein, for example:

- The experiments performed in this thesis can be replicated in real and larger power systems. By using a specific real power systems, we can observe to what extend the proposed formulation can further improve the current operating practices in that system, so conclusions and advice for the specific power systems can be outlined.
- Many studies have been performed for integrating renewable energy sources in power systems, using the traditional energy-block approach. Similar studies can be done using the proposed ramp-based scheduling approach and perhaps different conclusions could be achieved.
- Different commitment strategies can be implemented, e.g., multi-stage or rolling UC, and they can be evaluated using more detailed real-time simulations of power systems. These real-time simulations can be tailored considering specific characteristics of different real power systems.

Other case studies can be carried out focused on markets that are physically cleared on an hourly (or half-hourly) basis, such as those in Europe. These markets are presenting large deterministic frequency deviations. A change of market approach from the energy-block to the ramp-based scheduling may contribute to diminish this problem. Generators should be penalized if they deviate from their power schedule, which satisfies the energy and ramp schedule. Although these markets follow

hourly trading periods, measurements for shorter periods are needed to measure the ramp, and thus being able to penalize deviations from the power schedule. Energy measurements every few minutes (around 5-10) would be enough to monitor the ramp profiles. Actually, these measurements are usually available and needed by the secondary reserve control to work adequately (AGC usually uses continuous measurements every few seconds). Consequently, generators would have the incentive to follow their smooth power profile, thus considerably diminishing these deterministic frequency deviations.

4.3.5. Pricing

The ramp-based scheduling approach proposed in this thesis should be further extended to obtain a complete UC-based market-clearing mechanism. So apart from using this approach to schedule optimal quantities, as done in this thesis, it could be also used to determine the prices that allows the different parties to recover their production costs.

As a possible starting point, one can use the pricing mechanisms implemented by the current UC-based markets (e.g., those in USA). However, the proposed approach provides a power price \$/MW (which is the dimension of the shadow price of the demand-balance constraint) instead of the traditional energy price \$/MWh. This power price needs to be completely understood since it reflects the need of a given energy profile together with a given power profile, hence a unique ramp profile. In comparison, the energy price that results from the traditional energy-block approach just reflects an energy requirement, but not a ramp requirement, then the pure energy pricing cannot provide the right signal to avoid ramping scarcity events.

Furthermore, to introduce price-sensitive demand, a new trading product must be defined since the traditional energy-block bidding from the demand side is not valid under the proposed ramp-scheduling approach. Therefore, extending the ideas of the piecewise-linear formulation to the demand side would require a deeper analysis and further research. One possible solution could be to change from the squared energy blocks to piecewise-linear (or triangular shape) functions, which reflects both the energy and ramping requirements. That is, the demand can be modelled as a generator, so it can be included in the demand power-balance equation as if it were a negative generator, and the energy payment can be added in the objective function having only variable cost (the price assigned to each one of the energy blocks).

Apart from this, many questions have not been (completely) answered about pricing the stochastic paradigm yet, which also apply to the proposed robust reserve-based paradigm. If a stochastic UC is used as a market-clearing mechanism, how should the prices be calculated? Because a stochastic UC produces as part of its solution many shadow prices (e.g., one per energy-balance constraint scenario), instead of the traditional single set of deterministic shadow prices for energy at each location. Perhaps, a multi-price commodity can then be derived, similar to those traditional

joint reserve-energy markets (based on the deterministic paradigm). In those joint markets, the reserve price compensates the units for not exploiting their maximum capacity in the energy market, thus guaranteeing that the units have some reserve available in case it is needed later.

A. The Worst-case Wind Power Scenario for Adaptive Robust Unit Commitment Problems

Contents

This appendix presents a simple deterministic formulation for the unit commitment (UC) problem under the adaptive robust optimization (ARO) paradigm for the case of wind production uncertainty. We show that the worst-case wind power scenario can be obtained before solving the UC. This way the ARO-UC problem becomes a simple single-scenario deterministic UC, avoiding the bilinear optimization problem associated with the second-stage dispatch actions in traditional ARO formulations.

A.1. Obtaining the Worst-case Wind Scenario

The two-stage adaptive robust UC seeks to minimize the worst-case dispatch cost considering any possible realization of wind nodal injection $\boldsymbol{\xi}$ within the deterministic uncertainty set Ξ (or uncertainty range). In the adaptive robust UC, the first-stage commitment decisions and the second-stage dispatch decisions are robust against all uncertain wind nodal injection realizations. Furthermore, the second-stage dispatch solutions are fully adaptable to the uncertainty [8, 10, 12]. Here, we present a compact matrix formulation:

$$\min_{\boldsymbol{x}} \quad \left(\mathbf{b}^\top \boldsymbol{x} + \max_{\boldsymbol{\xi}\in\Xi} \min_{\boldsymbol{p}(\cdot),\boldsymbol{w}(\cdot)} \left(\mathbf{c}^\top \boldsymbol{p}\left(\boldsymbol{\xi}\right) + \mathbf{d}^\top \boldsymbol{w}\left(\boldsymbol{\xi}\right)\right)\right)$$

$$\text{s.t.} \quad \mathbf{F}\boldsymbol{x} \leq \mathbf{f},\ \boldsymbol{x} \text{ is binary} \tag{A.1}$$

$$\mathbf{H}\boldsymbol{p}\left(\boldsymbol{\xi}\right) + \mathbf{J}\boldsymbol{w}\left(\boldsymbol{\xi}\right) \leq \mathbf{h},\ \forall \boldsymbol{\xi} \in \Xi \tag{A.2}$$

$$\mathbf{A}\boldsymbol{x} + \mathbf{B}\boldsymbol{p}\left(\boldsymbol{\xi}\right) + \mathbf{C}\boldsymbol{w}\left(\boldsymbol{\xi}\right) \leq \mathbf{g},\ \forall \boldsymbol{\xi} \in \Xi \tag{A.3}$$

$$\boldsymbol{w}\left(\boldsymbol{\xi}\right) \leq \boldsymbol{\xi},\ \forall \boldsymbol{\xi} \in \Xi \tag{A.4}$$

where $\boldsymbol{x}, \boldsymbol{p}$ and $\boldsymbol{w}$ are variables. The binary variable $\boldsymbol{x}$ is a vector of commitment related decisions (e.g., on/off and startup/shutdown) of each generation unit for each time interval over the planning horizon. The continuous variable $\boldsymbol{p}$ is a vector of each unit dispatch decision for each time interval. The continuous variable $\boldsymbol{w}$ is a vector of each wind production dispatch decision for each node and for each time interval. The parameter $\boldsymbol{\xi}$ is a vector of each uncertain maximum wind nodal injection for each time interval, and the set of uncertainty Ξ is defined by the continuous interval $\xi_{bt} = [\underline{\mathrm{w}}_{bt}, \overline{\mathrm{w}}_{bt}]$ for all $t \in \mathcal{T}$, $b \in \mathcal{B}^{\mathrm{w}}$, where t is the time index in the planning horizon $\mathcal{T}$, b is the index representing buses and $\mathcal{B}^{\mathrm{w}}$ is the set of buses that have uncertain wind power injections.

Constraint (Equation A.1) involves only commitment-related constraints, e.g., minimum up and down. Constraint (Equation A.2) contains dispatch-related constraints, e.g., energy balance (equality can always be written as two opposite inequalities), transmission limit constraints, ramping constraints. Constraint (Equation A.3) couples the commitment and dispatch decisions, e.g., minimum and maximum generation capacity constraints. Finally, (Equation A.14) guarantees that the wind dispatch cannot exceed the available wind power. The reader is referred to [91] for a detailed UC formulation.

Note that only the right hand side of (Equation A.4) have an explicit dependence on the uncertain parameter $\boldsymbol{\xi}$, while the vectors $\mathbf{b}, \mathbf{c}, \mathbf{d}, \mathbf{f}, \mathbf{h}$, and $\mathbf{g}$ together with matrices $\mathbf{A}, \mathbf{B}, \mathbf{C}, \mathbf{F}, \mathbf{H}$ and $\mathbf{J}$ are taken to be deterministically and exactly known. On the other hand, the second-stage variables $\boldsymbol{p}(\boldsymbol{\xi})$ and $\boldsymbol{w}(\boldsymbol{\xi})$ are a function of the uncertain parameter $\boldsymbol{\xi}$, hence fully adaptive to any realization of the uncertainty.

Wind dispatch cost is usually considered to be zero. However, the parameter $\mathbf{d}$ is explicitly included to consider the possibility where this cost is different than zero (in some power systems, this cost can even be negative, e.g. -40 \$/MWh in ERCOT [7]). Defining negative values for parameter $\mathbf{d}$ is equivalent to penalize curtailments in the objective function.

The objective function is to minimize the sum of commitment cost $\mathbf{b}^{\top}\boldsymbol{x}$ and worst-case dispatch cost (max-min expression) $\max_{\boldsymbol{\xi}\in\Xi} \min_{\boldsymbol{y},\boldsymbol{w}} \left(\mathbf{c}^{\top}\boldsymbol{p} + \mathbf{d}^{\top}\boldsymbol{w}\right)$ over the planning horizon. Notice that the max-min form for the worst-case dispatch cost seeks to minimize the economic dispatch costs for a fixed commitment $\boldsymbol{x}$ and wind nodal injection $\boldsymbol{\xi}$, which is then maximized under the uncertainty set Ξ.

A.1.1. The Second Stage Problem

The second stage optimization problem of (Equation A.1)-(Equation A.4) can be reformulated as a single stage optimization problem with adaptability. This corresponds to the single-stage problem once the first-stage variables $\boldsymbol{x}$ have been fixed.

The completely adaptive linear formulation of this second-stage problem is now:

$$\max_{\boldsymbol{\xi}\in\boldsymbol{\Xi}} \min_{\boldsymbol{p}(\cdot),\boldsymbol{w}(\cdot)} \mathbf{c}^{\top}\boldsymbol{p}(\boldsymbol{\xi}) + \mathbf{d}^{\top}\boldsymbol{w}(\boldsymbol{\xi})$$

$$\text{s.t.} \quad \mathbf{H}\boldsymbol{p}(\boldsymbol{\xi}) + \mathbf{J}\boldsymbol{w}(\boldsymbol{\xi}) \leq \mathbf{h},\ \forall \boldsymbol{\xi} \in \boldsymbol{\Xi} \tag{A.5}$$

$$\mathbf{B}\boldsymbol{p}(\boldsymbol{\xi}) + \mathbf{C}\boldsymbol{w}(\boldsymbol{\xi}) \leq \tilde{\mathbf{g}},\ \forall \boldsymbol{\xi} \in \boldsymbol{\Xi} \tag{A.6}$$

$$\boldsymbol{w}(\boldsymbol{\xi}) \leq \boldsymbol{\xi},\ \forall \boldsymbol{\xi} \in \boldsymbol{\Xi} \tag{A.7}$$

where $\tilde{\mathbf{g}} = \mathbf{g} - \mathbf{A}\boldsymbol{x}$.

Note that the uncertainty affecting every one of the constraints (Equation A.7) is independent of each other (i.e., no correlations are considered). As mentioned before, the uncertainty set Ξ is defined by the continuous interval $\xi_{bt} = [\underline{\mathrm{w}}_{bt}, \overline{\mathrm{w}}_{bt}]$ for all $t \in \mathcal{T}$, $b \in \mathcal{B}^{\mathrm{w}}$. Due to this special characteristic of the uncertainty set in LP problems, the adaptive and static (or non-adaptive) robust formulations are equivalent, as proven in [8] and further discussed in [27]. That is, we can obtain the solution of the adaptive robust model by finding the static robust formulation of (Equation A.5)-(Equation A.7).

It can be easily observed that the solution of the adaptive (and static) robust formulation of the LP problem (Equation A.5)-(Equation A.7) can be obtained by solving the following LP reformulation [10]:

$$\min_{\boldsymbol{p}(\cdot),\boldsymbol{w}(\cdot)} \mathbf{c}^{\top}\boldsymbol{p} + \mathbf{d}^{\top}\boldsymbol{w}$$

$$\text{s.t.} \quad \mathbf{H}\boldsymbol{p} + \mathbf{J}\boldsymbol{w} \leq \mathbf{h} \tag{A.8}$$

$$\mathbf{B}\boldsymbol{p} + \mathbf{C}\boldsymbol{w} \leq \tilde{\mathbf{g}} \tag{A.9}$$

$$\boldsymbol{w} \leq \underline{\mathbf{w}} \tag{A.10}$$

notice that (Equation A.10) only includes the lowest bound of the uncertainty set.

To the best of our knowledge, all the ARO UCs models introducing wind uncertainty in the formulation consider (Equation A.4) and (Equation A.7) as equalities. Therefore, wind production is not allowed to have any flexibility because modelling (Equation A.4) and (Equation A.7) as equalities impose that $\boldsymbol{w}$ takes a fixed wind realization. However, wind has some flexibility because it can be curtailed. Therefore, what is uncertain is not the wind production range but rather the upper bound of the possible wind dispatch. Furthermore, if (Equation A.4) and (Equation A.7) are modelled as equalities, the second-stage adaptive problem requires solving a bilinear problem which further complicate the MIP problem [12, 151].

A.1.2. Adaptive Robust Reformulation

The adaptive robust problem (Equation A.1)-(Equation A.4) can be easily reformulated by replacing the max-min second-stage problem by its LP equivalent (Equation A.8)-

(Equation A.10):

$$\begin{aligned} \min_{\boldsymbol{x},\boldsymbol{p},\boldsymbol{w}} \quad & \mathbf{b}^\top \boldsymbol{x} + \mathbf{c}^\top \boldsymbol{p} + \mathbf{d}^\top \boldsymbol{w} \\ \text{s.t.} \quad & \mathbf{F}\boldsymbol{x} \leq \mathbf{f},\ \boldsymbol{x} \text{ is binary} && \text{(A.11)} \\ & \mathbf{H}\boldsymbol{p} + \mathbf{J}\boldsymbol{w} \leq \mathbf{h} && \text{(A.12)} \\ & \mathbf{A}\boldsymbol{x} + \mathbf{B}\boldsymbol{p} + \mathbf{C}\boldsymbol{w} \leq \mathbf{g} && \text{(A.13)} \\ & \boldsymbol{w} \leq \underline{\mathbf{w}} && \text{(A.14)} \end{aligned}$$

Therefore, a two-stage ARO MIP problem presents the same solution as a static robust problem if 1) the uncertainty affecting every one of the constraints is independent of each other, and 2) the second-stage (adaptive) variables are all continuous, i.e., the integer variables only appear as first-stage (non-adjustable) decision variables [11].

It is important to highlight that this is a deterministic formulation where the only scenario that is needed to solve the ARO UC problem is the lowest expected bound of wind $\underline{\mathbf{w}}$ within the uncertainty set Ξ. If this formulation has a feasible optimal solution $\boldsymbol{w}^*$ then it guarantees that all other possible wind realizations within the uncertainty set are feasible. That is, all scenarios can become $\boldsymbol{w}^*$ by curtailment. Consequently, all scenarios can be dispatched and, in the worst case, the maximum quantity of wind that can be dispatched for any scenario would be $\mathbf{w}^*$.

In short, $\underline{\mathbf{w}}$ is the worst-case scenario for the ARO UC problem, which ensures feasibility, but it may be too conservative because it does not guarantee that wind scenarios above $\underline{\mathbf{w}}$ can be dispatched.

A.2. Illustrative Example

Not allowing wind curtailment in the ARO UC formulation leads to misleading solutions. To illustrate this, consider the following example for an one-period ARO UC problem, where a first-stage (binary) commitment decision needs to be taken (this integer decision only appears in the first-stage). We compare two ARO UC formulations: 1) the traditional ARO-UC, presented in [12, 151], which does not allow curtailment, and 2) the ARO UC formulation that allows curtailment (Equation A.1)-(Equation A.4). They are labelled as NotCurt. and WithCurt., respectively.

A fixed demand of 45 MWh needs to be supplied by one thermal and one wind generating units. The thermal unit has 20 and 40 MW as min and max generation capacity, respectively. The wind production is within the uncertainty range $[40, 70]$ MWh. To provide the demand, it is necessary to maintain an energy balance. Figure A.1 shows the demand-balance deviations (shortage/surplus) for every value of wind within its uncertainty range. Notice that for a given value of wind, the deviations are always lower if the thermal unit is offline. Following the NotCurt

ARO approach, where these unbalances are highly penalized [12, 151], the objective is to minimize the maximum penalization (the worst-case scenario). Consequently, from Figure A.1, the thermal unit will always be offline for this example. Therefore, following the NotCurt. formulation, there will always be non-suply energy if the wind production is bellow 45 MWh, which would not be acceptable in the electricity sector.

Now, let us study the case taking into account a budget of uncertainty $\Delta \in [0, 1]$ [12]. When $\Delta = 0$ the wind production corresponds to the nominal deterministic case, 55 MWh, which is usually the mean value of the uncertainty set. As Δ increases, the size of the uncertainty set enlarges. Notice that since ARO optimizes the worst-case scenario, the solution is then always on the solid line shown in Figure A.1. That is, the solution will always be to have the unit offline, despite the value of Δ. The optimal minimum worst-case demand-balance deviation is 10 MWh when $\Delta = 0$ and linearly increases to 25 MWh when $\Delta = 1$. In short, the NotCurt ARO approach cannot find a satisfactory solution for this example even if we consider a budget of uncertainty.

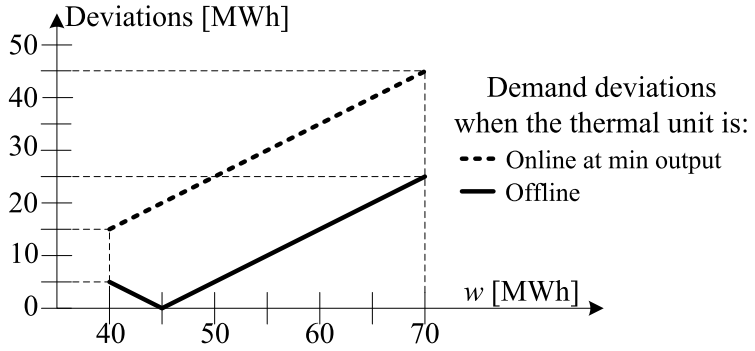

Figure A.1.: Demand balance deviations in function of expected wind production.

However, if we consider that wind production can be curtailed, it is easy to see that the optimal and satisfactory solution for this example is that the thermal unit produces at its minimum output 20 MWh and the wind production provides 25 MWh, thus matching the demand always. The remaining possible wind production would be spilled, thus always guaranteeing the energy supply despite any possible wind uncertainty realization. In fact, this is the solution that would be achieved by the WithCurt ARO formulation.

B. Deterministic Network-Constrained UC Formulations

Contents

This appendix presents the basic set of constraints for the proposed UC formulations under the traditional-energy-block and the proposed-ramp-based scheduling approaches.

Here, we present the set of constraints for quick-start units (which can startup within one hour) and single-startup costs. The proposed formulations also take into account slow-start units and variable startup costs, which depend on how long the unit have been offline. The reader is referred to [53, 91, 97, 99, 100] for further details.

B.1. Nomenclature

Upper-case letters are used for denoting parameters and sets. Lower-case letters denote variables and indexes.

Indexes and Sets

$g \in \mathcal{G}$ Generating units, running from 1 to G.

$b \in \mathcal{B}$ Buses, running from 1 to B.

$l \in \mathcal{L}$ Transmission lines, running from 1 to L.

$t \in \mathcal{T}$ Hourly periods, running from 1 to T hours.

System Parameters

D^{E}_{bt} Energy demand on bus b for hour t [MWh].

D^{P}_{bt} Power demand on bus b at the end of hour t [MW].

D^{-}_{t} System requirements for downward reserve for hour t [MW].

D^{+}_{t} System requirements for upward reserve for hour t [MW].

$\overline{F}_{l}$ Power flow limit on transmission line l [MW].

Γ_{lb} Shift factor for line l associated with bus b [p.u.].

Γ^{G}_{lg} Shift factor for line l associated with unit g [p.u.].

W^{E}_{bt} Nominal forecasted wind energy for hour t [MWh].

W^{P}_{bt} Nominal forecasted wind power at end of hour t [MW].

Unit's Parameters

C^{LV}_{g} Linear variable production cost [$/MWh].

C^{NL}_{g} No-load cost [$/h].

C^{SD}_{g} Shutdown cost [$].

C^{SU}_{g} Startup cost [$].

$\overline{P}_{g}$ Maximum power output [MW].

$\underline{P}_{g}$ Minimum power output [MW].

RD_{g} Ramp-down capability [MW/h].

RU_{g} Ramp-up capability [MW/h].

SD_{g} Shutdown ramping capability [MW/h].

SU_{g} Startup ramping capability [MW/h].

TD_{g} Minimum down time [h].

TU_{g} Minimum up time [h].

Decision Variables

w_{bt}^{E}	Wind energy output for hour t [MWh].
w_{bt}^{P}	Wind power output at the end of hour t [MW].
e_{gt}	Energy output above minimum output for hour t [MWh].
$\widehat{e}_{gt}$	Total energy output at the end of hour t, including startup and shutdown trajectories [MWh].
p_{gt}	Power output above minimum output at the end of hour t [MW].
$\widehat{p}_{gt}$	Total power output at the end of hour t, including startup and shutdown trajectories [MW].
r_{gt}^{-}	Down capacity reserve [MW].
r_{gt}^{+}	Up capacity reserve [MW].
u_{gt}	Binary variable which is equal to 1 if the unit is producing above minimum output and 0 otherwise.
v_{gt}	Binary variable which takes the value of 1 if the unit starts up and 0 otherwise.
z_{gt}	Binary variable which takes the value of 1 if the unit shuts down and 0 otherwise.

B.2. Traditional Energy-block UC

In the traditional energy-block UC, energy is considered to be the direct output of generating units, as shown in Figure B.1.

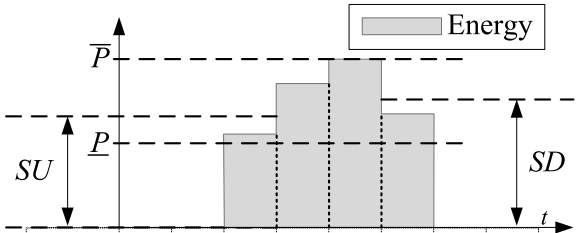

u_t	0	0	1	1	1	1	0	0
v_t	0	0	1	0	0	0	0	0
z_t	0	0	0	0	0	0	1	0

Figure B.1.: Unit's operation under the traditional energy-block scheduling approach.

The UC seeks to minimize all production costs:

$$\min \sum_{g\in\mathcal{G}}\sum_{t\in\mathcal{T}}\left[C_g^{\mathrm{LV}}\widehat{e}_{gt} + C_g^{\mathrm{NL}}u_{gt} + C_g^{\mathrm{SU}}v_{gt} + C_g^{\mathrm{SD}}z_{gt}\right] \tag{B.1}$$

B.2.1. System-wide Constraints

Energy demand balance for hour t and reserves requirements are guaranteed as follows:

$$\sum_{g\in\mathcal{G}} \widehat{e}_{gt} = \sum_{b\in\mathcal{B}} \left(D^{\mathrm{E}}_{bt} - w^{\mathrm{E}}_{bt}\right) \quad \forall t \tag{B.2}$$

$$\sum_{g\in\mathcal{G}} r^{+}_{gt} \geq D^{+}_{t} \quad \forall t \tag{B.3}$$

$$\sum_{g\in\mathcal{G}} r^{-}_{gt} \geq D^{-}_{t} \quad \forall t \tag{B.4}$$

and power-flow transmission limits are ensured with:

$$-\overline{F}_{l} \leq \sum_{g\in\mathcal{G}} \Gamma^{\mathrm{G}}_{lg}\widehat{e}_{gt} + \sum_{b\in\mathcal{B}} \Gamma_{lb}\left(w^{\mathrm{E}}_{bt} - D^{\mathrm{E}}_{bt}\right) \leq \overline{F}_{l} \quad \forall l,t \tag{B.5}$$

B.2.2. Individual Unit Constraints

The commitment, startup/shutdown logic and the minimum up/down times are guaranteed with:

$$u_{gt} - u_{g,t-1} = v_{gt} - z_{gt} \quad \forall g,t \tag{B.6}$$

$$\sum_{i=t-TU_g+1}^{t} v_{gi} \leq u_{gt} \quad \forall g, t\in[TU_g, T] \tag{B.7}$$

$$\sum_{i=t-TD_g+1}^{t} z_{gi} \leq 1 - u_{gt} \quad \forall g, t\in[TD_g, T] \tag{B.8}$$

Power production and reserves must be within the power capacity limits:

$$\begin{aligned} e_{gt} + r^{+}_{gt} \leq{}& \left(\overline{P}_{g} - \underline{P}_{g}\right) u_{gt} - \left(\overline{P}_{g} - SD_{g}\right) z_{g,t+1} \\ & - \max\left(SD_{g} - SU_{g}, 0\right) v_{g,t} \quad \forall g\in\mathcal{G}^{1}, t \end{aligned} \tag{B.9}$$

$$\begin{aligned} e_{gt} + r^{+}_{gt} \leq{}& \left(\overline{P}_{g} - \underline{P}_{g}\right) u_{gt} - \left(\overline{P}_{g} - SU_{g}\right) v_{gt} \\ & - \max\left(SU_{g} - SD_{g}, 0\right) z_{g,t+1} \quad \forall g\in\mathcal{G}^{1}, t \end{aligned} \tag{B.10}$$

$$\begin{aligned} e_{gt} + r^{+}_{gt} \leq{}& \left(\overline{P}_{g} - \underline{P}_{g}\right) u_{gt} - \left(\overline{P}_{g} - SU_{g}\right) v_{gt} \\ & - \left(\overline{P}_{g} - SD_{g}\right) z_{g,t+1} \quad \forall g\notin\mathcal{G}^{1}, t \end{aligned} \tag{B.11}$$

$$e_{gt} - r^{-}_{gt} \geq 0 \tag{B.12}$$

where $\mathcal{G}^{1}$ is defined as the units in $\mathcal{G}$ with $TU_{g}=1$.

Ramping-capability limits are ensured with:

$$\left(e_{gt} + r^{+}_{gt}\right) - e_{g,t-1} \leq RU_g \quad \forall g, t \tag{B.13}$$

$$-\left(e_{gt} - r^{-}_{gt}\right) + e_{g,t-1} \leq RD_g \quad \forall g, t \tag{B.14}$$

The total energy production for thermal units and wind are obtained as follows:

$$\widehat{e}_{gt} = \underline{P}_g u_{gt} + e_{gt} \quad \forall g, t \tag{B.15}$$

$$w^{\mathrm{E}}_{bt} \leq W^{\mathrm{E}}_{bt} \quad \forall b, t \tag{B.16}$$

Finally, non-negative constraints for decision variables:

$$e_{gt}, r^{+}_{gt}, r^{-}_{gt} \geq 0 \quad \forall g, t \tag{B.17}$$

$$w^{\mathrm{E}}_{bt} \geq 0 \quad \forall b, t \tag{B.18}$$

It is important to highlight that the set of constraints (Equation B.6)–(Equation B.12) is the tightest possible representation (convex hull) for a unit operation under the energy-block scheduling approach, see [53].

B.3. Ramp-Based UC

The proposed ramp-based UC draws a clear distinction between power and energy, where power is the direct output of generating units and the energy is then obtained from the power profile, as shown in Figure B.1.

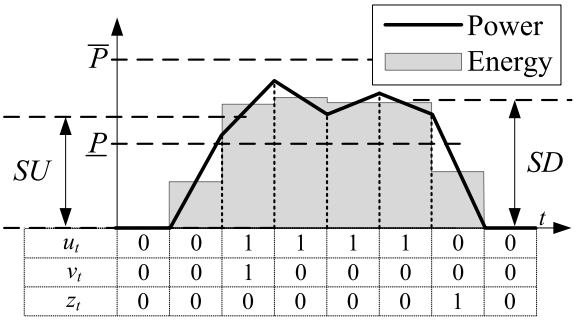

Figure B.2.: Unit's operation under the traditional ramp-based scheduling approach.

The UC seeks to minimize all production costs:

$$\min \sum_{g \in \mathcal{G}} \sum_{t \in \mathcal{T}} \left[C^{\mathrm{LV}}_g \widehat{e}_{gt} + C^{\mathrm{NL}}_g u_{gt} + C^{\mathrm{SU}'}_g v_{gt} + C^{\mathrm{SD}'}_g z_{gt} \right] \tag{B.19}$$

Note that the no-load cost (C_g^{NL}) in (Equation B.19) ignores the startup and shutdown periods, see Figure B.2. This is because the C_g^{NL} only multiplies the commitment during the up state u_{gt}. In order to take into account the no-load cost during the startup and shutdown periods, $C^{\mathrm{SU}'}$ and $C^{\mathrm{SD}'}$ are introduced in (Equation B.19) and defined as:

$$C^{\mathrm{SU}'} = C^{\mathrm{SU}} + C^{\mathrm{NL}} \tag{B.19a}$$
$$C^{\mathrm{SD}'} = C^{\mathrm{SD}} + C^{\mathrm{NL}} \tag{B.19b}$$

B.3.1. System-wide Constraints

Power demand balance at the end of hour t and reserves requirements are guaranteed as follows:

$$\sum_{g\in\mathcal{G}} \widehat{p}_{gt} = \sum_{b\in\mathcal{B}} \left(D_{bt}^{\mathrm{P}} - w_{bt}^{\mathrm{P}}\right) \quad \forall t \tag{B.20}$$
$$\sum_{g\in\mathcal{G}} r_{gt}^{+} \geq D_t^{+} \quad \forall t \tag{B.21}$$
$$\sum_{g\in\mathcal{G}} r_{gt}^{-} \geq D_t^{-} \quad \forall t \tag{B.22}$$

where (Equation B.20) is a power balance at the end of hour t. Be aware that the energy balance for the whole hour is automatically achieved by satisfying the power demand at the beginning and end of each hour, and by considering a piecewise-linear power profile for demand and generation [99].

Power-flow transmission limits are ensured with:

$$-\overline{F}_l \leq \sum_{g\in\mathcal{G}} \Gamma_{lg}^{\mathrm{G}} \widehat{p}_{gt} + \sum_{b\in\mathcal{B}} \Gamma_{lb} \left(w_{bt}^{\mathrm{P}} - D_{bt}^{\mathrm{P}}\right) \leq \overline{F}_l \quad \forall l, t \tag{B.23}$$

B.3.2. Individual Unit Constraints

The commitment, startup/shutdown logic and the minimum up/down times are guaranteed with:

$$u_{gt} - u_{g,t-1} = v_{gt} - z_{gt} \quad \forall g, t \tag{B.24}$$
$$\sum_{i=t-TU_g+1}^{t} v_{gi} \leq u_{gt} \quad \forall g, t \in [TU_g, T] \tag{B.25}$$
$$\sum_{i=t-TD_g+1}^{t} z_{gi} \leq 1 - u_{gt} \quad \forall g, t \in [TD_g, T] \tag{B.26}$$

Power production and reserves must be within the power capacity limits:

$$p_{gt} + r_{gt} \leq \left(\overline{P}_g - \underline{P}_g\right) u_{gt} - \left(\overline{P}_g - SD_g\right) z_{g,t+1} + \left(SU_g - \underline{P}_g\right) v_{g,t+1} \quad \forall g, t \tag{B.27}$$

$$p_{gt} - r^-_{gt} \geq 0 \quad \forall g, t \tag{B.28}$$

Ramping-capability limits are ensured with:

$$\left(p_{gt} + r^+_{gt}\right) - p_{g,t-1} \leq RU_g \quad \forall g, t \tag{B.29}$$

$$-\left(p_{gt} - r^-_{gt}\right) + p_{g,t-1} \leq RD_g \quad \forall g, t \tag{B.30}$$

The total power and energy production for thermal units are obtained as follows:

$$\widehat{p}_{gt} = \underline{P}_g \left(u_{gt} + v_{g,t+1}\right) + p_{gt} \quad \forall g, t \tag{B.31}$$

$$\widehat{e}_{gt} = \frac{\widehat{p}_{g,t-1} + \widehat{p}_{gt}}{2} \quad \forall g, t \tag{B.32}$$

$$w^{\mathrm{P}}_{bt} \leq W^{\mathrm{P}}_{bt} \quad \forall b, t \tag{B.33}$$

$$w^{\mathrm{E}}_{bt} = \frac{w^{\mathrm{P}}_{bt} + w^{\mathrm{P}}_{b,t-1}}{2} \quad \forall b, t \tag{B.34}$$

Finally, non-negative constraints for decision variables:

$$p_{gt}, r^+_{gt}, r^-_{gt} \geq 0 \quad \forall g, t \tag{B.35}$$

$$w^{\mathrm{P}}_{bt} \geq 0 \quad \forall b, t \tag{B.36}$$

It is interesting to note that even though $SU_g, SD_g \geq \underline{P}_g$ (by definition), the resulting energy from (Equation B.32) from the ramp-based UC may take values below $\underline{P}_g$ during the startup and shutdown processes, see Figure B.2, unlike the traditional energy-block UC.

It is important to highlight that the set of constraints (Equation B.24)–(Equation B.28) together with (Equation B.31) and (Equation B.32) is the tightest possible representation (convex hull) for a unit operation under the ramp-based scheduling approach, see [97].

C. IEEE-118 Bus System Data

This appendix provides the data of the IEEE-118 bus system used in this thesis.

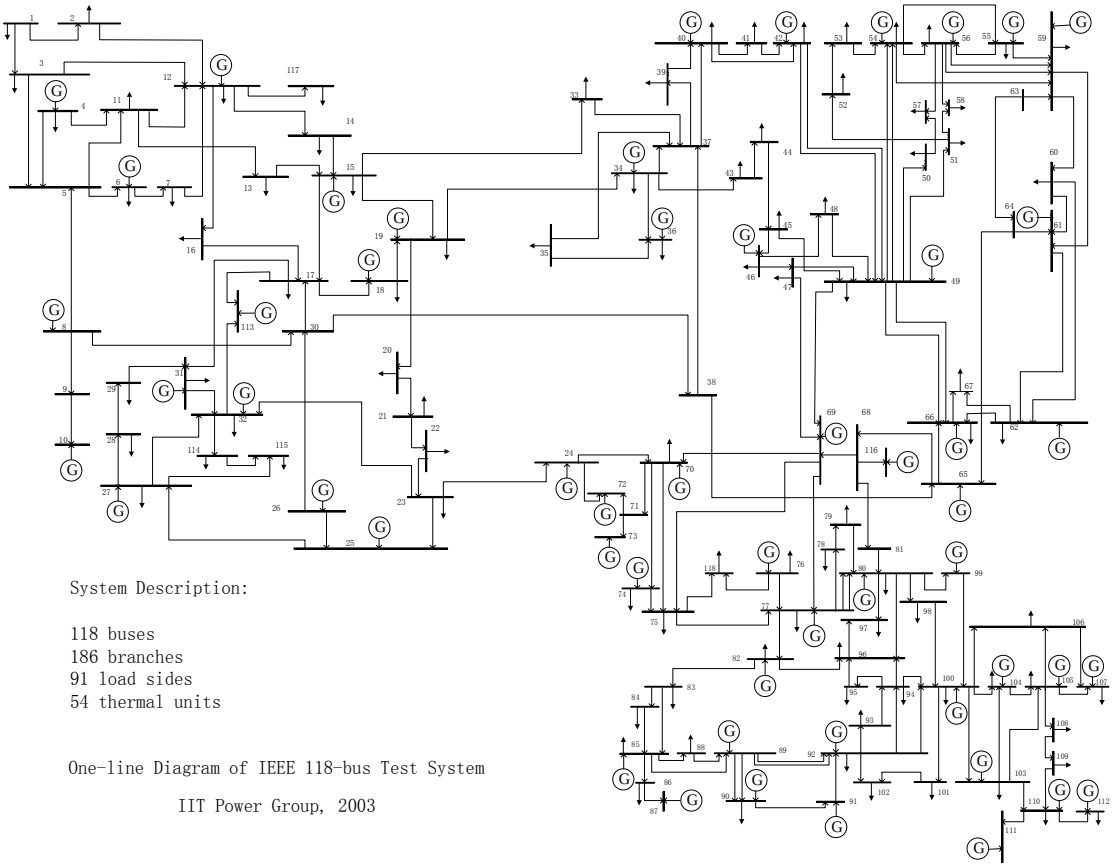

Figure C.1.: IEEE-118 bus system

The IEEE-118 bus system is shown in Figure C.1. The power system data are based on that in [121] and it was adapted to consider startup and shutdown power trajectories. This system has been widely used in UC studies, for example [4, 50, 65–67, 72–74, 76, 77, 121, 123, 134, 135, 137, 145–147, 151, 152]. In this thesis, we used the modified IEEE 118-bus test system in Article VI and chapter 3 for a time span of 24 hours.

The IEEE-118 bus system has 118 buses; 186 transmission lines; 54 thermal units; 91 loads, with average and maximum levels of 3991 MW and 5592 MW, respectively; and three wind units, with aggregated average and maximum production of 867 MW and 1333 MW, respectively, for the nominal wind case (see Figure 3.3).

Table C.1 and Table C.2 provide the generator data. Table C.3 and Table C.4 show the transmission network technical data. The load distribution profile and total system-wide power demand is given in Table C.6 and Table C.5, respectively. The 20 scenarios for wind power injection in three different buses are given in Table C.6, Table C.7 and Table C.8. Notice that the demand and wind data are given as power profiles (in MW) rather than the commonly used energy profiles (in MWh). However, obtaining the energy profiles is straightforward, for example, the energy profile for the demand is obtained as $D^{\mathrm{E}} = \frac{D_t^{\mathrm{P}} + D_{t-1}^{\mathrm{P}}}{2}$.

The symbols that appear in the header of Table C.1 to Table C.4 are defined as follows (in the same order as they appear in the tables):

Generator Data:

$\overline{P}$	Maximum power output [MW].
$\underline{P}$	Minimum power output [MW].
P_0	Initial power output [MW].
State_0	Initial state: hours that the unit has been online (+) or offline (-) prior to the first period of the time span.
RU	Ramp-up capability [MW/h].
RD	Ramp-down capability [MW/h].
C^{NL}	No-load cost [$/h].
C^{LV}	Linear variable production cost [$/MWh].
TU	Minimum up time [h].
TD	Minimum down time [h].
C^{SD}	Shutdown cost [$].
SD^{D}	Duration of the shutdown process [h].
C_h^{SU}	Hot-startup cost [$].
SU_h^{D}	Duration of the hot-startup process[h].
C_c^{SU}	Cold-startup cost [$].
SU_c^{D}	Duration of the cold-startup process[h].

T_c^{SU}	Time defining the interval limit of the cold startup segment [h]. That is, the unit has a hot startup if it has been offline for less than T_c^{SU} hours, and it has a cold startup if it has been offline for more than or equal to T_c^{SU} hours.
SU	Shutdown ramping capability [MW/h].
SD	Startup ramping capability [MW/h].

Network Data:

R	Resistance of transmission line (per unit).
X	Reactance of transmission line (per unit).
$\overline{F}$	Flow limit on transmission line [MW].

	Bus	$\overline{P}$ [MW]	$\underline{P}$ [MW]	P_0 [MW]	State$_0$ [h]	RU [MW/h]	RD [MW/h]	C^{NL} [$/h]	C^{LV} [$/MWh]	TU [h]	TD [h]	C^{SD} [$]	SD^{D} [h]	C_h^{SU} [$]	SU_h^{D} [h]	C_e^{SU} [$]	SU_e^{D} [h]	T_e^{SU} [h]	SU [MW/h]	SD [MW/h]
gen1	4	30	5	30	1	25	25	26.55	27.08	1	1	0	1	40	1	120	2	3	5	5
gen2	6	30	5	30	1	25	25	25.85	31.30	1	1	0	1	40	1	120	2	3	5	5
gen3	8	30	5	30	1	25	25	26.10	27.90	1	1	0	1	40	1	120	2	3	5	5
gen4	10	300	150	0	-8	60	60	8.05	12.06	8	8	0	2	440	4	1320	7	13	150	150
gen5	12	300	100	300	8	60	60	7.82	11.04	8	8	0	2	110	4	330	7	13	100	100
gen6	15	30	10	30	1	25	25	28.87	28.51	1	1	0	1	40	1	120	2	3	10	10
gen7	18	100	25	0	-5	20	20	12.26	14.64	5	5	0	1	50	2	150	4	9	25	25
gen8	19	30	5	30	1	25	25	28.51	30.45	1	1	0	1	40	1	120	2	3	5	5
gen9	24	30	5	30	1	25	25	26.38	26.44	1	1	0	1	40	1	120	2	3	5	5
gen10	25	300	100	300	8	60	60	7.12	11.72	8	8	0	2	100	4	300	7	13	100	100
gen11	26	350	100	300	8	70	70	35.59	10.11	8	8	0	2	100	4	300	7	13	100	100
gen12	27	30	8	0	-1	25	25	29.49	29.17	1	1	0	1	40	1	120	2	3	8	8
gen13	31	30	8	0	-1	25	25	27.62	30.89	1	1	0	1	40	1	120	2	3	8	8
gen14	32	100	25	0	-5	20	20	11.96	14.13	5	5	0	1	50	2	150	4	9	25	25
gen15	34	30	8	30	1	25	25	27.95	29.76	1	1	0	1	40	1	120	2	3	8	8
gen16	36	100	25	0	-5	20	20	11.61	16.76	5	5	0	1	50	2	150	4	9	25	25
gen17	40	30	8	0	-1	25	25	29.17	26.76	1	1	0	1	40	1	120	2	3	8	8
gen18	42	30	8	0	-1	25	25	27.25	28.10	1	1	0	1	40	1	120	2	3	8	8
gen19	46	100	25	0	-5	20	20	10.64	14.85	5	5	0	1	59	2	177	4	9	25	25
gen20	49	250	50	0	-8	50	50	30.48	10.83	8	8	0	2	100	4	300	7	13	50	50
gen21	54	250	50	50	8	50	50	30.74	10.60	8	8	0	2	100	4	300	7	13	50	50
gen22	55	100	25	0	-5	20	20	12.59	15.37	5	5	0	1	50	2	150	4	9	25	25
gen23	56	100	25	0	-5	20	20	11.87	15.19	5	5	0	1	50	2	150	4	9	25	25
gen24	59	200	50	0	-8	40	40	43.01	11.31	8	8	0	2	100	4	300	7	13	50	50
gen25	61	200	50	0	-8	40	40	39.49	13.01	8	8	0	2	100	4	300	7	13	50	50
gen26	62	100	25	0	-5	20	20	12.12	15.34	5	5	0	1	50	2	150	4	9	25	25
gen27	65	420	100	100	10	84	84	72.78	7.93	10	10	0	2	250	5	750	8	15	100	100

Table C.1.: Generator data (continued on next page)

	Bus	$\overline{P}$ [MW]	$\underline{P}$ [MW]	P_0 [MW]	State$_0$ [h]	RU [MW/h]	RD [MW/h]	C^{NL} [$/h]	C^{LV} [$/MWh]	TU [h]	TD [h]	C^{SD} [$]	SD^{D} [h]	C_h^{SU} [$]	SU_h^{D} [h]	C_c^{SU} [$]	SU_c^{D} [h]	T_c^{SU} [h]	SU [MW/h]	SD [MW/h]
gen28	66	420	100	100	10	84	84	69.33	8.28	10	10	0	2	250	5	750	8	15	100	100
gen29	69	300	80	0	-8	60	60	7.91	10.99	8	8	0	2	100	4	300	7	13	80	80
gen30	70	80	30	80	4	66.7	66.7	66.83	17.83	4	4	0	1	45	2	135	4	7	30	30
gen31	72	30	10	0	-1	25	25	29.35	29.59	1	1	0	1	40	1	120	2	3	10	10
gen32	73	30	5	0	-1	25	25	27.59	30.83	1	1	0	1	40	1	120	2	3	5	5
gen33	74	20	5	0	-1	16.7	16.7	15.75	43.75	1	1	0	1	30	1	90	2	3	5	5
gen34	76	100	25	25	5	20	20	11.94	15.09	5	5	0	1	50	2	150	4	9	25	25
gen35	77	100	25	25	5	20	20	11.93	15.18	5	5	0	1	50	2	150	4	9	25	25
gen36	80	300	150	0	-8	60	60	8.22	12.28	8	8	0	2	440	4	1320	7	13	150	150
gen37	82	100	25	25	5	20	20	11.73	14.73	5	5	0	1	50	2	150	4	9	25	25
gen38	85	30	10	0	-1	25	25	29.17	29.44	1	1	0	1	40	1	120	2	3	10	10
gen39	87	300	100	100	8	60	60	35.29	10.17	8	8	0	2	440	4	1320	7	13	100	100
gen40	89	200	50	50	8	40	40	7.73	11.14	8	8	0	2	400	4	1200	7	13	50	50
gen41	90	20	8	0	-1	16.7	16.7	15.22	44.87	1	1	0	1	30	1	90	2	3	8	8
gen42	91	50	20	40	1	41.7	41.7	48.05	23.87	1	1	0	1	45	1	135	2	3	20	20
gen43	92	300	100	100	8	60	60	7.28	12.65	8	8	0	2	100	4	300	7	13	100	100
gen44	99	300	100	100	8	60	60	7.92	11.17	8	8	0	2	100	4	300	7	13	100	100
gen45	100	300	100	100	8	60	60	7.41	12.10	8	8	0	2	110	4	330	7	13	100	100
gen46	103	20	8	0	-1	16.7	16.7	16.74	40.36	1	1	0	1	30	1	90	2	3	8	8
gen47	104	100	25	0	-5	20	20	11.24	14.73	5	5	0	1	50	2	150	4	9	25	25
gen48	105	100	25	0	-5	20	20	11.25	15.41	5	5	0	1	50	2	150	4	9	25	25
gen49	107	20	8	0	-1	16.7	16.7	15.77	40.55	1	1	0	1	30	1	90	2	3	8	8
gen50	110	50	25	40	2	41.7	41.7	48.88	25.28	2	2	0	1	45	1	135	2	4	25	25
gen51	111	100	25	0	-5	20	20	11.18	15.01	5	5	0	1	50	2	150	4	9	25	25
gen52	112	100	25	0	-5	20	20	10.93	15.01	5	5	0	1	50	2	150	4	9	25	25
gen53	113	100	25	0	-5	20	20	12.04	16.22	5	5	0	1	50	2	150	4	9	25	25
gen54	116	50	25	50	2	41.7	41.7	50.68	26.73	2	2	0	1	45	1	135	2	4	25	25

Table C.2.: Generator Data

Line	From Bus	To Bus	Circuit ID	R (p.u)	X (p.u.)	$\overline{F}$ [MW]	Line	From Bus	To Bus	Circuit ID	R (p.u)	X (p.u.)	$\overline{F}$ [MW]
1	1	2	1	0.0303	0.0999	175	48	33	37	1	0.0415	0.142	175
2	1	3	1	0.0129	0.0424	175	49	34	36	1	0.00871	0.0268	175
3	4	5	1	0.00176	0.00798	500	50	34	37	1	0.00256	0.0094	500
4	3	5	1	0.0241	0.108	175	51	38	37	1	0	0.0375	500
5	5	6	1	0.0119	0.054	175	52	37	39	1	0.0321	0.106	175
6	6	7	1	0.00459	0.0208	175	53	37	40	1	0.0593	0.168	175
7	8	9	1	0.00244	0.0305	500	54	30	38	1	0.00464	0.054	175
8	8	5	1	0	0.0267	500	55	39	40	1	0.0184	0.0605	175
9	9	10	1	0.00258	0.0322	500	56	40	41	1	0.0145	0.0487	175
10	4	11	1	0.0209	0.0688	175	57	40	42	1	0.0555	0.183	175
11	5	11	1	0.0203	0.0682	175	58	41	42	1	0.041	0.135	175
12	11	12	1	0.00595	0.0196	175	59	43	44	1	0.0608	0.2454	175
13	2	12	1	0.0187	0.0616	175	60	34	43	1	0.0413	0.1681	175
14	3	12	1	0.0484	0.16	175	61	44	45	1	0.0224	0.0901	175
15	7	12	1	0.00862	0.034	175	62	45	46	1	0.04	0.1356	175
16	11	13	1	0.02225	0.0731	175	63	46	47	1	0.038	0.127	175
17	12	14	1	0.0215	0.0707	175	64	46	48	1	0.0601	0.189	175
18	13	15	1	0.0744	0.2444	175	65	47	49	1	0.0191	0.0625	175
19	14	15	1	0.0595	0.195	175	66	42	49	1	0.0715	0.323	175
20	12	16	1	0.0212	0.0834	175	67	42	49	2	0.0715	0.323	175
21	15	17	1	0.0132	0.0437	500	68	45	49	1	0.0684	0.186	175
22	16	17	1	0.0454	0.1801	175	69	48	49	1	0.0179	0.0505	175
23	17	18	1	0.0123	0.0505	175	70	49	50	1	0.0267	0.0752	175
24	18	19	1	0.01119	0.0493	175	71	49	51	1	0.0486	0.137	175
25	19	20	1	0.0252	0.117	175	72	51	52	1	0.0203	0.0588	175
26	15	19	1	0.012	0.0394	175	73	52	53	1	0.0405	0.1635	175
27	20	21	1	0.0183	0.0849	175	74	53	54	1	0.0263	0.122	175
28	21	22	1	0.0209	0.097	175	75	49	54	1	0.073	0.289	175
29	22	23	1	0.0342	0.159	175	76	49	54	2	0.0869	0.291	175
30	23	24	1	0.0135	0.0492	175	77	54	55	1	0.0169	0.0707	175
31	23	25	1	0.0156	0.08	500	78	54	56	1	0.00275	0.00955	175
32	26	25	1	0	0.0382	500	79	55	56	1	0.00488	0.0151	175
33	25	27	1	0.0318	0.163	500	80	56	57	1	0.0343	0.0966	175
34	27	28	1	0.01913	0.0855	175	81	50	57	1	0.0474	0.134	175
35	28	29	1	0.0237	0.0943	175	82	56	58	1	0.0343	0.0966	175
36	30	17	1	0	0.0388	500	83	51	58	1	0.0255	0.0719	175
37	8	30	1	0.00431	0.0504	175	84	54	59	1	0.0503	0.2293	175
38	26	30	1	0.00799	0.086	500	85	56	59	1	0.0825	0.251	175
39	17	31	1	0.0474	0.1563	175	86	56	59	2	0.0803	0.239	175
40	29	31	1	0.0108	0.0331	175	87	55	59	1	0.04739	0.2158	175
41	23	32	1	0.0317	0.1153	140	88	59	60	1	0.0317	0.145	175
42	31	32	1	0.0298	0.0985	175	89	59	61	1	0.0328	0.15	175
43	27	32	1	0.0229	0.0755	175	90	60	61	1	0.00264	0.0135	500
44	15	33	1	0.038	0.1244	175	91	60	62	1	0.0123	0.0561	175
45	19	34	1	0.0752	0.247	175	92	61	62	1	0.00824	0.0376	175
46	35	36	1	0.00224	0.0102	175	93	63	59	1	0	0.0386	500
47	35	37	1	0.011	0.0497	175	94	63	64	1	0.00172	0.02	500

Table C.3.: Transmission line data (continued on next page)

Line	From Bus	To Bus	Circuit ID	R (p.u)	X (p.u.)	$\overline{F}$ [MW]	Line	From Bus	To Bus	Circuit ID	R (p.u)	X (p.u.)	$\overline{F}$ [MW]
95	64	61	1	0	0.0268	500	141	89	92	1	0.0099	0.0505	500
96	38	65	1	0.00901	0.0986	500	142	89	92	2	0.0393	0.1581	500
97	64	65	1	0.00269	0.0302	500	143	91	92	1	0.0387	0.1272	175
98	49	66	1	0.018	0.0919	500	144	92	93	1	0.0258	0.0848	175
99	49	66	2	0.018	0.0919	500	145	92	94	1	0.0481	0.158	175
100	62	66	1	0.0482	0.218	175	146	93	94	1	0.0223	0.0732	175
101	62	67	1	0.0258	0.117	175	147	94	95	1	0.0132	0.0434	175
102	65	66	1	0	0.037	500	148	80	96	1	0.0356	0.182	175
103	66	67	1	0.0224	0.1015	175	149	82	96	1	0.0162	0.053	175
104	65	68	1	0.00138	0.016	500	150	94	96	1	0.0269	0.0869	175
105	47	69	1	0.0844	0.2778	175	151	80	97	1	0.0183	0.0934	175
106	49	69	1	0.0985	0.324	175	152	80	98	1	0.0238	0.108	175
107	68	69	1	0	0.037	500	153	80	99	1	0.0454	0.206	200
108	69	70	1	0.03	0.127	500	154	92	100	1	0.0648	0.295	175
109	24	70	1	0.00221	0.4115	175	155	94	100	1	0.0178	0.058	175
110	70	71	1	0.00882	0.0355	175	156	95	96	1	0.0171	0.0547	175
111	24	72	1	0.0488	0.196	175	157	96	97	1	0.0173	0.0885	175
112	71	72	1	0.0446	0.18	175	158	98	100	1	0.0397	0.179	175
113	71	73	1	0.00866	0.0454	175	159	99	100	1	0.018	0.0813	175
114	70	74	1	0.0401	0.1323	175	160	100	101	1	0.0277	0.1262	175
115	70	75	1	0.0428	0.141	175	161	92	102	1	0.0123	0.0559	175
116	69	75	1	0.0405	0.122	500	162	101	102	1	0.0246	0.112	175
117	74	75	1	0.0123	0.0406	175	163	100	103	1	0.016	0.0525	500
118	76	77	1	0.0444	0.148	175	164	100	104	1	0.0451	0.204	175
119	69	77	1	0.0309	0.101	175	165	103	104	1	0.0466	0.1584	175
120	75	77	1	0.0601	0.1999	175	166	103	105	1	0.0535	0.1625	175
121	77	78	1	0.00376	0.0124	175	167	100	106	1	0.0605	0.229	175
122	78	79	1	0.00546	0.0244	175	168	104	105	1	0.00994	0.0378	175
123	77	80	1	0.017	0.0485	500	169	105	106	1	0.014	0.0547	175
124	77	80	2	0.0294	0.105	500	170	105	107	1	0.053	0.183	175
125	79	80	1	0.0156	0.0704	175	171	105	108	1	0.0261	0.0703	175
126	68	81	1	0.00175	0.0202	500	172	106	107	1	0.053	0.183	175
127	81	80	1	0	0.037	500	173	108	109	1	0.0105	0.0288	175
128	77	82	1	0.0298	0.0853	200	174	103	110	1	0.03906	0.1813	175
129	82	83	1	0.0112	0.03665	200	175	109	110	1	0.0278	0.0762	175
130	83	84	1	0.0625	0.132	175	176	110	111	1	0.022	0.0755	175
131	83	85	1	0.043	0.148	175	177	110	112	1	0.0247	0.064	175
132	84	85	1	0.0302	0.0641	175	178	17	113	1	0.00913	0.0301	175
133	85	86	1	0.035	0.123	500	179	32	113	1	0.0615	0.203	500
134	86	87	1	0.02828	0.2074	500	180	32	114	1	0.0135	0.0612	175
135	85	88	1	0.02	0.102	175	181	27	115	1	0.0164	0.0741	175
136	85	89	1	0.0239	0.173	175	182	114	115	1	0.0023	0.0104	175
137	88	89	1	0.0139	0.0712	500	183	68	116	1	0.00034	0.00405	500
138	89	90	1	0.0518	0.188	500	184	12	117	1	0.0329	0.14	175
139	89	90	2	0.0238	0.0997	500	185	75	118	1	0.0145	0.0481	175
140	90	91	1	0.0254	0.0836	175	186	76	118	1	0.0164	0.0544	175

Table C.4.: Transmission line data

Bus	D [%]	Bus	D [%]
1	1.450280868	57	0.321451245
2	0.568700828	58	0.321451245
3	1.109006796	59	7.420166244
4	0.85318518	60	2.089433094
6	1.478675728	62	2.06264549
7	0.540305968	66	1.044716547
11	1.990586836	67	0.750052906
12	1.336433552	70	1.767981849
13	0.96676462	74	1.821557056
14	0.398063792	75	1.259017377
15	2.559287664	76	1.821557056
16	0.710943004	77	1.63404383
17	0.312879212	78	1.901919868
18	1.706102484	79	1.044716547
19	1.279643832	80	3.48238849
20	0.511911108	82	1.446530603
21	0.398063792	83	0.535752075
22	0.284484352	84	0.294663641
23	0.199031896	85	0.64290249
27	1.76316008	86	0.562539679
28	0.483516248	88	1.285804981
29	0.682548144	90	2.089433094
31	1.222854112	92	1.741194245
32	1.677707624	93	0.321451245
33	0.654153284	94	0.803628113
34	1.677707624	95	1.125079358
35	0.93836976	96	1.017928943
36	0.88158004	97	0.401814057
39	0.723265302	98	0.910778528
40	0.535752075	100	0.991141339
41	0.991141339	101	0.589327283
42	0.991141339	102	0.133938019
43	0.482176868	103	0.616114887
44	0.42860166	104	1.017928943
45	1.419743	105	0.830415717
46	0.750052906	106	1.151866962
47	0.910778528	107	0.750052906
48	0.535752075	108	0.053575208
49	2.330521528	109	0.21430083
50	0.455389264	110	1.044716547
51	0.455389264	112	0.669690094
52	0.482176868	114	0.227426756
53	0.616114887	115	0.625490548
54	3.026999226	117	0.568700828
55	1.687619037	118	0.883990924
56	2.250158717		

Table C.5.: Load distribution profile

	D	Wind Power Scenarios at Bus 36 [MW]																			
	[MW]	sc01	sc02	sc03	sc04	sc05	sc06	sc07	sc08	sc09	sc10	sc11	sc12	sc13	sc14	sc15	sc16	sc17	sc18	sc19	sc20
h00	3466.24	304.79	304.79	304.79	304.79	304.79	304.79	304.79	304.79	304.79	304.79	304.79	304.79	304.79	304.79	304.79	304.79	304.79	304.79	304.79	304.79
h01	3314.40	298.35	287.74	324.89	307.64	328.93	303.61	308.10	291.12	279.94	310.82	296.89	287.01	330.87	326.55	300.81	321.75	313.94	306.22	283.85	286.84
h02	3010.72	286.41	292.37	323.46	310.82	308.08	292.58	310.31	277.03	273.28	293.47	287.24	273.15	307.94	325.72	289.70	293.24	290.30	290.78	291.49	272.86
h03	2403.36	262.36	277.77	306.50	285.49	294.79	266.12	298.57	266.72	257.30	262.40	257.50	237.26	281.61	309.55	264.09	261.70	270.56	270.57	265.66	245.38
h04	1036.80	245.34	241.20	293.76	255.70	238.90	248.20	265.92	264.17	235.98	240.94	224.09	214.84	269.52	277.13	252.47	221.39	274.19	249.82	246.83	211.59
h05	1796.00	241.48	236.80	287.98	236.45	200.39	249.51	246.10	261.67	223.05	248.44	247.95	212.10	262.97	244.87	287.28	197.19	263.32	237.94	251.90	202.33
h06	2555.20	236.17	254.91	278.88	219.18	181.18	250.27	219.76	239.12	187.31	252.19	241.82	218.03	240.38	198.55	303.05	166.28	244.84	231.84	239.32	206.65
h07	3314.40	206.80	218.10	252.93	191.73	123.95	221.63	190.91	201.73	146.78	225.43	207.98	189.60	202.64	161.99	275.32	116.50	211.57	195.07	214.54	173.18
h08	3921.76	189.99	190.00	221.37	183.66	103.61	179.22	189.30	199.14	120.17	234.36	199.34	161.56	196.09	158.00	270.04	82.66	197.83	169.96	179.70	154.81
h09	4225.44	199.06	207.58	201.42	187.53	132.52	161.42	240.12	203.80	128.47	262.30	221.65	171.30	201.08	178.73	268.10	92.00	186.44	171.44	166.14	201.65
h10	4680.96	201.84	208.49	209.30	194.32	130.56	150.84	262.94	197.81	142.68	254.91	202.84	178.11	182.29	185.77	237.62	82.91	180.55	169.77	165.98	215.14
h11	4756.88	200.22	198.57	224.45	186.55	141.36	144.32	264.65	205.93	175.07	262.33	183.94	191.47	180.47	182.11	214.21	95.51	202.32	178.61	151.82	225.17
h12	4377.28	193.86	213.47	243.64	144.02	136.68	143.05	238.39	217.87	207.51	235.65	181.36	197.66	204.82	161.36	217.01	113.64	220.17	185.45	156.75	227.93
h13	4073.60	191.51	232.44	225.23	143.88	156.37	144.96	231.07	235.14	222.84	197.96	158.38	207.90	209.43	170.93	189.88	137.98	231.78	196.06	165.56	236.64
h14	3769.92	183.06	225.40	204.21	172.60	165.06	150.16	206.65	225.38	221.37	166.58	145.44	182.56	198.86	194.41	169.24	143.96	212.15	187.96	186.18	198.14
h15	4680.96	180.04	208.68	204.86	172.43	168.04	160.88	175.39	229.66	233.62	162.45	149.53	143.32	192.05	191.08	182.15	134.54	206.34	184.45	191.49	152.85
h16	4832.80	188.70	210.83	211.61	180.23	194.87	143.03	178.60	213.55	244.61	185.33	171.46	155.41	196.04	192.87	184.33	152.66	190.51	184.92	180.98	170.28
h17	4453.20	172.98	177.32	201.23	153.53	213.26	119.35	170.79	188.99	212.00	190.20	143.27	137.19	210.48	187.53	156.21	164.08	193.53	176.76	124.97	165.20
h18	4756.88	150.41	155.56	181.91	125.41	188.92	96.66	142.76	161.34	172.76	156.77	143.86	151.23	219.45	165.82	144.40	183.72	178.74	157.28	110.77	161.34
h19	5136.48	168.07	191.36	197.27	133.39	209.99	109.56	140.05	184.79	166.90	149.03	163.39	165.58	235.62	165.03	178.79	194.20	190.05	176.21	126.47	169.57
h20	5440.16	209.10	231.40	213.58	173.04	259.66	140.33	169.57	232.88	187.42	168.14	190.94	148.07	273.98	214.84	222.41	204.19	213.05	207.20	157.31	173.01
h21	5592.00	222.74	226.62	248.73	153.03	272.61	147.47	204.92	234.41	186.20	178.77	207.86	133.09	285.32	219.29	237.93	203.41	217.04	213.71	145.63	181.73
h22	4832.80	237.36	221.95	278.94	174.34	259.27	196.58	255.22	261.23	194.83	219.54	246.21	133.21	277.87	238.79	282.54	190.40	237.17	226.45	175.85	182.42
h23	4605.04	273.69	253.21	319.88	233.70	277.89	253.52	302.24	288.87	218.20	288.99	300.59	181.14	328.75	292.24	339.08	229.37	279.71	261.52	229.90	220.57
h24	4225.44	300.66	281.72	339.34	282.23	276.11	265.34	314.75	286.24	243.25	330.21	323.10	252.13	341.56	305.10	350.61	253.27	291.67	278.87	266.57	269.60

Table C.6.: Demand and wind injection (continued on next page)

	Wind Power Scenarios at Bus 77 [MW]																			
	sc01	sc02	sc03	sc04	sc05	sc06	sc07	sc08	sc09	sc10	sc11	sc12	sc13	sc14	sc15	sc16	sc17	sc18	sc19	sc20
h00	518.79	518.79	518.79	518.79	518.79	518.79	518.79	518.79	518.79	518.79	518.79	518.79	518.79	518.79	518.79	518.79	518.79	518.79	518.79	518.79
h01	516.23	455.27	551.95	495.37	519.71	493.86	503.73	514.73	585.98	490.75	562.82	503.11	530.53	486.66	541.77	513.88	552.15	467.69	536.75	552.84
h02	502.94	463.11	539.97	487.59	508.59	481.72	508.28	515.09	572.26	505.55	532.46	483.59	524.21	492.37	525.20	512.36	538.53	482.76	533.47	538.37
h03	478.78	472.33	522.24	463.78	470.53	442.52	520.38	470.30	529.31	505.49	502.86	446.88	509.48	495.30	493.03	483.47	518.33	492.72	505.65	502.45
h04	458.94	485.33	483.91	451.46	444.27	413.38	497.84	428.15	503.87	508.48	483.09	436.27	506.18	487.29	474.72	473.09	485.03	492.88	477.86	466.58
h05	422.09	466.38	441.85	406.01	420.68	353.68	453.72	399.10	476.86	512.20	430.56	423.81	480.06	448.30	459.37	463.52	453.41	465.51	448.22	432.19
h06	345.05	366.28	354.56	337.36	352.47	271.06	353.48	315.25	401.99	478.04	340.52	340.41	424.99	376.35	389.40	403.39	378.07	372.50	370.42	343.97
h07	268.87	250.63	276.09	266.31	279.11	167.21	266.55	225.60	311.03	432.59	252.10	248.83	350.27	307.59	320.90	330.82	319.16	267.33	285.79	257.95
h08	196.88	175.94	207.62	169.53	201.10	89.97	195.51	156.05	220.96	350.22	160.86	168.47	293.33	230.58	247.85	250.68	240.04	203.97	211.93	186.34
h09	141.81	145.22	165.40	114.66	155.52	84.59	131.38	83.65	149.24	257.62	114.95	97.38	252.91	178.64	163.92	175.78	174.71	156.33	148.26	112.14
h10	143.37	163.77	159.59	118.75	155.33	131.19	133.57	76.69	169.97	257.75	142.25	95.26	240.95	170.54	143.19	173.94	167.88	166.35	142.92	92.16
h11	195.69	268.47	159.85	133.23	203.46	217.04	212.93	106.14	256.42	328.41	195.03	122.04	290.86	214.69	161.40	236.19	185.55	280.68	188.58	78.26
h12	217.02	314.30	161.32	116.55	243.90	249.23	195.69	123.03	275.22	358.73	199.39	111.87	353.76	235.44	176.46	275.46	199.51	324.20	198.84	56.86
h13	225.00	310.74	148.46	118.09	246.33	238.45	171.17	156.04	284.04	359.29	201.39	137.70	387.60	235.25	212.87	298.47	191.78	327.04	208.78	85.62
h14	226.80	292.83	157.00	151.10	185.73	227.18	202.75	166.72	334.82	373.67	198.68	117.71	379.24	239.56	194.19	289.52	161.36	356.13	238.60	126.53
h15	199.76	240.50	155.67	146.68	149.18	208.34	213.75	133.91	343.87	318.61	173.76	88.56	362.91	214.16	158.00	242.59	119.41	325.59	247.36	138.95
h16	201.66	198.71	163.62	178.61	145.65	240.62	233.87	142.69	353.02	278.23	179.49	148.72	366.06	192.52	169.51	221.25	86.13	291.42	273.59	195.85
h17	198.56	164.66	195.64	191.63	117.20	260.90	256.73	197.44	306.15	243.90	171.98	212.26	337.12	171.01	185.81	190.84	75.11	266.98	280.29	271.93
h18	184.96	158.84	202.69	174.16	123.33	229.58	262.31	164.32	263.08	172.50	164.01	192.61	268.76	158.21	159.84	150.20	91.51	234.15	253.38	247.25
h19	189.54	182.16	197.89	192.40	164.14	158.67	248.11	148.80	241.20	138.05	177.69	160.30	234.52	201.35	175.48	162.20	148.60	219.60	235.01	219.18
h20	235.43	203.65	211.52	246.86	203.43	138.71	315.87	248.97	213.59	171.68	171.57	173.68	256.71	297.23	240.48	211.49	205.02	277.45	272.41	271.62
h21	299.83	220.92	270.64	328.19	276.36	147.70	398.60	356.13	212.12	226.41	204.83	260.87	307.19	388.75	348.47	275.69	291.17	309.93	336.71	374.93
h22	316.88	227.74	308.56	337.09	305.82	156.90	407.36	398.92	188.82	289.93	209.54	280.66	308.44	412.91	379.18	304.28	350.17	312.26	338.41	389.41
h23	299.96	213.87	266.29	319.67	277.75	155.77	395.97	406.73	125.65	300.14	210.93	281.33	258.02	401.29	371.62	291.54	346.57	293.73	287.73	355.27
h24	266.38	163.99	270.52	287.19	237.46	134.06	351.72	339.25	58.67	223.68	215.52	288.42	237.07	347.38	351.11	222.88	323.50	212.47	237.05	348.62

Table C.7.: Wind injection (continued on the next page)

	Wind Power Scenarios at Bus 69 [MW]																			
	sc01	sc02	sc03	sc04	sc05	sc06	sc07	sc08	sc09	sc10	sc11	sc12	sc13	sc14	sc15	sc16	sc17	sc18	sc19	sc20
h00	501.39	501.39	501.39	501.39	501.39	501.39	501.39	501.39	501.39	501.39	501.39	501.39	501.39	501.39	501.39	501.39	501.39	501.39	501.39	501.39
h01	514.28	485.36	512.79	545.44	483.31	496.63	466.48	480.06	546.47	499.62	495.90	505.33	469.90	532.51	486.18	466.75	508.84	514.47	525.38	492.16
h02	525.54	484.21	535.89	554.09	499.86	501.40	477.49	497.21	545.73	521.87	499.39	529.81	481.41	538.30	505.41	482.02	529.86	529.90	532.03	512.55
h03	520.65	487.80	549.72	536.67	499.44	486.41	485.45	513.80	530.19	526.03	510.47	540.22	472.03	543.60	510.30	498.17	538.37	523.18	515.37	507.76
h04	501.93	468.88	529.33	523.95	486.84	451.40	493.40	518.45	502.19	509.37	526.70	491.45	478.57	520.40	491.72	519.37	535.68	514.13	512.30	472.52
h05	491.28	457.68	505.32	535.29	478.94	460.33	491.01	513.92	509.60	477.47	485.42	458.55	488.60	496.95	480.11	497.44	517.91	526.17	505.65	455.77
h06	489.43	476.34	466.30	533.61	467.82	478.16	462.35	507.42	528.56	485.68	440.25	468.35	473.14	497.41	499.77	470.02	493.51	501.82	490.12	457.12
h07	448.81	404.21	386.59	498.42	432.62	435.82	435.19	482.63	480.90	458.12	382.58	448.95	446.22	405.67	448.52	434.92	474.14	449.97	452.69	425.95
h08	362.34	310.87	307.52	425.31	355.37	341.81	397.04	377.14	380.63	390.70	286.32	360.91	416.10	293.49	377.88	372.65	402.30	383.79	386.49	374.89
h09	295.17	262.59	265.34	324.56	269.13	251.31	350.51	291.85	305.24	350.67	232.36	299.88	366.15	236.03	328.01	320.75	332.52	301.93	325.03	311.00
h10	277.37	248.04	238.73	291.34	245.53	253.52	335.29	268.14	272.91	348.75	220.58	261.04	334.82	228.55	310.42	296.95	302.97	275.97	315.43	276.08
h11	283.69	238.91	241.87	284.10	283.43	276.16	326.66	262.34	269.34	387.25	220.59	252.68	323.86	239.24	331.69	288.89	299.84	275.69	330.95	302.87
h12	280.44	227.68	249.87	308.67	287.15	270.01	310.20	229.52	249.36	360.11	209.99	282.79	327.40	226.62	320.86	281.55	298.97	285.68	317.26	339.22
h13	265.38	244.02	224.50	292.85	268.54	249.63	283.21	190.14	239.28	333.98	208.95	269.54	308.72	226.26	309.76	269.18	265.08	251.53	295.79	334.79
h14	251.39	231.85	204.71	262.37	263.94	253.42	236.48	196.03	183.80	316.40	226.93	297.03	272.49	211.31	289.07	265.85	251.98	220.38	258.86	327.25
h15	252.81	211.78	198.21	233.90	260.91	245.85	262.43	203.98	131.44	288.04	266.31	327.90	280.20	159.94	240.91	290.33	268.36	203.32	246.43	322.66
h16	271.07	228.80	222.30	226.18	256.46	232.61	269.26	228.27	126.13	239.56	310.56	372.20	287.52	147.28	209.50	316.52	284.18	200.95	230.39	314.71
h17	285.41	277.20	244.62	242.07	261.44	240.14	270.78	216.74	131.96	205.51	312.24	412.58	352.62	140.74	230.99	338.44	273.32	220.28	223.31	358.39
h18	307.08	288.48	246.94	268.03	262.80	246.09	304.25	172.92	225.53	233.66	356.30	424.58	366.94	163.88	204.12	317.01	290.92	216.09	293.20	388.41
h19	309.61	262.97	257.27	299.68	261.73	228.99	336.38	172.60	294.11	227.98	375.74	418.64	356.88	172.06	162.16	300.00	324.39	232.17	326.37	381.83
h20	327.83	255.79	295.77	298.40	241.71	266.95	362.78	215.95	323.70	239.62	387.14	462.67	360.60	183.53	142.50	287.26	357.40	261.21	346.01	358.13
h21	406.57	314.64	355.63	339.81	256.88	379.67	408.83	279.20	403.81	301.78	464.84	573.52	425.24	236.60	162.63	309.96	416.80	316.41	432.79	391.42
h22	463.39	331.94	419.84	403.41	312.75	391.85	413.49	372.11	452.74	335.18	528.63	657.75	434.05	284.50	197.48	368.15	497.55	363.68	461.11	426.00
h23	499.16	397.56	458.63	459.71	324.62	354.33	461.68	378.07	498.83	368.07	563.94	671.67	433.80	358.00	250.63	428.96	535.71	373.84	480.15	449.31
h24	516.16	440.72	483.28	454.93	346.61	372.40	513.59	380.12	592.68	431.91	607.43	634.63	397.46	445.47	269.01	419.93	546.82	368.12	530.49	443.68

Table C.8.: Wind injection

D. Optimal Schedules of The Deterministic Case

This appendix presents the optimal unit schedules of the EnSch and RmpSch approaches for the deterministic study case presented in section 3.3 in chapter 3.

chapter 3, section 3.3 describes the deterministic case study for two different power demand profiles D1 and D2 (in MW), which present the same energy profile D^E (in MWh). The IEEE-118 bus system (see Appendix C) is used for this case study, where we assumed that the power demand profiles are perfectly known and given in Table 3.1, without uncertain events (i.e., no wind).

Table D.1 and Table D.2 show the optimal power schedules of the *RmpSch* approach for D1. Table D.3 and Table D.4 list the optimal power schedules of the *RmpSch* approach for D2; and Table D.5 and Table D.6 show the optimal energy schedules obtained by the *EnSch* approach for the energy profile D^E. Numbers between parenthesis indicate that the unit is either starting up or shutting down (productions which are bellow the unit's minimum output). Note that all these tables contain the initial conditions for the case studies.

	State$_0$	h00	h01	h02	h03	h04	h05	h06	h07	h08	h09	h10	h11	h12	h13	h14	h15	h16	h17	h18	h19	h20	h21	h22	h23	h24
gen1	1	30	5	5	.	.	.	.	.	.	.	.	.	.	.	.	.	.	.	.	.	.	.	.	.	.
gen2	1	30	5	5	.	.	.	.	.	.	.	.	.	.	.	.	.	.	.	.	.	.	.	.	.	.
gen3	1	30	5	5	.	.	.	.	.	.	.	.	.	.	.	.	.	.	.	.	.	.	.	.	.	.
gen4	-8	.	(37.5)	(75)	(112.5)	150	210	150	180	240	300	300	300	240	180	210	150	150	150	210	270	210	150	(75)	.	.
gen5	8	100	160	220	280	250	300	300	300	300	300	300	300	300	300	240	180	120	180	240	300	300	240	180	120	100
gen6	1	30	10	10	.	.	.	.	.	.	.	.	.	.	.	.	.	.	.	.	.	.	.	.	.	.
gen7	-5	.	.	.	.	.	.	(6.25)	(12.5)	(18.75)	25	45	65	45	25	25	.	.	.	.	.	.	.	.	.	.
gen8	1	30	5	5	.	.	.	.	.	.	.	.	.	.	.	.	.	.	.	.	.	.	.	.	.	.
gen9	1	30	5	5	.	.	.	.	.	.	.	.	.	.	.	.	.	.	.	.	.	.	.	.	.	.
gen10	8	200	140	100	160	113.75	173.75	233.75	180	240	300	300	300	240	180	160	100	100	160	220	280	220	160	100	(50)	.
gen11	8	200	270	300.5	350	350	350	350	350	350	350	350	350	350	350	350	295	350	350	280	350	350	280	210	207	137
gen12	-1	.	.	.	.	.	.	.	.	.	.	.	.	.	.	.	.	.	.	.	.	.	.	.	.	.
gen13	-1	.	.	.	.	.	.	.	.	.	.	.	.	.	.	.	.	.	.	.	.	.	.	.	.	.
gen14	-5	.	.	.	.	(6.25)	(12.5)	(18.75)	25	40	60	80	100	80	60	40	25	25	25	45	65	45	25	.	.	.
gen15	1	30	8	8	.	.	.	.	.	.	.	.	.	.	.	.	.	.	.	.	.	.	.	.	.	.
gen16	-5	.	.	.	.	.	.	.	.	.	.	.	.	.	.	.	.	.	.	.	.	.	.	.	.	.
gen17	-1	.	.	.	.	.	.	.	.	.	.	.	.	.	.	.	.	.	.	.	.	.	.	.	.	.
gen18	-1	.	.	.	.	.	.	.	.	.	.	.	.	.	.	.	.	.	.	.	.	.	.	.	.	.
gen19	-5	.	.	.	.	.	(6.25)	(12.5)	(18.75)	25	45	65	45	25	25	25	25	25	25	25	45	25	.	.	.	.
gen20	-8	.	(12.5)	(25)	(37.5)	50	100	150	200	250	250	250	250	250	250	235	185	135	150	200	250	250	200	150	100	50
gen21	8	50	100	150	200	250	250	250	250	250	250	250	250	250	250	250	200	150	150	200	250	250	200	150	100	50
gen22	-5	.	.	.	.	.	.	.	.	.	.	.	.	.	.	.	.	.	.	.	.	.	.	.	.	.
gen23	-5	.	.	.	.	.	.	.	.	.	.	.	.	.	.	.	.	.	.	.	.	.	.	.	.	.
gen24	-8	.	(12.5)	(25)	(37.5)	50	90	130	120	160	200	200	200	180	160	120	80	80	120	160	200	160	120	80	50	50
gen25	-8	.	(12.5)	(25)	(37.5)	50	50	50	50	80	120	160	200	160	120	80	50	50	50	90	130	90	50	(25)	.	.
gen26	-5	.	.	.	.	.	.	.	.	.	.	.	.	.	.	.	.	.	.	.	.	.	.	.	.	.
gen27	10	100	184	268	352	420	420	420	420	420	420	420	420	420	420	420	420	420	414	420	420	420	420	336	420	420

Table D.1.: Optimal Power Schedules of the *RmpSch* approach for D1 [MW] (continued on next page)

	$State_0$	h00	h01	h02	h03	h04	h05	h06	h07	h08	h09	h10	h11	h12	h13	h14	h15	h16	h17	h18	h19	h20	h21	h22	h23	h24
gen28	10	200	284	368	420	420	420	420	420	420	420	420	420	420	420	420	420	420	420	336	420	420	340	319	403	363
gen29	-8	.	(20)	(40)	(60)	80	140	200	260	300	300	300	300	300	300	240	180	120	180	240	300	300	240	180	140	80
gen30	-4	.	.	.	.	.	.	.	.	.	.	.	.	.	.	.	.	.	.	.	.	.	.	.	.	.
gen31	-1	.	.	.	.	.	.	.	.	.	.	.	.	.	.	.	.	.	.	.	.	.	.	.	.	.
gen32	-1	.	.	.	.	.	.	.	.	.	.	.	.	.	.	.	.	.	.	.	.	.	.	.	.	.
gen33	-1	.	.	.	.	.	.	.	.	.	.	.	.	.	.	.	.	.	.	.	.	.	.	.	.	.
gen34	5	35	25	25	.	.	.	.	.	(12.5)	25	45	65	45	25	25	.	.	.	.	.	.	.	.	.	.
gen35	-5	.	.	.	.	.	.	.	.	.	.	.	.	.	.	.	.	.	.	.	.	.	.	.	.	.
gen36	-8	.	(37.5)	(75)	(112.5)	150	150	150	160	220	280	290	300	240	180	150	150	150	150	210	270	210	150	(75)	.	.
gen37	5	25	.	.	.	.	.	.	(12.5)	25	45	65	85	65	45	25	25	25	25	25	45	45	25	.	.	.
gen38	-1	.	.	.	.	.	.	.	.	.	.	.	.	.	.	.	.	.	.	.	.	.	.	.	.	.
gen39	8	100	160	220	280	300	300	300	300	300	300	300	300	300	300	300	240	255	300	240	300	300	240	180	160	100
gen40	8	50	81.5	120.5	160.5	160	200	200	200	200	200	200	200	200	200	160	120	80	120	160	200	170	130	90	50	50
gen41	-1	.	.	.	.	.	.	.	.	.	.	.	.	.	.	.	.	.	.	.	.	.	.	.	.	.
gen42	1	40	20	20	.	.	.	.	.	.	.	.	.	.	.	.	.	.	.	.	.	.	.	.	.	.
gen43	8	100	(50)	.	.	.	(25)	(50)	(75)	100	160	220	280	220	160	100	100	100	160	220	280	220	160	100	(50)	.
gen44	-8	.	(25)	(50)	(75)	100	160	220	255	265	300	300	300	300	300	240	180	120	180	240	300	270	210	150	100	100
gen45	-8	.	(25)	(50)	(75)	100	136.25	120	180	240	300	300	300	240	180	160	100	100	160	220	280	220	160	100	(50)	.
gen46	-1	.	.	.	.	.	.	.	.	.	.	.	.	.	.	.	.	.	.	.	.	.	.	.	.	.
gen47	-5	.	.	.	.	.	(6.25)	(12.5)	(18.75)	25	45	65	85	65	45	25	25	25	25	25	45	25	.	.	.	.
gen48	-5	.	.	.	.	.	.	.	.	.	.	.	.	.	.	.	.	.	.	.	.	.	.	.	.	.
gen49	-1	.	.	.	.	.	.	.	.	.	.	.	.	.	.	.	.	.	.	.	.	.	.	.	.	.
gen50	2	40	25	25	.	.	.	.	.	.	.	.	.	.	.	.	.	.	.	.	.	.	.	.	.	.
gen51	-5	.	.	.	.	.	(6.25)	(12.5)	(18.75)	25	25	45	65	45	25	.	.	.	.	.	.	.	.	.	.	.
gen52	-5	.	.	.	.	.	.	.	.	.	.	.	.	.	.	.	.	.	.	.	.	.	.	.	.	.
gen53	-5	.	.	.	.	.	.	.	.	.	.	.	.	.	.	.	.	.	.	.	.	.	.	.	.	.
gen54	2	50	25	25	.	.	.	.	.	.	.	.	.	.	.	.	.	.	.	.	.	.	.	.	.	.

Table D.2.: Optimal Power Schedules of the *RmpSch* approach for D1 [MW]

	$State_0$	h00	h01	h02	h03	h04	h05	h06	h07	h08	h09	h10	h11	h12	h13	h14	h15	h16	h17	h18	h19	h20	h21	h22	h23	h24
gen1	1	30	5	5	.	.	.	.	.	.	.	.	.	.	.	.	.	.	(2.5)	5	30	5	.	.	.	.
gen2	1	30	5	5	.	.	.	.	.	.	.	.	.	.	.	.	.	.	.	.	.	.	.	.	.	.
gen3	1	30	5	5	.	.	.	.	.	.	.	.	.	.	.	.	.	.	.	(2.5)	5	22	5	.	.	.
gen4	-8	.	(37.5)	(75)	(112.5)	150	150	210	150	210	240	300	300	300	240	210	150	150	150	210	270	210	150	(75)	.	.
gen5	8	200	140	200	240	300	300	300	240	300	300	300	300	300	240	240	180	120	180	240	300	300	240	180	120	100
gen6	1	30	10	10	.	.	.	.	.	.	.	.	.	.	.	.	.	.	.	.	.	.	.	.	.	.
gen7	-5	.	.	.	.	(6.25)	(12.5)	(18.75)	25	25	45	65	45	25	.	.	.	(12.5)	25	25	45	53	33	25	.	.
gen8	1	30	5	5	.	.	.	.	.	.	.	.	.	.	.	.	.	.	.	.	.	.	.	.	.	.
gen9	1	30	5	5	.	.	.	.	.	.	.	.	.	.	.	.	.	.	.	(2.5)	5	30	5	.	.	.
gen10	8	200	140	199.5	139.5	168	110	170	230	290	240	300	300	300	240	180	120	100	160	220	280	220	160	100	(50)	.
gen11	8	200	210	280	350	350	350	350	350	350	350	350	350	350	350	350	280	350	280	350	350	350	280	210	140	205
gen12	-1	.	.	.	.	.	.	.	.	.	.	.	.	.	.	.	.	.	.	.	.	.	.	.	.	.
gen13	-1	.	.	.	.	.	.	.	.	.	.	.	.	.	.	.	.	.	.	.	.	.	.	.	.	.
gen14	-5	.	.	.	.	(6.25)	(12.5)	(18.75)	25	37.93	57.93	77.93	65	45	25	45	25	25	25	25	45	25	.	.	.	.
gen15	1	30	8	8	.	.	.	.	.	.	.	.	.	.	.	.	.	.	.	.	.	.	.	.	.	.
gen16	-5	.	.	.	.	.	.	.	.	.	.	.	.	.	.	.	.	.	.	.	.	.	.	.	.	.
gen17	-1	.	.	.	.	.	.	.	.	.	.	.	.	.	.	.	.	.	.	.	.	.	.	.	.	.
gen18	-1	.	.	.	.	.	.	.	.	.	.	.	.	.	.	.	.	.	.	.	.	.	.	.	.	.
gen19	-5	.	.	.	.	.	(6.25)	(12.5)	(18.75)	25	45	60	40	25	25	25	25	25	25	25	37.5	25	.	.	.	.
gen20	-8	.	(12.5)	(25)	(37.5)	50	100	150	200	250	250	250	250	200	250	200	200	150	150	200	250	250	200	150	100	50
gen21	8	50	50	100	150	200	250	250	206.68	250	250	250	250	250	250	250	200	152.5	200	250	250	250	200	150	100	50
gen22	-5	.	.	.	.	.	.	.	.	.	.	.	.	.	.	.	.	.	.	.	.	.	.	.	.	.
gen23	-5	.	.	.	.	.	.	.	.	.	.	.	.	.	.	.	.	.	.	.	.	.	.	.	.	.
gen24	-8	.	(12.5)	(25)	(37.5)	50	90	130	160	200	180	200	200	200	160	120	80	80	120	160	200	200	160	120	80	50
gen25	-8	.	(12.5)	(25)	(37.5)	50	50	50	80	120	160	200	200	160	120	90	50	50	50	62.5	102.5	90	50	(25)	.	.
gen26	-5	.	.	.	.	.	.	.	.	.	.	.	.	.	.	.	.	.	.	.	.	.	.	.	.	.
gen27	10	225	309	393	420	420	420	420	420	420	420	420	420	420	420	420	354	420	420	420	420	420	336	420	420	420

Table D.3.: Optimal Power Schedules of the *RmpSch* approach for D2 [MW] (continued on next page)

	$State_0$	h00	h01	h02	h03	h04	h05	h06	h07	h08	h09	h10	h11	h12	h13	h14	h15	h16	h17	h18	h19	h20	h21	h22	h23	h24
gen28	10	100	184	268	352	420	420	420	420	420	420	420	420	420	420	420	336	420	420	420	420	420	336	360	375	420
gen29	-8	.	(20)	(40)	(60)	80	140	200	240	300	300	300	300	300	240	240	180	120	180	240	300	300	240	180	120	80
gen30	-4	.	.	.	.	.	.	.	.	.	.	.	.	.	.	.	.	.	.	.	.	.	.	.	.	.
gen31	-1	.	.	.	.	.	.	.	.	.	.	.	.	.	.	.	.	.	.	.	.	.	.	.	.	.
gen32	-1	.	.	.	.	.	.	.	.	.	.	.	.	.	.	.	.	.	.	.	.	.	.	.	.	.
gen33	-1	.	.	.	.	.	.	.	.	.	.	.	.	.	.	.	.	.	.	.	.	.	.	.	.	.
gen34	5	35	25	25	.	.	.	.	.	(12.5)	25	45	40	25	25	25	25	25	25	25	25	25	.	.	.	.
gen35	-5	.	.	.	.	.	.	.	.	.	.	.	.	.	.	.	.	.	.	.	.	.	.	.	.	.
gen36	-8	.	(37.5)	(75)	(112.5)	150	150	188.75	150	210	240	300	300	300	240	210	150	150	150	150	210	150	(75)	.	.	.
gen37	5	25	.	.	.	.	.	.	(12.5)	25	42.07	62.07	65	45	25	25	25	25	25	25	45	25	.	.	.	.
gen38	-1	.	.	.	.	.	.	.	.	.	.	.	.	.	.	.	.	.	.	.	.	.	.	.	.	.
gen39	8	100	121.5	181.5	241.5	300	300	300	300	300	300	300	300	300	300	300	240	300	240	300	300	300	240	180	120	100
gen40	8	50	50	90	84.5	124.5	160	200	160	200	200	200	200	200	160	160	120	80	120	160	200	200	160	120	80	50
gen41	-1	.	.	.	.	.	.	.	.	.	.	.	.	.	.	.	.	.	.	.	.	.	.	.	.	.
gen42	1	40	20	20	.	.	.	.	.	.	.	.	.	.	.	.	.	.	.	.	.	.	.	.	.	.
gen43	8	100	100	160	100	100	100	100	120	180	240	300	300	245	185	160	100	100	100	160	220	160	100	(50)	.	.
gen44	-8	.	(25)	(50)	(75)	100	160	220	228.32	288.32	300	300	300	300	240	195	135	120	180	240	300	300	240	180	120	100
gen45	-8	.	(25)	(50)	(75)	100	100	160	120	180	240	300	300	280	220	160	100	100	100	160	220	220	160	100	(50)	.
gen46	-1	.	.	.	.	.	.	.	.	.	.	.	.	.	.	.	.	.	.	.	.	.	.	.	.	.
gen47	-5	.	.	.	.	.	.	(6.25)	(12.5)	(18.75)	25	45	65	45	25	25	25	25	25	25	45	25	.	.	.	.
gen48	-5	.	.	.	.	.	.	.	.	.	.	.	.	.	.	.	.	.	.	.	.	.	.	.	.	.
gen49	-1	.	.	.	.	.	.	.	.	.	.	.	.	.	.	.	.	.	.	.	.	.	.	.	.	.
gen50	2	40	25	25	.	.	.	.	.	.	.	.	.	.	.	.	.	.	.	.	.	.	.	.	.	.
gen51	-5	.	.	.	.	.	.	.	.	.	.	.	.	.	.	.	.	.	.	.	.	.	.	.	.	.
gen52	-5	.	.	.	.	.	.	(6.25)	(12.5)	(18.75)	25	45	45	25	25	25	25	25	25	25	25	25	.	.	.	.
gen53	-5	.	.	.	.	.	.	.	.	.	.	.	.	.	.	.	.	.	.	.	.	.	.	.	.	.
gen54	2	50	25	25	.	.	.	.	.	.	.	.	.	.	.	.	.	.	.	.	.	.	.	.	.	.

Table D.4.: Optimal Power Schedules of the *RmpSch* approach for D2 [MW]

	State$_0$	h00	h01	h02	h03	h04	h05	h06	h07	h08	h09	h10	h11	h12	h13	h14	h15	h16	h17	h18	h19	h20	h21	h22	h23	h24
gen1	1	30	5	.	.	.	.	.	.	.	.	.	.	.	.	.	.	.	.	.	.	.	.	.	.	.
gen2	1	30	5	.	.	.	.	.	.	.	.	.	.	.	.	.	.	.	.	.	.	.	.	.	.	.
gen3	1	30	5	.	.	.	.	.	.	.	.	.	.	.	.	.	.	.	.	.	.	.	.	.	.	.
gen4	-8	.	.	.	.	150	150	150	180	240	300	300	300	300	240	180	150	150	150	210	270	300	250	190	150	150
gen5	8	200	149	209	269	300	240	300	300	300	300	300	300	300	300	292.44	232.44	172.44	180	240	300	300	240	180	120	100
gen6	1	30	10	.	.	.	.	.	.	.	.	.	.	.	.	.	.	.	.	.	.	.	.	.	.	.
gen7	-5	.	.	.	.	.	.	.	.	.	.	.	.	.	.	.	.	.	.	.	.	.	.	.	.	.
gen8	1	30	5	.	.	.	.	.	.	.	.	.	.	.	.	.	.	.	.	.	.	.	.	.	.	.
gen9	1	30	5	.	.	.	.	.	.	.	.	.	.	.	.	.	.	.	.	.	.	.	.	.	.	.
gen10	8	200	140	100	100	100	100	115	165	225	285	300	300	300	240	180	120	100	122.44	182.44	242.44	280	220	160	100	100
gen11	8	200	270	340	350	350	350	350	350	350	350	350	350	350	350	350	350	350	350	350	350	350	310	240	170	100
gen12	-1	.	.	.	.	.	.	.	.	.	.	.	.	.	.	.	.	.	.	.	.	.	.	.	.	.
gen13	-1	.	.	.	.	.	.	.	.	.	.	.	.	.	.	.	.	.	.	.	.	.	.	.	.	.
gen14	-5	.	.	.	.	25	25	25	25	40	60	80	100	80	60	40	25	.	.	.	.	.	.	.	.	.
gen15	1	30	8	.	.	.	.	.	.	.	.	.	.	.	.	.	.	.	.	.	.	.	.	.	.	.
gen16	-5	.	.	.	.	.	.	.	.	.	.	.	.	.	.	.	.	.	.	.	.	.	.	.	.	.
gen17	-1	.	.	.	.	.	.	.	.	.	.	.	.	.	.	.	.	.	.	.	.	.	.	.	.	.
gen18	-1	.	.	.	.	.	.	.	.	.	.	.	.	.	.	.	.	.	.	.	.	.	.	.	.	.
gen19	-5	.	.	.	.	.	.	.	.	.	.	.	.	.	.	.	.	.	.	.	.	.	.	.	.	.
gen20	-8	.	.	50	100	150	200	250	250	250	250	250	250	250	250	250	235	185	150	200	250	250	200	150	100	50
gen21	8	50	100	150	200	250	200	250	250	250	250	250	250	250	250	250	250	200	170	200	250	250	200	150	100	50
gen22	-5	.	.	.	.	.	.	.	.	.	.	.	.	.	.	.	.	.	.	.	.	.	.	.	.	.
gen23	-5	.	.	.	.	.	.	.	.	.	.	.	.	.	.	.	.	.	.	.	.	.	.	.	.	.
gen24	-8	.	.	.	.	.	50	90	130	160	200	200	200	200	160	160	120	80	120	160	200	190	150	110	70	50
gen25	-8	.	.	.	.	.	50	50	50	80	120	160	200	170	130	90	50	50	50	50	90	90	50	.	.	.
gen26	-5	.	.	.	.	.	.	.	.	.	.	.	.	.	.	.	.	.	.	.	.	.	.	.	.	.
gen27	10	225	309	393	420	420	420	420	420	420	420	420	420	420	420	420	420	420	420	420	420	420	420	344	358	302

Table D.5.: Optimal Energy Schedules of the *EnSch* approach for D^E [MWh] (continued on next page)

	$State_0$	h00	h01	h02	h03	h04	h05	h06	h07	h08	h09	h10	h11	h12	h13	h14	h15	h16	h17	h18	h19	h20	h21	h22	h23	h24
gen28	10	100	184	268	352	420	420	420	420	420	420	420	420	420	420	420	420	420	420	420	420	420	420	336	252	168
gen29	-8	.	.	80	140	200	180	240	300	300	300	300	300	300	300	300	240	180	180	240	300	300	240	180	120	80
gen30	-4	.	.	.	.	.	.	.	.	.	.	.	.	.	.	.	.	.	.	.	.	.	.	.	.	.
gen31	-1	.	.	.	.	.	.	.	.	.	.	.	.	.	.	.	.	.	.	.	.	.	.	.	.	.
gen32	-1	.	.	.	.	.	.	.	.	.	.	.	.	.	.	.	.	.	.	.	.	.	.	.	.	.
gen33	-1	.	.	.	.	.	.	.	.	.	.	.	.	.	.	.	.	.	.	.	.	.	.	.	.	.
gen34	5	35	25	.	.	.	.	.	.	25	45	65	85	65	45	25	.	.	.	.	.	.	.	.	.	.
gen35	-5	.	.	.	.	.	.	.	.	.	.	.	.	.	.	.	.	.	.	.	.	.	.	.	.	.
gen36	-8	.	.	.	.	.	150	150	150	150	210	270	300	300	240	180	150	150	150	180	240	300	240	180	150	150
gen37	5	25	25	25	25	25	25	25	25	40	60	80	100	80	60	40	25	.	.	.	.	.	.	.	.	.
gen38	-1	.	.	.	.	.	.	.	.	.	.	.	.	.	.	.	.	.	.	.	.	.	.	.	.	.
gen39	8	100	160	220	280	300	300	300	300	300	300	300	300	300	300	300	300	280	300	250	300	300	280	220	160	100
gen40	8	50	50	65	64	104	65	105	145	185	200	200	200	200	200	160	120	80	120	160	200	200	160	120	80	50
gen41	-1	.	.	.	.	.	.	.	.	.	.	.	.	.	.	.	.	.	.	.	.	.	.	.	.	.
gen42	1	40	20	.	.	.	.	.	.	.	.	.	.	.	.	.	.	.	.	.	.	.	.	.	.	.
gen43	8	100	100	100	100	100	100	100	100	120	180	240	300	285	225	165	105	100	100	100	160	220	160	100	100	100
gen44	-8	.	.	.	100	106	100	160	220	275	300	300	300	300	260	227.56	167.56	107.56	167.56	227.56	287.56	300	240	180	120	100
gen45	-8	.	.	.	.	.	100	100	100	140	200	260	300	300	240	180	120	100	100	160	220	280	220	160	100	100
gen46	-1	.	.	.	.	.	.	.	.	.	.	.	.	.	.	.	.	.	.	.	.	.	.	.	.	.
gen47	-5	.	.	.	.	25	25	25	25	40	60	80	100	80	60	40	25	.	.	.	.	.	.	.	.	.
gen48	-5	.	.	.	.	.	.	.	.	.	.	.	.	.	.	.	.	.	.	.	.	.	.	.	.	.
gen49	-1	.	.	.	.	.	.	.	.	.	.	.	.	.	.	.	.	.	.	.	.	.	.	.	.	.
gen50	2	40	25	.	.	.	.	.	.	.	.	.	.	.	.	.	.	.	.	.	.	.	.	.	.	.
gen51	-5	.	.	.	.	.	.	.	.	.	.	.	.	.	.	.	.	.	.	.	.	.	.	.	.	.
gen52	-5	.	.	.	.	.	.	.	.	.	.	.	.	.	.	.	.	.	.	.	.	.	.	.	.	.
gen53	-5	.	.	.	.	.	.	.	.	.	.	.	.	.	.	.	.	.	.	.	.	.	.	.	.	.
gen54	2	50	25	.	.	.	.	.	.	.	.	.	.	.	.	.	.	.	.	.	.	.	.	.	.	.

Table D.6.: Optimal Energy Schedules of the *EnSch* approach for D^E [MWh]

Bibliography

[1] "CPLEX 12," IBM ILOG CPLEX, User's Manual, 2013. [Online]. Available: http://gams.com/dd/docs/solvers/cplex.pdf

[2] A. Abiri-Jahromi, M. Fotuhi-Firuzabad, and E. Abbasi, "Optimal scheduling of spinning reserve based on well-being model," *Power Systems, IEEE Transactions on*, vol. 22, no. 4, pp. 2048–2057, 2007.

[3] M. Amelin, "Comparison of capacity credit calculation methods for conventional power plants and wind power," *Power Systems, IEEE Transactions on*, vol. 24, no. 2, pp. 685–691, 2009.

[4] F. Aminifar, M. Fotuhi-Firuzabad, and M. Shahidehpour, "Unit commitment with probabilistic spinning reserve and interruptible load considerations," *Power Systems, IEEE Transactions on*, vol. 24, no. 1, pp. 388–397, 2009.

[5] L. T. Anstine, R. E. Burke, J. E. Casey, R. Holgate, R. S. John, and H. G. Stewart, "Application of probability methods to the determination of spinning reserve requirements for the pennsylvania-new jersey-maryland interconnection," *IEEE Transactions on Power Apparatus and Systems*, vol. 82, no. 68, pp. 726–735, Oct. 1963.

[6] J. M. Arroyo and A. Conejo, "Modeling of start-up and shut-down power trajectories of thermal units," *IEEE Transactions on Power Systems*, vol. 19, no. 3, pp. 1562–1568, Aug. 2004.

[7] R. Baldick, "Wind and energy markets: A case study of texas," *IEEE Systems Journal*, vol. 6, no. 1, pp. 27–34, Mar. 2012.

[8] A. Ben-Tal, A. Goryashko, E. Guslitzer, and A. Nemirovski, "Adjustable robust solutions of uncertain linear programs," *Mathematical Programming*, vol. 99, no. 2, pp. 351–376, Mar. 2004.

[9] A. Ben-Tal and A. Nemirovski, "Robust solutions of linear programming problems contaminated with uncertain data," *Mathematical Programming*, vol. 88, no. 3, pp. 411–424, Sep. 2000. [Online]. Available: http://link.springer.com.focus.lib.kth.se/article/10.1007/PL00011380

[10] A. Ben-Tal, L. E. Ghaoui, and A. Nemirovski, *Robust Optimization*. Princeton University Press, Aug. 2009.

[11] A. Ben-Tal, A. Nemirovski, and D. den Hertog, "ARO MIP problems," 2014, personal correspondence.

[12] D. Bertsimas, E. Litvinov, X. A. Sun, J. Zhao, and T. Zheng, "Adaptive robust optimization for the security constrained unit commitment problem," *IEEE Transactions on Power Systems*, vol. 28, no. 1, pp. 52–63, Feb. 2013.

[13] D. Bertsimas and M. Sim, "The price of robustness," *Operations Research*, vol. 52, no. 1, pp. 35 –53, Jan. 2004. [Online]. Available: http://or.journal.informs.org/content/52/1/35.abstract

[14] D. Bertsimas, D. B. Brown, and C. Caramanis, "Theory and applications of robust optimization," *SIAM Review*, vol. 53, no. 3, pp. 464–501, Jan. 2011. [Online]. Available: http://epubs.siam.org/doi/abs/10.1137/080734510

[15] J. R. Birge and F. Louveaux, *Introduction to Stochastic Programming*, corrected ed. Springer, Jul. 1997.

[16] R. Bixby, M. Fenelon, Z. Gu, E. Rothberg, and R. Wunderling, "MIP: theory and practice–closing the gap," in *System Modelling and Optimization: Methods, Theory and Applications*, M. J. D. Powell and S. Scholtes, Eds. Boston: Kluwer Academic Publishers, 2000, vol. 174, p. 19–49.

[17] R. Bixby and E. Rothberg, "Progress in computational mixed integer programming—A look back from the other side of the tipping point," *Annals of Operations Research*, vol. 149, no. 1, pp. 37–41, Jan. 2007.

[18] R. E. Bixby, "Solving real-world linear programs: A decade and more of progress," *Operations Research*, vol. 50, no. 1, pp. 3–15, Jan. 2002.

[19] R. E. Bixby, M. Fenelon, Z. Gu, E. Rothberg, and R. Wunderling, "Mixed-integer programming: A progress report," in *The Sharpest Cut: The Impact of Manfred Padberg and his Work*, ser. MPS-SIAM Series on Optimization, M. Grötschel, Ed. 3600 Market Street, 6th Floor Philadelphia, PA 19104-2688: SIAM, Jan. 2004, pp. 309—325.

[20] A. Botterud, J. Wang, V. Miranda, and R. J. Bessa, "Wind power forecasting in U.S. electricity markets," *The Electricity Journal*, vol. 23, no. 3, pp. 71–82, Apr. 2010. [Online]. Available: http://www.sciencedirect.com/science/article/pii/S104061901000062X

[21] F. Bouffard and F. Galiana, "Stochastic security for operations planning with significant wind power generation," *Power Systems, IEEE Transactions on*, vol. 23, no. 2, pp. 306–316, 2008.

[22] F. Bouffard, F. Galiana, and A. Conejo, "Market-clearing with stochastic security-part i: formulation," *IEEE Transactions on Power Systems*, vol. 20, no. 4, pp. 1818–1826, Nov. 2005.

[23] ——, "Market-clearing with stochastic security-part II: case studies," *Power Systems, IEEE Transactions on*, vol. 20, no. 4, pp. 1827–1835, 2005.

[24] CAISO, "Multi-stage generator unit modeling enhancements," Tech. Rep., Sep. 2011. [Online]. Available: http://www.caiso.com/Documents/DraftFinalProposal-Multi-StageGenerationEnhancements.pdf

[25] ——, "White paper - integrated day-ahead market: Technical description for flexible ramping product," Midwest Independent Transmission System Operator, USA, Tech. Rep., Sep. 2012. [Online]. Available: http://www.caiso.com/Documents/IntegratedDay-AheadMarketDraftTechnicalDescription-FlexibleRampingProduct.pdf

[26] F. Campos, "Modelos de evaluación de reservas de generación en el mercado eléctrico español," Institute for Research in Technology (IIT), Technical Report, 2002.

[27] C. C. M. Caramanis, "Adaptable optimization: theory and algorithms," Thesis, Massachusetts Institute of Technology, 2006, thesis (Ph. D.)–Massachusetts Institute of Technology, Dept. of Electrical Engineering and Computer Science, 2006. [Online]. Available: http://dspace.mit.edu/handle/1721.1/38301

[28] M. Carrion and J. Arroyo, "A computationally efficient mixed-integer linear formulation for the thermal unit commitment problem," *IEEE Transactions on Power Systems*, vol. 21, no. 3, pp. 1371–1378, 2006.

[29] H. Chavez, R. Baldick, and S. Sharma, "Regulation adequacy analysis under high wind penetration scenarios in ERCOT nodal," *IEEE Transactions on Sustainable Energy*, vol. 3, no. 4, pp. 743 –750, Oct. 2012.

[30] T. Christof and A. Löbel, "PORTA: POlyhedron representation transformation algorithm, version 1.4.1," *Konrad-Zuse-Zentrum für Informationstechnik Berlin, Germany*, 2009. [Online]. Available: http://typo.zib.de/opt-long_projects/Software/Porta/

[31] E. DeMeo, G. Jordan, C. Kalich, J. King, M. Milligan, C. Murley, B. Oakleaf, and M. Schuerger, "Accommodating wind's natural behavior," *Power and Energy Magazine, IEEE*, vol. 5, no. 6, pp. 59–67, 2007.

[32] R. Doherty and M. O'Malley, "A new approach to quantify reserve demand in systems with significant installed wind capacity," *Power Systems, IEEE Transactions on*, vol. 20, no. 2, pp. 587–595, 2005.

[33] I. Egido, L. Rouco, J. Alonso, E. Porras, and J. Ruiz, "Impacto en regulación frecuencia-potencia de los cambios de programa en escalón de las unidades generadoras," *Anales de Mecánica y Electricidad*, vol. LXXXVIII, no. 3, pp. 26—32, May 2011.

[34] ENTSO-e, "Frequency quality investigation, excerpt of the final report," UCTE AD-HOC, Report, Aug. 2008. [Online]. Available: www.entsoe.eu/fileadmin/user_upload/_library/publications/ce/otherreports/090330_UCTE_FrequencyInvestigationReport_Abstract.pdf

[35] ——, "Operation handbook, P1–Policy 1: Load-frequency control and performance [c]," European Network of Transmission Systems Operators for Electricity (ENTSO-e), Tech. Rep., Apr. 2009. [Online]. Available: https://www.entsoe.eu/nc/resources/publications/former-associations/ucte/operation-handbook

[36] ——, "Operational reserve ad hoc team report (AHT-Report)," European Network of Transmission Systems Operators for Electricity (ENTSO-e), Tech. Rep., May 2012. [Online]. Available: https://www.entsoe.eu/fileadmin/user_upload/_library/consultations/Network_Code_OR/2012-06-14_SOC-AhT-OR_Report_final_V9.pdf

[37] ——, "Network code on load-frequency control and reserves," European Network of Transmission Systems Operators for Electricity (ENTSO-e), Tech. Rep., Jun. 2013. [Online]. Available: https://www.entsoe.eu/major-projects/network-code-development/load-frequency-control-reserves/

[38] ——, "Supporting document for the network code on load-frequency control and reserves," European Network of Transmission Systems Operators for Electricity (ENTSO-e), Tech. Rep., Jun. 2013. [Online]. Available: https://www.entsoe.eu/fileadmin/user_upload/_library/resources/LCFR/130628-NC_LFCR-Supporting_Document-Issue1.pdf

[39] ENTSO-e and Eurelectric, "Deterministic frequency deviations – root causes and proposals for potential solutions," ENTSO-e, Report, Dec. 2011. [Online]. Available: https://www.entsoe.eu/fileadmin/user_upload/_library/publications/entsoe/120222_Deterministic_Frequency_Deviations_joint_ENTSOE_Eurelectric_Report___Final_.pdf

[40] ——, "Deterministic frequency deviations: 2nd stage impact analysis," ENTSO-e, Report, Dec. 2012. [Online]. Available: https://www.entsoe.eu/fileadmin/user_upload/_library/publications/entsoe/130325_Deterministic_Frequency_Deviations_Final_Report.pdf

[41] ERCOT, "ERCOT operations report on the EECP event of february 26, 2008," Electric Reliability Council of Texas (ERCOT), Texas - USA, Tech. Rep., Jul. 2008. [Online]. Available: http://www.ercot.com/meetings/ros/keydocs/2008/0313/07._ERCOT_OPERATIONS_REPORT_EECP022608_public.doc

[42] ——, "White paper functional description of core market management system (MMS) applications for "Look-Ahead SCED", version 0.1.2," Electric Reliability Council of Texas (ERCOT), Texas - USA, Tech. Rep., Nov. 2011. [Online]. Available: http://www.ercot.com/content/meetings/metf/keydocs/2012/0228/04_white_paper_funct_desc_core_mms_applications_for_la_sced.doc

[43] ——, "ERCOT nodal protocols: Transmission security analysis and reliability unit commitment," Electric Reliability Council of Texas (ERCOT), Texas - USA, Tech. Rep., Mar. 2014. [Online]. Available: http://ercot.com/content/mktrules/nprotocols/current/05-050114_Nodal.doc

[44] ——, "ERCOT nodal protocols: Day-ahead operations," Electric Reliability Council of Texas (ERCOT), Texas - USA, Tech. Rep., Mar. 2014. [Online]. Available: http://ercot.com/content/mktrules/nprotocols/current/04-030114_Nodal.doc

[45] ——, "ERCOT nodal protocols: Adjustment period and real-time operations," Electric Reliability Council of Texas (ERCOT), Texas - USA, Tech. Rep., May 2014. [Online]. Available: http://ercot.com/content/mktrules/nprotocols/current/06-050114_Nodal.doc

[46] FERC, "Recent ISO software enhancements and future software and modeling plans," Federal Energy Regulatory Commission, Staff Report, Nov. 2011. [Online]. Available: http://www.ferc.gov/industries/electric/indus-act/rto/rto-iso-soft-2011.pdf

[47] ——, "RTO unit commitment test system," Federal Energy and Regulatory Commission, Washington DC, USA, Tech. Rep., Jul. 2012.

[48] A. Frangioni, C. Gentile, and F. Lacalandra, "Tighter approximated MILP formulations for unit commitment problems," *IEEE Transactions on Power Systems*, vol. 24, no. 1, pp. 105–113, Feb. 2009.

[49] J. Frunt, I. Lampropoulos, and W. L. Kling, "The impact of electricity market design on periodic network frequency excursions," in *Energy Market (EEM), 2011 8th International Conference on the European.* IEEE, May 2011, pp. 550–555.

[50] Y. Fu, M. Shahidehpour, and Z. Li, "AC contingency dispatch based on security-constrained unit commitment," *Power Systems, IEEE Transactions on*, vol. 21, no. 2, pp. 897–908, 2006.

[51] F. Galiana, F. Bouffard, J. Arroyo, and J. Restrepo, "Scheduling and pricing of coupled energy and primary, secondary, and tertiary reserves," *Proceedings of the IEEE*, vol. 93, no. 11, pp. 1970–1983, 2005.

[52] J. Garcia-Gonzalez, A. San Roque, F. Campos, and J. Villar, "Connecting the intraday energy and reserve markets by an optimal redispatch," *IEEE Transactions on Power Systems*, vol. 22, no. 4, pp. 2220–2231, Nov. 2007.

[53] C. Gentile, G. Morales-Espana, and A. Ramos, "A tight MIP formulation of the unit commitment problem with start-up and shut-down constraints," *European Journal of Operational Research*, 2014, under Review.

[54] A. Gil, M. de la Torre, T. Dominguez, and R. Rivas, "Influence of wind energy forecast in deterministic and pobabilistic sizing of reserves," Quebec, Canada, Oct. 2009, p. 6.

[55] P. Glasserman, *Monte Carlo methods in financial engineering.* New York: Springer, 2003.

[56] X. Guan, F. Gao, and A. Svoboda, "Energy delivery scheduling and realizability in deregulated electric energy market," in *Proceedings of the 32nd Annual Hawaii International Conference on System Sciences, 1999. HICSS-32*, vol. Track3. IEEE, 1999.

[57] ——, "Energy delivery capacity and generation scheduling in the deregulated electric power market," *IEEE Transactions on Power Systems*, vol. 15, no. 4, pp. 1275–1280, Nov. 2000.

[58] X. Guan, Q. Zhai, Y. Feng, and F. Gao, "Optimization based scheduling for a class of production systems with integral constraints," *Science in China Series E: Technological Sciences*, vol. 52, no. 12, pp. 3533–3544, Dec. 2009.

[59] K. Hedman, M. Ferris, R. O'Neill, E. Fisher, and S. Oren, "Co-optimization of generation unit commitment and transmission switching with n-1 reliability," *Power Systems, IEEE Transactions on*, vol. 25, no. 2, pp. 1052 –1063, May 2010.

[60] B. F. Hobbs, M. H. Rothkopf, R. P. O'Neill, and H.-p. Chao, Eds., *The Next Generation of Electric Power Unit Commitment Models*, 1st ed. Springer, 2001.

[61] B. F. Hobbs, W. R. Stewart, R. E. Bixby, M. H. Rothkopf, R. P. O'Neill, and H.-p. Chao, "Why this book? new capabilities and new needs for unit commitment modeling," in *The Next Generation of Electric Power Unit Commitment Models*, B. F. Hobbs, M. H. Rothkopf, R. P. O'Neill, and H.-p. Chao, Eds. Boston: Kluwer Academic Publishers, 2002, vol. 36, pp. 1–14.

[62] H. Holttinen, M. Milligan, B. Kirby, T. Acker, V. Neimane, and T. Molinski, "Using standard deviation as a measure of increased operational reserve requirement for wind power," *Wind Engineering*, vol. 32, no. 4, pp. 355–377, Jun. 2008. [Online]. Available: http://dx.doi.org/10.1260/0309-524X.32.4.355

[63] H. Holttinen, P. Meibom, A. Orths, B. Lange, M. O'Malley, J. O. Tande, A. Estanqueiro, E. Gomez, L. Söder, G. Strbac, J. C. Smith, and F. van Hulle, "Impacts of large amounts of wind power on design and operation of power systems, results of IEA collaboration," *Wind Energy*, vol. 14, no. 2, pp. 179–192, Mar. 2011. [Online]. Available: http://onlinelibrary.wiley.com/doi/10.1002/we.410/abstract

[64] J. Hooker, *Logic-Based Methods for Optimization: Combining Optimization and Constraint Satisfaction*, 1st ed. Wiley-Interscience, May 2000.

[65] B. Hu, L. Wu, and M. Marwali, "On the robust solution to SCUC with load and wind uncertainty correlations," *IEEE Transactions on Power Systems*, vol. Early Access Online, 2014.

[66] R. Jiang, J. Wang, M. Zhang, and Y. Guan, "Two-stage minimax regret robust unit commitment," *IEEE Transactions on Power Systems*, vol. Early Access Online, 2013.

[67] R. Jiang, M. Zhang, G. Li, and Y. Guan, "Two-stage network constrained robust unit commitment problem," *European Journal of Operational Research*, vol. 234, no. 3, pp. 751–762, May 2014. [Online]. Available: http://www.sciencedirect.com/science/article/pii/S0377221713007832

[68] P. Kall and S. W. Wallace, *Stochastic programming*, 2nd ed., ser. Wiley-Interscience Series in Systems and Optimization. Chichester: John Wiley & Sons, Ltd., 1994. [Online]. Available: http://stoprog.org/index.html?introductions.html

[69] T. Koch, T. Achterberg, E. Andersen, O. Bastert, T. Berthold, R. E. Bixby, E. Danna, G. Gamrath, A. M. Gleixner, S. Heinz, A. Lodi, H. Mittelmann, T. Ralphs, D. Salvagnin, D. E. Steffy, and K. Wolter, "MIPLIB 2010," *Mathematical Programming Computation*, vol. 3, no. 2, pp. 103–163, Jun. 2011.

[70] J. Lee, J. Leung, and F. Margot, "Min-up/min-down polytopes," *Discrete Optimization*, vol. 1, no. 1, pp. 77–85, Jun. 2004.

[71] K. Leuven and T. Engineering, "Study of the interactions and dependencies of balancing markets, intraday trade and automatically activated reserves," Katholieke Universiteit Leuven (KULeuven) and Tractebel Engineering, Tech. Rep., 2009. [Online]. Available: http://ec.europa.eu/energy/gas_electricity/studies/doc/electricity/2009_balancing_markets.pdf

[72] T. Li and M. Shahidehpour, "Price-based unit commitment: a case of lagrangian relaxation versus mixed integer programming," *IEEE Transactions on Power Systems*, vol. 20, no. 4, pp. 2015–2025, Nov. 2005.

[73] Z. Li and M. Shahidehpour, "Security-constrained unit commitment for simultaneous clearing of energy and ancillary services markets," *Power Systems, IEEE Transactions on*, vol. 20, no. 2, pp. 1079–1088, 2005.

[74] C. Liu, M. Shahidehpour, Z. Li, and M. Fotuhi-Firuzabad, "Component and mode models for the short-term scheduling of combined-cycle units," *IEEE Transactions on Power Systems*, vol. 24, no. 2, pp. 976 –990, May 2009.

[75] A. Lodi, "Mixed integer programming computation," in *50 Years of Integer Programming 1958-2008*, M. Jünger, T. M. Liebling, D. Naddef, G. L. Nemhauser, W. R. Pulleyblank, G. Reinelt, G. Rinaldi, and L. A. Wolsey, Eds. Berlin, Heidelberg: Springer Berlin Heidelberg, 2010, pp. 619–645.

[76] A. Lotfjou, M. Shahidehpour, Y. Fu, and Z. Li, "Security-constrained unit commitment with AC/DC transmission systems," *Power Systems, IEEE Transactions on*, vol. 25, no. 1, pp. 531–542, 2010.

[77] B. Lu and M. Shahidehpour, "Unit commitment with flexible generating units," *Power Systems, IEEE Transactions on*, vol. 20, no. 2, pp. 1022–1034, 2005.

[78] ——, "Short-term scheduling of combined cycle units," *IEEE Transactions on Power Systems*, vol. 19, no. 3, pp. 1616 – 1625, Aug. 2004.

[79] S. Lu, C. A. McKinstry, A. J. Brothers, and S. Jin, "Low probability tail event analysis and mitigation in the BPA control area," Pacific Northwest National Laboratory, Texas - USA, Tech. Rep., Oct. 2010. [Online]. Available: http://www.pnl.gov/main/publications/external/technical_reports/PNNL-20120.pdf

[80] J. Matevosyan, "Real-time operations in ERCOT," 2014, personal correspondence.

[81] M. Matos, J. P. Lopes, M. Rosa, R. Ferreira, A. Leite da Silva, W. Sales, L. Resende, L. Manso, P. Cabral, M. Ferreira, N. Martins, C. Artaiz, F. Soto, and R. López, "Probabilistic evaluation of reserve requirements of generating systems with renewable power sources: The portuguese and spanish cases," *International Journal of Electrical Power & Energy Systems*, vol. 31, no. 9, pp. 562–569, Oct. 2009. [Online]. Available: http://www.sciencedirect.com/science/article/B6V2T-4W73H68-2/2/05a6af8b1097af984d9a5e2f96a89744

[82] P. Meibom, R. Barth, B. Hasche, H. Brand, C. Weber, and M. O'Malley, "Stochastic optimization model to study the operational impacts of high wind penetrations in ireland," *IEEE Transactions on Power Systems*, vol. 26, no. 3, pp. 1367–1379, Aug. 2011.

[83] M. Milligan, K. Porter, E. DeMeo, P. Denholm, H. Holttinen, B. Kirby, N. Miller, A. Mills, M. O'Malley, M. Schuerger, and L. Soder, "Wind power myths debunked," *Power and Energy Magazine, IEEE*, vol. 7, no. 6, pp. 89–99, 2009. [Online]. Available: 10.1109/MPE.2009.934268

[84] MISO, "Ramp capability for load following in the MISO markets," Midwest Independent Transmission System Operator, USA, Tech. Rep., Jul. 2011. [Online]. Available: https://www.midwestiso.org/_layouts/MISO/ECM/Redirect.aspx?ID=112806

[85] I. Momber, G. Morales-Espana, A. Ramos, and T. Gomez, "PEV storage in multi-bus scheduling problems," *IEEE Transactions on Smart Grid*, vol. 5, no. 2, pp. 1079–1087, Mar. 2014.

[86] J. Morales, A. Conejo, and J. Perez-Ruiz, "Economic valuation of reserves in power systems with high penetration of wind power," *Power Systems, IEEE Transactions on*, vol. 24, no. 2, pp. 900–910, 2009.

[87] G. Morales-España, J. M. Latorre, and A. Ramos, "Modeling start-up & shut-down ramps of thermal units in unit-commitment formulations," in *Workshop on Advanced Optimisation Methods and their Applications to Unit Commitment in Energy Management*, Paris, France, Nov. 2011, pp. 1–4.

[88] G. Morales-Espana, J. Garcia-Gonzalez, and A. Ramos, "Impact on reserves and energy delivery of current UC-based market-clearing formulations," in *European Energy Market (EEM), 2012 9th International Conference on the*, Florence, Italy, May 2012, pp. 1–7.

[89] G. Morales-España, J. Garcia-Gonzalez, and A. Ramos, "Tight and compact MILP formulation for the thermal unit commitment problem," in *PowerTech 2013*, Grenoble, Francia, Jun. 2013, (Invited Presentation).

[90] G. Morales-España, J. M. Latorre, J. Garcia-Gonzalez, and A. Ramos, "Tight and compact MILP formulations for unit commitment problems," in *FERC Technical Conference on Increasing Real-Time And Day-Ahead Market Efficiency Through Improved Software*, Washington D.C., USA, Jun. 2013, (Invited Presentation).

[91] G. Morales-Espana, J. M. Latorre, and A. Ramos, "Tight and compact MILP formulation for the thermal unit commitment problem," *IEEE Transactions on Power Systems*, vol. 28, no. 4, pp. 4897–4908, Nov. 2013.

[92] G. Morales-España, J. M. Latorre, and A. Ramos, "Tight and compact MILP formulation of start-up and shut-down ramping in unit commitment," in *2013 IEEE Power and Energy Society General Meeting*, Vancouver, Canada, Jul. 2013.

[93] G. Morales-España, R. Baldick, J. Garcia-Gonzalez, and A. Ramos, "Robust reserve modeling for wind power integration in day-ahead unit commitment," in *FERC Technical Conference on Increasing Real-Time And Day-Ahead Market Efficiency Through Improved Software*, Washington D.C., USA, Jun. 2014, (Invited Presentation).

[94] ——, "Robust reserve modeling for wind power integration in ramp-based unit commitment," in *ERCOT: KERMIT Summit*, Austin-Texas, USA, Mar. 2014, (Invited Presentation).

[95] G. Morales-Espana, R. Baldick, J. Garcia-Gonzalez, and A. Ramos, "Robust reserve modelling for wind power integration in ramp-based unit commitment," *IEEE Transactions on Power Systems*, 2014, under review.

[96] G. Morales-Espana, C. M. Correa-Posada, and A. Ramos, "Tight and compact MIP formulation of configuration-based combined-cycle units," *IEEE Transactions on Power Systems*, 2014, to be submitted.

[97] G. Morales-Espana, C. Gentile, and A. Ramos, "Tight MIP formulations of the power-based unit commitment problem," *Optimization Letters*, 2014, under Review. [Online]. Available: http://www.iit.upcomillas.es/aramos/papers/Power-UC_ConvexHull.pdf

[98] G. Morales-España, C. Gentile, and A. Ramos, "Accelerating the convergence of stochastic unit-commitment problems by using a tight and compact MIP formulation," in *20th Conference of The International Federation of Operational Research Societies*, Barcelona, Spain, Jul. 2014.

[99] G. Morales-Espana, A. Ramos, and J. Garcia-Gonzalez, "An MIP formulation for joint market-clearing of energy and reserves based on ramp scheduling," *IEEE Transactions on Power Systems*, vol. 29, no. 1, pp. 476–488, 2014.

[100] G. Morales-Espana, J. M. Latorre, and A. Ramos, "Tight and compact MILP formulation of start-up and shut-down ramping in unit commitment," *IEEE Transactions on Power Systems*, vol. 28, no. 2, pp. 1288–1296, 2013.

[101] Morales Juan Miguel, "Impact on system economics and security economics of a high penetration of wind power," Ph.D. dissertation, University of Castilla - La Mancha, Ciudad Real, Spain, Dec. 2010. [Online]. Available: www.uclm.es/area/gsee/tesis/Tesis_JMMorales.pdf

[102] G. L. Nemhauser and L. A. Wolsey, *Integer and combinatorial optimization.* New York: John Wiley and Sons, 1999.

[103] NERC, ""22:00" frequency excursion (final report)," NERC, Report 20020828, Aug. 2002. [Online]. Available: www.nerc.com/docs/oc/rs/FETF-Report_20020828.doc

[104] ——, "Accommodating high levels of variable generation," North American Electric Reliability Corporation, Tech. Rep., 2010. [Online]. Available: http://www.nerc.com/files/IVGTF_Report_041609.pdf

[105] ——, "Balancing and frequency control," North American Electric Reliability Corporation, Tech. Rep., Jan. 2011. [Online]. Available: http://www.nerc.com/docs/oc/rs/NERC%20Balancing%20and%20Frequency%20Control%20040520111.pdf

[106] ——, "Reliability standards for the bulk electric systems in north america," North American Electric Reliability Corporation, Tech. Rep., May 2011. [Online]. Available: http://www.nerc.com/files/Reliability_Standards_Complete_Set.pdf

[107] G. Nilssen, "Planned actions to remedy the weakning nordic frequency quality," Strategic System Operation Development, Tech. Rep. Cokument ID 1438187, Jun. 2010.

[108] M. Ortega-Vazquez and D. Kirschen, "Estimating the spinning reserve requirements in systems with significant wind power generation penetration," *Power Systems, IEEE Transactions on*, vol. 24, no. 1, pp. 114–124, 2009.

[109] J. Ostrowski, M. F. Anjos, and A. Vannelli, "Tight mixed integer linear programming formulations for the unit commitment problem," *IEEE Transactions on Power Systems*, vol. 27, no. 1, pp. 39–46, Feb. 2012.

[110] A. L. Ott, "Evolution of computing requirements in the PJM market: Past and future," in *2010 IEEE Power and Energy Society General Meeting*. IEEE, Jul. 2010, pp. 1–4.

[111] N. Padhy, "Unit commitment-a bibliographical survey," *IEEE Transactions on Power Systems*, vol. 19, no. 2, pp. 1196–1205, May 2004.

[112] A. Papavasiliou, S. S. Oren, and R. P. O'Neill, "Reserve requirements for wind power integration: A scenario-based stochastic programming framework," *IEEE Transactions on Power Systems*, vol. 26, no. 4, pp. 2197–2206, Nov. 2011.

[113] D. Rajan and S. Takriti, "Minimum Up/Down polytopes of the unit commitment problem with start-up costs," IBM, Research Report RC23628, Jun. 2005. [Online]. Available: http://domino.research.ibm.com/library/cyberdig.nsf/1e4115aea78b6e7c85256b360066f0d4/cdcb02a7c809d89e8525702300502ac0?OpenDocument

[114] A. Ramos, J. M. Latorre, F. Báñez, Á. Hernández, G. Morales-Espana, K. Dietrich, and L. Olmos, "Modeling the operation of electric vehicles in an operation planning model," in *17th Power Systems Computation Conference (PSCC'11)*, Stockholm, Sweden, Aug. 2011, pp. 1–7.

[115] A. Ramos, G. Morales-España, J. Garcia-Gonzalez, and M. Rivier, "Operation reserve usage for different unit time periods of a stochastic unit commitment," in *20th Conference of The International Federation of Operational Research Societies*, Barcelona, Spain, Jul. 2014.

[116] Y. G. Rebours, D. S. Kirschen, M. Trotignon, and S. Rossignol, "A survey of frequency and voltage control ancillary Services—Part i: Technical features," *Power Systems, IEEE Transactions on*, vol. 22, no. 1, pp. 350–357, 2007.

[117] ——, "A survey of frequency and voltage control ancillary Services—Part II: economic features," *Power Systems, IEEE Transactions on*, vol. 22, no. 1, pp. 358–366, 2007.

[118] G. Relaño, J. I. de la Fuente, T. Gómez, D. Soler, O. Largo, R. Martínez, and F. Apartero, "A linearization algorithm for hourly power scheduling in a competitive framework," in *Universities Power Engineering Conference (UPEC), Belfast, September*, 2000.

[119] E. Rothberg, "The CPLEX library: Presolve and cutting planes," in *4th Max-Planck Advanced Course on the Foundations of Computer Science (ADFOCS)*, Saarbrücken, Germany, Sep. 2003, pp. 1–17.

[120] P. A. Ruiz, C. R. Philbrick, E. Zak, K. W. Cheung, and P. W. Sauer, "Uncertainty management in the unit commitment problem," *Power Systems, IEEE Transactions on*, vol. 24, no. 2, pp. 642–651, May 2009.

[121] C. Sahin, M. Shahidehpour, and I. Erkmen, "Allocation of hourly reserve versus demand response for security-constrained scheduling of stochastic wind energy," *IEEE Transactions on Sustainable Energy*, vol. 4, no. 1, pp. 219–228, 2013.

[122] P. Sanchez-Martin, G. Sanchez, and G. Morales-Espana, "Direct load control decision model for aggregated EV charging points," *IEEE Transactions on Power Systems*, vol. 27, no. 3, pp. 1577–1584, Aug. 2012. [Online]. Available: http://dx.doi.org/10.1109/TPWRS.2011.2180546

[123] M. Shahidehpour, H. Yamin, and Z. Li, *Market Operations in Electric Power Systems: Forecasting, Scheduling, and Risk Management*, 1st ed. Wiley-IEEE Press, Mar. 2002.

[124] A. Shapiro, D. Dentcheva, and A. Ruszczynski, *Lectures on Stochastic Programming: Modeling and Theory*. SIAM-Society for Industrial and Applied Mathematics, Sep. 2009.

[125] C. Simoglou, P. Biskas, and A. Bakirtzis, "Optimal self-scheduling of a thermal producer in short-term electricity markets by MILP," *IEEE Transactions on Power Systems*, vol. 25, no. 4, pp. 1965–1977, Nov. 2010.

[126] J. Smith, M. Milligan, E. DeMeo, and B. Parsons, "Utility wind integration and operating impact state of the art," *Power Systems, IEEE Transactions on*, vol. 22, no. 3, pp. 900–908, 2007. [Online]. Available: 10.1109/TPWRS.2007.901598

[127] S. Stoft, *Power System Economics: Designing Markets for Electricity*, 1st ed. Wiley-IEEE Press, May 2002.

[128] M. Tahanan, W. van Ackooij, A. Frangioni, and F. Lacalandra, "Large-scale unit commitment under uncertainty: a literature survey," University of Pisa, Pisa, Italy, Technical Report TR-14-01, Jan. 2014. [Online]. Available: http://compass2.di.unipi.it/TR/Files/TR-14-01.pdf.gz

[129] S. Takriti, J. Birge, and E. Long, "A stochastic model for the unit commitment problem," *Power Systems, IEEE Transactions on*, vol. 11, no. 3, pp. 1497–1508, 1996.

[130] N. Troy, E. Denny, and M. O'Malley, "Base-load cycling on a system with significant wind penetration," *IEEE Transactions on Power Systems*, vol. 25, no. 2, pp. 1088–1097, May 2010.

[131] A. Tuohy, P. Meibom, E. Denny, and M. O'Malley, "Unit commitment for systems with significant wind penetration," *Power Systems, IEEE Transactions on*, vol. 24, no. 2, pp. 592–601, 2009.

[132] F. Vanderbeck and L. A. Wolsey, "Reformulation and decomposition of integer programs," in *50 Years of Integer Programming 1958-2008*, M. Jünger, T. M. Liebling, D. Naddef, G. L. Nemhauser, W. R. Pulleyblank, G. Reinelt, G. Rinaldi, and L. A. Wolsey, Eds. Berlin, Heidelberg: Springer Berlin Heidelberg, 2010, pp. 431–502.

[133] C. Wang and S. M. Shahidehpour, "Effects of ramp-rate limits on unit commitment and economic dispatch," *IEEE Transactions on Power Systems*, vol. 8, no. 3, pp. 1341–1350, Aug. 1993.

[134] J. Wang, M. Shahidehpour, and Z. Li, "Security-constrained unit commitment with volatile wind power generation," *Power Systems, IEEE Transactions on*, vol. 23, no. 3, pp. 1319–1327, 2008.

[135] ——, "Contingency-constrained reserve requirements in joint energy and ancillary services auction," *Power Systems, IEEE Transactions on*, vol. 24, no. 3, pp. 1457–1468, 2009.

[136] J. Wang, J. Valenzuela, A. Botterud, H. Keko, R. Bessa, and V. Miranda, "Reliability assessment unit commitment with uncertain wind power," in *Handbook of Wind Power Systems*, ser. Energy Systems, P. M. Pardalos, S. Rebennack, M. V. F. Pereira, N. A. Iliadis, and V. Pappu, Eds. Springer Berlin Heidelberg, Jan. 2013, pp. 3–20. [Online]. Available: http://link.springer.com.focus.lib.kth.se/chapter/10.1007/978-3-642-41080-2_1

[137] Q. Wang, J.-P. Watson, and Y. Guan, "Two-stage robust optimization for n -k contingency-constrained unit commitment," *IEEE Transactions on Power Systems*, vol. Early Access Online, 2013.

[138] T. Weissbach and E. Welfonder, "High frequency deviations within the european power system: Origins and proposals for improvement," in *Power Systems Conference and Exposition, 2009. PSCE '09. IEEE/PES*. IEEE, Mar. 2009, pp. 1–6.

[139] H. P. Williams, *Model Building in Mathematical Programming*, 5th ed. John Wiley & Sons Inc, Feb. 2013.

[140] L. Wolsey, "Strong formulations for mixed integer programs: valid inequalities and extended formulations," *Mathematical programming*, vol. 97, no. 1, p. 423–447, 2003.

[141] ——, "Strong formulations for mixed integer programming: A survey," *Mathematical Programming*, vol. 45, no. 1-3, pp. 173–191, Aug. 1989.

[142] ——, *Integer Programming*. Wiley-Interscience, 1998.

[143] A. J. Wood and B. F. Wollenberg, *Power Generation, Operation, and Control*, 2nd ed. Wiley-Interscience, Jan. 1996.

[144] H. Wu, Q. Zhai, X. Guan, F. Gao, and H. Ye, "Security-constrained unit commitment based on a realizable energy delivery formulation," *Mathematical Problems in Engineering*, vol. 2012, pp. 1–22, 2012.

[145] L. Wu, M. Shahidehpour, and T. Li, "Stochastic security-constrained unit commitment," *IEEE Transactions on Power Systems*, vol. 22, no. 2, pp. 800–811, May 2007.

[146] ——, "Cost of reliability analysis based on stochastic unit commitment," *Power Systems, IEEE Transactions on*, vol. 23, no. 3, pp. 1364–1374, 2008.

[147] L. Wu, M. Shahidehpour, and Z. Li, "Comparison of scenario-based and interval optimization approaches to stochastic SCUC," *Power Systems, IEEE Transactions on*, vol. 27, no. 2, pp. 913 –921, May 2012.

[148] L. Xie, P. Carvalho, L. Ferreira, J. Liu, B. Krogh, N. Popli, and M. Ilic, "Wind integration in power systems: Operational challenges and possible solutions," *Proceedings of the IEEE*, vol. 99, no. 1, pp. 214–232, 2011.

[149] H. Y. Yamin, "Review on methods of generation scheduling in electric power systems," *Electric Power Systems Research*, vol. 69, no. 2-3, pp. 227–248, May 2004.

[150] Y. Yang, J. Wang, X. Guan, and Q. Zhai, "Subhourly unit commitment with feasible energy delivery constraints," *Applied Energy*, 2012, to be published.

[151] C. Zhao and Y. Guan, "Unified stochastic and robust unit commitment," *IEEE Transactions on Power Systems*, vol. 28, no. 3, pp. 3353–3361, Aug. 2013.

[152] C. Zhao, J. Wang, J.-P. Watson, and Y. Guan, "Multi-stage robust unit commitment considering wind and demand response uncertainties," *IEEE Transactions on Power Systems*, vol. Early Access Online, 2013.

[153] L. Zhao and B. Zeng, "Robust unit commitment problem with demand response and wind energy," in *2012 IEEE Power and Energy Society General Meeting*, Jul. 2012, pp. 1–8.

Collection of JCR Papers

Contents

This appendix includes the collection of the current version of the papers, which were result of this doctoral thesis.

Article I

G. Morales-España, J. M. Latorre, and A. Ramos, "Tight and compact MILP formulation of start-up and shut-down ramping in unit commitment," *IEEE Transactions on Power Systems*, vol. 28, no. 2, pp. 1288–1296. May 2013. JCR 2012 data: impact factor 2.921 and 5-year impact factor 3.601.

Tight and Compact MILP Formulation of Start-Up and Shut-Down Ramping in Unit Commitment

Germán Morales-España, *Student Member, IEEE*, Jesus M. Latorre, *Member, IEEE*, and Andres Ramos

***Abstract*—This paper presents a mixed-integer linear programming (MILP) formulation of start-up (SU) and shut-down (SD) power trajectories of thermal units. Multiple SU power-trajectories and costs are modeled according to how long the unit has been offline. The proposed formulation significantly reduces the computational burden in comparison with others commonly found in the literature. This is because the formulation is 1) tighter, i.e., the relaxed solution is nearer to the optimal integer solution; and 2) more compact, i.e., it needs fewer constraints, variables and nonzero elements in the constraint matrix. For illustration, the self-unit commitment problem faced by a thermal unit is employed. We provide computational results comparing the proposed formulation with others found in the literature.**

***Index Terms*—Mixed-integer linear programming, start-up and shut-down ramps, thermal units, unit commitment.**

NOMENCLATURE

The main definitions and notation used are presented in this section for quick reference. Upper-case letters are used for denoting parameters and sets; and lower-case letters for variables and indexes.

Definitions: The following terminology is used in this paper to reference the different unit operation states, see Fig. 1.

online	Unit is synchronized with the system.
offline	Unit is not synchronized with the system.
up	Unit is producing above its minimum output. During the *up* state, the unit output is controllable.
down	Unit is producing below its minimum output, when *offline*, starting up or shutting down.

Indexes and Sets:

$l \in L$	Start-up type, running from 1 (hottest) to N_L (coldest).
$t \in T$	Hourly periods, running from 1 to N_T hours.

Variables:

e_t	Energy production during period t [MWh].
p_t	Power output at the end of period t, production above the minimum output [MW].
u_t	Commitment of the unit during period t $\{0,1\}$. Binary variable which is equal to 1 if the unit is up and 0 if it is down, see Fig. 1.
v_t	Start-up in period t $[0,1]$. Continuous variable which takes the value of 1 if the unit starts up in period t and 0 otherwise, see Fig. 1.
w_t	Shut-down in period t $[0,1]$. Continuous variable which takes the value of 1 if the unit shuts down in period t and 0 otherwise, see Fig. 1.
$\delta_{t,l}$	Start-up type l in period t $[0,1]$. Continuous variable which takes the value of 1 in the period where the unit starts up for the start-up type l and 0 otherwise.

Parameters:

EP_t	Forecasted price of energy in period t [$/MWh].
C^{LV}	Linear variable production cost [$/MWh].
C^{NL}	No-load cost [$/h].
C^{SD}	Shut-down cost [$].
C_l^{SU}	Start-up cost for the start-up type l [$].
$\overline{P}$	Maximum power output [MW].
$\underline{P}$	Minimum power output [MW].
P_i^{SD}	Power output at the beginning of the ith interval of the shut-down ramp process [MW], see Fig. 1.
$P_{l,i}^{SU}$	Power output at the beginning of the ith interval of the start-up ramp process type l [MW], see Fig. 1.
P_l^{syn}	Power output at which the unit is synchronized for start-up type l [MW], $P_{l,1}^{SU} = P_l^{syn}$, see Fig. 1.
SD^D	Duration of the shut-down ramp process [h].
SU_l^D	Duration of the start-up type l ramp process [h].
RD	Maximum ramp-down rate [MW/h].
RU	Maximum ramp-up rate [MW/h].
TD	Minimum down time [h].
TU	Minimum up time [h].
T_l^{SU}	Minimum number of periods that the unit must be down for the start-up type l [h].

Manuscript received January 26, 2012; revised February 20, 2012, June 10, 2012, and August 20, 2012; accepted September 29, 2012. Date of publication November 29, 2012; date of current version April 18, 2013. Paper no. TPWRS-00080-2012.

The authors are with the Institute for Research in Technology (IIT), School of Engineering (ICAI), Universidad Pontificia Comillas, Madrid, Spain (e-mail: german.morales@iit.upcomillas.es; gmorales@kth.se; jesus.latorre@iit.upcomillas.es; andres.ramos@upcomillas.es).

Color versions of one or more of the figures in this paper are available online at http://ieeexplore.ieee.org.

Digital Object Identifier 10.1109/TPWRS.2012.2222938

I. INTRODUCTION

THE actual operation of power generation units must be considered in detail in order to rigorously model their generation schedules. Moreover, with the introduction of competi-

tion, accurate modeling and solutions for unit commitment (UC) problems are even more necessary to achieve efficiency and feasibility in energy production [1].

Most of the literature about modeling constraints of thermal units in UC problems deals with the unit operation above the minimum output [2], [3]. Units are considered to start/end their production at the minimum output while the start-up (SU) and shut-down (SD) ramps (or power trajectories) are ignored. Some papers are aware of the importance of considering these ramps in the UC optimization problem. However, they do not include these ramps because the resulting model will be considerably more complex, causing prohibitive solving times [4]–[6]. In addition, due to the increasing penetration of wind generation nowadays, thermal units are being shut down and started up more often [7]; therefore, a detailed modeling of the SU and SD processes in UC is required.

The application of direct mixed-integer linear programming (MILP) to solving UC is becoming increasingly popular due to improvements in MILP solvers. For example, PJM has switched from Lagrangian relaxation (LR) to MILP to solve the UC-based problems [8]. LR was the dominant optimization technique for solving UC problems through problem decomposition, mainly because LR does not present a high memory requirement as does MILP. However, this problem is being overcome due to the breakthrough of MILP solvers. Currently, combination of pure algorithmic speedup and the progress in computing machinery has meant that solving MILPs has become around 100 million times faster over the last 20 years [9]. Furthermore, MILP provides significant advantages over LR such as the fact that 1) there is a proven global optimal solution and 2) MILP models are easier to modify, which enhances modeling capabilities and adaptability, among other things [1], [10], [11].

The SU and SD ramps are explicitly modeled under the LR approach in [12] and under the MILP framework in [13] and [11]. In [12] and [13], only a single power trajectory for the SU process is modeled, while [11] considers different SU power trajectories depending on the unit's prior down time. Furthermore, [11] proposes a complete self-UC formulation which takes into account different constraints (e.g., power reserves and quadratic production costs) and is adapted to the Greek market rules.

References [13] and [11] made the important contribution in proposing the first MILP formulations for single and multiple SU and SD ramps, respectively. However, their main drawback is the creation of large models which greatly increase the complexity of UC problems, thereby making them unattractive for practical implementation. These models are large due to the introduction of many constraints in order to deal with the power trajectories above and below the minimum output of generating units. Apart from this, [11] needs many binary variables to model the different SU power trajectories.

The use of MILP-based UC formulations has increased significantly over the last 50 years [14]. As computational and algorithmic power increases, so does the complexity of the MILP formulations, with the addition of features such as ramping constraints, minimum up and down times and exponential SU costs [2]. The computational burden of UC problems needs to be further reduced, by improving the MILP formulations, so that even more advanced and computationally demanding problems can be implemented, such as stochastic formulations [15], contingency-constrained models [16], and generation expansion planning [17].

Improving an MILP formulation allows a faster search for optimality by tightening (removing inefficient solutions from) the original feasible region. Tightening requires strong lower bounds for minimization problems [18]. This means formulating the problem in such a way that the associated linear programming (LP) relaxation provides a better approximation of the value of the integer optimal solution. The time required for providing optimality is often prohibitive because the gap between the integer optimal solution and its associated LP relaxation is very large. Furthermore, a poor lower bound provided by the LP relaxation will not be adequate to guide the search for good feasible solutions during the solving phase (branch-and-cut) of standard MILP solvers [19]. MILP formulations are frequently tightened by adding a huge number of constraints and (sometimes) variables. However, the resulting expanded model must close the gap enough to be worth the extra time taken to solve the LP relaxations during the solving phase [20]. In other words, usually, tightening an MILP formulation comes at the expense of expanding the model which implies extra time consumption. Therefore, creating tight and compact MILP formulations is a nontrivial task because the obvious formulations are commonly either very weak or very large.

Creating tight (or strong) MILP formulations has been widely researched [21]. In the case of UC problems, there has been work in a number of specific areas. In [22], a strong formulation of the minimum up/down time constraints is presented; in [23], a tighter linear approximation for quadratic generation costs is proposed; and [24] presents a new class of inequalities giving a tighter description of the feasible operating schedules for generators.

The main contribution of this paper is two-fold:

1) A tighter MILP formulation of SU and SD ramps for UC problems is proposed in order to reduce the computational burden of analogous existent MILP formulations.
2) This MILP formulation is also compact and hence overcoming the main disadvantage of previous models [11], [13]. If a single power trajectory is modeled for the SU and SD ramps, then there is neither a need to increase the number of constraints nor a necessity to increase the number of variables in comparison to a formulation without the SU and SD ramps. Furthermore, when considering different SU trajectories, the proposed formulation requires the introduction of merely continuous variables compared to [11].

Additionally, this formulation of SU and SD ramps is suitable for any UC problem, whether under centralized or competitive environments, and further model expansion will not require the introduction of numerous terms in the constraints in order to avoid conflicts between the up and down states, unlike [13] and [11].

In order to illustrate the effectiveness of the proposed formulation, the self-UC for a price-taker thermal generator is used. The objective of a thermal generator, in the self-UC, is to maximize the profits from selling energy in the day-ahead market, while satisfying all the technical constraints.

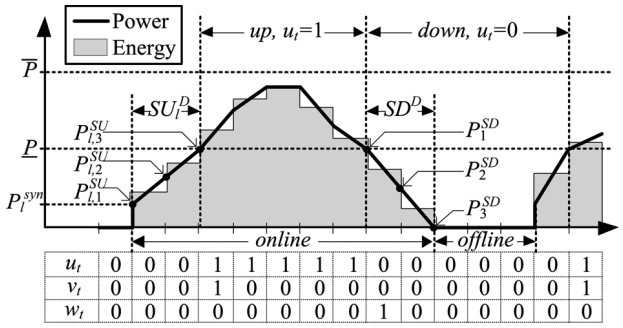

Fig. 1. Operation states of a thermal unit, including SU and SD ramps.

The remainder of this paper is organized as follows: Section II presents the formulation of the SU and SD constraints in detail. Section III provides and discusses results from several case studies, where the impact of neglecting the SU and SD ramps is shown and a comparison of the proposed formulation with those in [13] and [11] is made. Finally, some relevant conclusions are drawn in Section IV.

II. Proposed Approach

This section presents the mathematical formulation of the SU and SD power trajectories. With the purpose of illustrating how this formulation works, the objective function is formulated for the case of a price taker self-UC problem. This section is divided into two parts: Section II-A details the mathematical formulation and Section II-B shows how the online and offline unit states can be obtained (see Fig. 1) after the optimization problem has been solved.

Hourly time intervals are considered, but it should be noted that the formulation can be easily adapted to handle shorter time periods. For the sake of simplicity, reserve constraints are not considered; however, they can be easily introduced in the model. The interested reader is referred to [5], [11], and [25].

A. Mathematical Formulation

The different operation states of a thermal unit are presented in Fig. 1. The up and down states are distinguished from the online and offline states. During the up period, the unit has the flexibility to follow any trajectory being bounded between the maximum and minimum output and by the ramping-rate limits. On the other hand, the power output when the unit is starting up or shutting down follows a predefined power trajectory. Unlike the SD ramp, the SU ramp trajectory depends on the unit's previous down time.

1) Up/Down versus Online/Offline States: By considering the commitment variable u_t as up/down rather than offline/online states, the generation output above and below $\underline{P}$ can be managed independently. This characteristic makes the proposed formulation 1) compact, unlike [13] and [11], where most of the constraints involving p_t contain summations of binary variables in order to avoid conflicts between the power output above and below $\underline{P}$; and 2) tight where, by considering the generation output (p_t) above $\underline{P}$, the feasible region for p_t is between $\underline{P}$ and $\overline{P}$, which is tighter than the region that is usually considered, between 0 and $\overline{P}$.

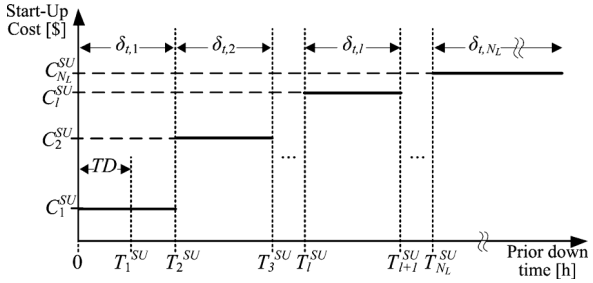

Fig. 2. Start-up costs as a function of the unit's previous down time.

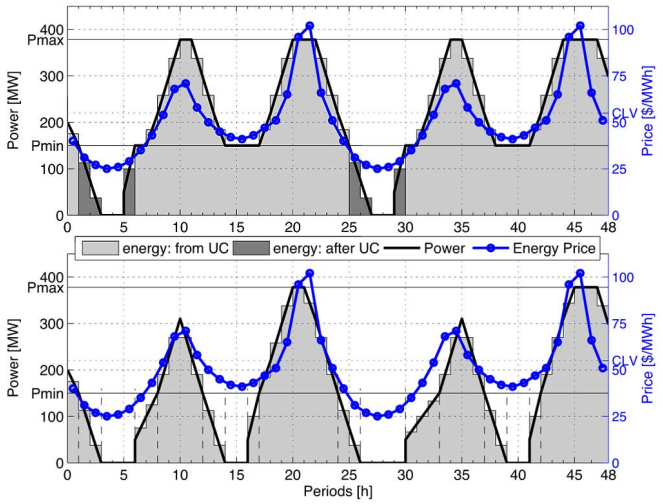

Fig. 3. Optimal generation scheduling for the *Traditional* and *Improved* formulations in the up and bottom part of the figure respectively. The darker gray area shows the SU and SD energy that the unit will produce in order to follow the optimal schedule that results from the *Traditional* formulation (this extra energy is added after solving the *Traditional* problem).

The down times are a function of the offline times (see Fig. 1). For example, the number of periods that the unit must be down to activate the SU type l, T_l^{SU}, is equal to the SU and SD ramp durations (SU_l^D and SD^D) plus the offline time required to activate the SU type l. Similarly, the down time TD is expressed as a function of the minimum offline time (see Section II-A3).

2) Start-Up Type: Different SU types are modeled depending on how long the unit has been down. The SU type $\delta_{t,l}$ is selected if the unit has been previously down within the interval $\left[T_l^{SU}, T_{l+1}^{SU}\right)$, see Fig. 2. Each SU type has a different SU power trajectory associated to it, where the colder the SU type, the longer the SU power trajectory duration (see example shown in Fig. 3 in Section III-A). As in the case of [26] and [11], new variables are introduced to select the SU type:

$$\delta_{t,l} \leq \sum_{i=T_l^{SU}}^{T_{l+1}^{SU}-1} w_{t-i} \quad \forall t \in \left[T_{l+1}^{SU}, N_T\right],\ l \in [1, N_L) \qquad (1)$$

where the right side of (1) is equal to 1 if the unit has been down within the interval $\left[T_l^{SU}, T_{l+1}^{SU}\right)$ before hour t. Therefore, $\delta_{t,l}$ can only be activated $(\delta_{t,l} \leq 1)$ if the unit has previously been down within this interval.

Note that (1) is not defined for the first hours. Appendix A details how the first SU types $\delta_{t,l}$ are obtained depending on the initial conditions of the unit.

The following constraint ensures that just one SU type is selected when the unit starts up:

$$\sum_{l=1}^{N_L} \delta_{t,l} = v_t \quad \forall t. \tag{2}$$

Equation (1) constrains all SU types except the coldest one δ_{t,N_L}. However, constraints (1) and (2) ensure $\delta_{t,N_L} = 1$ when the unit starts up $(v_t = 1)$, and has been down for at least $T^{SU}_{N_L}$ hours. This is because (1) makes $\delta_{t,l} = 0$ for all $l \neq N_L$ and then (2) forces $\delta_{t,N_L} = 1$. In the event that more than one SU type variable can be activated $(\delta_{t,l} \leq 1)$ then (2) together with the objective function ensure that the hottest, which is the cheapest, possible option is always selected. Therefore, just one of the variables is activated (equal to one). That is, these variables take binary values even though they are modeled as continuous variables. This is due to the convex (monotonically increasing) characteristic of the exponential SU costs of thermal units [2], see Fig. 2.

Constraint (1) is made even more compact by taking into account the minimum down time constraint (see Section II-A3). The hottest SU $\delta_{t,1}$ must be activated when the unit has been down within the interval $\left[0, T_2^{SU}\right)$. However, the minimum down time constraint (4) ensures that the unit cannot be down for less than TD hours. Therefore, the hottest SU is only possible within the interval $\left[TD, T_2^{SU}\right)$. By defining $T_1^{SU} = TD$, see Fig. 2, constraint (1) together with the minimum down time constraint (4) ensure that the hottest SU $\delta_{t,1}$ can be activated only when the unit has been down less than T_2^{SU} hours.

3) Minimum Up/Down Times: Constraints (3) and (4) ensure the minimum up and down times respectively [22]. This formulation has been compared with others and has shown a better performance [22], [24]:

$$\sum_{i=t-TU+1}^{t} v_i \leq u_t \quad \forall t \in [TU, N_T] \tag{3}$$

$$\sum_{i=t-TD+1}^{t} w_i \leq 1 - u_t \quad \forall t \in [TD, N_T]. \tag{4}$$

The minimum down time TD in (4) is equal to 1) the SD ramp duration (SD^D), plus 2) the hottest SU ramp duration (SU_1^D), plus 3) the minimum time that the unit must be offline. Therefore, (4) is needed to avoid overlapping between the SU and SD ramps. Appendix A describes how the initial conditions force the unit to remain up/down during the first hours.

4) Commitment, Start-Up, and Shut-Down: The following constraint can be found in models published approximately fifty years ago [14]:

$$u_t - u_t = v_t - w_t \quad \forall t. \tag{5}$$

Once u_t is defined as a binary variable, (5) forces v_t and w_t to take binary values.

5) Capacity Limits: The generation level in UC problems is usually expressed as hourly energy blocks; however, it has been demonstrated that taking a generation level schedule as an energy delivery schedule may not be realizable [27], [28]. Therefore, a clear difference between power and energy is made and all technical constraints are then imposed over the power output variable. The power generation output of the unit above its minimum output is modeled as

$$0 \leq p_t \leq \left(\overline{P} - \underline{P}\right)(u_t - w_{t+1}) \quad \forall t. \tag{6}$$

Constraint (6) ensures that the total power output is equal to $\underline{P}$ $(p_t = 0)$ at the beginning and at the end of a continuous up period. On the other hand, the SU (SD) trajectory ends (begins), during the down period, at $\underline{P}$ level, thereby making the connection with the up period that starts (ends) at this level, see Fig. 1.

6) Operating Ramp Constraints: As mentioned in Section II-A1, the proposed formulation avoids the introduction of many variables in most of the equations, unlike [13] and [11]. This is the case for the ramping constraints that only depend on the generation variables between two consecutive hours:

$$-RD \leq p_t - p_{t-1} \leq RU \quad \forall t. \tag{7}$$

7) Energy Production: The total unit's energy production, including the energy produced during the SU and SD processes, is presented in (8). Note that the energy is obtained for hourly periods and piecewise-linear power trajectories (see Fig. 1). However, the conversion to shorter time periods is straightforward:

$$\begin{aligned} e_t = {} & \underline{P} u_t + \frac{p_t + p_{t-1}}{2} \\ & + \sum_{i=1}^{SD^D} \frac{P^{SD}_{i+1} + P^{SD}_{i}}{2} w_{t-i+1} \\ & + \sum_{l=1}^{N_L} \sum_{i=1}^{SU_l^D} \frac{P^{SU}_{l,i+1} + P^{SU}_{l,i}}{2} \delta_{\left(t-i+SU_l^D+1\right),l} \quad \forall t. \end{aligned} \tag{8}$$

The terms of the summations in (8) include the energy produced during the SU and SD procedures.

Equation (8), together with (1) and (2), make a tight description of the SU and SD ramps in the energy output variable e_t. This could be observed from the fact that on the one hand, when the unit is starting up $(v_t = 1)$, (1) and (2) will choose the correct SU type $(\delta_{t,l})$, and then the associated SU energy trajectory is immediately fixed in (8), while on the other hand, when the unit is not starting up $(v_t = 0)$ then (2) forces all SU types to be zero $(\delta_{t,l} = 0)$ and thus the SU energy in (8) is immediately fixed to zero. Similarly, the SD decision (w_t) will fix the SD energy trajectory in (8). Besides, the tightness of the formulation is experimentally checked in Section III, where the integrality gap of the proposed formulation is lower than those in [13] and [11].

Note that when just a single SU power trajectory is modeled, there is no need to introduce variables $\delta_{t,l}$. Therefore, constraints (1) and (2) are not needed and the scheduled energy in (8) must be modified to be directly affected by the SU variable v_t instead of $\delta_{t,l}$.

8) Objective Function: The goal of a price-taker producer in a self-UC is to maximize his profit during the planning period,

which is the difference between the revenue and the total operating cost (9). For the sake of simplicity, a linear production cost is used in this paper:

$$\max \sum_{t=1}^{N_T} \Bigg[EP_t e_t - \Bigg(C^{NL} u_t + C^{LV} e_t + \sum_{l=1}^{N_L} C_l^{SU'} \delta_{t,l} + C^{SD'} w_t \Bigg) \Bigg]. \quad (9)$$

Note that the no-load cost (C^{NL}) considered in (9) ignores the SU and SD periods. This is because the C^{NL} only multiplies the commitment during the up state u_t. In order to consider the no-load cost during the SU and SD periods, $C_l^{SU'}$ and $C^{SD'}$ are introduced in (9) and defined as

$$C_l^{SU'} = C_l^{SU} + C^{NL} SU_l^D \quad \forall l \quad (9a)$$

$$C^{SD'} = C^{SD} + C^{NL} SD^D. \quad (9b)$$

B. Final Power Schedule

The complete energy profile, including SU and SD power trajectories, was presented in (8). Nevertheless, the complete power output as well as the unit states online/offline have not yet been obtained. This information can be explicitly modeled as variables in the optimization problem, which will create a considerably larger formulation. However, these values can be obtained after the optimization problem has been solved without changing the optimal results and then with negligible computational cost. Furthermore, this also contributes to the compactness of the formulation. The total power output P_t, and online/offline states U_t^{ON} are presented as follows:

$$P_t = \underline{P}\,(u_t + v_{t+1}) + p_t + \sum_{i=2}^{SD^D+1} P_i^{SD} w_{t-i+2} + \sum_{l=1}^{N_L} \sum_{i=1}^{SU_l^D} P_i^{SU} \delta_{\left(t-i+SU_l^D+2\right),l} \quad \forall t \quad (10)$$

$$U_t^{ON} = u_t + \sum_{l=1}^{N_L} \sum_{i=1}^{SU_l^D} \delta_{(t-i+SU^D+1),l} + \sum_{i=1}^{SD^D} w_{t-i+1} \quad \forall t. \quad (11)$$

Furthermore, analogously to the SU and SD decisions v_t and w_t which represent the changes between the up and down states, the turn-on V_t^{ON} and turn-off W_t^{OFF} decisions representing the changes between the online and offline states are now obtained with

$$V_t^{ON} = \sum_{l=1}^{N_L} \delta_{\left(t+SU_l^D\right),l} \quad \forall t \quad (12)$$

$$W_t^{OFF} = w_{t-SD^D} \quad \forall t. \quad (13)$$

TABLE I
THERMAL UNIT DATA

Technical Information					Cost Coefficients		
$\overline{P}$ [MW]	$\underline{P}$ [MW]	RU/RD [MW/h]	TU/TD [h]	SD^D [h]	C^{NL} [$]	C^{LV} [$/MWh]	C^{SD} [$]
378.0	150.0	80	4	2	200	55	20

Start-Up Ramping Information				
SU Type l	C_l^{SU} [$]	P_l^{syn} [MW]	SU_l^D [h]	T_l^{SU} [h]
01	16	50	1	4
02	28	50	2	6
03	36	50	3	8
04	40	50	4	11
05	41	50	5	14

III. TEST RESULTS

The proposed formulation is tested for the self-UC of a price-taker producer. The technical and economic data for the thermal unit, including five different SU ramps, are presented in Table I, and the expected electricity prices for a 48-hour time span are shown in Appendix B. These data are based on information presented in [11]. The power outputs $P_l^{SU}(P^{SD})$ for the SU (SD) power trajectories are obtained as an hourly linear change from $P_l^{syn}(\underline{P})$ to $\underline{P}$ (0) for a duration of $SU_l^D(SD^D)$ hours, see Fig. 1. With respect to initial conditions, the unit has been up for 6 hours before the scheduling horizon and its initial power output is 200 MW. All tests in this paper were carried out using CPLEX 12.3 under GAMS [29] on an Intel i7 2.4-GHz personal computer with 4 GB of RAM memory. Problems are solved to optimality, more precisely to 1e-6 of relative optimality tolerance.

This section is divided into two parts. The first part shows the impact of SU and SD ramps on the unit commitment. The second part presents a comparison of the proposed formulation with those presented in [13] and [11].

A. Scheduling and Economic Impact

In order to illustrate how the unit operation is affected if the SU and SD ramps are considered, the case study has been solved with and without the ramp trajectories. The formulation with SU and SD ramps is labeled as *Improved* and the formulation considering just the exponential-SU and SD costs is labeled as *Traditional*.

Unlike the *Traditional* formulation, considering the energy produced during the SU and SD ramps makes the *Improved* formulation perceive revenues during these ramping processes. To make a fair comparison between both formulations, the inherent energy produced during the SU and SD ramps is introduced into the *Traditional* formulation after the problem has been solved (see darker gray area in Fig. 3). That is, even when the *Traditional* formulation ignores these ramps in the scheduling stage, they are inevitably present during the operation stage. Subsequently, this energy can be added to the solution and this extra energy can also be sold. The total revenues for the *Traditional* formulation are then obtained by adding the revenues obtained from the UC solution to the revenues obtained from the energy produced during the SU and SD processes. These latter revenues

TABLE II
PRODUCER COSTS AND PROFITS

	Costs ($)	Revenues ($)	Profits ($)
Traditional	576417	617252	40835
Improved	402201	461674	59473
% of change	-30.22	-25.20	45.64

are calculated by multiplying the electricity price by the energy produced during the SU and SD ramps.

Fig. 3 and Appendix B show the optimal power and energy schedules for the *Traditional* and *Improved* formulations. Note the different duration of the SU power trajectories for the *Improved* formulation in Fig. 3. SU durations of one, two and three can be observed (starting at hours 16, 6, and 30, respectively) as a consequence of the different unit's down (and thus offline) time durations.

The optimal scheduling decision taken by the *Traditional* formulation around hours 15–17 and 39–41 was to produce at minimum output $\underline{P}$ (P_{min} in Fig. 3) even when electricity prices were lower than the unit's linear variable production cost C^{LV} (CLV in Fig. 3). This is a very common behavior, where producing at $\underline{P}$ generates fewer losses than shutting down and starting up the unit within a short period. On the other hand, when SU and SD ramps are considered, the optimal scheduling decision is to turn off the unit during these hours. The reason is that the SU and SD costs are offset by the revenues received from the energy produced during the SU and SD ramping processes. In short, unlike the *Improved* formulation, in the *Traditional* model, the SU and SD processes are perceived as pure losses. Therefore, the optimal decision of the *Traditional* UC formulation is to not turn off the unit for short periods to avoid these losses.

The main problem affecting the *Traditional* formulation is that revenues during the SU and SD processes are not considered in the optimization problem. Therefore, there is a tendency to produce at least at minimum output, even when electricity prices are lower than C^{LV}, and thus obtain some revenues that compensate for the losses. This drawback is overcome by considering the SU and SD power production in the formulation.

Table II shows the difference between costs, revenues and profits for the solutions of both formulations. As mentioned before, the total revenue for the *Traditional* model is obtained by adding the revenues due to the ramping process ($14 800) to the revenues obtained from the optimal solution ($602 452). For this illustrative case, the profits when considering the SU and SD ramps are around 46% higher than when these ramps are not taken into account.

B. Comparing Different Formulations

The proposed formulation is compared with those available in [13] and [11]. Reference [13] proposes a formulation to deal with a single SU and SD ramp trajectory, whereas [11] deals with different SU trajectories depending on the unit's prior down time. The different SU types, their associated costs and power-trajectories are inherent characteristics of thermal units and these data are provided by the manufacturer. However, in order to compare the different formulations, the proposed formulation is implemented considering one, three and five different SU ramp types, and these models are labeled as R1, R3, and R5, respectively. The single ramp type model R1 can be directly compared with the single-ramp formulation proposed in [13]. The model presented in [11] was implemented considering three SU ramp types, and hence it can be directly compared with R3. Model R5 is presented in order to observe the extra computational burden which results from considering extra SU ramp trajectories.

In order to assess the impact of the problem size on the computational performance of the models, several case studies of different sizes were solved. The price profile of one day (see Appendix B) has been replicated over different time spans from 4 to 256 days (each case is solved in one step for the complete time span). The unit data are presented in Table I, where the information for the single-ramp models (R1 and [13]) is the SU ramp type 02, the three-ramp models (R3 and [11]) are the first three SU types, and the five-ramp model (R5) are the five SU types.

1) Assumptions for the Formulations: In order to compare all the formulations, [13] and [11] were implemented using the same objective function and the same set of constraints as the formulation presented in Section II. Therefore, all the models are characterizing the same problem; the difference between them is how the constraints are formulated. In other words, two models considering the same SU types (R3 and [11], or R1 and [13]) obtain the same optimal results, e.g., commitments, generating outputs and profits.

The distinction between power and energy was made when implementing [13] and [11]. Additionally, as modeled here, the (usual) power variable is considered to be the power at the end of the period; and the energy is obtained by applying a piecewise-linear power profile. [11] was implemented with the same minimum up/down constraints presented in Section II-A3 as those are the constraints they also use. The synchronization time was set to zero in [11] as we believe this time does not need to be explicitly modeled, thus making the formulation simpler. That is to say, the synchronization time can be considered as a part of the offline time and obtained after the problem has been solved, without changing the optimal results (similar to the turn-on state presented in Section II-B). Finally, the other constraints presented in [11], which are not related to the SU and SD ramps, were not implemented (e.g., quadratic production costs and different power reserves).

Table III presents the optimal solutions for all the models for different time spans. As expected, the optimal solution for models R1 and [13] are the same, as well as the solution for models R3 and [11]. Interestingly, model R5, which considers five ramp types, also presents the same solution as R3 and [11]. This is because, in R5, ramp types 04 and 05 were never activated for this example case because the unit was not down for long enough. As in the case of the difference between R1 and R3 (see Table III), if the five different ramps had been activated in R5, this would have decreased the operational costs in comparison with R3 because more flexibility is possible (more SU ramp types).

1) Problem Size: Table III shows the dimension of all the models for the different case studies. Models R1 and [13] have the same number of variables, but [13] presents three times as many binary variables as R1. This is because [13] defines the

TABLE III
COMPARISON OF DIFFERENT FORMULATIONS

Case	Problem Size																			
	# of Constraints					# of Real Variables					# of Binary Variables				Nonzero elements				
(# of days)	R1	[13]	R3	[11]	R5	R1	[13]	R3	[11]	R5	R1	[13]	R3&R5	[11]	R1	[13]	R3	[11]	R5
4	668	1444	944	2395	1113	384	192	657	382	824	96	288	96	1540	3131	7515	4576	15050	6352
16	2684	5764	3824	9595	4569	1536	768	2673	1534	3416	384	1152	384	6148	12635	30267	18688	75808	26512
64	10748	23044	15344	38395	18393	6144	3072	10737	6142	13784	1536	4608	1536	24580	50651	121275	75136	318880	107152
256	43004	92164	61424	153595	73689	24576	12288	42993	24574	55256	6144	18432	6144	98308	202715	485307	300928	1291168	429712

Case	Computational Performance														
	Optimal Solution ($)		Integrality Gap (%)					# of Nodes					CPU Time (s)				
(# of days)	R1&[13]	R3,R5&[11]	R1	[13]	R3	[11]	R5	R1	[13]	R3	[11]	R5	R1	[13]	R3	[11]	R5
4	120250.5	118899.5	15.61	29.06	16.18	27.56	15.97	0	64	14	453	21	0.047	0.234	0.125	1.264	0.109
16	486382.5	475459.4	14.76	28.71	16.53	29.78	16.48	0	550	477	473	604	0.156	3.494	1.545	6.474	2.013
64	1950910.5	1901699.2	14.56	28.62	16.62	30.33	16.60	0	496	508	498	488	0.998	16.255	7.956	37.908	8.565
256	7809022.5	7606658.5	14.50	28.60	16.64	30.47	16.63	0	483	467	490	494	10.405	84.599	48.422	268.665	53.181

SU and SD variables as binary; however, they can be considered as continuous variables (see Section II-A4). The formulation in [13] also requires more than twice the quantity of constraints and nonzero elements than the proposed formulation R1.

As shown in Table III, [11] presents about 16 times more binary variables than the proposed formulation R3. Models R3 and R5 have more real variables than [11]. However, the total number of variables in R3 and R5 is smaller than the number of binary variables in [11]. R3 and R5 also present less than half the number of constraints than [11]. Furthermore, [11] presents up to 4.3 and 3 times more nonzero elements than R3 and R5 respectively. Similarly to [11], [13] needs these extra variables and nonzero elements to deal with the different SU ramp types and to avoid conflicts between the up and down states.

Note that model R5 is slightly larger than R3, with respect to the number of variables and constraints, because R5 considers two more ramp types than R3. This also shows that the compact formulation does not increase considerably when considering more SU types.

2) Computational Performance: Apart from the compactness of the proposed MILP formulation, the tightness has a significant impact on the computational performance, as mentioned in the Introduction. In fact, a compact formulation usually presents a weak LP relaxation that can dramatically increase the MILP resolution time. The tightness of an MILP can be measured with the integrality gap [24]. The integrality gap, for a maximization problem, is defined as $(Z_{LP} - Z_{MILP})/Z_{MILP}$, where Z_{LP} is the optimal value of the relaxed LP problem, and Z_{MILP} is the best integer solution found after the MILP problem is solved.

Table III shows the integrality gaps for the different formulations. Compared to [13], the proposed single-ramp formulation R1 has improved (reduced) the integrality gap between 46% and 49%. Similarly, with respect to [11], R3 improves the integrality gap between 41% and 45%. Table III also shows the nodes explored during the branch-and-cut phase; these are usually decreased with tighter formulations. Note that, for all the different cases, CPLEX was able to solve R1 with the required optimality tolerance without needing to branch, because the nodes were pruned earlier by the initial heuristics and cuts applied. Apart from the number of nodes, the performance of an MILP formulation is dramatically affected by the use of heuristics and cuts, and all of these are influenced by the tightness of the formulation [19]. Therefore, we will only comment about CPU times which offer a more complete view of the model's performance.

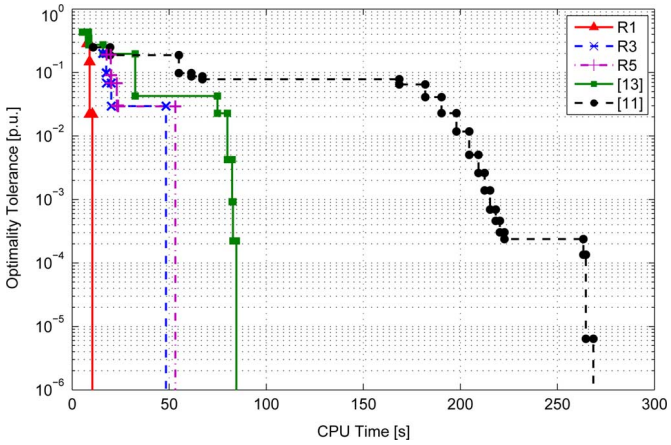

Fig. 4. Convergence evolution until low optimality tolerances for the different formulations.

The CPU times for the different case studies are presented in Table III, where R1 and R3 are up to 22.4 and 10.1 times faster than [13] and [11], respectively. This significant speed up is due to the simultaneous tightness and compactness of the proposed formulation. It is interesting to note that the formulation in [13], which models a single ramp trajectory and does not take into account exponential SU costs, is a larger model (presents more constraints and nonzero elements) and also requires more time to solve the problem than R5, which considers five different SU ramps and also exponential SU costs.

Finally, Fig. 4 shows the convergence evolution for the different formulations to small optimality tolerances for the case study of 256 days. The proposed formulation converges significantly faster than [13] and [11]. This is mainly due to its tightness.

IV. CONCLUSIONS

This paper presented an MILP formulation of the SU and SD power trajectories of thermal units. This formulation is si-

TABLE IV
PRICE DATA AND OPTIMAL GENERATION SCHEDULE

t	EP_t \$/MWh	p_t^I MW	e_t^I MWh	p_t^T MW	e_t^T MWh	t	EP_t \$/MWh	p_t^I MW	e_t^I MWh	p_t^T MW	e_t^T MWh	t	EP_t \$/MWh	p_t^I MW	e_t^I MWh	p_t^T MW	e_t^T MWh	t	EP_t \$/MWh	p_t^I MW	e_t^I MWh	p_t^T MW	e_t^T MWh
0	—	200	—	200	—	—	—	—	—	—	—	—	—	—	—	—	—	—	—	—	—	—	—
1	40	150	175	150	175	13	50	75	112.5	218	258	25	40	75	112.5	150	184	37	50	150	190	218	258
2	31	75	112.5	(75)	(112.5)	14	45	0	37.5	150	184	26	31	0	37.5	(75)	(112.5)	38	45	75	112.5	150	184
3	27	0	37.5	(0)	(37.5)	15	42	0	0	150	150	27	27	0	0	(0)	(37.5)	39	42	0	37.5	150	150
4	25	0	0	0	0	16	41	50	0	150	150	28	25	0	0	0	0	40	41	0	0	150	150
5	26	0	0	(50)	0	17	43	150	100	150	150	29	26	0	0	(50)	0	41	43	50	0	150	150
6	29	50	0	150	(100)	18	47	218	184	218	184	30	29	50	0	150	(100)	42	47	150	100	218	184
7	35	100	75	150	150	19	51	298	258	298	258	31	35	83.33	66.67	150	150	43	51	230	190	298	258
8	43	150	125	218	184	20	65	378	338	378	338	32	43	116.67	100	218	184	44	65	310	270	378	338
9	54	230	190	298	258	21	96	378	378	378	378	33	54	150	133.33	298	258	45	96	378	344	378	378
10	68	310	270	378	338	22	102	310	344	378	378	34	68	230	190	378	338	46	102	378	378	378	378
11	71	230	270	378	378	23	66	230	270	298	338	35	71	310	270	378	378	47	66	378	378	378	378
12	58	150	190	298	338	24	51	150	190	218	258	36	58	230	270	298	338	48	51	298	338	298	338

multaneously tighter and more compact than equivalent formulations found in the literature. Consequently, the computation time is dramatically reduced. The proposed MILP formulation was analyzed in the context of a price taker self-unit commitment problem. However, its application to any unit commitment problem is straightforward, either under centralized or competitive environments. Several case studies were analyzed to show the improvements of this formulation with respect to others available in the literature. Although SU and SD ramps are usually not considered, mainly because of the computation complexity, simulation results showed that ignoring them changes the commitment decisions causing a negative economic impact.

APPENDIX

A. Initial Conditions

The following parameters are needed to deal with the unit state during the first periods:

- u_0 Initial commitment state {0,1}.
- TU_0 Number of hours that the unit has been up before the scheduling horizon.
- TD_0 Number of hours that the unit has been down before the scheduling horizon.

1) Initial Minimum Up/Down Times: The following condition must be satisfied if $(TU_R + TD_R) \geq 1$:

$$u_t = u_0 \quad \forall t \in [1, TU_R + TD_R] \tag{14}$$

where TU_R and TD_R are the number of initial hours during which the unit must remain up or down at the beginning of the scheduling horizon. TU_R and TD_R are defined as follows:

$$TU_R = \max\{0, (TU - TU_0)\, u_0\} \tag{14a}$$
$$TD_R = \max\{0, (TD - TD_0)\,(1 - u_0)\}. \tag{14b}$$

2) Initial Start-Up Type: Equation (15a) complements (1) taking into account the initial conditions if $TD_0 \geq 2$:

$$\delta_{t,l} = 0 \quad \forall l \in [1, N_L),\ t \in \left(T_{l+1}^{SU} - TD_0, T_{l+1}^{SU}\right). \tag{15a}$$

Finally, the following equation guarantees that the SU $\delta_{t,l}$ is not activated before the SU ramp duration SU_l^D:

$$\delta_{t,l} = 0 \quad \forall l,\ t \in \left[1, SU_l^D\right]. \tag{15b}$$

In other words, this condition ensures that if the unit is turned on in the first hour, the power output above $\underline{P}$ is produced after the ramp duration SU_l^D.

B. Generator-Schedules and Price-Data

The expected electricity prices and optimal power schedules mentioned in Section III are shown in Table IV, where super-indexes T and I refer to the *Traditional* and *Improved* formulations. The numbers in parentheses are the power and energy that were included after the UC problem was solved.

ACKNOWLEDGMENT

G. Morales-España has been awarded an Erasmus Mundus Ph.D. Fellowship. The authors would like to express their gratitude to all partner institutions within the programme as well as the European Commission for their support. The authors also would like to thank Prof. J. M. Arroyo for his valuable comments.

REFERENCES

[1] B. F. Hobbs, W. R. Stewart, R. E. Bixby, M. H. Rothkopf, R. P. O'Neill, and H.-P. Chao, "Why this book? new capabilities and new needs for unit commitment modeling," in *The Next Generation of Electric Power Unit Commitment Models*, B. F. Hobbs, M. H. Rothkopf, R. P. O'Neill, and H.-p Chao, Eds. Boston, MA: Kluwer, 2002, vol. 36, pp. 1–14.

[2] A. J. Wood and B. F. Wollenberg, *Power Generation, Operation, and Control*, 2nd ed. New York: Wiley-Interscience, 1996.

[3] N. Padhy, "Unit commitment-a bibliographical survey," *IEEE Trans. Power Syst.*, vol. 19, no. 2, pp. 1196–1205, May 2004.

[4] J. Garcia-Gonzalez, A. S. Roque, F. Campos, and J. Villar, "Connecting the intraday energy and reserve markets by an optimal redispatch," *IEEE Trans. Power Syst.*, vol. 22, no. 4, pp. 2220–2231, Nov. 2007.

[5] P. Meibom, R. Barth, B. Hasche, H. Brand, C. Weber, and M. O'Malley, "Stochastic optimization model to study the operational impacts of high wind penetrations in Ireland," *IEEE Trans. Power Syst.*, vol. 26, no. 3, pp. 1367–1379, Aug. 2011.

[6] White Paper Functional Description of Core Market Management System (MMS) Applications for Look-Ahead SCED, Version 0.1.2, Electric Reliability Council of Texas (ERCOT), 2011. [Online]. Available: http://www.ercot.com/content/meetings/metf/keydocs/2012/0228/04_white_paper_funct_desc_core_mms_applications_for_la_sced.doc.
[7] N. Troy, E. Denny, and M. O'Malley, "Base-load cycling on a system with significant wind penetration," *IEEE Trans. Power Syst.*, vol. 25, no. 2, pp. 1088–1097, May 2010.
[8] A. L. Ott, "Evolution of computing requirements in the PJM market: Past and future," in *Proc. IEEE 2010 IEEE Power and Energy Soc. General Meeting*, Jul. 2010, pp. 1–4.
[9] T. Koch, T. Achterberg, E. Andersen, O. Bastert, T. Berthold, R. E. Bixby, E. Danna, G. Gamrath, A. M. Gleixner, S. Heinz, A. Lodi, H. Mittelmann, T. Ralphs, D. Salvagnin, D. E. Steffy, and K. Wolter, "MIPLIB 2010," *Math. Program. Comput.*, vol. 3, no. 2, pp. 103–163, Jun. 2011.
[10] T. Li and M. Shahidehpour, "Price-based unit commitment: a case of Lagrangian relaxation versus mixed integer programming," *IEEE Trans. Power Syst.*, vol. 20, no. 4, pp. 2015–2025, Nov. 2005.
[11] C. Simoglou, P. Biskas, and A. Bakirtzis, "Optimal self-scheduling of a thermal producer in short-term electricity markets by MILP," *IEEE Trans. Power Syst.*, vol. 25, no. 4, pp. 1965–1977, Nov. 2010.
[12] C. Wang and S. M. Shahidehpour, "Effects of ramp-rate limits on unit commitment and economic dispatch," *IEEE Trans. Power Syst.*, vol. 8, no. 3, pp. 1341–1350, Aug. 1993.
[13] J. M. Arroyo and A. Conejo, "Modeling of start-up and shut-down power trajectories of thermal units," *IEEE Trans. Power Syst.*, vol. 19, no. 3, pp. 1562–1568, Aug. 2004.
[14] L. L. Garver, "Power generation scheduling by integer programming-development of theory," *Power App. Syst., Part III. Trans. Amer. Inst. Elect. Engineers*, vol. 81, no. 3, pp. 730–734, Apr. 1962.
[15] F. Bouffard, F. Galiana, and A. Conejo, "Market-clearing with stochastic security—Part I: Formulation," *IEEE Trans. Power Syst.*, vol. 20, no. 4, pp. 1818–1826, Nov. 2005.
[16] A. Street, F. Oliveira, and J. M. Arroyo, "Contingency-constrained unit commitment with n-k security criterion: A robust optimization approach," *IEEE Trans. Power Syst.*, vol. 26, no. 3, pp. 1581–1590, Aug. 2011.
[17] B. Palmintier and M. Webster, "Impact of unit commitment constraints on generation expansion planning with renewables," in *Proc. 2011 IEEE Power and Energy Soc. General Meeting*, Jul. 2011, pp. 1–7.
[18] L. Wolsey, *Integer Programming*. New York: Wiley-Interscience, 1998.
[19] R. Bixby, M. Fenelon, Z. Gu, E. Rothberg, and R. Wunderling, "MIP: Theory and practice-closing the gap," in *System Modelling and Optimization: Methods, Theory and Applications*, M. J. D. Powell and S. Scholtes, Eds. Boston, MA: Kluwer, 2000, vol. 174, pp. 19–49.
[20] F. Vanderbeck and L. A. Wolsey, "Reformulation and Decomposition of Integer Programs," in *50 Years of Integer Programming 1958–2008*, M. Jünger, T. M. Liebling, D. Naddef, G. L. Nemhauser, W. R. Pulleyblank, G. Reinelt, G. Rinaldi, and L. A. Wolsey, Eds. Berlin, Germany: Springer, 2010, pp. 431–502.
[21] L. Wolsey, "Strong formulations for mixed integer programs: Valid inequalities and extended formulations," *Math. Program.*, vol. 97, no. 1, pp. 423–447, 2003.
[22] D. Rajan and S. Takriti, Minimum Up/Down Polytopes of the Unit Commitment Problem With Start-up Costs, IBM, Research Report RC23628, Jun. 2005. [Online]. Available: http://domino.research.ibm.com/library/cyberdig.nsf/1e4115aea78b6e7c85256b360066f0d4/cdcb02a7c809d89e8525702300502ac0?OpenDocument.
[23] A. Frangioni, C. Gentile, and F. Lacalandra, "Tighter approximated MILP formulations for unit commitment problems," *IEEE Trans. Power Syst.*, vol. 24, no. 1, pp. 105–113, Feb. 2009.
[24] J. Ostrowski, M. F. Anjos, and A. Vannelli, "Tight mixed integer linear programming formulations for the unit commitment problem," *IEEE Trans. Power Syst.*, vol. 27, no. 1, pp. 39–46, Feb. 2012.
[25] G. Morales-España, A. Ramos, and J. García-González, "An MIP formulation for joint market-clearing of energy and reserves including ramp scheduling," *IEEE Trans. Power Syst.* [Online]. Available: http://www.iit.upcomillas.es/~aramos/papers/V3.4_UC-based_MC.pdf, to be published
[26] J. A. Muckstadt and R. C. Wilson, "An application of mixed-integer programming duality to scheduling thermal generating systems," *IEEE Trans. Power App. Syst.*, vol. PAS-87, no. 12, pp. 1968–1978, Dec. 1968.
[27] X. Guan, F. Gao, and A. Svoboda, "Energy delivery capacity and generation scheduling in the deregulated electric power market," *IEEE Trans. Power Syst.*, vol. 15, no. 4, pp. 1275–1280, Nov. 2000.
[28] G. Morales-España, J. Garcia-Gonzalez, and A. Ramos, "Impact on reserves and energy delivery of current UC-based market-clearing formulations," in *Proc. 2012 9th Int. Conf. Eur. Energy Market (EEM)*, Florence, Italy, May 2012, pp. 1–7.
[29] The GAMS Development Corporation Website, 2012. [Online]. Available: http://www.gams.com.

Germán Morales-España (S'10) received the B.Sc. degree in electrical engineering from the Universidad Industrial de Santander, Bucaramanga, Colombia, in 2007 and the M.Sc. degree from the Delft University of Technology, Delft, The Netherlands, in 2010. He is now pursuing the (Ph.D.) Erasmus Mundus Joint Doctorate in sustainable energy technologies and strategies (SETS) hosted by the Universidad Pontificia Comillas, Madrid, Spain; the Royal Institute of Technology, Stockholm, Sweden; and Delft University of Technology, Delft, The Netherlands.

He is currently an assistant researcher at the Institute for Research in Technology (IIT) at the Universidad Pontificia Comillas, and he is also a member of the Research Group on Electric Power Systems (GISEL) at the Universidad Industrial de Santander. His areas of interest are power systems operation, economics and reliability, as well as power quality and protective relaying.

Jesus M. Latorre (S'00–M'07) was born in Madrid, Spain, in 1977. He received the degree of Electronic Engineer in 2001 and the Ph.D. degree in November 2007, from Comillas Pontifical University, Madrid, Spain.

He is currently a postdoctoral researcher at the Institute for Research in Technology, of the Comillas Pontifical University. His main interest areas include operations research and mathematical modeling, stochastic programming, parallel and distributed computing, algorithms, and numerical methods.

Andres Ramos received the degree of Electrical Engineering from Universidad Pontificia Comillas, Madrid, Spain, in 1982 and the Ph.D. degree in Electrical Engineering from Universidad Politécnica de Madrid, Madrid, Spain, in 1990.

He is a Research Fellow at Instituto de Investigación Tecnológica, Madrid, Spain, and a Full Professor at Comillas' School of Engineering, Madrid, Spain, where he has been the Head of the Department of Industrial Organization. His areas of interest include the operation, planning, and economy of power systems and the application of operations research to industrial organization.

Article II

G. Morales-España, A. Ramos, and J. García-González, "An MIP Formulation for Joint Market-Clearing of Energy and Reserves Based on Ramp Scheduling," *IEEE Transactions on Power Systems*, vol. 29, no. 1, pp. 476–488, Jan. 2014. JCR 2012 data: impact factor 2.921 and 5-year impact factor 3.601.

Remark: This paper is part of a special section of the IEEE TPWRS journal "Electricity Markets Operation".

An MIP Formulation for Joint Market-Clearing of Energy and Reserves Based on Ramp Scheduling

Germán Morales-España, *Student Member, IEEE*, Andres Ramos, and Javier García-González, *Member, IEEE*

***Abstract*—The day-ahead unit-commitment (UC)-based market-clearing (MC) is widely acknowledged to be the most economically efficient mechanism for scheduling resources in power systems. In conventional UC problems, power schedules are used to represent the staircase energy schedule. However, the realizability of this schedule cannot be guaranteed due to the violation of ramping limits, and hence conventional UC formulations do not manage the flexibility of generating units efficiently. This paper provides a UC-based MC formulation, drawing a clear distinction between power and energy. Demand and generation are modeled as hourly piecewise-linear functions representing their instantaneous power trajectories. The schedule of generating unit output is no longer a staircase function, but a smoother function that respects all ramp constraints. The formulation represents in detail the operating reserves (online and offline), their time deployment limits (e.g., 15 min), their potential substitution, and their limits according to the actual ramp schedule. Startup and shutdown power trajectories are also modeled, and thus a more efficient energy and reserves schedule is obtained. The model is formulated as a mixed-integer programming (MIP) problem, and was tested with a 10-unit and 100-unit system in which its computational performance was compared with a traditional UC formulation.**

***Index Terms*—Mixed-integer programming, operating reserves, startup and shutdown ramps, UC-based market-clearing.**

NOMENCLATURE

Uppercase letters are used for denoting parameters and sets. Lowercase letters denote variables and indexes.

Indexes and Sets:

$g \in \mathcal{G}$	Generating units, running from 1 to G.
$s \in \mathcal{S}_g$	Startup segments, running from 1 (the hottest) to S_g (the coldest).
$t \in \mathcal{T}$	Hourly periods, running from 1 to T hours.
$\kappa \in \mathcal{K}$	Index for reserve type: $2+$ and $2-$ for secondary up and down; $3+$ and $3-$ for tertiary up and down; $3\mathrm{N}+$ and $3\mathrm{N}-$ for offline tertiary up and down.
$\tau \in \Gamma$	Index for time interval: $15'$ for 15 min, $30'$ for 30 min, and op for 1 h.

Manuscript received May 15, 2012; revised May 31, 2012, October 14, 2012, April 03, 2013, and April 19, 2013; accepted April 20, 2013. Date of publication May 13, 2013; date of current version December 16, 2013. The work of G. Morales-España was supported through an Erasmus Mundus Ph.D. Fellowship. Paper no. TPWRS-00510-2012.

The authors are with the Institute for Research in Technology (IIT), School of Engineering (ICAI), Universidad Pontificia Comillas, Madrid, Spain (e-mail: german.morales@iit.upcomillas.es; gmorales@kth.se; andres.ramos@upcomillas.es; javiergg@iit.upcomillas.es).

Color versions of one or more of the figures in this paper are available online at http://ieeexplore.ieee.org.

Digital Object Identifier 10.1109/TPWRS.2013.2259601

Parameters:

C_{gt}^{LV}	Linear variable production cost bid [$/MWh].
C_{gt}^{NL}	No-load cost bid [$/h].
C_{gt}^{SD}	Shutdown cost bid [$].
C_{gst}^{SU}	Startup cost bid for starting up at segment s [$].
C_{gt}^{κ}	Cost bid for reserve type κ [$/MW].
D_t	Instantaneous demand at the end of hour t [MW].
D_t^{κ}	System requirements for reserve type κ [MW].
E_{gt}	Energy capacity bid [MWh].
$\overline{P}_g$	Maximum power output [MW].
$\underline{P}_g$	Minimum power output [MW].
P_{gi}^{SD}	Power output at the beginning of the ith interval of the shutdown ramp process [MW]; see Fig. 2.
P_{gsi}^{SU}	Power output at the beginning of the ith interval of the startup ramp process type s [MW]; see Fig. 2.
$Q_g^{\mathrm{SD}\tau}$	Quick shutdown capability for $\tau \in \{30', op\}$ [MW].
$Q_g^{\mathrm{SU}\tau}$	Quick startup capability for $\tau \in \{30', op\}$ [MW].
R_{gt}^{κ}	Capacity bid for reserve type κ [MW].
RD_g^{τ}	Ramp-down capability for interval τ [MW/min].
RU_g^{τ}	Ramp-up capability for interval τ [MW/min].
SD_g^{D}	Duration of the shutdown process [h]; see Fig. 2.
SU_{gs}^{D}	Duration of the startup process type s [h]; see Fig. 2.
T_{gs}^{SU}	Time defining the interval limits of the startup segment s, $\left[T_{gs}^{\mathrm{SU}}, T_{g,s+1}^{\mathrm{SU}}\right)$ [h].
TD_g	Minimum down time [h].
TU_g	Minimum up time [h].

Decision Variables:

e_{gt}	Energy schedule for hour t, excluding energy production during the startup and shutdown processes [MWh].
p_{gt}	Power output schedule at the end of hour t, production above the minimum output [MW].

$\widehat{p}_{gt}$ Total power output schedule at the end of hour t, including startup and shutdown trajectories [MW].

r^{κ}_{gt} Reserve type κ schedule [MW].

u^{κ}_{gt} Binary variable which is equal to 1 if the unit is providing up/down offline tertiary reserve ($\kappa \in \{3N+, 3N-\}$) and 0 otherwise.

u_{gt} Binary variable which is equal to 1 if the unit is producing above $\underline{P}_g$ and 0 otherwise; see Fig. 2.

v_{gt} Binary variable which takes the value of 1 if the unit starts up and 0 otherwise; see Fig. 2.

w_{gt} Binary variable which takes the value of 1 if the unit shuts down and 0 otherwise; see Fig. 2.

δ_{gst} Startup type s. Binary variable which takes the value of 1 if the unit starts up and has been previously down within $\left[T^{\mathrm{SU}}_{gs}, T^{\mathrm{SU}}_{g,s+1}\right)$ hours.

I. Introduction

A. Motivation

DAY-AHEAD market-clearing (MC) is the central mechanism in electricity markets, despite the large variety in market designs across the world. Unit commitment (UC)-based MC, in which energy and operating reserves are simultaneously cleared, is widely, if not universally, acknowledged to be the most economically efficient way to run day-ahead markets [1], [2]. The UC problem schedules the cheapest resources to supply the demand, while operating the system and units within secure technical limits [1], [3]. Moreover, simultaneous clearing avoids uneconomical out-of-merit operation and mitigates potential market power when hierarchical substitution of reserves is considered [2], [4], [5].

Current day-ahead scheduling practices do not exploit the real flexibility of power systems and could even endanger security of supply. This problem is faced by markets that are (physically) cleared on an hourly basis as well as on a sub-hourly one. An inherent problem of hourly-cleared markets is that they make an (staircase) hourly energy balance between supply and demand rather than matching the instantaneous generating power profiles with the power demand profile. In these kind of markets, generators are penalized if they deviate from their hourly energy schedule. Therefore, units operate by trying to match their power profile with the staircase energy blocks. This staircase behavior creates large generation gradients at the beginning and at the end of every trading hour, causing large frequency deviations during these time intervals [6], [7]. As a consequence, even in the absence of uncertainty, power system security is being compromised and a significant quantity of operating reserves need to be deployed in real time to maintain the supply-demand balance. A report from The European Network of Transmission System Operators for Electricity (Entso-e) [8] summarizes the operational and economic impacts of this phenomenon on the power system and generating units.

Although sub-hour or real-time markets allow the mitigation of these problems, an inadequate day-ahead schedule may leave real-time markets unprepared to face real-time uncertainties. In fact, some power systems have experienced short-term scarcity events caused by resources with sufficient power capacity but insufficient ramp capability [9]. In response, independent system operators (ISOs) are developing market-based ramping products that will be acquired in day-ahead markets in order to increase real-time dispatch flexibility [9], [10].

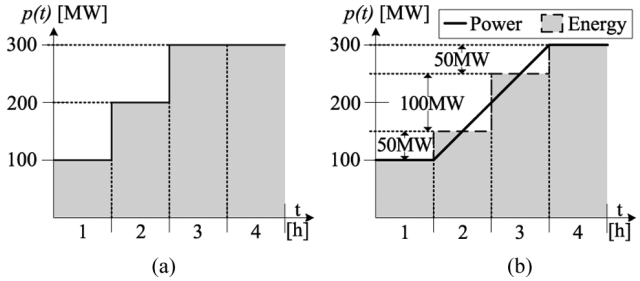

Fig. 1. Scheduling versus deployment. (a) Traditional energy schedule. (b) Actual deployment.

In order to better prepare the power system to face real-time uncertainties, day-ahead scheduling approaches are required to efficiently manage power system flexibility by adequately utilizing ramping resources.

B. Literature Review

1) Inefficient Ramp Management—Energy versus Power: Conventional day-ahead UC formulations fail to deal with ramp capabilities appropriately. Inefficient ramp management arises from applying ramp-constraints to energy levels or (hourly) averaged generation levels, which is standard practice in traditional UC models [1], [3], [5], [11]. As a result, energy schedules may not be feasible [12]. To illustrate this problem, consider the following scheduling example for one generating unit. This example assumes that the minimum and maximum generation outputs of the unit are 100 MW and 300 MW, respectively, and that the maximum ramp rate is 100 MW/h. As shown in Fig. 1(a), if the unit ramps up at its maximum capability and has been producing 100 MW during the first hour, then the expected hourly energy levels for the second and third hours will be 200 MWh and 300 MWh, respectively. However, the unit cannot reach its maximum output before the end of the third hour due to its limited ramp rate, as shown in Fig. 1(b). Consequently, the solution obtained in Fig. 1(a) is not feasible. In fact, the unit requires a ramping capability of 200 MW/h to be able to produce the energy presented in Fig. 1(a).

Note that representing the generation in a staircase fashion (energy blocks) may lead to misleading estimations of a system's ramp availability. This in turn could leave the system unprepared to face real-time uncertainties. For example, if the unit in the previous example were actually scheduled to produce the energy profile presented in Fig. 1(b) then, since the first energy increase is 50 MW (half of the unit's ramp capability), the unit would be erroneously considered to have 50 MW of remaining upward ramp flexibility.

Although it has been proven that delivering the energy schedule obtained from these energy-block formulations may not be feasible [12], insufficient attention has been paid to this issue. Formulations drawing a clear distinction between power and energy have been proposed, guaranteeing that staircase

energy schedules can be realized [13]–[15]. In [13] a smooth nonlinear programming problem which does not take into account discrete decisions is proposed (e.g., commitment). The work in [14] presents a formulation with feasible energy delivery constraints, which is further extended in [15], where a sub-hourly UC is formulated. These formulations are focused on feasible energy schedules rather than on matching generating and demand power profiles. In fact, these formulations supply hourly energy demand with power profiles that vary from staircase [15] to oscillating power trajectories [16], which are far from matching the instantaneous power demand forecast. This indiscriminate use of ramping resources from the scheduling stage does not permit the effective management of the system ramp capabilities to face real-time uncertainties. In addition, the formulations do not model operating reserves.

2) Startup and Shutdown Power Trajectories: Conventional day-ahead UC models assume that units start/end their production at their minimum output. That is, UC models ignore the intrinsic startup (SU) and shutdown (SD) power trajectories of thermal units. Consequently, there is an increasing amount of energy that is not being allocated by day-ahead scheduling approaches because, first, units provide energy (and ramp) during the SU and SD processes, affecting the total load balance; and second, thermal units are being shut down and started up more often due to the increasing penetration of variable generation [17]. As a result, there is an inefficient deployment in real time of resources that are required to accommodate the power trajectories that were ignored in the day-ahead schedule, so that the balance between supply and demand is maintained [18]. Furthermore, as discussed in [19], ignoring these power trajectories can significantly change commitment decisions, which in turn increases operating costs. Recent papers indicate an awareness of the importance of the SU and SD processes [20]–[22]. However, SU and SD power trajectories continue being ignored because the resulting model will supposedly be considerably more complex, and thus lead to prohibitive solving times.

An adequate day-ahead schedule not only must take into account these SU and SD power trajectories, but also must optimally schedule them to avoid the aforementioned drawbacks.

3) Reserve modeling: Another drawback of conventional UC-based MC formulations is related to the accuracy of reserve modeling. Reserves must be scheduled on the basis of their required time deployment (e.g., 15 min) and not as an hourly requirement, as has been commonly modeled [1], [5], [11]. The formulations presented in [4], [23], and [24] guarantee possible reserve deployments in a few minutes, although these models are on an hourly-basis. However, they do not consider the real reserve availability of a unit which depends on its actual ramp schedule.

A correct modeling of ramp constraints, which must be applied to power trajectories, is then required to guarantee the execution of the power schedules and correctly represent the real availability of operating reserves at any moment within the hour.

For further details of the drawbacks of conventional UC-based scheduling approaches, the reader is referred to [18].

C. Ramp-Based Scheduling Approach: An Overview

This paper proposes a day-ahead UC-based MC formulation in which the operating ramping of generators is optimally scheduled to supply an instantaneous power demand forecast. In addition, the formulation guarantees that operating reserves can be deployed in a given (required) time. The formulation is represented as a mixed-integer programming (MIP) problem. MIP is becoming widely used in the electricity sector due to significant improvements on MIP solvers [25].

The proposed formulation draws a clear distinction between power and energy. Ramp constraints are thus applied on power trajectories rather than on energy blocks, which is a common drawback of conventional UC formulations [1], [3], [5], [11]. Power production and demand are modeled as an hourly piecewise-linear function representing their instantaneous power trajectories. This overcomes the disadvantages of power-based scheduling models [13]–[15] by having the clear objective of matching the instantaneous power demand with the total power generation profile, thus avoiding an indiscriminate use of ramping resources in the scheduling stage.

Unlike previous works that have modeled reserves [1], [3], [5], [11], [23], [24], the proposed formulation provides the actual ramp schedules, and thus defines the available ramp capability that can be used to provide reserves. Although the formulation is based on time periods of one hour, it also guarantees that reserves can be deployed within the time requirements (a few minutes) imposed by the reliability authorities (for each type of reserve) [26].

In addition, the formulation considers SU and SD power trajectories, thus avoiding power discontinuities in the scheduling stage which result in an inefficient deployment of resources in the real-time operation.

The proposed formulation would help ISOs to draw up an efficient day-ahead ramp resources schedule in order to better prepare the system to face real-time uncertainties. For the case of an hourly-cleared market (such as those in Europe), if the proposed approach were followed, generating units would be penalized if they deviated within the hour from the scheduled power trajectory. As a result, in comparison with the staircase approach, the aggregated generation would better fit the power demand. This strategy would avoid large frequency deviations at the hour limits and the unnecessary reserve use caused by the mismatch between supply and demand. In addition, power systems with real-time markets would be better prepared to face real-time if their day-ahead schedules followed piecewise power profiles rather than staircase energy blocks. This is because, in comparison with the conventional staircase scheduling approach, the scheduled power profiles would be a better approximation of the units' real production and the optimal ramp scheduling would correctly estimate the ramp availability of power systems.

This paper is focused on scheduling quantities, and the problem of determining the prices that will allow generators to recover their non-convex costs, is beyond the scope of this work. However, a pricing mechanism for a multi-part bidding with different commodities [27], such as startup and shutdown costs, can be applied directly. It is important to highlight that the proposed ramp-based approach presents great challenges in terms of market design. Both the definition of a proper pricing mechanism that copes with continuous power profiles and the consideration of demand bids expressed as continuous functions are some examples that require further research. Nevertheless, the ideas presented in this paper have potential for broad applications, such as for reliability UC, which guarantee the feasibility of the scheduling obtained after forward markets

have been cleared [9], [10]. Finally, for the sake of simplicity and without loss of generality, transmission constraints are not considered in this paper.

D. Contributions

The principal contributions of this paper are as follows:

1) A day-ahead UC-based MC formulation is proposed in which the total power generation follows the instantaneous power profile of the demand forecast. This is achieved by taking into account piecewise-linear power-trajectories instead of staircase energy-blocks, and also scheduling the SU and SD power trajectories of thermal units.
2) The actual reserve availability is accurately defined, based on the units' ramp schedules. The formulation takes into account different ramp-rate limits, and it guarantees that reserves can be deployed within their different time requirements. Consequently, the reserve capabilities of a system are optimally scheduled, taking a better advantage of units' flexibility.
3) The core of the proposed MIP formulation is built upon the tight and compact formulations presented in [19] and [28], thus taking advantage of their mathematical properties. These formulations reinforce the convergence speed by reducing the search space (tightness) and at the same time by increasing the searching speed with which solvers explore that reduced space (compactness). That is, the formulations are simultaneously tight and compact. If compared with a traditional UC formulation, with no SU and SD ramps and representing a single reserve type, the proposed formulation involves a low computational burden and solving times were even decreased when a large study case was carried out.

E. Paper Organization

The remainder of this paper is organized as follows. Section II details the mathematical formulation of different operating reserves (secondary, tertiary online and tertiary offline) and their links with the ramp schedules. Section III presents some numerical examples as well as a comparison with a conventional UC. Finally, concluding remarks are made in Section IV.

II. Proposed Approach

This section details the mathematical formulation of the proposed UC-based market-clearing approach. This paper models secondary and tertiary reserves using European standards as a benchmark [26]. The up/down reserve provided by a generating unit is defined as the amount of power that the unit can increase/decrease over its scheduled power output within a time limit. Secondary up (r_{gt}^{2+}) and down (r_{gt}^{2-}) reserves are provided by online units that respond to a continuous automatic generation control (AGC). The secondary reserve must be fully available within 15 min. Tertiary reserve is composed of online up (r_{gt}^{3+}) and down (r_{gt}^{3-}) reserves, as well as offline up ($r_{gt}^{3\mathrm{N}+}$) and down ($r_{gt}^{3\mathrm{N}-}$) reserves. The tertiary reserve is manually activated by ISOs and it is used to release the secondary reserve or prevent its activation. After being called, the tertiary reserve must be fully available within 30 min. Although the formulation follows these time deployments, the adaptation to U.S. standards [29] is straightforward. For example, the 10-min spinning reserve can be modeled in the same way as the (15-min) secondary reserves by simply modifying the parameters established for the time deployments.

The formulation takes into account different ramp limits to model different reserve time deployments. These limits change depending on the duration of the ramping process, i.e., the shorter a sustained ramping process, the larger the ramp limits without shortening the rotor life [30]. For the sake of simplicity and without loss of generality, ramp-rate limits are considered to be constant during the unit's *up* state; however, the formulation can be further extended to deal with dynamic ramps [31].

The first part of this section presents the general formulation. The second part describes how to obtain the ramp-capability and power-capacity constraints using the proposed ramp-based scheduling approach. The following two parts are devoted to modeling the reserve constraints for slow- and quick-start units, respectively. Finally, the last subsection lists some specific characteristics that make the formulation computationally efficient.

A. General Formulation

In order to obtain computational advantage, the generation output above and bellow $\underline{P}$ is managed independently [28]. This also facilitates the inclusion of SU and SD power trajectories in the model [19]. Therefore, the *up* and *down* states are distinguished from the *online* and *offline* states, as shown in Fig. 2. The unit is *online* when providing energy to the system and *offline* otherwise. During the *up* period, the unit has the flexibility to follow any trajectory being limited by its power-capacity and ramp-capability limits. Consequently, the unit can only provide reserves when it is *up*. On the other hand, the unit's power output follows a predefined power trajectory when it is starting up or shutting down. The SU power trajectory depends on the unit's previous down time, unlike the SD process.

1) Objective Function: The objective of the MC is to procure energy and reserves at the minimum cost:

$$\min \sum_{g\in\mathcal{G}}\sum_{t\in\mathcal{T}}\Bigg[\sum_{\kappa\in\mathcal{K}} C_{gt}^{\kappa} r_{gt}^{\kappa} + \sum_{s\in\mathcal{S}_g} C_{gst}^{\mathrm{SU}}\delta_{gst} + C_{gt}^{\mathrm{SD}} w_{gt} + C_{gt}^{\mathrm{NL}} u_{gt} + C_{gt}^{\mathrm{LV}} e_{gt}\Bigg]. \quad (1)$$

Note that the startup cost C_{gst}^{SU} includes the energy spent by two different actions: first, the energy required to bring the thermal unit online, which does not result in any MW generation [32]; second, the cost of the energy that is provided to the system during the SU process, i.e., the energy which is produced until the unit achieves its minimum output, *up* state. Both the cost of bring the unit online and the duration of the SU ramp, depend on how long the unit has been down [19]. Similarly, the C_{gt}^{SD} includes the cost of the energy provided to the system during the SD ramp process.

2) Power System Requirements: The power system requirements for demand and reserves are presented as follows:

$$\sum_{g\in\mathcal{G}} \widehat{p}_{gt} = D_t \quad \forall t \quad (2)$$

$$\sum_{g\in\mathcal{G}} r_{gt}^{2+} \geq D_t^{2+} \quad \forall t \quad (3)$$

$$\sum_{g\in\mathcal{G}} r_{gt}^{2-} \geq D_t^{2-} \quad \forall t \quad (4)$$

$$\sum_{g\in\mathcal{G}}\left[r_{gt}^{2+}+r_{gt}^{3+}+r_{gt}^{3\mathrm{N}+}\right]\geq D_t^{3+}+D_t^{2+}\quad\forall t \tag{5}$$

$$\sum_{g\in\mathcal{G}}\left[r_{gt}^{2-}+r_{gt}^{3-}+r_{gt}^{3\mathrm{N}-}\right]\geq D_t^{3-}+D_t^{2-}\quad\forall t. \tag{6}$$

The demand balance in (2) is calculated at the end of hour t. Note that the energy balance for the whole hour is automatically achieved by satisfying the power demand at the beginning and end of each hour, and by considering a piecewise-linear power profile for demand and generation. Constraints (3) and (4) represent the supply of up and down secondary reserves. The constraints satisfying the tertiary reserve requirements, (5) and (6), also consider the substitution of a higher quality reserve for a lower quality reserve [2], [4], [22], [24]. In other words, the secondary reserves can technically substitute tertiary reserves as long as this reduces the total procurement costs.

3) Commitment Logic and Minimum Up/Down Times: The relation between the commitment, startup and shutdown variables is presented in (7). Constraints (8) and (9) ensure the minimum up and down times, respectively [33]:

$$u_{gt}-u_{g,t-1}=v_{gt}-w_{gt}\quad\forall g,t \tag{7}$$

$$\sum_{i=t-TU_g+1}^{t}v_{gi}\leq u_{gt}\quad\forall g,t\in[TU_g,T] \tag{8}$$

$$\sum_{i=t-TD_g+1}^{t}w_{gi}\leq 1-u_{gt}\quad\forall g,t\in[TD_g,T] \tag{9}$$

where the minimum up/down constraints ensure that a unit cannot start up and shut down simultaneously. Note that (8) and (9) guarantee (dominate over) the inequalities $v_{gt}\leq u_{gt}$ and $u_{gt}\leq 1-w_{gt}$, respectively, which, combined, become $v_{gt}+w_{gt}\leq 1$. In addition, given that u_{gt} is defined as a binary variable, (7) forces v_{gt} and w_{gt} to take binary values, even if they are defined as continuous.

4) Selection of SU Type: The SU type and the SU and SD power trajectories are obtained using the tight and compact formulation proposed in [19], which considerably reduces the computational burden in comparison with analogous formulations commonly found in the literature. The SU type is selected with

$$\delta_{gst}\leq\sum_{i=T_{gs}^{\mathrm{SU}}}^{T_{g,s+1}^{\mathrm{SU}}-1}w_{g,t-i}\quad\forall g,s\in[1,S_g),t\in\left[T_{g,s+1}^{\mathrm{SU}},T\right] \tag{10}$$

$$\sum_{s\in\mathcal{S}_g}\delta_{gst}=v_{gt}\quad\forall g,t \tag{11}$$

where (10) allows that the startup segment s can be selected ($\delta_{gst}\leq 1$) if the unit has been previously down within $\left[T_{gs}^{\mathrm{SU}},T_{g,s+1}^{\mathrm{SU}}\right)$ hours. Constraint (11) forces the selection of a unique SU type if the unit actually starts up.

As discussed in [19] and [28], the variables δ_{gst} take binary values even if they are defined as continuous. This is due to the tightness characteristic of the startup-cost formulation. Note that (10) is not defined for the first hours. See [19] for details of how the initial conditions define δ_{gst} for these first hours.

5) Total Power Output: Although all units' technical constraints are applied to the output variable p_{gt}, which is production above $\underline{P}_g$, the total power production $\widehat{p}_{gt}$ is needed to satisfy the power demand (2).

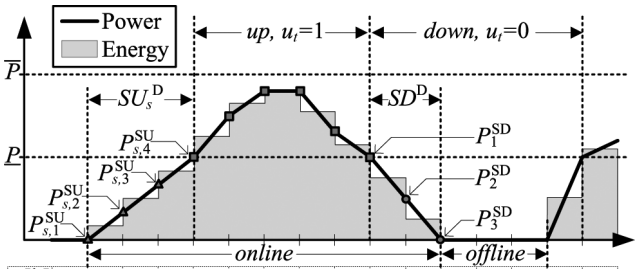

t [h]	1	2	3	4	5	6	7	8	9	10	11	12	13	14	15	16
u_t	0	0	0	0	1	1	1	1	1	0	0	0	0	0	0	1
v_t	0	0	0	0	1	0	0	0	0	0	0	0	0	0	0	1
w_t	0	0	0	0	0	0	0	0	0	1	0	0	0	0	0	0

Fig. 2. Unit operation states, including SU and SD power trajectories.

As presented in [19], the total power output including the SU and SD power trajectories for slow-start units is obtained with

$$\widehat{p}_{gt}=\underbrace{\sum_{s=1}^{S_g}\sum_{i=1}^{\mathrm{SU}_{gs}^{\mathrm{D}}}P_{gsi}^{\mathrm{SU}}\delta_{gs,\left(t-i+SU_{gs}^{\mathrm{D}}+2\right)}}_{\text{(iii) SU trajectory}}+\underbrace{\sum_{i=2}^{\mathrm{SD}_g^{\mathrm{D}}+1}P_{gi}^{\mathrm{SD}}w_{g,(t-i+2)}}_{\text{(ii) SD trajectory}}+\underbrace{\underline{P}_g\left(u_{gt}+v_{g,t+1}\right)+p_{gt}}_{\text{(i) Output when being } up}\quad\forall g,t. \tag{12}$$

For a better understanding of this constraint, we can analyze how the power trajectory example in Fig. 2 is obtained from the three different parts in (12):

1) Output when the unit is *up*: Although the unit is *up* for five consecutive hours, there are six total power values, from $\widehat{p}_{g,4}$ to $\widehat{p}_{g,9}$, greater than or equal to $\underline{P}_g$ (see the squares in Fig. 2). When $t=4$, the term $v_{g,t+1}$ in (i) becomes $v_{g,5}$ ensuring (the first) $\underline{P}_g$ at the beginning of the *up* period, and the term u_{gt} adds (the remaining five) $\underline{P}_g$ for $t=5\ldots 9$. In addition, p_{gt} adds the power production above $\underline{P}_g$.
2) SD power trajectory: This process lasts for two hours, $SD_g^{\mathrm{D}}=2$; then, the summation term (ii) becomes $P_{g,2}^{\mathrm{SD}}w_{gt}+P_{g,3}^{\mathrm{SD}}w_{g,t-1}$, which is equal to $P_{g,2}^{\mathrm{SD}}$ for $t=10$ and $P_{g,3}^{\mathrm{SD}}$ for $t=11$, being zero otherwise. This provides the SD power trajectory (see the circles in Fig. 2).
3) SU power trajectory: the SU power trajectory can be obtained using a procedure similar to that used in 2) (see the triangles in Fig. 2). The possible SU trajectory is given by the chosen segment s (see Section II-A4), which depends on how long the unit has been down.

6) Energy Schedule: The energy produced by a unit during the *up* state, following an hourly piecewise-linear power profile, is obtained with

$$e_{gt}=\underline{P}_g u_{gt}+\frac{p_{g,t-1}+p_{gt}}{2}\quad\forall g,t. \tag{13}$$

This energy is used to represent the unit's production cost during the *up* state in (1). The energy produced during the SU and SD processes is internalized in the SU and SD costs, as discussed in Section II-A1. The total energy schedule can easily be calculated using $\widehat{p}_{gt}$ after the optimization problem is solved.

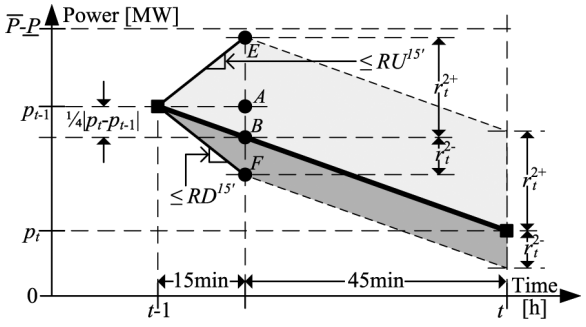

Fig. 3. Relation between secondary reserves, power trajectory, and ramps.

7) Operating Ramps: The traditional ramp constraints for the unit operation are presented as follows:

$$-60RD_g^{op} \leq p_{gt} - p_{g,t-1} \leq 60RU_g^{op} \quad \forall g,t. \tag{14}$$

B. Obtaining the Reserve Constraints

This subsection is made for illustrative purposes in order to aid understanding of how the ramping and capacity constraints are derived. For the sake of simplicity only secondary reserves are considered here. The complete formulation also taking into account the tertiary reserves is presented in Sections II-C and II-D for slow- and quick-start units, respectively. In other words, the equations (1)–(14) together with (21)–(45) provide the complete formulation that is proposed in this paper. A formulation that only models secondary reserve, ignoring online and offline tertiary reserves, is described by (1)–(14) together with (15)–(20).

1) Ramping Limits: The up (down) secondary reserve provided by a generating unit is the amount of power that the unit can increase (decrease) over its scheduled power output within 15 minutes. Therefore, as observed in Fig. 3, the segment *EB (BF)* defines the up (down) secondary reserve, which is the power above (below) the scheduled power output level *B*. The following constraints ensure that the unit has the ramp capability to provide up *(EB)* and down *(BF)* secondary reserves:

$$\underbrace{\underbrace{\frac{1}{4}\left(p_{gt} - p_{g,t-1}\right)}_{BA} + \underbrace{r_{gt}^{2+}}_{EB}}_{EA} \leq 15RU_g^{15'} \quad \forall g,t \tag{15}$$

$$\underbrace{\underbrace{-\frac{1}{4}\left(p_{gt} - p_{g,t-1}\right)}_{AB} + \underbrace{r_{gt}^{2-}}_{BF}}_{AF} \leq 15RD_g^{15'} \quad \forall g,t. \tag{16}$$

As shown in Fig. 3, when the unit is ramping up, the 15-min ramp excursion resulting from the scheduled power trajectory *(BA)* and the down up secondary reserve *(EB)* cannot exceed the 15-min ramp capability (15). Similarly, when the unit is ramping down, the 15-min ramp excursion due to the scheduled power trajectory *(AB)* plus the down secondary reserve *(BF)* cannot exceed the 15-min ramp capability (16).

As shown in Fig. 3, due to the hourly piecewise-linear power profile, the ramp excursion of the power trajectory during a 15 min period is a quarter of that obtained during an hour.

The reserve that is available within one hour depends directly on the unit power trajectory during that hour. For example, the up (down) secondary reserve availability increases (decreases) if the scheduled power is ramping down. This is the case in Fig. 3, where the up secondary reserve *(EB)* can even be greater than the 15-min ramp rate limit.

2) Capacity Limits: The reserve interval (grey areas in Fig. 3) must not exceed the unit's capacity limits at the end of the hour:

$$p_{gt} + r_{gt}^{2+} \leq \left(\overline{P}_g - \underline{P}_g\right)\left(u_{gt} - w_{g,t+1}\right) \quad \forall g,t \tag{17}$$

$$p_{gt} - r_{gt}^{2-} \geq 0 \quad \forall g,t. \tag{18}$$

Constraint (17) also guarantees that the unit is at the minimum output $\underline{P}_g$ at the instant when the SU (SD) power trajectory finishes (starts), thus connecting the production above $\underline{P}_g$ with the SU (SD) power trajectory, as discussed in Section II-A5. This can be observed in the example presented in Fig. 2, where (17) makes p_{gt} equal to zero at the end of hours 4 ($p_{g,4} = 0$) and 9 ($p_{g,9} = 0$), which are the beginning and end of the *up* state period, respectively.

It is important to note that (17) and (18) do not ensure that the unit operates within its capacity limits during the whole hour. When the unit is ramping down (up), the unit can violate its maximum (minimum) power limit at minute 15, as indicated with point *E* (*F*) in Fig. 3. This problem is avoided by ensuring that point *E* is below the maximum power limit (19) and *F* is above the minimum (20):

$$\underbrace{\underbrace{\frac{1}{4}p_{gt} + \frac{3}{4}p_{g,t-1}}_{B} + \underbrace{r_{gt}^{2+}}_{EB}}_{E} \leq \overline{P}_g - \underline{P}_g \quad \forall g,t \tag{19}$$

$$\underbrace{\underbrace{\frac{1}{4}p_{gt} + \frac{3}{4}p_{g,t-1}}_{B} - \underbrace{r_{gt}^{2-}}_{BF}}_{F} \geq 0 \quad \forall g,t. \tag{20}$$

In short, secondary reserves can be provided at any time within the hour by guaranteeing that the reserve interval (grey areas in Fig. 3) does not exceed the ramp-capability and power-capacity limits at the end of the hour and at minute 15.

C. Secondary and Tertiary Reserves for Slow-Start Units

The complete formulation for secondary and tertiary reserves is presented in this subsection. The formulation guarantees a simultaneous or independent (either secondary or tertiary) reserve deployment. All equations are derived in a similar fashion to the constraints presented in Section II-B.

1) Ramping Limits: The simultaneous deployment of secondary and tertiary reserves cannot exceed the unit ramping limits. The following constraints ensure that the unit operates within its 30-min ramp limits

$$\underbrace{\underbrace{\frac{1}{2}p_{gt} - \frac{1}{2}p_{g,t-1}}_{JI} + \underbrace{r_{gt}^{3+}}_{MJ}}_{MI} \leq 30RU_g^{30'} \quad \forall g,t \tag{21}$$

$$-\frac{1}{2}p_{gt} + \frac{1}{2}p_{g,t-1} + r_{gt}^{3-} \leq 30RD_g^{30'} \quad \forall g,t \tag{22}$$

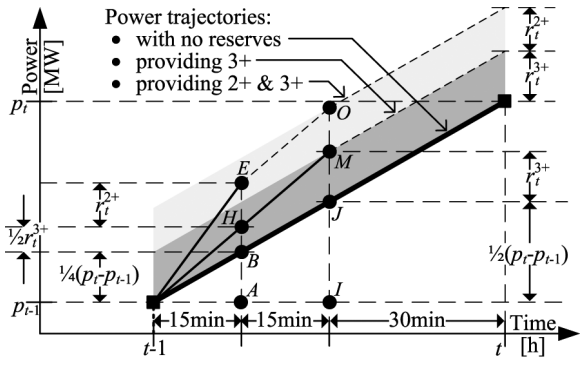

Fig. 4. Relation between upward reserves, power trajectory, and ramps.

and the operation within the unit's 15-min ramp limits are ensured with

$$\underbrace{\underbrace{\frac{1}{4}p_{gt}-\frac{1}{4}p_{g,t-1}}_{BA}+\underbrace{\frac{1}{2}r_{gt}^{3+}}_{HB}+\underbrace{r_{gt}^{2+}}_{EH}}_{EA}\leq 15RU_g^{15'}\quad\forall g,t \tag{23}$$

$$-\frac{1}{4}p_{gt}+\frac{1}{4}p_{g,t-1}+\frac{1}{2}r_{gt}^{3-}+r_{gt}^{2-}\leq 15RD_g^{15'}\quad\forall g,t. \tag{24}$$

As shown in Fig. 4, the 30-min ramp excursion due to the scheduled power trajectory *(JI)* plus the up tertiary reserve *(MJ)* cannot exceed the 30-min ramp rate limit (21). Similarly, the 15-min ramp excursion due to the scheduled power trajectory *(BA)*, plus the possible 15-min ramp excursion due to up tertiary reserve *(HB)*, plus the up secondary reserve *(EH)* cannot exceed the 15-min ramp rate limit (23). Analogously to these constraints, down reserve limits, (22) and (24), can be easily obtained.

Note that if all ramp limits are the same $RU_g^{op}=RU_g^{30'}=RU_g^{15'}$ and $RD_g^{op}=RD_g^{30'}=RD_g^{15'}$, then the 15-min ramp constraints (23)–(24) dominate over the 30-min (21)–(22) and one-hour (14) constraints. Consequently, although (21)–(22) and (14) would not be necessary, these constraints take advantage of the different units' ramp limits. To illustrate how this formulation works with different ramping limits, $RU_g^{15'}>RU_g^{30'}>RU_g^{op}$, we can analyze the upwards reserve deployment for the following example. Consider that unit g presents a zero ramping excursion during a given hour t, then $p_{gt}-p_{g,t-1}=0$ and thus (14) is automatically satisfied. Constraint (23) now ensures $1/2r_{gt}^{3+}+r_{gt}^{2+}\leq 15RU_g^{15'}$, then we have the two extreme feasible solutions $r_{gt}^{2+}=15RU_g^{15'}, r_{gt}^{3+}=0$ and $r_{gt}^{2+}=0, r_{gt}^{3+}=30RU_g^{15'}$. The former solution does not violate the ramp limits, but the latter implies that the unit may operate 30 min at 15-min ramp rate which clearly violates the 30-min ramp limit. Therefore, (21) is necessary to ensure that deploying r_{gt}^{3+} does not violate the unit's 30-min ramp limit $30RU_g^{30'}$.

2) Capacity Limits: The following constraints ensure that the reserve intervals remain within the power capacity limits at the end of the hour:

$$p_{gt}+r_{gt}^{2+}+r_{gt}^{3+}\leq\left(\overline{P}_g-\underline{P}_g\right)\left(u_{gt}-w_{g,t+1}\right)\ \forall g,t \tag{25}$$

$$p_{gt}-r_{gt}^{2-}-r_{gt}^{3-}\geq 0\quad\forall g,t. \tag{26}$$

As discussed in Section II-B, these capacity limits at the end of the hour (25)–(26) do not guarantee that the unit operates within its capacity limits during the whole hour. Note in Fig. 4 that either the point *O* or the point *E* may exceed the maximum power limit when the unit is ramping down. Therefore, (27) and (28) are needed to keep the points *O* and *E* below the maximum power limit:

$$\underbrace{\underbrace{\frac{1}{2}p_{gt}+\frac{1}{2}p_{g,t-1}}_{J}+\underbrace{r_{gt}^{2+}}_{OM}+\underbrace{r_{gt}^{3+}}_{MJ}}_{O}\leq\overline{P}_g-\underline{P}_g\quad\forall g,t \tag{27}$$

$$\underbrace{\underbrace{\frac{1}{4}p_{gt}+\frac{3}{4}p_{g,t-1}}_{B}+\underbrace{r_{gt}^{2+}}_{EH}+\underbrace{\frac{1}{2}r_{gt}^{3+}}_{HB}}_{E}\leq\overline{P}_g-\underline{P}_g\quad\forall g,t. \tag{28}$$

Analogously, (29) and (30) ensure that the unit is always producing above its minimum:

$$\frac{1}{2}p_{gt}+\frac{1}{2}p_{g,t-1}-r_{gt}^{2-}-r_{gt}^{3-}\geq 0\quad\forall g,t \tag{29}$$

$$\frac{1}{4}p_{gt}+\frac{3}{4}p_{g,t-1}-r_{gt}^{2-}-\frac{1}{2}r_{gt}^{3-}\geq 0\quad\forall g,t. \tag{30}$$

Finally, apart from keeping the units' energy and reserve within their technical limits, the formulation must also constrain energy and reserves by the bidding limits:

$$0\leq r_{gt}^{\kappa}\leq R_{gt}^{\kappa}\quad\forall\kappa,g,t \tag{31}$$

$$0\leq e_{gt}\leq E_{gt}\quad\forall\kappa,g,t \tag{32}$$

where the energy bid E_{gt} should be greater than or equal to $\underline{P}_g$, so that the unit can be committed.

In conclusion, constraints (14) and (21)–(32) guarantee that the unit can provide simultaneously (or independently) secondary and tertiary reserves at any time within the hour without violating its technical and bidding limits (ramp capability and power capacity).

D. Secondary and Tertiary Reserves for Quick-Start Units

Unlike the slow-start units, the quick-start units can ramp up (down) from 0 (more than $\underline{P}_g$) to more than $\underline{P}_g$ (0) within one hour. This makes them technically capable of providing offline tertiary reserves. Similarly to (12), which includes the SU and SD trajectories for slow-start units, (33) presents the total power output for quick-start units:

$$\widehat{p}_{gt}=\underline{P}_g u_{gt}+p_{gt}\quad\forall g,t. \tag{33}$$

1) Up and Down Offline Tertiary Reserves: Due to the minimum power output $\underline{P}_g$, the offline up reserve that is scheduled must be above $\underline{P}_g$ and below the 30-min quick-SU power capability of the unit, as presented in (34). Models commonly found in the literature fail to capture this technical characteristic ($\underline{P}_g$) when modeling offline (or non-spinning) reserves. Similarly, the offline down reserve must be between $\underline{P}_g$ and the 30-min quick-SD capability, as is shown in (35). We consider the tertiary offline down reserve as the down reserve that involves the shut down of the unit:

$$\underline{P}_g u_{gt}^{3N+}\leq r_{gt}^{3+}\leq Q_g^{SU30'}u_{gt}^{3N+}\quad\forall g,t \tag{34}$$

$$\underline{P}_g u_{gt}^{3N-}\leq r_{gt}^{3-}\leq Q_g^{SD30'}u_{gt}^{3N-}\quad\forall g,t. \tag{35}$$

Constraint (36) ensures that the unit can provide offline up reserves if the unit is down but not shutting down, and (37) ensures that the unit must be up but not starting up to provide the offline down reserve:

$$u_{gt}^{3\mathrm{N}+} + u_{gt} + w_{gt} \leq 1 \quad \forall g,t \tag{36}$$

$$u_{gt}^{3\mathrm{N}-} - u_{gt} + v_{gt} \leq 0 \quad \forall g,t. \tag{37}$$

Although two binary variables are needed to deal with offline tertiary reserves, one of them is always fixed by u_{gt}. If $u_{gt}=0$, then (37) implies $u_{gt}^{3\mathrm{N}-}=0$, and when $u_{gt}=1$, then (36) makes $u_{gt}^{3\mathrm{N}+}=0$.

2) Capacity Limits: To provide the offline down reserve for a given hour, the unit must be operating below the 30-min SD capability during that hour. This is ensured by the upper limit constraints of the unit at the beginning of the hour (38), at the end (39):

$$\begin{aligned} p_{gt} + r_{gt}^{2+} + r_{gt}^{3+} \leq{}& \left(\overline{P}_g - \underline{P}_g\right) u_{gt} \\ &- \left(\overline{P}_g - Q_g^{\mathrm{SD}30'}\right) u_{g,t+1}^{3\mathrm{N}-} \\ &- \left(\overline{P}_g - Q_g^{\mathrm{SU}}\right) v_{gt} - \left(\overline{P}_g - Q_g^{\mathrm{SD}}\right) w_{g,t+1} \quad \forall g,t \end{aligned} \tag{38}$$

$$\begin{aligned} p_{gt} + r_{gt}^{2+} + r_{gt}^{3+} \leq{}& \overline{P}_g - \underline{P}_g \\ &- \left(\overline{P}_g - Q_g^{\mathrm{SD}30'}\right) u_{g,t}^{3\mathrm{N}-} \quad \forall g,t \end{aligned} \tag{39}$$

and at minute 30 (40) and 15 (41):

$$\frac{1}{2}p_{gt} + \frac{1}{2}p_{g,t-1} + r_{gt}^{2+} + r_{gt}^{3+} \leq \overline{P}_g - \underline{P}_g - \left(\overline{P}_g - Q_g^{\mathrm{SD}30'}\right) u_{gt}^{3\mathrm{N}-} \quad \forall g,t \tag{40}$$

$$\frac{1}{4}p_{gt} + \frac{3}{4}p_{g,t-1} + r_{gt}^{2+} + \frac{1}{2}r_{gt}^{3+} \leq \overline{P}_g - \underline{P}_g - \left(\overline{P}_g - Q_g^{\mathrm{SD}30'}\right) u_{gt}^{3\mathrm{N}-} \quad \forall g,t. \tag{41}$$

Finally, the total power output must be greater than the summation of all downward reserves. This is guaranteed in the lower limit constraints of the unit at the beginning of the hour (42), at the end (43):

$$p_{g,t-1} - r_{g,t-1}^{2-} - r_{g,t-1}^{3-} - \left(r_{gt}^{3\mathrm{N}-} - \underline{P}_g u_{gt}^{3\mathrm{N}-}\right) \geq 0 \quad \forall g,t \tag{42}$$

$$p_{gt} - r_{gt}^{2-} - r_{gt}^{3-} - \left(r_{gt}^{3\mathrm{N}-} - \underline{P}_g u_{gt}^{3\mathrm{N}-}\right) \geq 0 \quad \forall g,t \tag{43}$$

and at minutes 30 (44) and 15 (45):

$$\begin{aligned} &\frac{1}{2}p_{gt} + \frac{1}{2}p_{g,t-1} - r_{gt}^{2-} - r_{gt}^{3-} \\ &\quad - \left(r_{gt}^{3\mathrm{N}-} - \underline{P}_g u_{gt}^{3\mathrm{N}-}\right) \geq 0 \quad \forall g,t \end{aligned} \tag{44}$$

$$\begin{aligned} &\frac{1}{4}p_{gt} + \frac{3}{4}p_{g,t-1} \\ &\quad - r_{gt}^{2-} - \frac{1}{2}r_{gt}^{3-} - \left(r_{gp}^{3\mathrm{N}-} - \underline{P}_g u_{gt}^{3\mathrm{N}-}\right) \geq 0 \\ &\forall g,t. \end{aligned} \tag{45}$$

E. Computational Efficiency

The computational performance of an MIP formulation depends mainly on its tightness (distance between relaxed and integer solutions) and compactness (quantity of data to process), as stated in the literature of integer programming [34], [35]. The full exploitation of these two characteristics has meant a breakthrough in off-the-shelf MIP solvers (through cutting planes and root presolve) [36], [37].

The core of the proposed MIP formulation is built upon the tight and compact formulations presented in [19] and [28], and thus takes advantage of these mathematical properties. Although detailing the mathematical properties of the proposed formulation is beyond the scope of this paper, some specific aspects are worth mentioning to aid the understanding of its computational efficiency:

1) The number of binary variables is a very poor indicator of the difficulty of an MIP model [34], [35]. Increasing the number of binary variables, as in the case of the proposed formulation, is actually used as a tightening strategy [35]. See [19] and [28] for further details. In addition, the variables v_{gt}, w_{gt} and δ_{gst} can be defined as continuous because the formulation (tightness of the model) forces them to take binary values. Therefore, declaring these variables as binary does not increase the combinatorial complexity and allow MIP solvers to use powerful strategies that exploit their integrality characteristic [28], [35], [36].
2) The only binary variable that is actually needed for slow-start units is u_{gt}. On the other hand, the quick-start units require two extra binary variables $u_{gt}^{3\mathrm{N}+}$ and $u_{gt}^{3\mathrm{N}-}$. However, one of them is always fixed by u_{gt} (see Section II-D1). In the worst case, they only add the complexity of one-single binary variable. In any case, and fortunately, quick-start units are usually a minority in the power system mixes.
3) The modeling of variable SU costs with δ_{gst} and (10)–(11) make a formulation significantly more tight and compact in comparison with common SU-cost models (e.g., [11]), as reported in [28]. Apart from taking this computational advantage, this paper fully exploits the inclusion of δ_{gst} to model the SU power trajectories in 12 [19].
4) Including r_{gt}^{κ} together with the equations in Section II-C (Section II-D) further constrains the operation of slow (quick)-start units. This means that the formulation is actually being further tightened. A similar conclusion was drawn in [38], where including ramping constraints actually improved the MIP formulation.
5) Finally, the variables $\widehat{p}_{gt}$ and e_{gt} are used in this work for the sake of clarity. However, they are not strictly needed, as the former could be directly included in (2) and the latter in (1). Their values can be obtained after solving the problem, without changing the results.

III. Numerical Results

The following case studies were conducted to illustrate the proposed market-clearing formulation, given by (1)–(14) together with (21)–(45). The power system data was based on that in [11]. This power system was adapted to consider SU and SD power trajectories. Table I presents the technical and economic data of the thermal units, including different SU ramps. Units 8 to 10 are quick-start units with hourly SU and SD capabilities of 55 MW, and 50 MW for the 30-min SU and SD capabilities. For slow-start units, the power outputs P_{gsi}^{SU} (P_{gi}^{SD}) for the SU (SD) power trajectories are obtained as an hourly linear change from 0 ($\underline{P}_g$) to $\underline{P}_g$ (0) for a duration of SU_{gs}^{D} (SD_g^{D}) hours. The energy costs due to SU and SD processes are added to the SU and SD costs shown in Table I.

All tests were carried out using CPLEX 12.4 under GAMS [39] on an Intel-i7 2.4 GHz with 4 GB of RAM memory. Prob-

TABLE I
GENERATOR DATA

Unit	Technical Data							Cost Coefficients		StartUp Ramping Information								
	$\overline{P}$ [MW]	$\underline{P}$ [MW]	TU/TD [h]	RU/RD [MW/min]	p_0 [MW]	IniState [h]	SD^{D} [h]	C^{NL} [$/h]	C^{LV} [$/MWh]	SU_1^{D} [h]	T_1^{SU} [h]	C_1^{SU} [$]	SU_2^{D} [h]	T_2^{SU} [h]	C_2^{SU} [$]	SU_3^{D} [h]	T_3^{SU} [h]	C_3^{SU} [$]
1	455	150	8	3.75	455	8	3	1000	16.19	3	8	3000	5	11	7500	6	14	9000
2	455	150	8	3.75	245	8	3	970	17.26	3	8	4000	5	11	8000	7	14	10000
3	130	20	5	0.83	0	-5	2	700	16.60	2	5	300	3	7	800	5	10	1100
4	130	20	5	0.83	0	-5	2	680	16.50	2	5	560	3	7	950	5	10	1120
5	162	25	6	1.00	0	-6	2	450	19.70	2	6	600	3	8	1400	5	11	1800
6	80	20	3	1.00	0	-3	1	370	22.26	1	3	170	3	8	340	—	—	—
7	85	25	3	1.00	0	-3	1	480	27.74	1	3	260	3	6	520	—	—	—
8*	55	10	1	2.25	0	-1	—	660	25.92	—	1	30	—	2	60	—	—	—
9*	55	10	1	2.25	0	-1	—	665	27.27	—	1	30	—	2	60	—	—	—
10*	55	10	1	2.25	0	-1	—	670	27.79	—	1	30	—	2	60	—	—	—

*This is a quick-start unit

TABLE II
POWER AND ENERGY DEMAND PROFILES (MW)

Hour	1	2	3	4	5	6	7	8	9	10	11	12
$D1^*$	750	850	950	1000	1100	1150	1200	1300	1400	1450	1500	1400
$D2^*$	725	875	925	1025	1075	1175	1175	1325	1375	1475	1475	1425
$D^{\mathrm{E}\dagger}$	725	800	900	975	1050	1125	1175	1250	1350	1425	1475	1450
Hour	**13**	**14**	**15**	**16**	**17**	**18**	**19**	**20**	**21**	**22**	**23**	**24**
$D1^*$	1300	1200	1050	1000	1100	1200	1400	1300	1100	900	800	700
$D2^*$	1475	1425	1275	1225	1025	1025	1075	1225	1375	1325	1075	925
$D^{\mathrm{E}\dagger}$	1350	1250	1125	1025	1050	1150	1300	1350	1200	1000	850	750

*Power [MW] at the end of the hour †Total Energy [MWh] for the hour

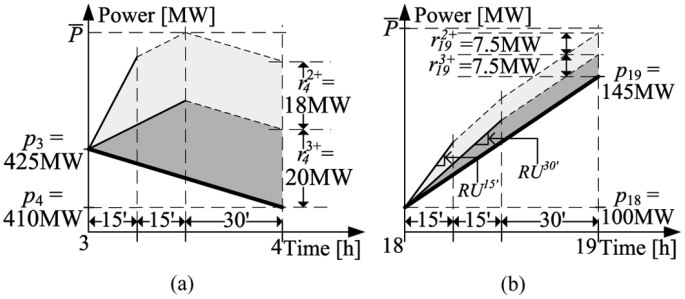

Fig. 5. Examples of units power and upwards reserve schedules. (a) Unit 2 hour 4. (b) Unit 5 hour 19.

lems were solved until they hit a CPU time limit of 1000 s or until they reached optimality (more precisely to 10^{-6} of relative optimality tolerance). Apart from this, CPLEX default values were used for all the experiments.

This section is divided into three parts. The first part illustrates how the formulation deals with the reserves. The second part compares the difference in commitment schedules between the proposed formulation and the conventional energy-block scheduling. The last part compares the computational performance of the proposed formulation with a UC formulation commonly found in the literature [11].

A. Ramp and Reserve Schedules

For this case study, the previously described power system must meet the power demand D1, shown in Table II, at the end of each hour. The up/down secondary and tertiary reserve requirements of 2.5% and 5% of the power demand have to be met for each hour. The 15- and 30-min ramp capabilities of the units are assumed to be equal to 150% and 100% of their operation ramp rates, respectively. For simplicity, we assume that all units offer secondary, tertiary and offline-tertiary reserves at 20%, 10% and 40% of their energy variable cost C_g^{LV}, respectively. Each unit is considered to have the same bids for upward and downward reserves. The maximum reserve offered by each unit is set to the maximum available reserve.

Fig. 6 shows the generation and reserve schedules for each generation unit. Note the piecewise-linear profiles of power schedules which follow the instantaneous demand forecast profile. Reserves are scheduled as constant power availability for each hour. Note in Fig. 6 (bottom section) that all the scheduled offline tertiary reserves are above the units' minimum output (10 MW for quick-start units 7 to 10). As mentioned in Section II-D, the units providing offline tertiary reserves cannot be called to produce below their minimum output.

We will now examine some cases in which the available reserve of units were bound by the capacity and ramping limits:

1) *Reserves bound by capacity limits*: Interestingly, unit 2 is scheduled to ramp down in hour 4 while the demand is increasing during that hour, as shown in Fig. 6. Unit 2 reduces its production during hour 4 in order to provide upward reserves to the system. Fig. 5(a) shows the power production and upward-reserve schedules for unit 2 during hour 4. In the event that unit 2 provides all the upward scheduled reserves, the resulting power trajectory (see the uppermost solid line in Fig. 5) will ramp up and achieve the maximum unit capacity output (455 MW) after 30 min. Note that the capacity limit is only reached if the unit starts providing all the upward reserves at the beginning of the hour.
2) *Reserves bound by ramping limits*: Fig. 5(b) shows the power production and upward-reserve schedules for unit 5 during hour 19. The unit is scheduled to ramp up at 0.75 MW/min during normal operation. The unit 30-min ramping limit $RU^{30'}$ is 1 MW/min, which means that the unit has an extra ramp capability of 0.25 MW/min, which results in 7.5 MW in the reserve that the unit can provide within 30 min r^{3+}. In addition, the unit has a 15-min ramping limit $RU^{15'}$ of 1.5 MW/min. This means that for 15-min reserve deployment r^{2+}, the unit has an available ramp capability of 0.5 MW/min, which results in a power reserve capacity of 7.5 MW that can be provided in 15 min.

TABLE III
OPTIMAL ENERGY SCHEDULES

	Unit	Hour																							
		1	2	3	4	5	6	7	8	9	10	11	12	13	14	15	16	17	18	19	20	21	22	23	24
PropRmpSch - D1	1	455	455	455	455	455	455	455	455	455	455	455	455	455	455	455	455	455	455	455	455	455	455	455	455
	2	266.67	327.5	405.83	437.5	430	421.67	417.5	438.33	455	455	455	455	455	435	362.5	285	302.5	355	410	455	422.5	335	241.25	176.25
	3	.	3.33	10	16.67	45	95	125	130	130	130	130	130	130	130	130	130	130	130	125	95	45	15	5	.
	4	3.33	10	16.67	45	95	125	130	130	130	130	130	130	130	130	130	130	130	130	130	130	130	130	130	112.5
	5	.	4.17	12.5	20.83	25	25	37.5	80	136	162	162	162	146	100	47.5	25	32.5	70	130	152.5	115	55	18.75	6.25
	6	.	.	.	.	.	3.33	10	16.67	44	74	80	50	10	.	.	.	.	10	50	62.5	32.5	10	.	.
	8	.	.	.	.	.	.	.	.	.	.	27.5	51.5	24	.	.	.	.	.	.	.	.	.	.	.
	9	.	.	.	.	.	.	.	.	.	19	35.5	16.5	.	.	.	.	.	.	.	.	.	.	.	.
PropRmpSch - D2	1	455	455	455	455	455	455	455	455	455	455	455	455	455	455	455	455	455	455	455	455	455	455	455	455
	2	266.67	327.5	405.83	437.5	430	425	412.5	417.5	455	455	455	455	446.5	446.5	370	285	310	370	430	455	385	256.25	173.75	150
	3	.	3.33	10	16.67	45	95	125	130	130	130	130	130	130	130	130	130	130	130	130	130	130	130	105	55
	4	3.33	10	16.67	45	95	125	130	130	130	130	130	130	130	130	130	130	130	130	130	130	130	130	110	90
	5	.	4.17	12.5	20.83	25	25	45	95	142.5	161	162	162	132	78.5	40	25	25	55	115	115	55	18.75	6.25	.
	6	.	.	.	.	.	.	3.33	10	16.67	50	80	74	44	10	.	.	.	10	40	65	45	10	.	.
	7	.	.	.	.	.	.	4.17	12.5	20.83	44	63	44	12.5	.	.	.	.	.	.	.	.	.	.	.
ConvlEnSch - D1&D2	1	455	455	455	455	455	455	455	455	455	455	455	455	455	455	455	455	455	455	455	455	455	455	455	455
	2	270	320	420	455	455	455	440	435	455	455	455	455	455	455	385	285	310	385	455	455	380	260	150	150
	3	.	.	.	.	20	70	120	130	130	130	130	130	130	130	130	130	130	130	130	130	130	130	90	40
	4	.	.	.	.	20	70	120	130	130	130	130	130	130	130	130	130	130	130	130	130	130	130	130	80
	5	.	25	25	65	100	75	40	100	160	162	162	162	135	80	25	25	25	50	110	145	85	25	25	25
	6	.	.	.	.	.	.	.	.	20	68	80	80	20	.	.	.	.	.	20	35	20	.	.	.
	7	.	.	.	.	.	.	.	.	.	25	63	38	25	.	.	.	.	.	.	.	.	.	.	.

Highlighted cells indicate that the unit is either starting up or shutting down

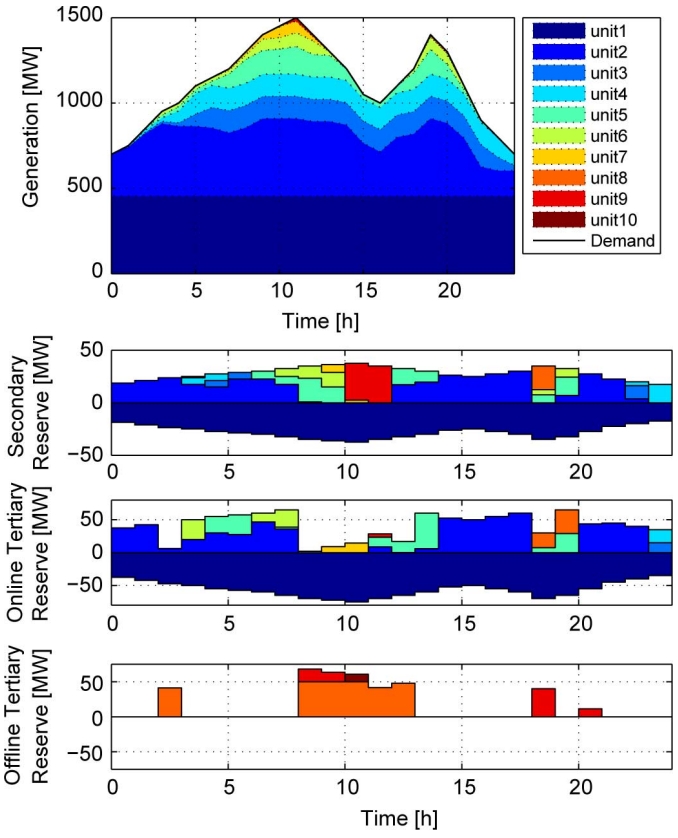

Fig. 6. Generation and reserves schedules. For the reserve schedules, positive and negative values refer to up and down reserves, respectively.

In conclusion, as discussed in Section II, even though the formulation is on an hourly basis, it guarantees that the unit (capacity and ramping) limits are not violated within the hour when providing reserves with shorter deployment times.

B. Conventional versus Ramp-Based Scheduling Approaches: Commitment and Economic Impact

To illustrate the difference in schedules between the conventional and the proposed scheduling approaches, the lowest production cost is obtained for two different demand profiles assuming full knowledge of system conditions. That is, it is assumed that the power demand profile is known perfectly and that no uncertain events will happen. Therefore, there should be no need for operating reserves and hence they are not considered (i.e., $D_t^{\kappa}, r_{gt}^{\kappa} = 0\,\forall\kappa$). Although this situation is hypothetical, it helps to evaluate [40] and compare the two scheduling approaches.

The proposed ramp-based scheduling formulation, labelled as *PropRmpSch*, and the conventional staircase energy approach, labelled as *ConvlEnSch*, are used to optimally schedule the 10-unit system, in Table I, to supply the power demand profiles $D1$ and $D2$ presented in Table II. Note that $D1$ and $D2$ present the same energy profile (D^{E} in Table II) but different ramp requirements. Table III shows the optimal energy schedules found by *PropRmpSch* and *ConvlEnSch* to supply $D1$ and $D2$. While *TradEnSch* directly provides the energy schedules, *PropRmpSch* provides the piecewise-linear power schedules (see Table IV), and obtaining the resulting energy schedule is straightforward ($\widehat{p}_{gt}/2 + \widehat{p}_{g,t-1}/2$). Note that in Table III, *ConvlEnSch* provides the same optimal scheduling solution for $D1$ and $D2$ because they present the same energy profile. On the other hand, *PropRmpSch* provides different optimal scheduling for $D1$ and $D2$, although both scheduling solutions satisfy the same total energy demand.

One power profile has a unique energy profile and hence satisfying a power profile automatically satisfies the energy profile. However, one energy profile has infinite possible power profiles [12], [14], [16]; therefore, even though *ConvlEnSch* could provide a given energy profile, it cannot guarantee that all possible

TABLE IV
OPTIMAL POWER SCHEDULES

	Unit	Hour																								
		0	1	2	3	4	5	6	7	8	9	10	11	12	13	14	15	16	17	18	19	20	21	22	23	24
PropRampSch - D1	1	455	455	455	455	455	455	455	455	455	455	455	455	455	455	455	455	455	455	455	455	455	455	455	455	455
	2	245	288.33	366.67	445	430	430	413.33	421.67	455	455	455	455	455	455	415	310	260	345	365	455	455	390	280	202.5	150
	3	.	.	6.67	13.33	20	70	120	130	130	130	130	130	130	130	130	130	130	130	130	120	70	20	10	.	.
	4	.	6.67	13.33	20	70	120	130	130	130	130	130	130	130	130	130	130	130	130	130	130	130	130	130	130	95
	5	.	.	8.33	16.67	25	25	25	50	110	162	162	162	162	130	70	25	25	40	100	160	145	85	25	12.5	.
	6	.	.	.	.	.	.	6.67	13.33	20	68	80	80	20	.	.	.	.	.	20	80	45	20	.	.	.
	8	.	.	.	.	.	.	.	.	.	.	.	55	48	.	.	.	.	.	.	.	.	.	.	.	.
	9	.	.	.	.	.	.	.	.	.	.	38	33	.	.	.	.	.	.	.	.	.	.	.	.	.
PropRampSch– D2	1	455	455	455	455	455	455	455	455	455	455	455	455	455	455	455	455	455	455	455	455	455	455	455	455	455
	2	270	263.33	391.67	420	455	405	445	380	455	455	455	455	455	438	455	285	285	335	405	455	455	315	197.5	150	150
	3	.	.	6.67	13.33	20	70	120	130	130	130	130	130	130	130	130	130	130	130	130	130	130	130	130	80	30
	4	.	6.67	13.33	20	70	120	130	130	130	130	130	130	130	130	130	130	130	130	130	130	130	130	130	90	90
	5	.	.	8.33	16.67	25	25	25	65	125	160	162	162	162	102	55	25	25	25	85	145	85	25	12.5	.	.
	6	.	.	.	.	.	.	.	6.67	13.33	20	80	80	68	20	.	.	.	.	.	60	70	20	.	.	.
	7	.	.	.	.	.	.	.	8.33	16.67	25	63	63	25	.	.	.	.	.	.	.	.	.	.	.	.

Highlighted cells indicate that the unit is either starting up or shutting down

resulting power profiles can be supplied [12]. Moreover, *ConvlEnSch* suffer from the following shortcomings in comparison with *PropRmpSch*, due to the inability of *ConvlEnSch* to perceive a given power profile:

1) *Ramp Scarcity*: The power demand $D2$ is ramping at 100 MW/h during hour 4 (see Table II) and the optimal schedule of *ConvlEnSch* only provides 60 MW/h of ramp capability. Note that in Table III only three units are up during hour four, where units 1 and 2 are producing at their maximum capacity. Consequently, unit 5 is the only unit that can ramp up and its ramping capability is 1 MW/min (see Table I).
2) *Capacity Scarcity*: The demand peak of $D1$ is 1500 MW and occurs at the end of hour 11. Note that *ConvlEnSch* scheduled seven units for this hour having a total production capacity of 1497 MW. This is in contrast to *PropRmpSch*, which committed seven units at hour 11 to satisfy the peak demand of $D1$.
3) *Infeasible Energy Delivery*: There are many hours where units cannot comply with their scheduled energy profile provided by *ConvlEnSch*. For example, unit 5 must produce at its minimum output (25 MW) during the whole hour 3 to deliver its scheduled 25 MWh. If the unit ramps up at its maximum capability (60 MW/h), then the production at the end of hour 4 will be 85 MW, providing a maximum of 55 MWh for hour 4, and thus failing to deliver its scheduled energy level of 65 MWh. Similarly, unit 6 must produce 80 MW at the end of hour 12 to provide its schedule energy for that hour. If the unit ramps down at its maximum capability, it can provide a minimum of 50 MWh for hour 13, thus failing to deliver its scheduled energy level of 20 MWh.

Table V shows the comparison of the optimal scheduling costs where *ConvlEnSch* presents the highest scheduling costs. This can be explained as follows: Although both *PropRmpSch* and *ConvlEnSch* consider the cost of the intrinsic energy produced during the SU and SD processes, *ConvlEnSch* does not include this energy in the scheduling stage. As a consequence, *ConvlEnSch* cannot accommodate the SU and SD power trajectories, which contribute to satisfying the demand (energy and ramp). This also causes an inefficient deployment of resources in real time to accommodate these trajectories that were ignored in the scheduling stage [18], [19].

TABLE V
COMPARISON OF TOTAL OPTIMAL SCHEDULING COSTS

Approach	Demand	Scheduling Cost ($)
PropRmpSch	$D1$	562738.61
	$D2$	562573.80
ConvlEnSch	$D1$ and $D2$	567392.22

In short, the conventional energy scheduling approach does not guarantee that enough resources will be available to satisfy an expected power profile. Furthermore, *ConvlEnSch* cannot even guarantee a feasible energy delivery of its resulting energy profile, as also previously reported in [12], [14], and [21]. Consequently, *ConvlEnSch* would require *ad-hoc* operations in real time in order to deal with these problems and keep the balance between supply and demand. However, *PropRmpSch* overcomes these problems by an adequate resource scheduling.

C. Computational Performance

In order to assess the computational burden of the proposed formulation, its computational performance was compared with the UC model proposed in [11]. The work in [11] presents a basic formulation that only considers one-single upward reserve and ignores the SU and SD power trajectories. The model in [11] is implemented using the case study detailed in Section III-A and the hourly spinning reserve is assumed to be 10% of the hourly demand (which is similar to the 5% of the hourly demand assumed for the half-hour tertiary reserve in the proposed formulation).

Two different problem sizes were simulated: 10-unit (presented in Table I) and 100-unit power systems, the latter being the 10-unit power system replicated ten times. This replication introduces symmetry in the MIP problem which makes it harder to solve than usual [35]. The load demand was accordingly multiplied by 10 for the latter power system case.

Table VI shows the model size and computational performance of [11] and the proposed formulation, which is labelled as "Prop". The proposed model presents around 8% and 5% more constraints and non-zeros in the constraint matrix than [11]. This is an insignificant increase taking into account the fact that the

TABLE VI
COMPARISON OF DIFFERENT FORMULATIONS

Case	Model Size								Computational Performance							
	# of Constraints		# of Real Variables		# of Binary Variables		Non-zero elements		Time (s)		OptTol (p.u.)		Nodes		Int. Gap ($\times 10^{-3}$)	
(# Gens)	Prop	[11]	Prop	[11]	Prop	[11]	Prop	[11]	Prop	[11]	Prop	[11]	Prop	[11]	Prop	[11]
10	4436	4089	1584	984	1365	240	21767	20867	9.11	1.42	4e-15	2e-15	1123	1058	6.41	21.92
100	43271	40449	15840	9624	13650	2400	217661	208445	1001	1000	2e-4	6.3e-3	33257	62098	3.33	17.6

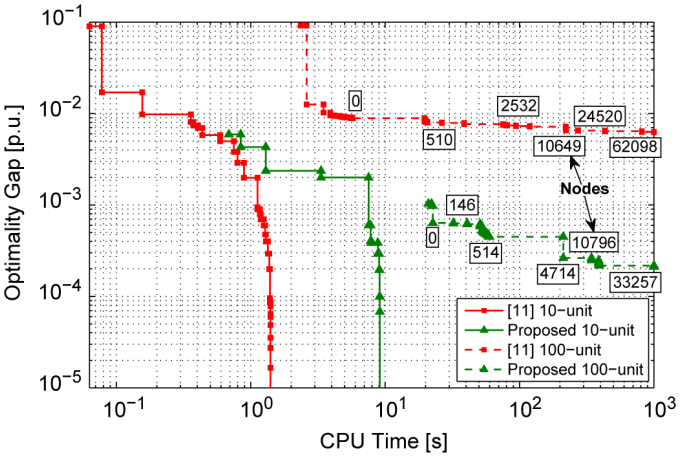

Fig. 7. Comparison of convergence evolution to optimal solutions. Values inside squares indicate the number of explored nodes by the solver.

proposed formulation includes SU and SD power trajectories and five types of reserves more than [11]. However, although the proposed formulation needs around 1.6 and 5.7 times as many real and binary variables as [11], respectively, this does not necessarily mean an increase in computational burden. In fact, increasing the number of binary variables may lower the complexity of an MIP formulation [35] as in the case of the tight and compact formulations presented in [19] and [28], which are the core of the formulation proposed in this paper.

As stated in Section II-E, the computational burden of an MIP formulation mainly depends on the strength of its linear program (LP) relaxation, where the LP relaxation of an MIP problem is obtained by relaxing its integrality requirements. In other words, the nearer the LP relaxed solution is to its MIP integer solution, the faster the search for optimality. The strength (or tightness) of a MIP formulation can be measured with the integrality gap [28], [35] which is defined as $(Z_{\mathrm{MIP}} - Z_{\mathrm{LP}})/Z_{\mathrm{MIP}}$, where Z_{MIP} and Z_{LP} are the optimal values of the MIP and the relaxed LP, respectively. The integrality gap of the two formulations which are not modeling exactly the same problem should not be directly compared; however, these gaps provide an indication of the strength of each formulation. Note that in Table VI, the proposed formulation presents a smaller integrality gap (around 5 times lower) in comparison with [11], which indicates that the proposed formulation is significantly tighter.

Finally, Fig. 7 shows the convergence evolution, for both formulations, for the two different system sizes. The proposed formulation took longer to find an initial feasible solution mainly due to the greater number of binary variables (In general, a large number of integer variables complicates the process of finding initial feasible solutions). For the 10-unit case, the impact is significant due to the short solving times (less than 10 s). However, for the 100-unit case, even though the proposed formulation took longer to find an initial feasible solution, the optimality gap achieved by this solution (with zero nodes explored) is better than all the solutions found by [11] within the time limit. This evolution of convergence, as well as the quality of the initial solutions, is mainly due to the tightness of the proposed formulation.

IV. CONCLUSIONS

A UC-based market clearing formulation was proposed using continuous power trajectories for both generating units and demand instead of the commonly established staircase profile for energy blocks. The use of an instantaneous power profile allows the model to efficiently schedule reserve and ramping resources. In comparison with conventional UC models, the proposed formulation guarantees that, first, energy schedules can be delivered and, second, that operating reserves (secondary, tertiary online and tertiary offline) can be deployed within their given time requirements while respecting the ramping and capacity limits of generating units. In addition, the model takes into account the normally neglected power trajectories that occur during the startup and shutdown processes, thus optimally scheduling them to provide energy (and ramp), which help to satisfy the power demand. The formulation was tested on a 10-unit and 100-unit system, where the computational burden was lowered in comparison with common UC formulations.

V. ACKNOWLEDGEMENT

The authors would like to thank all partner institutions within the Erasmus Mundus Joint Doctorate Programme in Sustainable Energy Technologies and Strategies (SETS) as well as to the European Commission for their support.

REFERENCES

[1] B. F. Hobbs, M. H. Rothkopf, R. P. O'Neill, and H.-p Chao, *The Next Generation of Electric Power Unit Commitment Models*, 1st ed. New York, NY, USA: Springer, 2001.

[2] R. Baldick, U. Helman, B. F. Hobbs, and R. P. O'Neill, "Design of efficient generation markets," *Proc. IEEE*, vol. 93, no. 11, pp. 1998–2012, Nov. 2005.

[3] M. Shahidehpour, H. Yamin, and Z. Li, *Market Operations in Electric Power Systems: Forecasting, Scheduling, and Risk Management*, 1st ed. New York, NY, USA: Wiley-IEEE Press, 2002.

[4] T. Wu, M. Rothleder, Z. Alaywan, and A. Papalexopoulos, "Pricing energy and ancillary services in integrated market systems by an optimal power flow," *IEEE Trans. Power Syst.*, vol. 19, no. 1, pp. 339–347, Feb. 2004.

[5] F. Galiana, F. Bouffard, J. Arroyo, and J. Restrepo, "Scheduling and pricing of coupled energy and primary, secondary, and tertiary reserves," *Proc. IEEE*, vol. 93, no. 11, pp. 1970–1983, Nov. 2005.

[6] NERC, 22:00 Frequency Excursion (Final Report), NERC, Report 20020828, Aug. 2002. [Online]. Available: http://www.nerc.com/docs/oc/rs/FETF-Report_20020828.doc.

[7] ENTSO-e, Frequency Quality Investigation, Excerpt of the Final Report, UCTE AD-HOC, Report, Aug. 2008. [Online]. Available: http://www.entsoe.eu/fileadmin/user_upload/_library/publications/ce/ otherreports/090330_UCTE_FrequencyInvestigationReport_Abstract.pdf.

[8] ENTSO-e and Eurelectric, Deterministic Frequency Deviations Root Causes and Proposals for Potential Solutions, ENTSO-e, Report, Dec. 2011. [Online]. Available: https://www.entsoe.eu/fileadmin/user_upload/_library/publications/entsoe/120222_Deterministic_Frequency_Deviations_joint_ENTSOE_Eurelectric_Report__Final_.pdf.
[9] MISO, Ramp Capability for Load Following in the MISO Markets, Midwest Independent Transmission System Operator, USA, Tech. Rep., Jul. 2011. [Online]. Available: https://www.midwestiso.org/_layouts/MISO/ECM/Redirect.aspx?ID=112806.
[10] CAISO, Flexible Ramping Products: Second Revised Draft Final Proposal, California Independent System Operator, USA, Tech. Rep., Oct. 2012. [Online]. Available: http://www.caiso.com/Documents/SecondRevisedDraftFinalProposal-FlexibleRampingProduct.pdf.
[11] M. Carrion and J. Arroyo, "A computationally efficient mixed-integer linear formulation for the thermal unit commitment problem," *IEEE Trans. Power Syst.*, vol. 21, no. 3, pp. 1371–1378, Aug. 2006.
[12] X. Guan, F. Gao, and A. Svoboda, "Energy delivery capacity and generation scheduling in the deregulated electric power market," *IEEE Trans. Power Syst.*, vol. 15, no. 4, pp. 1275–1280, Nov. 2000.
[13] X. Guan, Q. Zhai, Y. Feng, and F. Gao, "Optimization based scheduling for a class of production systems with integral constraints," *Sci. China Series E: Technol. Sci.*, vol. 52, no. 12, pp. 3533–3544, Dec. 2009.
[14] H. Wu, Q. Zhai, X. Guan, F. Gao, and H. Ye, "Security-constrained unit commitment based on a realizable energy delivery formulation," *Math. Problems Eng.*, vol. 2012, pp. 1–22, 2012.
[15] Y. Yang, J. Wang, X. Guan, and Q. Zhai, "Subhourly unit commitment with feasible energy delivery constraints," *Appl. Energy*, 2012.
[16] G. Rela, J. I. de la Fuente, T. Gómez, D. Soler, O. Largo, R. Martínez, and F. Apartero, "A linearization algorithm for hourly power scheduling in a competitive framework," in *Proc. Universities Power Eng. Conf. (UPEC)*, Belfast, Ireland, Sep. 2000.
[17] N. Troy, E. Denny, and M. O'Malley, "Base-load cycling on a system with significant wind penetration," *IEEE Trans. Power Syst.*, vol. 25, no. 2, pp. 1088–1097, May 2010.
[18] G. Morales-Espana, J. Garcia-Gonzalez, and A. Ramos, "Impact on reserves and energy delivery of current UC-based market-clearing formulations," in *Proc. European Energy Market EEM*, Florence, Italy, May 2012, pp. 1–7.
[19] G. Morales-Espana, J. Latorre, and A. Ramos, "Tight and compact MILP formulation of start-up and shut-down ramping in unit commitment," *IEEE Trans. Power Syst.*, vol. 28, no. 2, pp. 1288–1296, May 2013.
[20] J. M. Arroyo and A. Conejo, "Modeling of start-up and shut-down power trajectories of thermal units," *IEEE Trans. Power Syst.*, vol. 19, no. 3, pp. 1562–1568, Aug. 2004.
[21] J. Garcia-Gonzalez, A. San Roque, F. Campos, and J. Villar, "Connecting the intraday energy and reserve markets by an optimal redispatch," *IEEE Trans. Power Syst.*, vol. 22, no. 4, pp. 2220–2231, Nov. 2007.
[22] ERCOT, White Paper Functional Description of Core Market Management System (MMS) Applications for Look-Ahead SCED, Version 0.1.2, Electric Reliability Council of Texas ERCOT, Texas, USA, Nov. 2011. [Online]. Available: http://www.ercot.com/content/meetings/metf/keydocs/2012/0228/04_white_paper_funct_desc_core_mms_applications_for_la_sced.doc.
[23] Z. Li and M. Shahidehpour, "Security-constrained unit commitment for simultaneous clearing of energy and ancillary services markets," *IEEE Trans. Power Syst.*, vol. 20, no. 2, pp. 1079–1088, May 2005.
[24] J. Wang, M. Shahidehpour, and Z. Li, "Contingency-constrained reserve requirements in joint energy and ancillary services auction," *IEEE Trans. Power Syst.*, vol. 24, no. 3, pp. 1457–1468, Aug. 2009.
[25] A. L. Ott, "Evolution of computing requirements in the PJM market," in *Proc. IEEE Power and Energy Soc. General Meeting*, Jul. 2010, pp. 1–4.
[26] ENTSO-e, Operation handbook, Policy 1: Load-frequency control and performance [c], European Network of Transmission Systems Operators for Electricity (ENTSO-e), Tech. Rep., Apr. 2009, p. 1. [Online]. Available: https://www.entsoe.eu/nc/resources/publications/former-associations/ucte/operation-handbook.
[27] R. P. O'Neill, P. M. Sotkiewicz, B. F. Hobbs, M. H. Rothkopf, and W. R. Stewart, Jr, "Efficient market-clearing prices in markets with nonconvexities," *Eur. J. Oper. Res.*, vol. 164, no. 1, pp. 269–285, Jul. 2005.
[28] G. Morales-Espana, J. M. Latorre, and A. Ramos, "Tight and compact MILP formulation for the thermal unit commitment problem," *IEEE Trans. Power Syst.*, to be published.
[29] NERC, Reliability Standards for the Bulk Electric Systems in North America, North American Electric Reliability Corporation, Tech. Rep., May 2011. [Online]. Available: http://www.nerc.com/files/Reliability_Standards_Complete_Set.pdf.
[30] C. Wang and S. M. Shahidehpour, "Optimal generation scheduling with ramping costs," *IEEE Trans. Power Syst.*, vol. 10, no. 1, pp. 60–67, Feb. 1995.
[31] T. Li and M. Shahidehpour, "Dynamic ramping in unit commitment," *IEEE Trans. Power Syst.*, vol. 22, no. 3, pp. 1379–1381, Aug. 2007.
[32] A. J. Wood and B. F. Wollenberg, *Power Generation, Operation, and Control*, 2nd ed. New York, NY, USA: Wiley-Interscience, 1996.
[33] D. Rajan and S. Takriti, Minimum Up/Down Polytopes of the Unit Commitment Problem With Start-up Costs, IBM, Research Report RC23628, Jun. 2005. [Online]. Available: http://domino.research.ibm.com/library/cyberdig.nsf/1e4115aea78b6e7c85256b360066f0d4/cdcb02a7c809d89e8525702300502ac0?OpenDocument.
[34] L. Wolsey, *Integer Programming*. New York, NY, USA: Wiley-Interscience, 1998.
[35] H. P. Williams, *Model Building in Mathematical Programming*, 4th ed. New York, NY, USA: Wiley, 1999.
[36] R. Bixby, M. Fenelon, Z. Gu, E. Rothberg, and R. Wunderling, *MIP: Theory and Practice Closing the Gap, in System Modelling and Optimization: Methods, Theory and Applications*, M. J. D. Powell and S. Scholtes, Eds. Boston, MA, USA: Kluwer, 2000, vol. 174, pp. 1949–1949.
[37] R. Bixby and E. Rothberg, "Progress in computational mixed integer programming a look back from the other side of the tipping point," *Ann. Oper. Res.*, vol. 149, no. 1, pp. 37–41, Jan. 2007.
[38] D. Streiffert, R. Philbrick, and A. Ott, "A mixed integer programming solution for market clearing and reliability analysis," in *Proc. IEEE Power Eng. Society General Meeting 2005*, Jun. 2005, vol. 3, pp. 2724–2731.
[39] The GAMS Development Corporation, 2012. [Online]. Available: http://www.gams.com.
[40] H. Chen and F. Bresler, "Practices on real-time market operation evaluation," *IET Gen., Transm., Distrib.*, vol. 4, no. 2, pp. 324–332, Feb. 2010.

Germán Morales-España (S'10) received the B.Sc. degree in electrical engineering from the Universidad Industrial de Santander (UIS), Colombia, in 2007 and the M.Sc. degree from the Delft University of Technology (TUDelft), The Netherlands, in 2010. He is now pursuing the (Ph.D.) Erasmus Mundus Joint Doctorate in Sustainable Energy Technologies and Strategies (SETS) hosted by the Universidad Pontificia Comillas (Comillas), Spain; the Royal Institute of Technology, Sweden; and TUDelft, The Netherlands.

He is currently an assistant researcher at the Institute for Research in Technology (IIT) at Comillas, and he is also a member of the Research Group on Electric Power Systems (GISEL) at the UIS. His areas of interest are power systems operation, economics and reliability, as well as power quality and protective relaying.

Andres Ramos received the Electrical Engineering degree from Universidad Pontificia Comillas, Madrid, Spain, in 1982 and the Ph.D. degree in electrical engineering from Universidad Politécnica de Madrid, Madrid, Spain, in 1990.

He is a Research Fellow at Instituto de Investigación Tecnológica, Madrid, Spain, and a Full Professor at Comillas' School of Engineering, Madrid, Spain, where he has been the Head of the Department of Industrial Organization. His areas of interest include the operation, planning, and economy of power systems and the application of operations research to industrial organization.

Javier García-González (S'99–M'01) received the Industrial Engineering degree, with specialization in electricity, from the Universidad Politécnica de Cataluña, Barcelona, Spain, in 1996, and the Ph.D. degree from the Universidad Pontificia Comillas, Madrid, Spain, in 2001.

Currently he is an Assistant Professor of electrical engineering at the Universidad Pontificia Comillas, and he belongs to the research staff of the Instituto de Investigación Tecnológica (IIT). His research interests include operations, planning, and economy of power systems.

Article III

G. Morales-España, J. M. Latorre, and A. Ramos, "Tight and compact MILP formulation for the thermal unit commitment problem," *IEEE Transactions on Power Systems*, vol. 28, no. 4, pp. 4897–4908. Nov. 2013. JCR 2012 data: impact factor 2.921 and 5-year impact factor 3.601.

Remark: This paper is part of a special section of the IEEE TPWRS journal "Analysis and simulation of very large power systems".

Tight and Compact MILP Formulation for the Thermal Unit Commitment Problem

Germán Morales-España, *Student Member, IEEE*, Jesus M. Latorre, *Member, IEEE*, and Andres Ramos

***Abstract*—This paper presents a mixed-integer linear programming (MILP) reformulation of the thermal unit commitment (UC) problem. The proposed formulation is simultaneously tight and compact. The tighter characteristic reduces the search space and the more compact characteristic increases the searching speed with which solvers explore that reduced space. Therefore, as a natural consequence, the proposed formulation significantly reduces the computational burden in comparison with analogous MILP-based UC formulations. We provide computational results comparing the proposed formulation with two others which have been recognized as computationally efficient in the literature. The experiments were carried out on 40 different power system mixes and sizes, running from 28 to 1870 generating units.**

***Index Terms*—Mixed-integer linear programming (MILP), strong lower bounds, thermal units, unit commitment (UC).**

NOMENCLATURE

Upper-case letters are used for denoting parameters and sets. Lower-case letters denote variables and indexes.

A. Indexes and Sets

$g \in \mathcal{G}$	Generating units, running from 1 to G.
$s \in \mathcal{S}_g$	Startup segments, running from 1 (hottest) to S_g (coldest), see Fig. 1.
$t \in \mathcal{T}$	Hourly periods, running from 1 to T hours.

B. Parameters

C_g^{LV}	Linear variable cost of unit g (\$/MWh).
C_g^{NL}	No-load cost of unit g (\$/h).
C^{NSE}	Nonserved energy cost (\$/MWh).
C_g^{SD}	Shutdown cost of unit g (\$).
C_{gs}^{SU}	Coefficients of the startup cost function of unit g, see Fig. 1 (\$).
D_t	Load demand in hour t (MW).
$\overline{P}_g$	Maximum power output of unit g (MW).
$\underline{P}_g$	Minimum power output of unit g (MW).
R_t	Spinning reserve requirement in hour t (MW).
RD_g	Ramp-down rate of unit g (MW/h).
RU_g	Ramp-up rate of unit g (MW/h).
SD_g	Shutdown capability of unit g (MW).
SU_g	Startup capability of unit g (MW).
TD_g	Minimum downtime of unit g (h).
TU_g	Minimum uptime of unit g (h).
T_{gs}^{SU}	Times defining the segment s limits, $[T_{gs}^{\mathrm{SU}}, T_{g,s+1}^{\mathrm{SU}})$, of the startup cost function of unit g (h), see Fig. 1.

C. Variables

1) Positive and Continuous Variables:

nse_t	Nonserved energy in hour t (MWh).
p_{gt}	Power output at hour t of unit g, production above the minimum output $\underline{P}_g$ (MW).
r_{gt}	Spinning reserve provided by unit g in hour t (MW)..

3) Binary Variables:

u_{gt}	Commitment status of the unit g for hour t, which is equal to 1 if the unit is online and 0 offline.
v_{gt}	Startup status of unit g, which takes the value of 1 if the unit starts up in hour t and 0 otherwise.
w_{gt}	Shutdown status of unit g, which takes the value of 1 if the unit shuts down in hour t and 0 otherwise.
δ_{gst}	Startup-type s of unit g, which takes the value of 1 in the hour where the unit starts up and has been previously offline within $[T_{gs}^{\mathrm{SU}}, T_{g,s+1}^{\mathrm{SU}})$ hours, see Fig. 1.

I. INTRODUCTION

A. Motivation

EFFICIENT resource scheduling is necessary in power systems to achieve an economical and reliable energy production and system operation, either under centralized or competitive environments. This can be achieved by solving the unit commitment (UC) problem, of which the main objective is to

Manuscript received July 05, 2012; revised October 20, 2012, January 22, 2013; accepted February 21, 2013. Date of publication March 22, 2013; date of current version October 17, 2013. The work of G. Morales-España was supported through an Erasmus Mundus Ph.D. Fellowship. Paper no. TPWRS-00779-2012.

The authors are with the Institute for Research in Technology (IIT), School of Engineering (ICAI), Universidad Pontificia Comillas, Madrid 28015, España (e-mail: german.morales@iit.upcomillas.es; gmorales@kth.se; jesus.latorre@iit.upcomillas.es; andres.ramos@upcomillas.es).

Digital Object Identifier 10.1109/TPWRS.2013.2251373

minimize the total system operational costs while operating the system and units within secure technical limits [1]–[3].

Mixed-integer linear programming (MILP) has become a very popular approach to solving UC problems due to significant improvements in off-the-shelf MILP solvers, based on the branch-and-cut algorithm. The combination of pure algorithmic speedup and the progress in computer machinery has meant that solving MILPs has become 100 million times faster over the last 20 years [4]. Recently, the world's largest competitive wholesale market, PJM, changed from Lagrangian Relaxation to MILP to tackle its UC-based scheduling problems [5]. There is extensive literature comparing the pros and cons of MILP with its competitors, see, for example, [2] and [6].

Despite the significant improvements in MILP solving, the time required to solve UC problems continues to be a critical limitation that restricts the size and scope of UC models. Nevertheless, improving an MILP formulation can dramatically reduce its computational burden and thus allow the implementation of more advanced and computationally demanding problems, such as stochastic formulations [7], accurate modelling of different types of (online and offline) reserves [8], or transmission switching [9].

B. Literature Review

1) Performance of MILP Formulations—Tightness vs. Compactness: The branch-and-cut algorithm solves MILP by solving a sequence of linear programming (LP) relaxations. The LP relaxation of a MILP problem is obtained by relaxing its integrality requirements. During the solving process (branching), upper bounds (feasible integer solutions) and lower bounds (LP relaxations) are computed. The quality of a feasible integer solution is measured with the optimality tolerance, which is the difference between upper and lower bounds. In order to reduce this difference, upper bounds are decreased by finding better integer solutions (e.g., heuristics), and lower bounds are increased by strengthening the LP relaxation (e.g., adding cutting planes) [10]. Providing an MILP formulation with strong lower bounds (LP relaxation near to the optimal integer solution) can dramatically reduce the length of the search for optimality [11], [12]. In addition, strong lower bounds effectively guide the search for better upper bounds (i.e., heuristics explore the neighborhood of the LP relaxation to find potentially better integer solutions).

The computational performance of an MILP formulation is mainly influenced by its tightness (distance between relaxed and integer solutions) and compactness (quantity of data to process when solving the problem). These two characteristics are actually fully exploited by off-the-shelf MILP solvers. Even though solvers' breakthrough is due to the synergy between different strategies (e.g., heuristics, cuts, and node presolve), introducing cutting planes has been recognized as the most effective strategy, followed by root presolve [13], [14]. The former strategy dynamically tightens the formulation around the integer feasible solution point. The latter makes the initial problem formulation more compact (by removing redundant variables and constraints) and also tighter (by strengthening constraints and variable bounds).

The tightness of an MILP formulation defines the search space (relaxed feasible region) that the solver needs to explore in order to find the (optimal integer) solution. A given MILP problem has many possible formulations. If F1 and F2 are two formulations for the same MILP problem, and the feasible region of F1 is contained inside the feasible region of F2, then F1 is a tighter formulation than F2, and thus the lower bound provided by the LP relaxation of F1 is always greater than or equal to that provided by F2 [11], [15], that is, F1 provides stronger lower bounds and the optimal solution of its LP relaxation is nearer to the optimal integer solution.

The compactness of an MILP formulation refers to its size and defines the searching speed that the solver takes to find the optimal solution, since, during the process, many LP relaxations are repeatedly solved. Although the number of constraints is considered to be the best simple predictor of the LP models' difficulty [16], [17], the number of nonzeros also has a significant impact on solution times [10]. Therefore, formulation F1 is considered more compact than F2 if F1 presents simultaneously fewer constraints and nonzeros than F2.

Research on improving MILP formulations is usually focused on tightening rather than on compacting. An MILP formulation is typically tightened by adding a huge number of constraints, which increases the problem size [18], [19]. Although this tightening reduces the search space, solvers may take more time exploring it because they are now required to repeatedly solve larger LPs. Consequently, when a formulation is tightened while significantly affecting its compactness, a more compact and less tight formulation may be solved faster, because the solver is able to explore the larger feasible region more rapidly [18]. On the other hand, compact formulations usually provide weak (not strong) lower bounds. In conclusion, creating tight or compact computationally efficient formulations is a nontrivial task because the obvious formulations are very weak (not tight) or very large, and trying to improve the tightness (compactness) usually means harming the compactness (tightness).

2) Improving UC Formulations: Improving MILP formulations, especially the tightness, has been widely researched. In fact, all of the cutting plane theory, which has meant the breakthrough in MILP solving, is about tightening the formulations [4], [10], [14], [20]. In the case of UC problems, there have been efforts affecting specific aspects. The work in [21] reduced the number of binary variables, claiming that this speeded up the search process compared with the three-binary models [2], [6]. In [22], a strong formulation of the minimum up/down time constraints is proposed; in [23], a tighter linear approximation for quadratic generation costs is described; the work in [19] presents a new class of inequalities giving a tighter description of the feasible operating schedules for generators; and the work in [24] proposes a tight and compact formulation for the startup and shutdown unit's power trajectories.

From the aforementioned formulations, the work in [21], [22], and [19] have focused on improving the basic technical constraints (e.g., ramping limits, generation limits, or minimum up/down times). As stated in [19], the main disadvantage of [21] is that avoiding the startup and shutdown variables hinders the possibility to generate and use strong valid inequalities, such as the minimum up/down time constraints proposed in

[22]. In [19], this problem is overcome by using the three-binary format, thus introducing many additional inequalities (using all of the binaries) to tighten the UC formulation. However, the main drawback of [19] is that it creates a huge model where, in order to obtain a computational advantage, the additional inequalities need to be appropriately introduced to the formulation during the solving process (dynamically). The work in [19] also presents the additional disadvantage of implementation complexity, where the modeller needs to make an *ad-hoc* configuration of the solving strategy of MILP solvers to dynamically introduce these inequalities.

C. Contributions

This paper presents an alternative UC reformulation that describes the same basic UC problem as in [21] and [19]. In other words, we provide a formulation containing the same feasible integer solutions as those in [21] and [19], and hence obtaining the same optimal results.

The main contribution of this paper is threefold.

1) A tight MILP formulation for the thermal UC problem is proposed in order to decrease the computational burden of analogous MILP formulations [19], [21].
2) The formulation is tightened at the same time as it is made more compact compared with both [21] and [19], hence overcoming the main disadvantage of usual tightening strategies [19]. The simultaneous tight and compact characteristics reinforce the convergence speed by reducing the search space and at the same time increasing the searching speed with which solvers explore that reduced space.
3) This reformulation can be used as the core of any UC problem, whether under centralized or competitive environments, from self-scheduling to centralized auction-based market clearing.

Furthermore, given the compactness of the formulation, additional extensions of the UC model will be less cumbersome. For example, in the case of a stochastic formulation the compactness and tightness can be fully exploited given the size and computational complexity of solving a large-scale stochastic UC problem. That is, a stochastic problem replicates the original deterministic structure to represent uncertainty; consequently, any reformulation will benefit from the characteristics of the deterministic formulation.

D. Paper Organization

The remainder of this paper is organized as follows. Section II details the UC reformulation. Section III provides and discusses results from several case studies, where a comparison with two other UC formulations is made. Finally, some relevant conclusions are drawn in Section IV.

II. Mathematical Formulation

Here, we detail the reformulation of a typical UC. The constraints presented here characterize the same UC problem as those in [21] and [19] (see [25]). Hourly time intervals are considered, but it should be noted that the formulation can be easily adapted to handle shorter time periods.

A. Objective Function

The UC problem seeks to minimize the power system operation costs, which are defined as the sum of: (i) the production cost; (ii) startup cost; (iii) shutdown cost; and (iv) in order to take into account situations in which there is a lack of energy, the nonserved energy cost is also included as follows:

$$\min \sum_{g\in\mathcal{G}}\sum_{t\in\mathcal{T}} \Bigg[\underbrace{C_g^{\mathrm{NL}}u_{gt} + C_g^{\mathrm{LV}}(\underline{P}_g u_{gt} + p_{gt})}_{i} + \underbrace{\sum_{s\in\mathcal{S}_g} C_{gs}^{\mathrm{SU}}\delta_{gst}}_{ii} + \underbrace{C_g^{\mathrm{SD}}w_{gt}}_{iii} + \underbrace{C^{\mathrm{NSE}}nse_t}_{iv} \Bigg]. \quad (1)$$

1) Production Cost: The production cost is usually expressed as a quadratic function of the power output. Typically, this cost is modeled as a piecewise-linear function [21]. A tight formulation for this piecewise-linear approximation is given in [23]. This paper focuses on the reformulation of the unit's technical constraints as well as of the exponential startup cost. Therefore, for the sake of simplicity, we represent the production cost as a linear function. Note in (1) that the linear variable cost multiplies the total power output, which is the minimum output $\underline{P}_g u_{gt}$ plus the production above that minimum p_{gt}.

2) Startup Cost: Fig. 1 shows a typical exponential startup cost function [26], where C_{gs}^{SU} is the cost incurred when the unit g has been offline within the interval $[T_{gs}^{\mathrm{SU}}, T_{g,s+1}^{\mathrm{SU}})$. This function is discrete since the time span has also been discretized into hourly periods. The work in [21] and [19] represent this startup cost function using the formulation proposed in [27]. We represent the same cost function using

$$\delta_{gst} \le \sum_{i=T_{gs}^{\mathrm{SU}}}^{T_{g,s+1}^{\mathrm{SU}}-1} w_{g,t-i} \quad \forall g, t \in \left[T_{g,s+1}^{\mathrm{SU}}, T\right], s \in [1, S_g) \quad (2)$$

$$\sum_{s\in\mathcal{S}_g} \delta_{gst} = v_{gt} \quad \forall g, t. \quad (3)$$

As presented in our previous work [24], the startup-type variable δ_{gst} that activates the cost C_{gs}^{SU} in the objective function is selected by (2) and (3), where (2) stands for the time passed since the last shutdown and (3) ensures that only one startup cost value is selected when the unit actually starts up.

Note that (2) does not bound the coldest startup-type $\delta_{g,S_g,t}$. However, if the unit starts up at hour t and has been offline for at least $T_{S_g}^{\mathrm{SU}}$ hours, then constraints (2) and (3) ensure $\delta_{g,S_g,t} = 1$. As discussed in [24], the variables δ_{gst} take binary values even if they are defined as continuous variables. This is due to the convex (monotonically increasing) characteristic of the exponential startup cost function of thermal units [26] (see Fig. 1).

Due to the minimum downtime constraint (see Section II-B2), the hottest startup-type is only possible within the interval $[TD_g, T_{g,2}^{\mathrm{SU}})$. Therefore, constraint (2) is made more compact

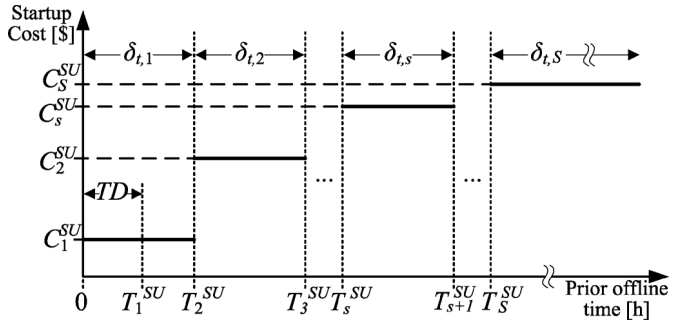

Fig. 1. Startup costs as a function of the unit's previous offline time.

by defining $T_{g,1}^{\mathrm{SU}} = TD_g$; see Fig. 1. Note that (2) is not defined for the first hours. Appendix A details how to obtain δ_{gst} for the first hours depending on the unit's initial conditions.

An easy way to observe that this startup cost formulation is tighter than the formulation in [19], [21] and [27] is that (2) and (3) provide upper bounds to the possible startup-cost values. For example, if the unit does not start up ($v_{gt} = 0$), then (3) forces the startup cost to be zero. This is in contrast to [21], which does not provide upper bounds to the startup cost variable and then the objective function always has to look for the lowest feasible value. In addition, the computational results in Section III shows that the integrality gap of the UC formulation is significantly lowered when modelling the startup costs using (2) and (3).

B. Power System and Thermal Unit Constraints

1) Power System Requirements: The following constraints guarantee the balance between generation and load and the provision of spinning reserve:

$$\sum_{g\in\mathcal{G}}[\underline{P}_g u_{gt} + p_{gt}] = D_t - nse_t \quad \forall t \tag{4}$$

$$\sum_{g\in\mathcal{G}} r_{gt} \geq R_t \quad \forall t \tag{5}$$

where the nonserved energy variable nse_t is included to take into account situations of lack of energy. Note in (4) that power (MW) and energy (MWh) units are mixed, which is numerically correct in models with hourly time intervals. However, the time-period duration must be included when considering different time intervals.

2) Minimum Up and Downtime: The minimum number of periods that the unit must be online and offline are ensured with [22]

$$\sum_{i=t-TU_g+1}^{t} v_{gi} \leq u_{gt} \quad \forall g, t \in [\mathrm{TU}_g, T] \tag{6}$$

$$\sum_{i=t-TD_g+1}^{t} w_{gi} \leq 1 - u_{gt} \quad \forall g, t \in [\mathrm{TD}_g, T]. \tag{7}$$

This formulation provides strong lower bounds in comparison with others [9], [19], [22] as also shown in Section III. Appendix A describes how the initial conditions force the unit to remain online or offline during the first hours.

3) Logical Constraint: The following equation guarantees that v_{gt} and w_{gt} take the appropriate values when the unit starts up or shuts down:

$$u_{gt} - u_{g,t-1} = v_{gt} - w_{gt} \quad \forall g, t. \tag{8}$$

The minimum up/down constraints ensure that a unit cannot start up and shut down simultaneously: note that (6) and (7) guarantee (dominate over) the inequalities $v_{gt} \leq u_{gt}$ and $u_{gt} \leq 1 - w_{gt}$, respectively, which combined become $v_{gt} + w_{gt} \leq 1$. In addition, if u_{gt} is defined as a binary variable, (8) forces v_{gt} and w_{gt} to take binary values even if they are defined as continuous.

4) Generation Limits: The total unit production is modelled in two blocks: the minimum power output $\underline{P}_g$ that is generated just by being committed and the generation over that minimum p_{gt}. The generation limits over the power output and the spinning reserve contribution are set as follows:

$$p_{gt} + r_{gt} \leq (\bar{P}_g - \underline{P}_g)u_{gt} - (\bar{P}_g - SU_g)v_{gt} \quad \forall g \in \mathcal{G}^1, t \tag{9}$$

$$p_{gt} + r_{gt} \leq (\bar{P}_g - \underline{P}_g)u_{gt} - (\bar{P}_g - SD_g)w_{g,t+1} \quad \forall g \in \mathcal{G}^1, t \tag{10}$$

where p_{gt} and r_{gt} are also constrained by the unit startup and shutdown capabilities.

Note that (9) and (10) are only applied for the subset $\mathcal{G}^1$, which is defined as the units in $\mathcal{G}$ with $\mathrm{TU}_g = 1$. For the cases in which $\mathrm{TU}_g \geq 2$, both constraints can be replaced by a tighter and more compact formulation

$$\begin{aligned} p_{gt} + r_{gt} \leq & (\bar{P}_g - \underline{P}_g)u_{gt} - (\bar{P}_g - SU_g)v_{gt} \\ & - (\bar{P}_g - SD_g)w_{g,t+1} \quad \forall g \notin \mathcal{G}^1, t. \end{aligned} \tag{11}$$

Constraint (11) is tighter than (9) and (10) because, in the event that the unit is online for just one period, the right side of (11) can be negative. Consequently, (11) is not valid for units with $\mathrm{TU}_g = 1$, because this constraint means that it is not feasible to operate the unit for just one online period, that is, (11) presents a tighter feasible region than (9) and (10) together. In addition, constraint (11) is also more compact because: 1) the two constraints (9) and (10) are lowered to one and 2) constraint (11) introduces five nonzero elements (per unit and per period) in the constraint matrix in comparison with the eight elements introduced by (9) and (10) together.

Note that (9) and (10) are valid in both cases when $g \notin \mathcal{G}^1$ and when $g \in \mathcal{G}^1$. However, if (11) is used for $g \notin \mathcal{G}^1$, the same solution is obtained at the same time as the formulation is made more compact and tighter. Hence, the combination of both groups of constraints is used in this model.

One simple way to observe that the proposed formulation is tighter than those in [21] and [19] is by checking the upper bound of the constraints. For example, note that the upper bounds of (9)–(11) decrease when the binary variables v_{gt} and w_{gt} are different from zero. This is in contrast to [21] and [19], where the bounds of the constraints increase if $v_{gp}, w_{gp} \neq 0$; see Appendix B for further details. In fact, the set of constraints (6)–(11) are the tightest possible representation (convex hull) for a unit operation without ramp constraints, although the mathematical proof for this is outside the scope of this paper.

5) Ramping Limits: The following constraints ensure that the unit operates within the ramp rate limits:

$$(p_{gt} + r_{gt}) - p_{g,t-1} \leq RU_g \quad \forall g, t \tag{12}$$

$$-p_{gt} + p_{g,t-1} \leq RD_g \quad \forall g, t \tag{13}$$

where (12) guarantees that the unit can provide spinning reserve without violating the upwards ramp limit. The reader is referred to [8] for a more accurately modelling of different (online and offline) types of reserves.

III. Numerical Results

This section is divided into four parts. The first part describes the different UC formulations that were implemented. The different case studies are detailed in the second part. The third part presents a comparison between all the UC formulations, in terms of size and computational performance. Finally, the last part assess the impact on computational performance due to different number of binary variables in the formulations.

A. UC Formulations

To assess the computational burden of the proposed model, we compare it with those UC formulations in [21] and [19]. These two formulations have been recognized as computationally efficient in the literature [9], [19], [21], [22], [28]. For the sake of simplicity, the production costs are considered linear for all the formulations.

The following four formulations are then implemented.

- *1bin:* This formulation is presented in [21] and requires a single set of binary variables (one per unit and per period), i.e., the startup and shutdown decisions are expressed as a function of the commitment decision variable.
- *3bin:* The minimum up/down time constraints proposed in [22] (see Section II-B2) are implemented with the three-binary equivalent formulation of [21]. This formulation is presented in [19] (see also [25]). Unlike [19], *3bin* is implemented without the extra cuts.
- *P1:* This formulation is the same as *3bin*; however, the exponential startup-cost constraints presented in Section II-A2 were used instead of that in [27], which is the formulation used by [21] and [19].
- *P2:* This is the complete formulation proposed in this paper.

It is important to note that all of the formulations were implemented using the same objective function and the same set of constraints as the formulation presented in Section II (see also [25]). As a result, all of them describe the same mixed-integer optimization problem. The difference between them is how the constraints are formulated. In other words, for a given case study, all of the formulations obtain the same optimal results, e.g., commitments, generating outputs and operation costs, as numerically shown in Section III-D.

Note that we define four sets of variables as binary u_{gt}, v_{gt}, w_{gt} and δ_{gst}. Thus, reducing the computational burden of the formulations, as discussed in Section III-D.

Although we focus the discussion on the performance of the proposed formulation *P2*, *P1* is implemented to observe the improvements in the proposed startup-cost formulation (see Section II-A2). Furthermore, when comparing *P2* with *P1*, one can clearly observe the additional improvements which result from considering the generation output variable above $\underline{P}_g$.

TABLE I
Number of Generators Per Problem Case

Small cases										Large Cases									
	Generator								Total		Generator								Total
Case	1	2	3	4	5	6	7	8	Gens	Case	1	2	3	4	5	6	7	8	Gens
1	12	11	0	0	1	4	0	0	28	11	46	45	8	0	5	0	12	16	132
2	13	15	2	0	4	0	0	1	35	12	40	54	14	8	3	15	9	13	156
3	15	13	2	6	3	1	1	3	44	13	50	41	19	11	4	4	12	15	156
4	15	11	0	1	4	5	6	3	45	14	51	58	17	19	16	1	2	1	165
5	15	13	3	7	5	3	2	1	49	15	43	46	17	15	13	15	6	12	167
6	10	10	2	5	7	5	6	5	50	16	50	59	8	15	1	18	4	17	172
7	17	16	1	3	1	7	2	4	51	17	53	50	17	15	16	5	14	12	182
8	17	10	6	5	2	1	3	7	51	18	45	57	19	7	19	19	5	11	182
9	12	17	4	7	5	2	0	5	52	19	58	50	15	7	16	18	7	12	183
10	13	12	5	7	2	5	4	6	54	20	55	48	18	5	18	17	15	11	187

TABLE II
Sets of Experiments

	Small cases		Large cases	
	Total gens	Time span	Total gens	Time span
$\times 7$-*day*	28 to 54	7 days	132 to 187	7 days
$\times 10$-*gen*	280 to 540	1 day	1320 to 1870	1 day

B. Case Studies

1) Set of Experiments: The following case study based on the power system data in [21] is conducted to assess the computational performance of the proposed UC formulation. As presented in [19], an eight-generator data set is replicated to create larger instances and different power-systems mixes. These generation mixes, also used in [19], are shown in Table I. The replication introduces symmetry in the problems which makes them harder to solve than usual. The spinning reserve requirement of 10% of the power demand has to be met for each hour. The non-served energy cost is considered to be 1000 $/MWh. For quick reference, the generator data and power demand can be found in Appendix C.

Two test-sets are created in order to obtain even larger instances.

- $\times 7$-*day*: for the first test-set, the problem is solved with all of the 20 instances presented in Table I for a time span of seven days. The demand for the last two days (the weekend) is considered to be 80% of the demand on a working day.
- $\times 10$-*gen*: for the second test-set, the 20 different power-system mixes in Table I are replicated ten times with a time span of one day, that is, the total number of generators for this test-set goes from 280 up to 1870.

Table II shows the different groups for all 40 cases that are considered here, where there are small and large cases for the two previous test-sets.

All tests were carried out using CPLEX 12.4 under GAMS [29] on a quad-core Intel-i7 2.4-GHz personal computer with 4 GB of RAM memory. The small and large cases, for both $\times 7$-*day* and $\times 10$-*gen*, are solved within 0.1% and 1.0% of relative optimality tolerance and a CPU time limit of 1 and 10 h, respectively. CPLEX defaults were used for all of the experiments.

TABLE III
PROBLEM SIZE (SELECTED INSTANCES)

	Case	# of constraints ($\times 10^3$)				# of nonzero elements ($\times 10^6$)				# real var ($\times 10^3$)			# binary var ($\times 10^3$)		
		1bin	*3bin*	*P1*	*P2*	*1bin*	*3bin*	*P1*	*P2*	*1bin*	*3bin*	*P**	*1bin*	*3bin*	*P**
×7-day	01	104	104	51	37	0.74	0.75	0.25	0.22	19	14	10	5	14	24
	10	177	177	99	73	1.13	1.15	0.44	0.39	36	27	18	9	27	45
	11	454	453	241	178	3.09	3.13	1.11	0.98	89	67	45	22	67	111
	20	639	637	342	250	4.22	4.28	1.56	1.37	126	94	63	31	94	157
×10-gen	01	148	144	67	47	0.92	0.92	0.30	0.26	27	20	13	7	20	33
	10	252	247	132	95	1.44	1.45	0.56	0.49	52	39	26	13	39	64
	11	647	633	319	229	3.88	3.89	1.39	1.21	127	95	63	32	95	158
	20	910	891	453	323	5.35	5.36	1.96	1.71	180	135	90	45	135	222

* *P1* is equal to *P2* for these cases

2) Performance Metrics: In order to summarize comparison results between formulations, geometric means of ratios are used since arithmetic means can be quite misleading when applied to a set of ratios [10], [14], that is, a number of model characteristics between two formulations, e.g., number of constraints or runtimes, are compared using ratios, and the geometric mean over a set of case studies is then used as a performance metric. For example, when comparing solution times between *P1* and *1bin*, for each case study, two runtimes are obtained, one for *P1* and one for *1bin*. Given the set of runtimes, ratios are computed dividing the runtimes of *P1* by the corresponding runtime of *1bin*. Finally, the geometric mean is computed over these ratios and multiplied by 100 to obtain percentages. Thus, a geometric mean of ratios lower than 100% means that *P1* is faster. For the sake of brevity, the summary of results is presented in this paper; however, the different formulations and the set of statistics are presented in [25].

The formulation *1bin* is used as a benchmark to obtain the ratios. In other words, the formulations *P1*, *P2* and *3bin* (in the numerator) are compared with *1bin* (in the denominator) unless otherwise specified.

C. Comparing Different Formulations

1) Problem Size: Table III shows the dimensions for all of the formulations for four selected instances. This sample is composed of the smallest and largest instances for the small cases (cases 01 and 10) and large cases (cases 11 and 20). There are instances which consist of almost a million constraints, present millions of nonzero elements in the constraint matrix, and contain 100 000+ real and binary variables.

Table IV summarizes the different model sizes for all 40 instances in comparison with *1bin*. This summary is obtained as a geometric mean of ratios as described in Section III-B2. Note that *3bin* has almost as many constraints and nonzero elements as *1bin*. However, *3bin* presents three times more binary variables due to the explicit modelling of the startup and shutdown decisions as binary variables.

Although *P1* and *P2* present around five times as many binary variables as *1bin* does, the number of constraints and nonzero elements was approximately reduced by two thirds. Consequently, *P2* is considerably more compact than *1bin* and *3bin* with respect to the nonzero elements and constraints (following the definition of compactness provided in the Introduction).

TABLE IV
PROBLEM SIZE SUMMARY COMPARED WITH *1bin* (%)

Case	# constraints			# nonzero elements			# real var		# binary var	
	3bin	*P1*	*P2*	*3bin*	*P1*	*P2*	*3bin*	*P**	*3bin*	*P**
Mean	98.8	51.0	36.9	100.8	36.1	31.7	75.0	50.1	300	497.3
min	98.6	47.1	33.7	100.4	32.8	28.8	75.0	50.0	300	495.9
max	98.9	54.8	39.9	101.1	39.8	34.9	75.1	50.2	300	498.9

* *P1* is equal to *P2* for these cases

Note in Table IV that the main improvements in compactness are due to the proposed startup-cost formulation *P1*. Finally, *P2* further reduces the formulation size by modelling the power output variable above $\underline{P}_g$.

2) Computational Performance: Although the proposed formulation is more compact than *1bin* and *3bin*, this does not necessarily lead to a better computational performance. In fact, a compact formulation usually presents a weak (not tight) LP relaxation that can dramatically increase the MILP resolution time, as mentioned in the Introduction. The tightness of an MILP can be measured with the integrality gap [19]. The integrality gap is defined as $(Z_{\mathrm{MILP}} - Z_{\mathrm{LP}})Z_{\mathrm{MILP}}$, where Z_{LP} is the optimal value of the (initial) relaxed LP problem, and Z_{MILP} is the optimal integer solution. In practice, the problems are not solved until optimality but within an optimality tolerance. Therefore, for a given case study, Z_{MILP} is considered to be the best integer solution that was found among the four formulations after that case study was solved.

Fig. 2 shows the CPU times and integrality gaps for all of the formulations and all the instances in comparison with *1bin* (using ratios), where *1bin* always represents 100%. The CPU times and the integrality gaps of *1bin* are shown within squares to give an idea of the different problem magnitudes. The instances that took more than 10 min to solve for *P2* can also be found within squares. The computational performance summary for the different formulations is presented in Table V for the small cases, large cases, and all of the cases together. Table V also shows the final optimality tolerance achieved as well as nodes explored and iterations.

In short, Fig. 2 and Table V shows that the proposed formulation *P2* considerably reduces the computational burden in comparison with *1bin* and *3bin* while achieving better solution qualities (lower final optimality tolerances) at the same time. Nevertheless, several aspects are worth mentioning:

1) *Relationship between integrality gap and runtime:* Fig. 2(b) and (d) shows that *P2* always presents the lowest integrality gaps, followed by *P1*, *3bin* and finally *1bin*. Table V shows that the average time taken by the different formulations presents a similar pattern as to that of the integrality gaps, with the exception of *3bin* for the $\times 7$-*day* test-set, which presented a worse performance than *1bin* (on average, *3bin* required more than 30% of the time that *1bin* required to solve all of the $\times 7$-*day* test-set). This is an unexpected result which can be explained as follows. In theory, lower integrality gaps lead to faster solving times when two formulations have similar sizes. However, in practice, MILP solvers use heuristics and cuts (among others) that may also dramatically influence performance. In addition, the enumeration tree and branching

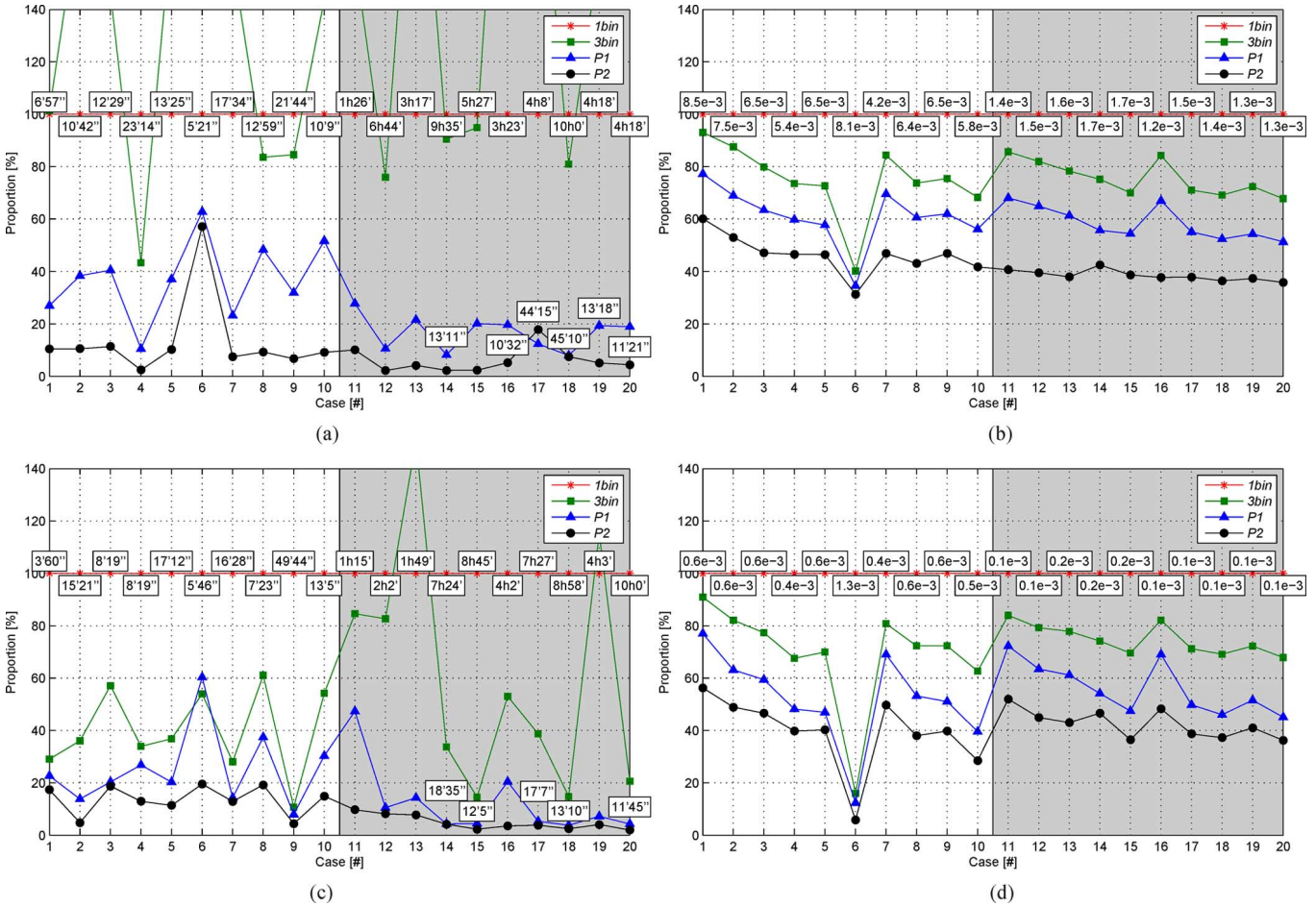

Fig. 2. Improvements in comparison with *1bin* (%). White areas correspond to small cases and gray to the large cases. (a) ×7-*day* CPU time. (b) ×7-*day* Integrality Gap. (c) ×10-*gen* CPU Time. (d) ×10-*gen* Integrality Gap.

strategies change completely when formulations with different integer variables are compared. *1bin* presents fewer binary variables than *3bin*, and this is an advantage for finding integer feasible solutions. In general, a high number of integer variables complicates the search for feasible solutions. For the ×10-*gen* test-set, *3bin* showed a significant improvement over *1bin*: *3bin* required, on average, 40.6% of the CPU time needed by *1bin*. Note that, overall, *3bin* performs better for the small cases than for the large cases. A clearer performance dominance of *3bin* over *1bin* was observed when the experiments were carried out without the exponential startup cost constraints (for the sake of brevity, these results are not shown here but the interested reader is referred to [25]).

2) *Overall performance of P2:* For *1bin*, all of the large cases (gray area in Fig. 2) took longer than one hour to solve within the required optimality tolerance. Two of the instances hit the ten hour time limit. On the other hand, *P2* solved all the tests in less than one hour and just two of them took more than 20 min. *P2* presented shorter runtimes than *1bin* and *3bin* for all the instances, being beaten just once by *P1* [instance 17 for the ×7-*day* test-set, see Fig. 2(a)]. Note in Fig. 2(a) and (c) that, for the instances where the proposed formulation showed the worst performances, *P2* required 57.1% and 19.5% of the CPU time required by *1bin* for the ×7-*day* and ×10-*gen* test-sets, respectively. Furthermore, *P2* obtained better solution quality in general (i.e., converged to smaller optimality tolerances) than *1bin*, especially for the large cases. However, *1bin* obtained better solution qualities for 5 of the 40 instances (3 for the ×7-*day* and 2 for the ×10-*gen*).

3) *Node enumeration versus LP complexity:* Table V shows that, for the ×10-*gen* test-set, all of the formulations enumerated more nodes than *1bin* to find a solution within the given optimality tolerance. As mentioned above, formulations with different integer variables lead to different enumeration tree and branching strategies. By default, an MILP solver's objective is to obtain satisfactory feasible solutions quickly using different strategies, such as branching, cuts and heuristics. The strategy that proves to be more effective is used more often (e.g., branching) and the others more seldom so that they do as little harm as possible [10]. That being said, larger enumerated nodes in one formulation do not mean longer solving times. In fact, exploring few nodes for long periods is an indication of the difficulty of the linear relaxed formulation [30]. Therefore, *P2* is able to explore more nodes than *1bin* in even shorter times mainly due to the compactness of the formulation. Focusing on the number of nodes explored can lead to misleading conclusions. That is why other

TABLE V
COMPUTATIONAL PERFORMANCE COMPARED WITH *1bin* (%)

		CPU Time			Integrality Gap			Opt. Tolerance			Nodes			Iterations		
		3bin	*P1*	*P2*	*3bin*	*P1*	*P2*	*3bin*	*P1*	*P2*	*3bin*	*P1*	*P2*	*3bin*	*P1*	*P2*
×7-*day*	Cases 01-10	120.9	33.7	9.7	73.3	59.8	45.8	97.3	59.9	47.0	88.9	105.6	57.7	42.9	33.0	14.5
	Cases 11-20	140.6	15.4	4.9	75.3	58.1	38.5	130.1	5.1	5.4	169.8	69.1	96.2	72.4	21.4	11.7
	Cases 01-20	130.4	22.8	6.9	74.3	59.0	42.0	112.5	17.4	16.0	122.8	85.4	74.5	55.7	26.6	13.0
×10-*gen*	Cases 01-10	36.3	22.0	12.2	64,0	47,6	34,7	71.2	8.0	11.1	136.5	122.6	121.7	56.2	45.8	35.7
	Cases 11-20	45.4	8.4	4.2	74,5	55,2	42,1	57.0	0.6	0.7	189.7	99.1	160.4	56.9	19.5	15.6
	Cases 01-20	40.6	13.6	7.1	69,1	51,3	38,3	63.7	2.3	2.9	160.9	110.2	139.7	56.6	29.9	23.6

TABLE VI
OVERALL SPEEDUPS

	3bin over *1bin*	*P1* over *1bin*	*P2* over *1bin*	*P1* over *3bin*	*P2* over *3bin*	*P2* over *P1*
Cases 01-10	1.5	3.7	9.2	2.4	6.1	2.5
Cases 11-20	1.3	8.8	22.1	7.0	17.7	2.5
Cases 01-20	1.4	5.7	14.3	4.1	10.4	2.5

works prefer to look at the number of simplex iterations rather than nodes in order to perform comparisons [15], [31].

Finally, Table VI presents the overall speedups of the formulations compared with each other. For a given instance, the speedup of, for example, *3bin* over *1bin* is obtained by dividing the runtime of *1bin* by the runtime of *3bin*, and the results are summarized using the geometric mean on the speedups of a group of instances. Both test-sets ×7-*day* and ×10-*gen* are grouped together, and now the instances are separated into small, large and all cases (see Table II). In general, *3bin* is 1.4 times faster than *1bin* and presented a better performance for the small cases. *P2* was around 14 and 10 times faster than *1bin* and *3bin*, respectively. *P2* presented the best performance for the large cases, where *P2* was around 22 and 18 times faster than *1bin* and *3bin*, respectively. Note that *P1* already presents significant improvements over *1bin* (5.7 times faster) and *3bin* (4.1 times faster). In addition, *P2* is a further improvement on *P1*, being generally 2.5 times faster.

D. Difficulty of an MILP Versus its Number of Binary Variables

In this part, we present two sets of experiments to assess the impact on the convergence evolution and solving times due to the number of binary variables, and the simultaneous tight and compact characteristic of the proposed formulation. The UC is solved for the eight-generator power system by 1) pure branch-and-bound method (BB), for one to three days, and 2) the solver defaults, which is the complete branch-and-cut method including heuristics (BC+H), for three to five days.

The eight-generator data and power demand can be found in Appendix C. The spinning reserve requirement of 5% of the power demand has to be met for each hour; the nonserved energy is not considered (i.e., the variable nse_t is removed from all formulations); and all UC problems are solved until they hit the time limit of 1 h or until they reach optimality (more precisely to 10^{-6} of relative optimality tolerance).

Five different formulations are now considered. Three of the formulations described in Section III-A, *1bin*, *3bin*, and *P2*. The other two formulations are the relaxed versions of *3bin* and *P2*, and they are denoted as *R3bin* and *RP2*, respectively. Similarly to *1bin*, the commitment variable u_t is the only variable that is defined as binary for *R3bin* and *RP2*. That is, for *R3bin* and *RP2*, the set of variables v_{gt}, w_{gt} and δ_{gst} are defined as continuous variables within the interval $[0, 1]$. As discussed in Sections II.A.2 and II.B.3, once u_{gt} is defined as binary, the formulations *3bin* and *P2* allow relaxing the integrality condition of variables v_{gt}, w_{gt} and δ_{gst} because the constraints guarantee that these variables always take binary values.

The problem size for the different formulations, the optimal solutions, and integrality gaps are shown in Table VII. The computational performances are presented in Table VIII. which includes runtimes, nodes explored, iterations, and memory required to solve the problems until optimality, otherwise the final optimality tolerance is shown within parentheses. Table VII shows that all formulations present the same optimal solution for a given time span. As expected, all formulations obtain the same integer solutions because they are characterizing the same integer problem (see Section II).

1) Pure Branch and Bound (BB): To assess the impact on the computational performance of formulations containing different number of binary variables, the UC is solved by only using the branch-and-bound method. The cutting planes and heuristics were then disabled, and CPLEX defaults were used for all remaining features. Therefore, the solver is forced to explore all the tree in order to prove optimality [11], [16].

Table VIII shows the computational performance for the one-, two-, and three-day cases that where solved by pure BB. Table IX presents the optimal generation schedule, where all of the formulations obtained the same schedule. All formulations could prove optimality for the case of one and two days. For the three-day case, none of the formulations could achieve optimality because they either exceeded the one-hour time limit or the 4-GB memory limit. *P2*, *3bin, RP2* and *R3bin* hit the time limit and the final optimality tolerances that they achieved are shown between parentheses in Table VIII. *1bin* hit the memory limit achieving the worst final optimality tolerance of 4.3×10^{-3} after about 500 s.

Although *P2* is the formulation with the highest number of binary variables, *P2* explored the least number of nodes and presented the best computational performance for the two-day case, in comparison with the other five formulations. On the other extreme, *1bin*, with the least number of binary variables (the same as *R3bin* and *RP2*), explored the highest number of nodes and presented the worst computational performance, followed by *R3bin* and *RP2*; see Table VIII.

Fig. 3 shows the convergence evolution until optimality of *P2*, *3bin* and *1bin*, for the two-day case. Note that the first value

TABLE VII
PROBLEM SIZE, OPTIMUM AND INTEGRALITY GAP FOR THE EIGHT-GENERATOR CASE

days	# constraints			# nonzero elements			# binary var			# total var			Optimum	Integrality Gap [$\times 10^{-3}$]		
	*P2**	*3bin*†	*1bin*	*P2**	*3bin*†	*1bin*	*P2*	*3bin*	*1bin*‡	*P2**	*3bin*†	*1bin*	All◇	*P2**	*3bin*†	*1bin*
1	1480	4587	4647	7105	30103	29897	960	576	192	1344	1152	960	573630.655	10.21	12.07	17.86
2	3088	9243	9303	15097	66151	65513	1920	1152	384	2688	2304	1920	1142132.128	9.01	10.43	15.00
3	4696	13899	13959	23089	102199	101129	2880	1728	576	4032	3456	2880	1710633.601	8.61	9.88	14.04
4	6304	18555	18615	31081	138247	136745	3840	2304	768	5376	4608	3840	2279135.074	8.41	9.60	13.55
5	7912	23211	23271	39073	174295	172361	4800	2880	960	6720	5760	4800	2847636.547	8.29	9.43	13.27

* *P2* is equal to *RP2* for these cases
† *3bin* is equal to *R3bin* for these cases
‡ *1bin*, *RP2* and *R3bin* are equal for these cases
◇ *P2*, *3bin*, *1bin*, *RP2* and *R3bin* are equal for these cases

TABLE VIII
COMPUTATIONAL PERFORMANCE FOR THE EIGHT-GENERATOR CASE

	days	Time [s] / (OptTol [$\times 10^{-3}$])					Nodes [$\times 10^3$]					Iterations [$\times 10^3$]					Memory [MB] / (OptTol [$\times 10^{-3}$])				
		P2	*3bin*	*1bin*	*RP2*	*R3bin*	*P2*	*3bin*	*1bin*	*RP2*	*R3bin*	*P2*	*3bin*	*1bin*	*RP2*	*R3bin*	*P2*	*3bin*	*1bin*	*RP2*	*R3bin*
BB	1	1.1	0.6	0.3	0.5	1.1	1.8	0.9	0.6	1.2	1.4	15.6	18.1	9.6	12.3	30.2	0.1	0.1	0.1	0.1	0.1
	2	92.0	169.8	242.7	171.5	205.5	92.4	170.6	220.5	232.0	130.6	1278.2	2140.0	3952.9	3082.2	2733.2	23.0	46.9	48.1	44.9	373.5
	3	(2.03)	(1.04)	518.3	(3.12)	(2.79)	3150.8	2692.7	248.7	3569.8	1552.3	49814.7	47095.2	5368.0	62240.6	51563.5	1349.2	1010.8	(4.3)	1079.2	1313.6
BC+H	3	7.9	9.9	4.3	7.5	6.6	1.1	1.1	0.8	0.7	0.8	38.6	80.0	37.5	27.8	52.4	1.2	0.2	0.3	0.3	1.4
	4	9.7	22.4	44.0	12.4	277.0	0.6	1.0	6.4	1.1	27.8	25.6	128.4	296.5	43.1	1884.8	0.7	1.7	4.4	5.5	7.8
	5	12.9	33.4	218.7	39.2	1594.5	0.9	1.4	29.6	4.8	220.6	34.5	158.9	1157.3	172.1	11339.5	1.0	2.3	247.8	1.9	128.2

TABLE IX
OPTIMAL GENERATION SCHEDULE FOR THE EIGHT-GENERATOR CASE AND ONE-DAY TIME SPAN (MW)

Gen	Hour																							
	1	2	3	4	5	6	7	8	9	10	11	12	13	14	15	16	17	18	19	20	21	22	23	24
1	375	455	455	455	455	455	455	455	455	455	455	455	455	455	455	455	455	455	455	455	455	455	455	455
2	375	418.45	455	451.2	420.16	420.16	443.26	418.67	444.28	455	455	455	455	455	453.7	433.51	426.16	455	455	455	455	455	437.4	408.48
3	70	20	.	.	.	.	.	20	70	120	130	130	130	130	130	130	130	130	130	130	130	130	130	130
4	70	20	.	.	.	.	.	20	70	120	130	130	130	130	130	130	130	130	130	130	130	130	130	130
5	85	40.35	52.24	25	25	25	32.94	79.61	93.68	91.6	82.64	98.16	82.64	71.6	57.38	77.57	102	162	162	150.76	129.2	113.68	53.68	25
6	80	20	.	.	.	.	.	.	.	.	20	20	20	.	.	.	20	55.32	39.8	20	20	20	20	.
7	25	25	.	.	.	.	.	.	.	.	.	.	.	.	.	.	25	25	25	25	.	.	.	.
8	21.92	10	.	.	.	.	.	.	.	.	.	.	.	.	.	.	.	.	.	.	.	.	.	.

of the lower bound of *P2*, which is the LP relaxed solution, was found sooner (due to the compactness) and nearer to the final integer solution (due to the tightness) than *3bin* and *1bin*. After 4 s, *P2* presented a better evolution of both lower and upper bounds and hence faster convergence to optimality in comparison with *3bin* and *1bin*.

If a model containing n binary variables is solved by the pure BB algorithm, this algorithm could potentially enumerate 2^n nodes to prove optimality. Consequently, one might expect the solution time to increase exponentially with the number of binary variables. However, the BB method cuts off large sections of the potential tree because some expected solutions may be infeasible or worse than solutions already known. For example, for the two-day case, *P2* potentially presents $2^{1920-384}$ times more nodes to explore than *1bin*, but the BB algorithm solved *P2* until optimality enumerating 42% of the number of nodes required to solve *1bin*. This very surprising efficiency that the BB method exhibits over the potential amount of computation is due to the tightness of the formulation, hence the number of binary variables is a very poor indicator of the difficulty of an MILP model [11], [16]. In fact, the BB will solve a problem exploring zero nodes if the whole model is the tightest possible (convex hull); that is, the LP relaxation solution will always be integer [11]. Furthermore, increasing the number of binary variables is actually a tightening strategy [32].

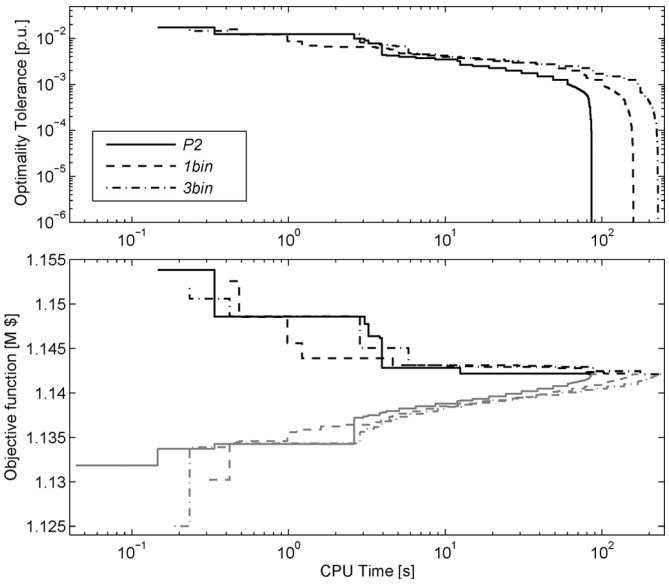

Fig. 3. Convergence evolution for the optimality tolerance and upper/lower bounds in the top and bottom parts of the figure, respectively. In the bottom figure, black lines refer to upper bounds and gray lines to lower bounds.

Increasing the number of binary variables can also provide a further advantage in the tree search strategy. This is the case of

formulations involving variables that take binary values even when these variables are defined as continuous, e.g., v_{gt}, w_{gt} and δ_{gst}. As also stated in [19], declaring all these variables as binary does not cause extra complexity during the enumeration process (branching), because when fixing some of the variables, many others can be immediately obtained due to the high correlation among each other. For example, if the variable v_{gt} is fixed to 1 then (6) fixes u_{gt} to 1 for the following TU_g periods, then (8) (together with (7)) fixes w_{gt} and v_{gt} to 0 for those TU_g periods, and finally (3) fixes δ_{gst}, for all s, for the same periods.

2) Branch-and-Cut+Heuristics (Bc+H)*:* The UC for the eight-generator system was solved for three, four and five days using BC+H strategy, which are CPLEX defaults. Similarly to the results previously obtained in Section III-D1, *P2* generally requires shorter runtimes to solve the problem until optimality than the other four formulations, see Table VIII. *P2* was up to 17 and 2.5 times faster than *1bin* and *3bin*, respectively. Note that, in general, the relaxed versions *R3bin* and *RP2* present a higher computational burden than their analogous formulations *3bin* and *P2*, respectively.

Note that, in Table VIII, the formulations with higher number of binary variables may keep the tree considerably smaller in size. For example, for the five-day case, *1bin* required around 250 and 110 times more memory to deal with the branch-and-bound tree than *P2* and *3bin*, respectively. In order to solve the five-day case until optimality, *P2* potentially presents $2^{4800-960}$ times more nodes to explore than *1bin*, but the BC+H algorithm solved *P2* and *3bin* by just enumerating around 3% of the number of nodes required to solve *1bin*. Similarly, *3bin* required around the 5% of the nodes enumerated by *1bin*, although *3bin* potentially presented $2^{2880-960}$ times more nodes to explore. As mentioned before, the tightness and the high correlation between binary variables of *3bin* and *P2* considerably reduce the size of the tree.

In short, the computational burden of a MILP formulation mainly depends on its tightness and compactness, as stated in the literature of integer programming [11], [12], [16], [18]. A further computational advantage can be obtained by defining as binary those variables that either way take binary values, because the constraints (and tightness of the model) force them to do so. In addition, branching on different variables may be more convenient [10], [19]. MILP solvers employ techniques to exploit the integrality characteristic of integer variables such as cutting planes and node presolve [10], [11], [20]. Consequently, declaring this type of variables as continuous will not allow the solver to look for opportunities to exploit their integrality characteristic.

IV. Conclusion

This paper presented an MILP reformulation for the thermal UC problem. The formulation is simultaneously tighter and more compact than equivalent formulations found in the literature. This simultaneous characteristic boosts the convergence speed that solvers take to solve the MILP formulation. This is done by reducing the search space (tightening) and at the same time increasing the searching speed (compacting) with which solvers explore that reduced space. Consequently, the computation time is dramatically reduced. Several case studies were analyzed to show the improvements achieved by this formulation with respect to others available in the literature. Results showed that the proposed UC formulation considerably reduced the computational burden while achieving better solution qualities. While the formulation is tested only on "standard" thermal UC problems, the tight and compact formulation can be further extended to many other variants of the UC problem, where analogous results should be expected.

Appendix

A. Initial Conditions

The initial behavior of the units is bound by their initial conditions. This is guaranteed by fixing the value of some variables before running the optimization model. The following parameters are needed to deal with the unit state during the first periods.

u_g^0	Initial commitment status of unit g $\{0,1\}$.
TU_g^0	Number of hours that the unit g has been online before the scheduling horizon.
TD_g^0	Number of hours that the unit g has been offline before the scheduling horizon.

a) Initial Minimum Up/Down Times: The number of hours during which the units must be initially online (TU_g^R) or offline (TD_g^R) due to their minimum up/down constraints are obtained as follows:

$$TU_g^R = \max\left\{0, \left(TU_g - TU_g^0\right) u_g^0\right\} \quad \forall g \tag{13a}$$

$$TD_g^R = \max\left\{0, \left(TD_g - TD_g^0\right)\left(1 - u_g^0\right)\right\} \quad \forall g. \tag{13b}$$

Now, the commitment variables for the initial periods where the units must remain online or offline $(TU_g^R + TD_g^R) \geq 1$ must be fixed:

$$u_{gt} = u_g^0 \quad \forall g, t \in \left[1, TU_g^R + TD_g^R\right]. \tag{14}$$

b) Initial Startup Type: Equation (15) complements (2), guaranteeing that the appropriate startup type will be chosen, taking into account the initial conditions. If $\mathrm{TD}_g^0 \geq 2$, then δ_{gst} must be fixed for some initial periods as follows:

$$\delta_{gst} = 0 \quad \forall g, s \in [1, S_g),\ t \in \left(T_{g,s+1}^{\mathrm{SU}} - \mathrm{TD}_g^0, T_{g,s+1}^{\mathrm{SU}}\right). \tag{15}$$

Equations (14) and (15) can also be respectively written as additional constraints in the optimization problem as follows:

$$\sum_{t=1}^{\mathrm{TU}_g^R + \mathrm{TD}_g^R} u_{gt} = TU_g^R u_g^0 \quad \forall g \tag{16}$$

$$\sum_{s=1}^{S_g - 1} \sum_{t=T_{g,s+1}^{\mathrm{SU}} - \mathrm{TD}_g^0 + 1}^{T_{g,s+1}^{\mathrm{SU}} - 1} \delta_{gst} = 0 \quad \forall g. \tag{17}$$

However, (14) and (15) are preferred over (16) and (17), because (14) and (15) turn the involved integer variables into constants before running the optimization problem, thus decreasing the problem size. Nevertheless, solvers usually provide the option to treat fixed variables as constants.

B. Comparing Feasible Regions of the Startup Capability Constraints

Here, we compare the tightness of the startup capability constraint of the proposed formulation with the one presented in [21]. Similar analysis and conclusions can be made for the shutdown capability constraint. For notational simplicity, the index g is dropped in this section.

For the following analysis, we consider $u_{t-1} = 0$. Therefore, the constraint imposing the unit's startup capability (9) becomes

$$p_t + r_t \leq (\bar{P} - \underline{P})u_t - (\bar{P} - \mathrm{SU})v_t \quad \forall t \tag{18}$$

and (6) together with (8) imposes $v_t = u_t$, that is, (6) guarantees $v_t \leq u_t$, and, if $u_{t-1} = 0$ then (8) ensures $v_t \geq u_t$, thus forcing $v_t = u_t$. Consequently, (18) can be rewritten as a function of u_t as

$$p_t + r_t \leq (\mathrm{SU} - \underline{P})u_t \quad \forall t. \tag{19}$$

The analogous constraint from [21, eq. (18)], imposing the unit's startup capability, becomes

$$\bar{p}_t \leq \mathrm{SU} \cdot u_t + \bar{P}(1 - u_t) \quad \forall t \tag{20}$$

when $u_{t-1} = 0$, where $\bar{p}_t$ is the maximum available power output at time t, which is the total power output plus the spinning reserve. Thus, in terms of the nomenclature used in this paper, $\bar{p}_t$ is equal to $\underline{P} \cdot u_t + p_t + r_t$. Hence, (20) can be rewritten as

$$p_t + r_t \leq (\mathrm{SU} - \underline{P})u_t + \bar{P}(1 - u_t) \quad \forall t. \tag{21}$$

Now, the tightness of inequalities (19) and (21) can be directly compared. Note that, if the unit starts up, $u_t = 1$, both (19) and (21) impose $p_t + r_t \leq SU - \underline{P}$. Therefore, the feasible integer region of both constraints is the same when the unit starts up. Be aware, however, that their relaxed feasible regions are completely different. Whereas the right side of (19) takes its maximum value when $u_t = 1$, the right side of (21) actually takes its minimum value, that is, the term involving $\bar{P}$ in (21) plays the role of the so-called big-M, so that (21) becomes inactive when $u_t = 1$. The big-M inequalities considerably harm the tightness of MILP formulations, so they must be avoided when possible [12], [16], [18].

Furthermore, if $\mathrm{SU} = \underline{P}$, which is a very common case [19], [21], [33], then (19) and (21) respectively become

$$p_t + r_t \leq 0 \quad \forall t \tag{22}$$

$$p_t + r_t \leq \bar{P}(1 - u_t) \quad \forall t. \tag{23}$$

Although these two constraints impose $p_t + r_t \leq 0$, when the unit starts up $u_t = 1$, the right side of (23) provides a very poor upper bound to p_t and r_t when $u_t \in [0, 1)$.

C. Power System Data

The eight-unit system data used in [21] and [19] are shown in Table X and the hourly demand (used in [19]) depending on the power system's total capacity is shown in Table XI.

The startup and shutdown rates are assumed equal to the unit minimum output ($SU_g = SD_g = \underline{P}_g$). For the numerical experiments in Section III-C, the initial power production of units 1 and 2, prior to the first period of the time span, is 455 and 245 MW, respectively. For the experiments in Section III-D, the initial power production of all units is their minimum output $\underline{P}$, hence the initial states Ste_0 in Table X are considered the same in magnitude but positive for all units.

TABLE X
GENERATOR DATA

Gen	Technical Information						Cost Coefficients			
	$\overline{P}$ [MW]	$\underline{P}$ [MW]	TU/TD [h]	RU/RD [MW/h]	Ste_0* [h]	$T_c^{SU\dagger}$ [h]	C^{NL} [$/h]	C^{LV} [$/MWh]	$C_h^{SU\dagger}$ [$]	$C_c^{SU\dagger}$ [$]
1	455	150	8	225	8	14	1000	16.19	4500	9000
2	455	150	8	225	8	14	970	17.26	5000	10000
3	130	20	5	50	-5	10	700	16.60	550	1100
4	130	20	5	50	-5	10	680	16.50	560	1120
5	162	25	6	60	-6	11	450	19.70	900	1800
6	80	20	3	60	-3	8	370	22.26	170	340
7	85	25	3	60	-3	6	480	27.74	260	520
8	55	10	1	135	-1	2	660	25.92	30	60

*Hours that the unit has been online (+) or offline (-) prior to the first period of the time span.

†Subindex h refers to hot startup $s = 1$, and subindex c to cold startup $s = 2$

TABLE XI
DEMAND (% OF TOTAL CAPACITY)

Time	1	2	3	4	5	6	7	8	9	10	11	12
Demand	71%	65%	62%	60%	58%	58%	60%	64%	73%	80%	82%	83%
Time	13	14	15	16	17	18	19	20	21	22	23	24
Demand	82%	80%	79%	79%	83%	91%	90%	88%	85%	84%	79%	74%

ACKNOWLEDGMENT

The authors would like to express their gratitude to all partner institutions within the Erasmus Mundus Joint Doctorate Programme in Sustainable Energy Technologies and Strategies (SETS) as well as to the European Commission for their support.

REFERENCES

[1] S. Stoft, *Power System Economics: Designing Markets for Electricity*, 1st ed. New York, NY, USA: Wiley/IEEE Press, May 2002.

[2] B. F. Hobbs, W. R. Stewart, R. E. Bixby, M. H. Rothkopf, R. P. O'Neill, and H.-P. Chao, , B. F. Hobbs, M. H. Rothkopf, R. P. O'Neill, and H.-P. Chao, Eds., "Why this book? New capabilities and new needs for unit commitment modeling," in *The Next Generation of Electric Power Unit Commitment Models*. Boston, MA, USA: Kluwer Academic, 2002, vol. 36, pp. 1–14.

[3] N. Padhy, "Unit commitment—A bibliographical survey," *IEEE Trans. Power Syst.*, vol. 19, no. 2, pp. 1196–1205, May 2004.

[4] T. Koch, T. Achterberg, E. Andersen, O. Bastert, T. Berthold, R. E. Bixby, E. Danna, G. Gamrath, A. M. Gleixner, S. Heinz, A. Lodi, H. Mittelmann, T. Ralphs, D. Salvagnin, D. E. Steffy, and K. Wolter, "MIPLIB 2010," *Math. Programming Computation*, vol. 3, no. 2, pp. 103–163, June 2011.

[5] A. L. Ott, "Evolution of computing requirements in the PJM market: Past and future," in *Proc. IEEE IEEE Power and Energy Soc. Gen. Meeting*, July 2010, pp. 1–4.

[6] T. Li and M. Shahidehpour, "Price-based unit commitment: A case of Lagrangian relaxation versus mixed integer programming," *IEEE Trans. Power Syst.*, vol. 20, no. 4, pp. 2015–2025, Nov. 2005.

[7] F. Bouffard, F. Galiana, and A. Conejo, "Market-clearing with stochastic security—Part I: Formulation," *IEEE Trans. Power Syst.*, vol. 20, no. 4, pp. 1818–1826, Nov. 2005.

[8] G. Morales-España, A. Ramos, and J. García-González, "An MIP formulation for 'joint market-clearing of energy and reserves including ramp scheduling'," *IEEE Trans. Power Syst.*, submitted for publication.

[9] K. Hedman, M. Ferris, R. O'Neill, E. Fisher, and S. Oren, "Cooptimization of generation unit commitment and transmission switching with n-1 reliability," *IEEE Trans. Power Syst.*, vol. 25, no. 2, pp. 1052–1063, May 2010.
[10] R. Bixby, M. Fenelon, Z. Gu, E. Rothberg, and R. Wunderling, , M. J. D. Powell and S. Scholtes, Eds., "MIP: Theory and practice-closing the gap," in *System Modelling and Optimization: Methods, Theory and Applications*. Boston, MA, USA: Kluwer Academic, 2000, vol. 174, pp. 19–49.
[11] L. Wolsey, *Integer Programming*. New York, NY, USA: Wiley-Interscience, 1998.
[12] F. Vanderbeck and L. A. Wolsey, , M. Jünger, T. M. Liebling, D. Naddef, G. L. Nemhauser, W. R. Pulleyblank, G. Reinelt, G. Rinaldi, and L. A. Wolsey, Eds., "Reformulation and decomposition of integer programs," in *50 Years of Integer Programming 1958-2008*. Berlin, Germany: Springer, 2010, pp. 431–502.
[13] E. Rothberg, "The CPLEX library: Presolve and cutting planes," in *Proc. 4th Max-Planck Adv. Course Foundations of Comput. Sci.*, Saarbrücken, Germany, Sep. 2003, pp. 1–17.
[14] R. Bixby and E. Rothberg, "Progress in computational mixed integer programming—A look back from the other side of the tipping point," *Ann. Oper. Res.*, vol. 149, no. 1, pp. 37–41, Jan. 2007.
[15] A. Lodi, , M. Jünger, T. M. Liebling, D. Naddef, G. L. Nemhauser, W. R. Pulleyblank, G. Reinelt, G. Rinaldi, and L. A. Wolsey, Eds., "Mixed integer programming computation," in *50 Years of Integer Programming 1958–2008*. Berlin, Germany: Springer, 2010, pp. 619–645.
[16] H. P. Williams, *Model Building in Mathematical Programming*, 4th ed. New York, NY, USA: Wiley, Aug. 1999.
[17] R. E. Bixby, "Solving real-world linear programs: A decade and more of progress," *Oper. Res.*, vol. 50, no. 1, pp. 3–15, Jan. 2002.
[18] J. Hooker, *Logic-Based Methods for Optimization: Combining Optimization and Constraint Satisfaction*, 1st ed. New York, NY, USA: Wiley-Interscience, May 2000.
[19] J. Ostrowski, M. F. Anjos, and A. Vannelli, "Tight mixed integer linear programming formulations for the unit commitment problem," *IEEE Trans. Power Syst.*, vol. 27, no. 1, pp. 39–46, Feb. 2012.
[20] L. Wolsey, "Strong formulations for mixed integer programs: Valid inequalities and extended formulations," *Math. Programming*, vol. 97, no. 1, pp. 423–447, 2003.
[21] M. Carrion and J. Arroyo, "A computationally efficient mixed-integer linear formulation for the thermal unit commitment problem," *IEEE Trans. Power Syst.*, vol. 21, no. 3, pp. 1371–1378, Aug. 2006.
[22] D. Rajan and S. Takriti, "Minimum up/down polytopes of the unit commitment problem with start-up costs," IBM, Res. Rep. RC23628, Jun. 2005. [Online]. Available: http://domino.research.ibm.com/library/cyberdig.nsf/1e4115aea78b6e7c85256b360066f0d4/cdcb02a7c809d89e8525702300502ac0?OpenDocument
[23] A. Frangioni, C. Gentile, and F. Lacalandra, "Tighter approximated MILP formulations for unit commitment problems," *IEEE Trans. Power Syst.*, vol. 24, no. 1, pp. 105–113, Feb. 2009.
[24] G. Morales-Espana, J. M. Latorre, and A. Ramos, "Tight and compact MILP formulation of start-up and shut-down ramping in unit commitment," *IEEE Trans. Power Syst.*, vol. PP, no. 99, p. 1, 2012, DOI: 10.1109/TPWRS.2012.2222938.
[25] G. Morales-España, J. M. Latorre, and A. Ramos, "Online companion for tight and compact MILP formulation for the thermal unit commitment problem," Res. Rep. IIT-12-072, 2012. [Online]. Available: http://www.iit.upcomillas.es/aramos/papers/OnlineCompanion_Tight&Compact_UC.pdf
[26] A. J. Wood and B. F. Wollenberg, *Power Generation, Operation, and Control*, 2nd ed. New York: Wiley-Interscience, Jan. 1996.
[27] M. P. Nowak and W. Römisch, "Stochastic Lagrangian relaxation applied to power scheduling in a hydro-thermal system under uncertainty," *Ann. Oper. Res.*, vol. 100, no. 1, pp. 251–272-272, Dec. 2000.
[28] K. Hedman, R. O'Neill, and S. Oren, "Analyzing valid inequalities of the generation unit commitment problem," in *Proc. IEEE PES Power Syst. Conf. Expo.*, 2009, pp. 1–6.
[29] "The GAMS development corporation website," 2012 [Online]. Available: www.gams.com
[30] R. E. Bixby, M. Fenelon, Z. Gu, E. Rothberg, and R. Wunderling, , M. Grötschel, Ed., "Mixed-integer programming: A progress report," in *The Sharpest Cut: The Impact of Manfred Padberg and His Work*, ser. ser. MPS-SIAM Series on Optimization. Philadelphia, PA, USA: SIAM, Jan. 2004, pp. 309–325.
[31] E. Danna, "Performance variability in mixed integer programming," in *Proc. 5th Workshop on Mixed Integer Programming*, 2008, pp. 1–40.
[32] H. P. Williams, *Logic and Integer Programming*, ser. Int. series in Oper. Res. Manag. Sci., 1st ed. New York: Springer, 2009.
[33] L. Wu, M. Shahidehpour, and T. Li, "Stochastic security-constrained unit commitment," *IEEE Trans. Power Syst.*, vol. 22, no. 2, pp. 800–811, May 2007.

Germán Morales-España (S'10) received the B.Sc. degree in electrical engineering from the Universidad Industrial de Santander, Bucaramanga, Colombia, in 2007, and the M.Sc. degree from the Delft University of Technology, Delft, The Netherlands, in 2010. He is currently working toward the Ph.D. Erasmus Mundus Joint Doctorate degree in sustainable energy technologies and strategies hosted by the Universidad Pontificia Comillas, Madrid, Spain; the Royal Institute of Technology, Stockholm, Sweden; and Delft University of Technology, Delft, The Netherlands.

He is currently an Assistant Researcher with the Institute for Research in Technology (IIT), Universidad Pontificia Comillas, Madrid, Spain, and he is also a member of the Research Group on Electric Power Systems (GISEL), Universidad Industrial de Santander, Bucaramanga, Colombia. His areas of interest are power systems operation, economics, and reliability, as well as power quality and protective relaying.

Jesus M. Latorre (S'00–M'07) was born in Madrid, Spain, in 1977. He received the degree of Electronic Engineer and Ph.D. degree from Universidad Pontificia Comillas, Madrid, Spain, in 2001 and 2007, respectively.

He is currently a Postdoctoral Researcher with the Institute for Research in Technology, Universidad Pontificia Comillas, Madrid, Spain. His main interest areas include operations research and mathematical modelling, stochastic programming, parallel and distributed computing, algorithms, and numerical methods.

Andres Ramos received the degree of Electrical Engineering from Universidad Pontificia Comillas, Madrid, Spain, in 1982, and the Ph.D. degree in electrical engineering from Universidad Politécnica de Madrid, Madrid, Spain, in 1990.

He is a Research Fellow with Institute for Research in Technology, Universidad Pontificia Comillas, Madrid, Spain, and a Full Professor with the School of Engineering, Universidad Pontificia Comillas, where he has been the Head of the Department of Industrial Organization. His areas of interest include the operation, planning, and economy of power systems and the application of operations research to industrial organization.

Article IV

C. Gentile, G. Morales-España, and A. Ramos, "A Tight MIP Formulation of the Unit Commitment Problem with Start-up and Shut-down Constraints," *Computers & Operations Research*, paper under review, 2014. JCR 2012 data: impact factor 1.909 and 5-year impact factor 2.374.

Additional Material: With the help of PORTA [30], all vertices of the polytope described in this paper were computed for different time spans and different set of parameters. As expected, since the proposed polytope describes a convex hull, it only contains integer vertices for all the cases. We also explored the vertices of other formulations commonly found in the literature and all of them presented plenty of fractional vertices. The complete set of experiments that were carried out can be found in http://goo.gl/wHqFMF.

A Tight MIP Formulation of the Unit Commitment Problem with Start-up and Shut-down Constraints

C. Gentile[a,1], G. Morales-España[b,2], A. Ramos[b]

[a] *Istituto di Analisi dei Sistemi ed Informatica "A. Ruberti", C.N.R., Viale Manzoni 30, 00185 Roma, Italy*

[b] *Institute for Research in Technology (IIT) of the School of Engineering (ICAI), Universidad Pontificia Comillas, Madrid, Spain*

Abstract

This paper provides the convex hull description for the following basic operating constraints of a single thermal generation unit in Unit Commitment (UC) problems: 1) generation limits, 2) startup and shutdown capabilities, and 3) minimum up and down times. Although the model does not consider some crucial constraints, such as ramping, the proposed constraints can be used as the core of any UC formulation, thus tightening the final UC model. We provide evidence that dramatic improvements in computational time are obtained by solving a self-UC problem for different case studies.

Keywords: Unit Commitment (UC), Mixed-Integer Programming (MIP), Facet/Convex hull description.

1. Introduction

The short-term Unit Commitment problem requires to optimally operate a set of power generation units over a time horizon ranging from a day to a week. Despite significant improvements in Mixed-Integer Programming (MIP) solvers, the time required to solve Unit Commitment (UC) problems continues to be a critical limitation that restricts its size and scope. Nevertheless, improving the UC formulation can dramatically reduce its computational burden and so allow the implementation of more advanced and computationally demanding problems.

Ideally, an MIP problem can be reformulated so that the feasible region of the corresponding Linear Programming (LP) model becomes the convex hull of the feasible points. If this is possible, we could solve an MIP as an LP since each vertex is a point satisfying the integrality constraints and hence it always exists an optimal solution of the LP that

Email addresses: gentile@iasi.cnr.it (C. Gentile), german.morales@iit.upcomillas.es; gmorales@kth.se (G. Morales-España), andres.ramos@upcomillas.es (A. Ramos)

[1] The work of C. Gentile was partially supported by the project MINO grant no. 316647 Initial Training Network of the "Marie Curie" program funded by the European Union.

[2] The work of G. Morales-España was supported by the European Commission through an Erasmus Mundus Ph.D. Fellowship.

is optimal for the corresponding MIP [14]. Unfortunately, in many practical problems there is an enormous number of inequalities needed to describe the convex hull, and the effort required to obtain them outweighs the computation needed to solve the original formulation of the MIP problem [14, 13]. For the UC case, however, it is possible to tighten the feasible region of the relaxed LP problem, consequently obtaining dramatic improvements in computation [14, 13, 11, 8, 7].

In particular, an UC formulation can be considerably tightened by providing the convex hull (or tight) description of some set of constraints. Even though other constraints in the problem might add some fractional vertices, this solution should be nearer to the optimal solution than would be the original model [14, 13]. Some efforts in tightening specific set of constraints have been done, such as: the convex hull of the minimum up and down times [5, 6, 12], cuts to tighten ramping limits [11], tighter approximation for quadratic generation costs [4], and simultaneously tight and compact description of thermal units operation [8, 7].

This paper further improves the work in Morales-Espana et al. [7] by providing the convex hull description for the following set of constraints: generation limits, startup and shutdown capabilities, and minimum up and down times. In addition, different case studies for a self-UC were solved as LP obtaining feasible MIP solutions; if compared with three other MIP formulations, the same optimal results were obtained but significantly faster.

The remainder of this paper is organized as follows. Section 2 introduces the main notation used to describe the proposed formulation. Section 3 details the basic operating constraints of a single generating unit. Section 4 contains the facet inducing and convex hull proofs for the proposed linear description of the self-UC subproblem. Section 5 provides and discusses results from several case studies, where a comparison with other three UC formulations is made. Finally, some relevant conclusions are drawn in Section 6.

2. Notation

Here we introduce the main notation used in this paper. Lowercase letters are used for denoting variables and indexes. Uppercase letters denote parameters.

2.1. Indexes

t	Time periods, running from 1 to T hours.

2.2. Unit's Technical Parameters

$\overline{P}$	Maximum power output [MW].
$\underline{P}$	Minimum power output [MW].
SD	Shutdown capability [MW].
SU	Startup capability [MW].
TD	Minimum down time [h].
TU	Minimum up time [h].

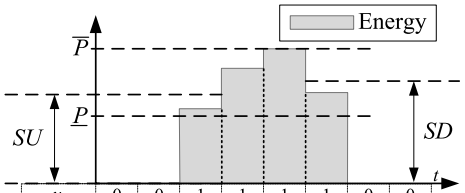

u_t	0	0	1	1	1	1	0	0
v_t	0	0	1	0	0	0	0	0
w_t	0	0	0	0	0	0	1	0

Figure 1: Unit's operation including its startup and shutdown capabilities

2.3. Continuous Decision Variables

p_t Power output of the unit for period t, production above the unit's minimum output $\underline{P}$ [MW].

2.4. Binary Decision Variables

u_t Commitment status of the unit for period t, which is equal to 1 if the unit is online and 0 offline

v_t Startup status of the unit, which takes the value of 1 if the unit starts up in period t and 0 otherwise.

w_t Shutdown status of the unit, which takes the value of 1 if the unit shuts down in period t and 0 otherwise.

3. Modelling the Unit's Operation

This section describes the mathematical formulation of the basic operation of a single generating unit in Unit Commitment (UC) problems. The following set of constraints are modelled: generation limits, minimum up and down times, and startup and shutdown capabilities. As shown in Figure 1, the startup capability SU is the maximum energy that a generating unit can produce when it starts up. Similarly, the unit should be producing bellow its shutdown capability SD when it shuts down. All these constraints are inherent to units' operation and they are included in recent Unit Commitment literature, see [1, 4, 11, 7, 9] and references therein for further details.

The unit's generation limits taking into account its maximum $\overline{P}$ and minimum $\underline{P}$ production, as well as its startup SU and shutdown SD capabilities are set as follows:

$$p_1 \leq \left(\overline{P} - \underline{P}\right) u_1 - \left(\overline{P} - SD\right) w_2 \tag{1}$$

$$p_t \leq \left(\overline{P} - \underline{P}\right) u_t - \left(\overline{P} - SU\right) v_t - \left(\overline{P} - SD\right) w_{t+1} \quad t \in [2, T-1] \tag{2}$$

$$p_T \leq \left(\overline{P} - \underline{P}\right) u_T - \left(\overline{P} - SU\right) v_T \tag{3}$$

It is important to highlight that the continuous decision variable p_t is the generation over $\underline{P}$. The total generation output can be obtained as $u_t\underline{P} + p_t$.

Be aware that (2) may be infeasible in the event that the unit is online for just one period. That is, $v_t = w_{t+1} = 1$ and the right side of (2) can be negative. Consequently, (2) is only valid for units with uptime $TU \geq 2$. Therefore, the correct formulation for units with $TU = 1$ is given by:

$$\begin{aligned} p_t \leq & \left(\overline{P} - \underline{P}\right) u_t - \left(\overline{P} - SD\right) w_{t+1} \\ & - \max\left(SD - SU, 0\right) v_t \quad \forall t \in [2, T-1] \end{aligned} \tag{4}$$

$$\begin{aligned} p_t \leq & \left(\overline{P} - \underline{P}\right) u_t - \left(\overline{P} - SU\right) v_t \\ & - \max\left(SU - SD, 0\right) w_{t+1} \quad \forall t \in [2, T-1]. \end{aligned} \tag{5}$$

Note that if $SU = SD$ then (4)-(5) would be equivalent to the power limit constraints proposed in [7].

The logical relationship between the decision variables u_t, v_t and w_t; and the minimum uptime TU and downtime TD limits are ensured with

$$u_t - u_{t-1} = v_t - w_t \quad \forall t \in [2, T] \tag{6}$$

$$\sum_{i=t-TU+1}^{t} v_i \leq u_t \quad \forall t \in [TU+1, T] \tag{7}$$

$$\sum_{i=t-TD+1}^{t} w_i \leq 1 - u_t \quad \forall t \in [TD+1, T] \tag{8}$$

where (6)-(8) are the constraints proposed in [12] to describe the convex hull formulation of the minimum-up and -down time constraints. Finally, the variable bounds are given by

$$0 \leq u_t \leq 1 \quad \forall t \tag{9}$$

$$v_t \geq 0, \quad w_t \geq 0 \quad \forall t \in [2, T] \tag{10}$$

$$p_t \geq 0 \quad \forall t. \tag{11}$$

In summary, inequalities (1)-(3) together with (6)-(11) describe the operation for units with $TU \geq 2$; and (1) together with (3)-(11) for the cases in which $TU = 1$.

4. Strength of the Proposed Inequalities

In this section, we prove that inequalities (1)-(5) and (11) are facet defining.

Note that constraints (6) uniquely define the value of the variables w as a function of variables u and v. Unless differently specified, in the following, we will consider only the space defined by the variables u, v, and p. Moreover, we suppose that all constraints (1)-(5) and (7)-(11) are rewritten by substituting the w variables accordingly.

Definition 1. Let $\overline{C}_T\left(TU, TD, \overline{P}, \underline{P}, SU, SD\right)$ be the convex hull of the feasible integer solution for the problem. That is, for $TU \geq 2$, we write

$$\begin{aligned} \overline{C}_T \ & (TU \geq 2, TD, \overline{P}, \underline{P}, SU, SD) = \\ & conv\{(u, v, p) \in \{0,1\}^{2T-1} \times R_+^T | \, (u, v, p) \text{ satisfy (1)-(3) and (7)-(11)}\}; \end{aligned}$$

	u_1	u_2	$\cdots$	u_{t-1}	u_t	u_{t+1}	$\cdots$	u_{T-1}	u_T	p_1	p_2	$\cdots$	p_{t-1}	p_t	p_{t+1}	$\cdots$	p_{T-1}	p_T	v_2	$\cdots$	v_{t-1}	v_t	v_{t+1}	$\cdots$	v_{T-1}	v_T	w_2	$\cdots$	w_{t-1}	w_t	w_{t+1}	$\cdots$	w_{T-1}	w_T
$x^{(1)}$	1	0	$\cdots$	0	0	0	$\cdots$	0	0	g_t^x	0	$\cdots$	0	0	0	$\cdots$	0	0	0	$\cdots$	0	0	0	$\cdots$	0	0	1	$\cdots$	0	0	0	$\cdots$	0	0
$x^{(2)}$	1	1	$\cdots$	0	0	0	$\cdots$	0	0	g_t^x	0	$\cdots$	0	0	0	$\cdots$	0	0	0	$\cdots$	0	0	0	$\cdots$	0	0	0	$\cdots$	0	0	0	$\cdots$	0	0
$\vdots$	$\vdots$	$\vdots$	$\ddots$	$\vdots$	$\vdots$	$\vdots$	$\ddots$	$\vdots$	$\vdots$	$\vdots$	$\vdots$	$\ddots$	$\vdots$	$\vdots$	$\vdots$	$\ddots$	$\vdots$	$\vdots$	$\vdots$	$\ddots$	$\vdots$	$\vdots$	$\vdots$	$\ddots$	$\vdots$	$\vdots$	$\vdots$	$\ddots$	$\vdots$	$\vdots$	$\vdots$	$\ddots$	$\vdots$	$\vdots$
$x^{(t-1)}$	1	1	$\cdots$	1	0	0	$\cdots$	0	0	g_t^x	0	$\cdots$	0	0	0	$\cdots$	0	0	0	$\cdots$	0	0	0	$\cdots$	0	0	0	$\cdots$	0	1	0	$\cdots$	0	0
$x^{(t)}$	1	1	$\cdots$	1	1	0	$\cdots$	0	0	g_t^x	0	$\cdots$	0	0	0	$\cdots$	0	0	0	$\cdots$	0	0	0	$\cdots$	0	0	0	$\cdots$	0	0	1	$\cdots$	0	0
$x^{(t+1)}$	1	1	$\cdots$	1	1	1	$\cdots$	0	0	g_t^x	0	$\cdots$	0	g_t	0	$\cdots$	0	0	0	$\cdots$	0	0	0	$\cdots$	0	0	0	$\cdots$	0	0	0	$\cdots$	0	0
$\vdots$	$\vdots$	$\vdots$	$\ddots$	$\vdots$	$\vdots$	$\vdots$	$\ddots$	$\vdots$	$\vdots$	$\vdots$	$\vdots$	$\ddots$	$\vdots$	$\vdots$	$\vdots$	$\ddots$	$\vdots$	$\vdots$	$\vdots$	$\ddots$	$\vdots$	$\vdots$	$\vdots$	$\ddots$	$\vdots$	$\vdots$	$\vdots$	$\ddots$	$\vdots$	$\vdots$	$\vdots$	$\ddots$	$\vdots$	$\vdots$
$x^{(T-1)}$	1	1	$\cdots$	1	1	1	$\cdots$	1	0	g_t^x	0	$\cdots$	0	g_t	0	$\cdots$	0	0	0	$\cdots$	0	0	0	$\cdots$	0	0	0	$\cdots$	0	0	0	$\cdots$	0	1
$x^{(T)}$	1	1	$\cdots$	1	1	1	$\cdots$	1	1	g_t^x	0	$\cdots$	0	g_t	0	$\cdots$	0	0	0	$\cdots$	0	0	0	$\cdots$	0	0	0	$\cdots$	0	0	0	$\cdots$	0	0
$y^{(1)}$	1	0	$\cdots$	0	0	0	$\cdots$	0	0	D	0	$\cdots$	0	0	0	$\cdots$	0	0	0	$\cdots$	0	0	0	$\cdots$	0	0	1	$\cdots$	0	0	0	$\cdots$	0	0
$y^{(2)}$	1	1	$\cdots$	0	0	0	$\cdots$	0	0	P	D	$\cdots$	0	0	0	$\cdots$	0	0	0	$\cdots$	0	0	0	$\cdots$	0	0	0	$\cdots$	0	0	0	$\cdots$	0	0
$\vdots$	$\vdots$	$\vdots$	$\ddots$	$\vdots$	$\vdots$	$\vdots$	$\ddots$	$\vdots$	$\vdots$	$\vdots$	$\vdots$	$\ddots$	$\vdots$	$\vdots$	$\vdots$	$\ddots$	$\vdots$	$\vdots$	$\vdots$	$\ddots$	$\vdots$	$\vdots$	$\vdots$	$\ddots$	$\vdots$	$\vdots$	$\vdots$	$\ddots$	$\vdots$	$\vdots$	$\vdots$	$\ddots$	$\vdots$	$\vdots$
$y^{(t-1)}$	1	1	$\cdots$	1	0	0	$\cdots$	0	0	P	P	$\cdots$	D	0	0	$\cdots$	0	0	0	$\cdots$	0	0	0	$\cdots$	0	0	0	$\cdots$	0	1	0	$\cdots$	0	0
$y^{(t)}$	1	1	$\cdots$	1	1	0	$\cdots$	0	0	P	P	$\cdots$	P	D	0	$\cdots$	0	0	0	$\cdots$	0	0	0	$\cdots$	0	0	0	$\cdots$	0	0	1	$\cdots$	0	0
$y^{(t+1)}$	1	1	$\cdots$	1	1	1	$\cdots$	0	0	P	P	$\cdots$	P	g_t^y	D	$\cdots$	0	0	0	$\cdots$	0	0	0	$\cdots$	0	0	0	$\cdots$	0	0	0	$\cdots$	0	0
$\vdots$	$\vdots$	$\vdots$	$\ddots$	$\vdots$	$\vdots$	$\vdots$	$\ddots$	$\vdots$	$\vdots$	$\vdots$	$\vdots$	$\ddots$	$\vdots$	$\vdots$	$\vdots$	$\ddots$	$\vdots$	$\vdots$	$\vdots$	$\ddots$	$\vdots$	$\vdots$	$\vdots$	$\ddots$	$\vdots$	$\vdots$	$\vdots$	$\ddots$	$\vdots$	$\vdots$	$\vdots$	$\ddots$	$\vdots$	$\vdots$
$y^{(T-1)}$	1	1	$\cdots$	1	1	1	$\cdots$	1	0	P	P	$\cdots$	P	g_t^y	P	$\cdots$	D	0	0	$\cdots$	0	0	0	$\cdots$	0	0	0	$\cdots$	0	0	0	$\cdots$	0	1
$y^{(T)}$	1	1	$\cdots$	1	1	1	$\cdots$	1	1	P	P	$\cdots$	P	g_t^y	P	$\cdots$	P	P	0	$\cdots$	0	0	0	$\cdots$	0	0	0	$\cdots$	0	0	0	$\cdots$	0	0
$z^{(1)}$	0	1	$\cdots$	1	1	1	$\cdots$	1	1	0	U	$\cdots$	0	g_t	0	$\cdots$	0	0	1	$\cdots$	0	0	0	$\cdots$	0	0	0	$\cdots$	0	0	0	$\cdots$	0	0
$\vdots$	$\vdots$	$\vdots$	$\ddots$	$\vdots$	$\vdots$	$\vdots$	$\ddots$	$\vdots$	$\vdots$	$\vdots$	$\vdots$	$\ddots$	$\vdots$	$\vdots$	$\vdots$	$\ddots$	$\vdots$	$\vdots$	$\vdots$	$\ddots$	$\vdots$	$\vdots$	$\vdots$	$\ddots$	$\vdots$	$\vdots$	$\vdots$	$\ddots$	$\vdots$	$\vdots$	$\vdots$	$\ddots$	$\vdots$	$\vdots$
$z^{(t-2)}$	0	0	$\cdots$	1	1	1	$\cdots$	1	1	0	0	$\cdots$	U	g_t	0	$\cdots$	0	0	0	$\cdots$	1	0	0	$\cdots$	0	0	0	$\cdots$	0	0	0	$\cdots$	0	0
$z^{(t-1)}$	0	0	$\cdots$	0	1	1	$\cdots$	1	1	0	0	$\cdots$	0	g_t^z	0	$\cdots$	0	0	0	$\cdots$	0	1	0	$\cdots$	0	0	0	$\cdots$	0	0	0	$\cdots$	0	0
$z^{(t)}$	0	0	$\cdots$	0	0	1	$\cdots$	1	1	0	0	$\cdots$	0	0	U	$\cdots$	0	0	0	$\cdots$	0	0	1	$\cdots$	0	0	0	$\cdots$	0	0	0	$\cdots$	0	0
$\vdots$	$\vdots$	$\vdots$	$\ddots$	$\vdots$	$\vdots$	$\vdots$	$\ddots$	$\vdots$	$\vdots$	$\vdots$	$\vdots$	$\ddots$	$\vdots$	$\vdots$	$\vdots$	$\ddots$	$\vdots$	$\vdots$	$\vdots$	$\ddots$	$\vdots$	$\vdots$	$\vdots$	$\ddots$	$\vdots$	$\vdots$	$\vdots$	$\ddots$	$\vdots$	$\vdots$	$\vdots$	$\ddots$	$\vdots$	$\vdots$
$z^{(T-2)}$	0	0	$\cdots$	0	0	0	$\cdots$	1	1	0	0	$\cdots$	0	0	0	$\cdots$	U	0	0	$\cdots$	0	0	0	$\cdots$	1	0	0	$\cdots$	0	0	0	$\cdots$	0	0
$z^{(T-1)}$	0	0	$\cdots$	0	0	0	$\ldots$	0	1	0	0	$\cdots$	0	0	0	$\ldots$	0	U	0	$\cdots$	0	0	0	$\ldots$	0	1	0	$\ldots$	0	0	0	$\ldots$	0	0
$z^{(T)}$	0	0	$\cdots$	0	0	0	$\ldots$	0	0	0	0	$\cdots$	0	0	0	$\ldots$	0	0	0	$\cdots$	0	0	0	$\ldots$	0	0	0	$\ldots$	0	0	0	$\ldots$	0	0
$q^{(t)}$	0	0	$\cdots$	0	1	0	$\ldots$	0	0	0	0	$\cdots$	0	g_t^q	0	$\ldots$	0	0	0	$\cdots$	0	1	0	$\ldots$	0	0	0	$\ldots$	0	1	0	$\ldots$	0	0
$y^{(T+1)}$	1	1	$\cdots$	1	1	1	$\cdots$	1	1	P	P	$\cdots$	P	g_t^y	P	$\cdots$	P	0	0	$\cdots$	0	0	0	$\cdots$	0	0	0	$\cdots$	0	0	0	$\cdots$	0	0

Figure 2: $3T$ Affinely independent points for $g_t^x, g_t = 0$ and $g_t^z = U$, where $U = SU - \underline{P}$, $D = SD - \underline{P}$ and $P = \overline{P} - \underline{P}$.

for $TU = 1$, we write

$$\overline{C}_T\ \big(TU = 1, TD, \overline{P}, \underline{P}, SU, SD\big) = \\ conv\left\{(u,v,p) \in \{0,1\}^{2T-1} \times R_+^T |\, (u,v,p)\ \text{ satisfy (1), (3)-(5), and (7)-(11)}\right\}.$$

For short we write $\overline{C}_T$ for $\overline{C}_T\left(TU, TD, \overline{P}, \underline{P}, SU, SD\right)$, $\overline{C}_T(TU \geq 2)$ for $\overline{C}_T(TU \geq 2, TD, \overline{P}, \underline{P}, SU, SD)$, and $\overline{C}_T(TU = 1)$ for $\overline{C}_T(TU = 1, TD, \overline{P}, \underline{P}, SU, SD)$.

In order to simplify the proofs, we introduce the points $x^i, y^i, z^i \in \overline{C}_T$, as shown in Figure 2. For short, we introduce the parameters U, D, and P which are equivalent to $U = SU - \underline{P}$, $D = SD - \underline{P}$, and $P = \overline{P} - \underline{P}$, respectively.

Proposition 2. *$\overline{C}_T\big(TU, TD, \overline{P}, \underline{P}, SU, SD\big)$ is full-dimensional in terms of u, v and p.*

Proof. From Figure 2, it can be easily shown that the $3T$ points x^i, y^i, and z^i for $i \in [1, T]$ are affinely independent when $g_t^x = g_t = 0$, $g_t^y = P$, and $g_t^z = U$. Note that in case $D = 0$ the point $y^{(1)}$ must be replaced by $y^{(T+1)}$, thus keeping the $3T$ affinely independent points. This applies for all the following proofs; but for the sake of brevity, we assume in the following that $D \neq 0$. □

Proposition 3. *The inequalities* (2) *describe facets of the polytope $\overline{C}_T\big(TU \geq 2\big)$.*

Proof. We show that (2) describe facets of $\overline{C}_T\big(TU \geq 2\big)$ by the direct method [14]. We do so by presenting $3T-1$ affinely independent points in $\overline{C}_T\big(TU \geq 2\big)$ that are tight (i.e., that satisfy as an equality) for inequality (2). Note in Figure 2 that the point z^T (the origin) satisfies (1)-(5) and (11) as equality. Therefore, to get $3T-1$ affinely independent points, we need $3T-2$ other linearly independent points.

The following $3T-2$ points are linearly independent and tight for (2) when $g_t^x = 0$, $g_t = g_t^y = P$ and $g_t^z = U$: $T-1$ points x^i for $i \in [1, t-1] \cup [t+1, T]$, T points y^i for $i \in [1, T]$, and $T-1$ points z^i for $i \in [1, T-1]$. □

Proposition 4. *The inequalities* (4) *and* (5) *describe facets of the polytope* $\overline{C}_T\big(TU = 1\big)$.

Proof. As z^T (the origin) satisfies both (4) and (5) as equality, it suffices to show $3T-2$ linearly independent points that are tight for (4) and the same for (5). The following $3T-2$ points are linearly independent and tight for (4) when $g_t^x = 0$, $g_t = g_t^y = P$: $T-1$ points x^i for $i \in [1, t-1] \cup [t+1, T]$, T points y^i for $i \in [1, T]$, $T-2$ points z^i for $i \in [1, t-2] \cup [t, T-1]$, and one point $q^{(t)}$ where $g_t^q = D$ if $SD \leq SU$ and $g_t^q = U$ if $SD \geq SU$.

The following $3T-2$ points are linearly independent and tight for (5) when $g_t^x = 0$, $g_t = g_t^y = P$, and $g_t^z = U$: $T-1$ points x^i for $i \in [1, t-1] \cup [t+1, T]$, $T-1$ points y^i for $i \in [1, t-1] \cup [t+1, T]$, $T-1$ points z^i for $i \in [1, T-1]$, and one point $q^{(t)}$ where $g_t^q = D$ if $SD \leq SU$ and $g_t^q = U$ if $SD \geq SU$. □

Proposition 5. *The inequalities* (1) *and* (3) *describe facets of the polytope* $\overline{C}_T$.

Proof. As z^T (the origin) satisfies both (1) and (3) as equality, it suffices to provide a set of $3T-2$ linearly independent points that are tight for each of the above inequalities. The following $3T-2$ points are linearly independent and tight for (1) when $g_t = 0$, $g_t^x = g_t^y = P$ and $g_t^z = U$: $T-1$ points x^i for $i \in, [2, T]$, T points y^i for $i \in [1, T]$, and $T-1$ points z^i for $i \in [1, T-1]$.

The following $3T-2$ points are linearly independent and tight for (3) when $g_t^x = 0$, $g_t = g_t^y = P$, and $g_t^z = U$: $T-1$ points x^i for $i \in [1, T]$, T points y^i for $i \in [1, T]$, and $T-1$ points z^i for $i \in [1, T-1]$. □

Proposition 6. *The inequality* (11) *describes a facet of the polytope* $\overline{C}_T$.

Proof. The point z^T satisfies the inequality (11) as equality. So, as above discussed, it suffices to show $3T-2$ linearly independent solutions that are tight for (11). The following $3T-2$ points are linearly independent and tight for (11) when $g_t = g_t^x = g_t^y = g_t^z = 0$: T points x^i for $i \in [1, T]$, $T-1$ points y^i for $i \in [1, t-1] \cup [t+1, T]$, and $T-1$ points z^i for $i \in [1, T-1]$. □

Summing up (1)-(5) and (11) describe facets of $\overline{C}_T$. Finally, we prove that the inequalities (1)-(11) are sufficient to describe the convex hull of the feasible solutions.

We need a preliminary lemma.

Lemma 7. *Let* $P = \{x \in \mathbb{R}^n | Ax \leq b\}$ *be an integral polyhedron, i.e,* $P = conv(P \cap \mathbb{Z}^n)$. *Define* $Q = \{(x, y) \in \mathbb{R}^n \times \mathbb{R}^m | x \in P, 0 \leq y_i \leq c_i x, i = 1, \ldots, k,\ y_i = d_i x, i = k+1, \ldots, m\}$, *where* $1 \leq k \leq m$, $c_i, d_i \in \mathbb{R}^n$, *and* $c_i x \geq 0$, $d_i x \geq 0$ *for* $i = 1, \ldots, m$ *and for each* $x \in P$. *Then every vertex* $(\tilde{x}, \tilde{y})$ *of* Q *has the property that* $\tilde{x}$ *is integral.*

Proof. Suppose by contradiction that there exists a vertex $(\tilde{x}, \tilde{y})$ of Q such that $\tilde{x}$ is not integral. Then $\tilde{x}$ is not a vertex of P and therefore there exist $\bar{x}^1, \bar{x}^2 \in P$ such that $\tilde{x} = \frac{1}{2}\bar{x}^1 + \frac{1}{2}\bar{x}^2$. Moreover, $\tilde{y}_i = c_i\tilde{x}$ for $i = 1, \ldots, k$, indeed if there exists r, $1 \leq r \leq k$, such that $0 \leq \tilde{y}_r < c_r\tilde{x}$, then $(\tilde{x}, \tilde{y})$ is a convex combination of the point $(\tilde{x}, \hat{y})$ and the point $(\tilde{x}, \check{y})$, where $\hat{y}_r = c_r\tilde{x}$, $\check{y}_r = 0$, and $\hat{y}_i = \check{y}_i = \tilde{y}_i$ for $1 \leq i \leq m$, $i \neq r$.

For $j = 1, 2$, let $\bar{y}_i^j = c_i\bar{x}^j$ for $i = 1, \ldots, k$ and $\bar{y}_i^j = d_i\bar{x}^j$ for $i = k+1, \ldots, m$. Then $(\tilde{x}, \tilde{y}) = \frac{1}{2}(\bar{x}^1, \bar{y}^1) + \frac{1}{2}(\bar{x}^2, \bar{y}^2)$, i.e., $(\tilde{x}, \tilde{y})$ is a convex combination of $(\bar{x}^1, \bar{y}^1)$ and $(\bar{x}^2, \bar{y}^2)$. Contradiction. □

Theorem 8. *Let* $\overline{D}_T\left(TU, TD, \overline{P}, \underline{P}, SU, SD\right)$ *be a polyhedron defined as follows:*

- *for* $TU \geq 2$

$$\begin{aligned}\overline{D}_T\ &\left(TU \geq 2, TD, \overline{P}, \underline{P}, SU, SD\right) = \\ &\left\{(u, v, p) \in [0,1]^{2T-1} \times R_+^T |\ (u, v, p)\ \textit{satisfy}\ (1)\text{-}(3)\ \textit{and}\ (7)\text{-}(11)\ \right\};\end{aligned}$$

- *for* $TU = 1$

$$\begin{aligned}\overline{D}_T\ &\left(TU = 1, TD, \overline{P}, \underline{P}, SU, SD\right) = \\ &\left\{(u, v, p) \in [0,1]^{2T-1} \times R_+^T |\ (u, v, p)\ \textit{satisfy}\ (1), (3)\text{-}(5), \textit{and}\ (7)\text{-}(11)\ \right\}.\end{aligned}$$

Then $\overline{C}_T\big(TU, TD, \overline{P}, \underline{P}, SU, SD\big) = \overline{D}_T\big(TU, TD, \overline{P}, \underline{P}, SU, SD\big)$.

Proof. As for $\overline{C}_T$, we use short notations $\overline{D}_T$, $\overline{D}_T\big(TU \geq 2\big)$, and $\overline{D}_T\big(TU = 1\big)$. The proof for $TU \geq 2$ easily follows from Lemma 7. Indeed, $\overline{D}_T\big(TU \geq 2\big)$ is described by the inequalities (6)-(10), that describe an integral polyhedron in u and v as proved in [12], together with inequalities (1)-(3) and (11) satisfying the hypothesis of Lemma 7.

For $TU = 1$ let us suppose that $SU \geq SD$. We follow Approach 8 in [14] (see Section 9.2.3, Problem 2, Approach 8). We first introduce an extended formulation of the problem, then we prove that the extended formulation is integral, and finally we prove that the projection of the new polyhedron correspond to $\overline{D}_T\big(TU = 1\big)$. To accomplish to this task we need to prove some preliminary claims. We define the following new binary variables for $t = 2, \ldots, T-1$:

- $x_t = 1$ if and only if $v_t = 1$ and $w_{t+1} = 1$,
- $\tilde{v}_t = 1$ if and only if $v_t = 1$ and $w_{t+1} = 0$,
- $\tilde{w}_{t+1} = 1$ if and only if $v_t = 0$ and $w_{t+1} = 1$,
- $\tilde{u}_t = 1$ if and only if $u_t = 1$, $v_t = 0$, and $w_{t+1} = 0$.

Moreover, $\tilde{u}_T = 1$ if and only if $u_T = 1$ and $v_T = 0$.

Claim 1. The polyhedron P defined by the points $(u, v, w, \tilde{u}, \tilde{v}, \tilde{w}, x)$ satisfying the

following inequalities is integral:

$$v_t \leq u_t \quad t = 2, \ldots, T \tag{12}$$

$$\sum_{i=t-TD+1}^{t} w_i \leq 1 - u_t \quad t \in [TD+1, T] \tag{13}$$

$$u_t - u_{t-1} = v_t - w_t \quad t \in [2, T] \tag{14}$$

$$w_{t+1} = \tilde{w}_{t+1} + x_t \quad t \in [2, T-1] \tag{15}$$

$$v_t = \tilde{v}_t + x_t \quad t \in [2, T-1] \tag{16}$$

$$u_t = \tilde{v}_t + \tilde{w}_{t+1} + x_t + \tilde{u}_t \quad t \in [2, T-1] \tag{17}$$

$$u_T = v_T + \tilde{u}_T \tag{18}$$

$$0 \leq u_t \leq 1 \quad t \in [1, T] \tag{19}$$

$$v_t \geq 0 \quad t \in [2, T] \tag{20}$$

$$w_t \geq 0 \quad t \in [2, T] \tag{21}$$

$$\tilde{v}_t, x_t \geq 0 \quad t \in [2, T-1] \tag{22}$$

$$\tilde{w}_t \geq 0 \quad t \in [3, T] \tag{23}$$

$$\tilde{u}_t \geq 0 \quad t \in [2, T] \tag{24}$$

Proof of Claim 1. The proof is carried on by showing that the coefficient matrix associated with the above linear system is totally unimodular.

We exploit this well-known property (proved by Ghouila-Houri, see [10], Chapter III.1, Theorem 2.7): let A be a $\{0, 1, -1\}$-matrix, if each subset J of columns of A can be partitioned into J_1 and J_2 such that

$$\left| \sum_{j \in J_1} a_{ij} - \sum_{j \in J_2} a_{ij} \right| \leq 1 \tag{25}$$

for each row i, then A is totally unimodular. This part of the proof has been inspired by the proof of Malkin [6] for the polyhedron defined by minimum-up and down-time constraints.

First we assign the variables $w_i \in J$ alternatively to J_1 and to J_2 in lexicographic order. Then the variables $u_t \in J$ are assigned either to J_1 if $w_k \in J_2$, where $k = \max\{i | 1 \leq i \leq t, w_i \in J\}$, or to J_2 if $w_k \in J_1$, or to the same set with respect to u_{t-1} if $\{i | 1 \leq i \leq t, w_i \in J\}$ is empty. Thus condition (25) is satisfied for constraints (13).

Variables $v_t \in J$ are assigned either to J_1 if $u_t \in J_1$, or to J_2 if $u_t \in J_2$, or to the opposite set with respect to u_{t-1} if $u_t \notin J$, or to the same set as w_t if both $u_{t-1}, u_t \notin J$. This ensures that condition (25) is satisfied for constraints (12) and (14).

If $v_t, w_{t+1} \in J$, then assign $\tilde{v}_t \in J$ to the same subset as v_t, $x_t \in J$ to the opposite set with respect to $\tilde{v}_t$, and $\tilde{w}_t \in J$ to the same subset as w_t. These assignments guarantee that condition (25) is satisfied for constraints (15) and (16) both in the case that v_t and w_{t+1} are in the same set or in different sets. Moreover, the assignment for $\tilde{u}_t$ can be chosen to satisfy condition (25) for constraints (17). If one between v_t and w_{t+1} does not belong to J then proceed as follows: suppose w.l.o.g. that $v_t \notin J$, then assign w_{t+1}, $\tilde{w}_{t+1}$, and $\tilde{v}_t$ to the same set and x_t to the other set, then $\tilde{u}_t$ can be chosen to satisfy

condition (25) for constraints (17). Similar choices can be done if some of the variables $\tilde{v}_t$, $\tilde{w}_{t+1}$, x_t, $\tilde{u}_t$ do not belong to J and the claim follows. **End of Claim 1.**

Then we define the polyhedron $\tilde{Q}$ by adding to the linear system defining P the following inequalities:

$$p_t^v \leq (SU - \underline{P})\tilde{v}_t \quad t \in [2, T-1] \tag{26}$$
$$p_t^x \leq (SD - \underline{P})x_t \quad t \in [2, T-1] \tag{27}$$
$$p_t^w \leq (SD - \underline{P})\tilde{w}_{t+1} \quad t \in [2, T-1] \tag{28}$$
$$p_t^u \leq (\overline{P} - \underline{P})\tilde{u}_t \quad t \in [2, T] \tag{29}$$
$$p_T^v \leq (SU - \underline{P})v_T \tag{30}$$
$$p_1 \leq (\overline{P} - \underline{P})u_1 - (\overline{P} - SD)w_2 \tag{31}$$

where p^v, p^x, p^w, p^u and p_1 are non-negative variables.

Claim 2. The polyhedron $\tilde{Q}$ is integral with respect to variables u, v, w, x, $\tilde{u}$, $\tilde{v}$, $\tilde{w}$. **End of Claim 2.**

The proof of Claim 2 is a direct application of Lemma 7 to the polyhedron P of Claim 1.

Then we define the polyhedron Q by adding to the linear system defining $\tilde{Q}$ the following inequalities

$$p_t = p_t^v + p_t^x + p_t^w + p_t^u \qquad t \in [2, \ldots, T-1] \tag{32}$$
$$p_T = p_T^v + p_T^u \tag{33}$$

where p_t for $t \in [2 \ldots T]$ are non-negative variables.

Claim 3. The polyhedron Q is integral with respect to variables u, v, w, x, $\tilde{u}$, $\tilde{v}$, $\tilde{w}$. **End of Claim 3.**

Claim 3 follows from Claim 2 and by the straightforward extension of Lemma 7, where the role of P is played by the integral polyhedron $\tilde{Q}$.

Finally we prove that

Claim 4. The projection of Q onto the space of the variables u, v, p is equivalent to $\overline{D}_T$.

Proof of Claim 4. We start by eliminating the variables p_t^v, p_t^x, p_t^w, and p_t^u by simply substituting constraints (32)-(33) with the following:

$$\begin{aligned} p_t \leq & (SU - \underline{P})\tilde{v}_t + (SD - \underline{P})x_t + \\ & + (SD - \underline{P})\tilde{w}_{t+1} + (\overline{P} - \underline{P})\tilde{u}_t \qquad t \in [2, T-1] \end{aligned} \tag{34}$$
$$p_T \leq (SU - \underline{P})v_T + (\overline{P} - \underline{P})\tilde{u}_T, \tag{35}$$

which are obtained by using constraints (26)-(30).

Now, we replace $\tilde{u}_T$ from (18) in (35) to obtain:

$$p_T \leq \left(\overline{P} - \underline{P}\right) u_T - \left(\overline{P} - SU\right) v_T \tag{36}$$

then we eliminate variables in (34) according to the following order

- $\tilde{u}_t$ by using the equation (17);

- $\tilde{w}_{t+1}$ by using the equation (15);
- $\tilde{v}_t$ by using the equation (16).

It is not difficult to see that for $t \in [2, T-1]$ we obtain the following constraints:

$$\begin{aligned} p_t \leq & (\overline{P} - \underline{P})u_t - (\overline{P} - SU)v_t \\ & - (\overline{P} - SD)w_{t+1} + (\overline{P} - SU)x_t && (37) \\ x_t \geq & 0 && (38) \\ x_t \geq & v_t + w_{t+1} - u_t && (39) \\ x_t \leq & v_t && (40) \\ x_t \leq & w_{t+1}. && (41) \end{aligned}$$

Now we can apply Fourier-Motzkin elimination to variables x_t by considering the following pairs of constraints:

- by constraints (40) and (37) we obtain

$$p_t \leq (\overline{P} - \underline{P})u_t - (\overline{P} - SD)w_{t+1}; \quad (42)$$

- by constraints (40) and (38) we obtain $v_t \geq 0$;
- by constraints (40) and (39) we obtain

$$w_{t+1} \leq u_t; \quad (43)$$

- by constraints (41) and (37) we obtain

$$p_t \leq (\overline{P} - \underline{P})u_t - (\overline{P} - SU)v_t - (SU - SD)w_{t+1}; \quad (44)$$

- by constraints (41) and (38) we obtain $w_{t+1} \geq 0$;
- by constraints (41) and (39) we obtain $u_t \geq v_t$.

By using equation (14), $w_{t+1} \leq u_t$ is equivalent to $v_{t+1} \leq u_{t+1}$, which is one of the inequalities (12). We can simply see that the new constraints (42) and (44) coincide with constraints (4) and (5) for the case $SU \geq SD$, respectively; and constraints (31) and (36) coincide with constraints (1) and (3), respectively. **End of Claim 4.**

From Claim 4 it follows that $\overline{D}_T$ is integral with respect to the variables u and v. The proof for $SD \geq SU$ can be performed in a symmetric way.

□

5. Numerical Results

To illustrate the computational performance of the Tight and Compact formulation proposed in this paper, the self-UC problem for a price-taker producer is solved for different time spans. The goal of a price-taker producer is to maximize his profit during the planning horizon (which is the difference between the revenue and the total operating

Table 1: Generator Data

Gen	Technical Information							Cost Coefficients†		
	$\overline{P}$ [MW]	$\underline{P}$ [MW]	TU/TD [h]	SU [MW]	SD [MW]	p_0* [MW/h]	$\text{Ste}_0\star$ [h]	C^{NL} [$/h]	C^{LV} [$/MWh]	C^{SU} [$]
1	455	150	8	252	303	150	8	1000	16.19	9000
2	455	150	8	252	303	150	8	970	17.26	10000
3	130	20	5	57	75	20	5	700	16.60	1100
4	130	20	5	57	75	20	5	680	16.50	1120
5	162	25	6	71	94	25	6	450	19.70	1800
6	80	20	3	40	50	20	3	370	22.26	340
7	85	25	3	45	55	25	3	480	27.74	520
8	55	10	1	25	33	10	1	660	25.92	60
9	55	10	1	25	33	10	1	665	27.27	60
10	55	10	1	25	33	10	1	670	27.79	60

* p_0 is the unit's initial production prior to the first period of the time span.

$\star\text{Ste}_0$ is the number of hours that the unit has been online prior to the first period of the time span.

†C^{NL}, C^{LV} and C^{SU} stand for non-load, linear-variable and startup costs, respectively.

Table 2: Energy Price ($/MWh)

$t = 1 \dots 12 \rightarrow$	13.0	7.2	4.6	3.3	3.9	5.9	9.8	15.0	22.1	31.3	33.2	24.8
$t = 13 \dots 24 \rightarrow$	19.5	16.3	14.3	13.7	15.0	17.6	20.2	29.3	49.5	53.4	30.0	20.2

cost [8]). The self-UC is also associated with the scheduling problem of a single generation unit [2], which arises when solving UC with decomposition methods such as Lagrangian Relaxation [3]. The 10-unit system data is presented in Table 1 and the energy prices are shown in Table 2. The power system data are based on information presented in [1, 7]. All tests were carried out using CPLEX 12.5 on an Intel-i7 3.4-GHz personal computer with 8 GB of RAM memory. The problems are solved until they hit the time limit of 10000 seconds or until they reach optimality (more precisely to 10^{-6} of relative optimality tolerance).

The formulation presented in this paper, labelled as *TC*, is compared with the previous Tight and Compact formulation presented in [7], labelled as *TC0,* and with those in [1] and [11], labelled as *1bin* and *3bin*, respectively.

Table 3 shows the computational performance for four cases with different time spans.

Table 3: Computational Performance Comparison

Case	Optimum	IntGap (%)				LP time (s)				MIP time (s)*				Nodes			
(days)	(M$)	*TC*	*TC0*	*3bin*	*1bin*	*TC*	*TC0*	*3bin*	*1bin*	*TC*	*TC0*	*3bin*	*1bin*	*TC*	*TC0*	*3bin*	*1bin*
64	7.259361	0	0.09	0.88	2.57	0.57	0.47	0.80	0.95	0.57	1.92	12.01	13.79	0	0	496	487
128	14.517096	0	0.09	0.87	2.57	1.17	1.20	2.06	2.60	1.17	4.81	45.54	(3.33E-4)	0	0	528	603915
256	29.032567	0	0.09	0.87	2.57	3.16	3.29	5.38	6.88	3.16	7.75	199.18	(5.21E-4)	0	0	533	229035
512	58.063509	0	0.09	0.87	2.57	8.08	8.39	14.29	18.83	8.08	17.29	734.03	(5.35E-4)	0	0	488	136128

* If the time limit is reached then the final optimality tolerance is shown between parentheses

Table 4: Problem Size Comparison

Case	# constraints			# nonzero elements				# real var		# binary var	
(days)	*TC**	*3bin*	*1bin*	*TC*	*TC0*	*3bin*	*1bin*	*TC*†	*1bin*	*TC*†	*1bin*
64	65997	107459	138225	338994	334389	417313	469719	15360	46080	46080	15360
128	132045	214979	276465	678450	669237	835105	939735	30720	92160	92160	30720
256	264141	430019	552945	1357362	1338933	1670689	1879767	61440	184320	184320	61440
512	528333	860099	1105905	2715186	2678325	3341857	3759831	12288	368640	368640	122880

* *TC* is equal to *TC0* for these cases

†*TC*, *TC0* and *3bin* are equal for these cases

All formulations achieve the same MIP optimum since all of them model the same MIP problem. However, they present different LP optimums, the relative distance between their MIP and LP optimums is measured with the Integrality Gap [13, 7]. Note that the MIP optimums of *TC* were achieved by just solving the LP over (1)-(11), IntGap$=0$, hence solving the problems in LP time. On the other hand, as usual, the branch-and-cut method was needed to solve the MIP for *TC0*, *3bin* and *1bin*. Table 3 also shows the MIP time and nodes explored that were required by the different formulations to reach optimality. It is interesting to note that although *TC0* reached optimality exploring zero nodes, *TC0* needed to make use of the solver's cutting planes strategy because the relaxed LP solution did not achieve the integer one, IntGap$\neq 0$ (the solver used 227 and 1224 cuts for the smallest and largest case, respectively). This tightening process took more time than the time required to solve the initial LP relaxation, that is why the MIP time for *TC0* is more than twice its LP relaxation time.

Table 4 shows the dimensions for all of the formulations for four selected instances. Note that *TC* and *TC0* are more compact, in terms of quantity of constraints and nonzero elements, than *3bin* and *1bin*. The formulation *1bin* presents a third of binary variables in comparison with the other formulations, but 3 times more continuous variables. This is because the work in [1] reformulated the units' operation model to avoid the startup and shutdown binary variables, claiming that this would reduce the node enumeration in the branch-and-bound process. Note however that this reformulation considerable damaged the strength of *1bin*, hence it presented the worst computational performance, similar results are obtained in [11, 7]. The formulation *1bin* presents more continuous variables than the other formulations because it requires the introduction of new continuous variables to model the startup and shutdown costs of generating units.

In conclusion, *TC* presents a dramatic improvement in computation in comparison with *3bin* and *1bin* due to its tightness (speedups above 90x and 8500x, respectively); and it also presents a lower LP burden due to its compactness, see Table 4. Compared with *TC0*, the formulation *TC* is tighter; consequently, *TC* requires less time to solve the MIP problem (speedup above 4.1x).

6. Conclusion

This paper presented the convex hull description of the basic constraints of generating units for unit commitment (UC) problems. These constraints are: generation limits, startup and shutdown capabilities, and minimum up and down times. The model does

not include some crucial constraints, such as ramping, but the proposed constraints can be used as the core of any UC formulation and they can help to tighten the final UC model. Finally, different case studies for a self-UC were solved as LP obtaining MIP solutions; if compared with three other formulations, the same optimal results were obtained but significantly faster.

Acknowledgments

The authors thank Laurence Wolsey, Santanu Dey, Antonio Frangioni, and Paolo Ventura for useful discussions on the paper.

References

[1] Carrion, M., Arroyo, J., 2006. A computationally efficient mixed-integer linear formulation for the thermal unit commitment problem. IEEE Transactions on Power Systems 21 (3), 1371–1378.

[2] Frangioni, A., Gentile, C., Aug. 2006. Solving nonlinear single-unit commitment problems with ramping constraints. Operations Research 54 (4), 767–775.

[3] Frangioni, A., Gentile, C., Lacalandra, F., Jun. 2008. Solving unit commitment problems with general ramp constraints. International Journal of Electrical Power & Energy Systems 30 (5), 316–326.
URL http://www.sciencedirect.com/science/article/pii/S0142061507001160

[4] Frangioni, A., Gentile, C., Lacalandra, F., Feb. 2009. Tighter approximated MILP formulations for unit commitment problems. IEEE Transactions on Power Systems 24 (1), 105–113.

[5] Lee, J., Leung, J., Margot, F., Jun. 2004. Min-up/min-down polytopes. Discrete Optimization 1 (1), 77–85.

[6] Malkin, P., 2003. Minimum runtime and stoptime polyhedra. manuscript.

[7] Morales-Espana, G., Latorre, J., Ramos, A., Nov. 2013. Tight and compact MILP formulation for the thermal unit commitment problem. IEEE Transactions on Power Systems 28 (4), 4897–4908.

[8] Morales-Espana, G., Latorre, J. M., Ramos, A., 2013. Tight and compact MILP formulation of start-up and shut-down ramping in unit commitment. IEEE Transactions on Power Systems 28 (2), 1288–1296.

[9] Morales-Espana, G., Ramos, A., Garcia-Gonzalez, J., 2014. An MIP formulation for joint market-clearing of energy and reserves based on ramp scheduling. IEEE Transactions on Power Systems 29 (1), 476–488.

[10] Nemhauser, G. L., Wolsey, L. A., 1999. Integer and combinatorial optimization. John Wiley and Sons, New York.

[11] Ostrowski, J., Anjos, M. F., Vannelli, A., Feb. 2012. Tight mixed integer linear programming formulations for the unit commitment problem. IEEE Transactions on Power Systems 27 (1), 39–46.

[12] Rajan, D., Takriti, S., Jun. 2005. Minimum Up/Down polytopes of the unit commitment problem with start-up costs. Research Report RC23628, IBM.
URL http://domino.research.ibm.com/library/cyberdig.nsf/1e4115aea78b6e7c85256b360066f0d4/cdcb02a7c809d89e8525702300502ac0?OpenDocument

[13] Williams, H. P., Feb. 2013. Model Building in Mathematical Programming, 5th Edition. John Wiley & Sons Inc.

[14] Wolsey, L., 1998. Integer Programming. Wiley-Interscience.

Article V

G. Morales-Espana, C. Gentile, and A. Ramos, "Tight MIP Formulations of the Power-Based Unit Commitment Problem," *Optimization Letters*, 2014, paper under review (Manuscript ID: OPTL-D-14-00276R1). JCR 2012 data: impact factor 1.654 and 5-year impact factor 1.602.

Additional Material: With the help of PORTA [30], all vertices of the polytope described in this paper were computed for different time spans and different set of parameters. As expected, since the proposed polytope describes a convex hull, it only contains integer vertices for all the cases. The complete set of experiments that were carried out can be found in goo.gl/wGNNnw.

Working Paper manuscript No.
(will be inserted by the editor)

Tight MIP Formulations of the Power-Based Unit Commitment Problem

Germán Morales-España · Claudio Gentile · Andres Ramos

Last update: 2014-05-26

Abstract This paper provides the convex hull description for the basic operation of slow- and quick-start units in power-based unit commitment (UC) problems. The basic operating constraints that are modelled for both types of units are: 1) generation limits and 2) minimum up and down times. Apart from this, the startup and shutdown processes are also modelled, using 3) startup and shutdown power trajectories for slow-start units, and 4) startup and shutdown capabilities for quick-start units. In the conventional UC problem, power schedules are used to represent the staircase energy schedule; however, this simplification leads to infeasible energy delivery, as stated in the literature. To overcome this drawback, this paper provides a power-based UC formulation drawing a clear distinction between power and energy. The proposed constraints can be used as the core of any power-based UC formulation, thus tightening the final mixed-integer programming UC problem. We provide evidence that dramatic improvements in computational time are obtained by solving a self-UC problem for different case studies.

Keywords Convex Hull · Unit Commitment (UC) · Mixed-Integer Programming (MIP) · Tight Formulation · Slow-Start units · Quick-Start Units

1 Introduction

The short-term Unit Commitment (UC) problem is one of the critical tasks that is daily performed by different actors in the electricity sector. [5]Depending on the purpose, the UC is solved under centralized or competitive environments, from self-scheduling to centralized auction-based market clearing, over a time horizon ranging from one day to one week.

Conventional UC formulations do not represent the unit operation adequately, because they fail to guarantee that the resulting energy schedules can be delivered [6,8]. To illustrate this problem, consider the following scheduling example for one generating unit. This example assumes that the minimum and maximum generation outputs of the unit are 100 MW and 300 MW, respectively, and that the unit can ramp up from the minimum to the maximum output in one hour. As shown in Figure 1a, if the unit has been producing 100 MW during the first hour then the unit can produce at its maximum output (300 MW) for the next hour. This would be a natural energy schedule resulting from the traditional UC formulations, which are based on the energy scheduling approach. However, the unit is just physically capable to reach its maximum output before the end of the second hour due to its limited ramp rate, as shown in Figure 1b.

The work of G. Morales-España was supported by the European Commission through an Erasmus Mundus Ph.D. Fellowship. The work of C. Gentile was partially supported by the project MINO grant no. 316647 Initial Training Network of the "Marie Curie" program funded by the European Union.

G. Morales-España
Institute for Research in Technology (IIT) of the School of Engineering (ICAI), Universidad Pontificia Comillas, Madrid, Spain
E-mail: german.morales@iit.upcomillas.es; gmorales@kth.se

C. Gentile
Istituto di Analisi dei Sistemi ed Informatica "A. Ruberti", C.N.R., Viale Manzoni 30, 00185 Roma, Italy
E-mail: gentile@iasi.cnr.it

A. Ramos
Institute for Research in Technology (IIT) of the School of Engineering (ICAI), Universidad Pontificia Comillas, Madrid, Spain
E-mail: andres.ramos@upcomillas.es

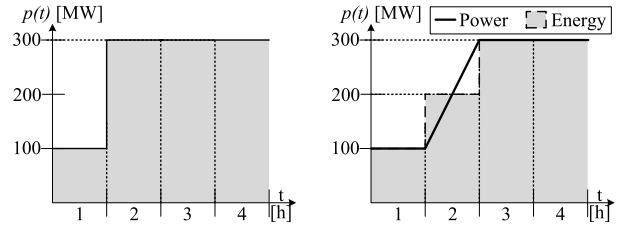

(a) Traditional Energy Schedule (b) Actual Deployment

Figure 1: Scheduling vs. Deployment

Consequently, the solution obtained in Figure 1a is not feasible. In fact, the unit requires an infinite ramping capability to be able to reproduce the energy schedule presented in Figure 1a.

Another drawback of conventional UC formulations is that generating units are assumed to start/end their production at their minimum output. That is, their intrinsic startup and shutdown power trajectories are ignored. As a consequence, there is a high amount of energy that is not allocated by UC but it is inherently present in real time, thus causing a negative economic impact [10]. For further details of the drawbacks of conventional UC scheduling approaches, the reader is referred to [8,11] and references therein.

Developing more accurate models would be pointless if they cannot be solved fast enough. Under the mixed integer programming (MIP) approach, it is important to develop tight formulations to reduce the UC computational burden. This allows the implementation of more advanced and computationally demanding problems. Different set of constraints have been proposed to tighten the UC problem [7,13,12,10,9,5]. The work in [7,13] formulate the convex hull of the minimum up and down times. Cuts to tighten ramping limits are presented in [12]. A tighter approximation for quadratic generation costs is proposed [4]. Simultaneously tight and compact MIP formulations for thermal units operation are devised in [10,9,5].

To overcome the drawbacks of conventional UC formulations, the model proposed in this paper draws a clear difference between power and energy, and it also takes into account the normally neglected power trajectories that occur during the startup and shutdown processes. Thus adequately representing the operation of generating units to efficiently exploit their flexibility and avoiding infeasible energy delivery. This paper further improves the work in [10] by including the operation of quick-start units and providing the convex hull description for the following set of constraints: generation limits, minimum up and down times, startup and shutdown power trajectories for slow-start units, and startup and shutdown capabilities for quick-start units. Although the model does not consider some crucial constraints, such as ramping, the proposed constraints can be used as the core of any power-based UC formulation, thus tightening the final UC model. In addition, different case studies for a self-UC were solved as a linear program (LP) obtaining feasible MIP solutions; thus solving the MIP problem significantly faster when compared with two other traditional UC formulations.

The remainder of this paper is organized as follows. Section 2 introduces the main nomenclature used in this paper. Section 3 details the operating constraints of a single slow- and quick-start unit. In Section 4, we provide a convex hull proof for the power-based UC including the constraints above cited. Section 5 provides and discusses results from several case studies, where a computational performance comparison with other two traditional UC formulations is made. Finally, some relevant conclusions are drawn in Section 6.

2 Nomenclature

Here we introduce the main notation used in this paper. Lowercase letters are used to denote variables and indexes. Uppercase letters denote parameters.

2.1 Definitions

In this paper, we use the terminology introduced in [10] to reference the different unit operation states, see Figure 2.

online	the unit is synchronized with the system.
offline	the unit is not synchronized with the system.
up	the unit is producing above its minimum output. During the *up* state, the unit output is controllable.

down the unit is producing below its minimum output, when *offline, s*tarting up or shutting down.

2.2 Indexes

t Time periods, running from 1 to T hours.

2.3 Unit's Technical Parameters

C^{LV} Linear variable cost [$/MWh].
C^{NL} No-load cost [$/h].
C^{SD} Shutdown cost [$].
C^{SU} Startup cost [$].
$\overline{P}$ Maximum power output [MW].
$\underline{P}$ Minimum power output [MW].
P_i^{SD} Power output at the beginning of the i^{th} interval of the shutdown ramp process [MW], see Figure 2.
P_i^{SU} Power output at the beginning of the i^{th} interval of the startup ramp process [MW], see Figure 2.
SD Shutdown capability [MW], see Figure 3.
SU Startup capability [MW], see Figure 3.
SD^{D} Duration of the shut-down process [h], see Figure 2.
SU^{D} Duration of the start-up process [h], see Figure 2.
TD Minimum down time [h].
TU Minimum up time [h].

2.4 Continuous Decision Variables

e_t Total energy production during period t [MWh].
p_t Power output at the end of period t, production above the minimum output $\underline{P}$ [MW].
$\widehat{p}_t$ Total power output schedule at the end of hour, including startup and shutdown power trajectories [MW].

2.5 Binary Decision Variables

u_t Commitment status of the unit for period t, which is equal to 1 if the unit is up and 0 if it is down, see Figure 2.
v_t Startup status of the unit, which takes the value of 1 if the unit starts up in period t and 0 otherwise, see Figure 2.
w_t Shutdown status of the unit, which takes the value of 1 if the unit shuts down in period t and 0 otherwise, see Figure 2.

3 Modelling the Unit's Operation

The constraints presented here are a further extension of our previous work in [10]. Here we generalize the formulation by considering quick-start units.

The quick-start units are defined as those that can ramp up (down) from 0 (more than $\underline{P}$ and up to SD) to more than $\underline{P}$ and up to SU (0) within one period, typically one hour, as shown in Figure 3. The slow-start units are defined as those units that require more than one period to ramp up (down) from 0 ($\underline{P}$) to $\underline{P}$ (0), see Figure 2.

The up and down states are distinguished from the online and offline states. Figure 2 shows the different operation states of a thermal unit, as defined in Section 2. During the up period ($u_t = 1$), the unit has the flexibility to follow any power trajectory being bounded between the maximum and minimum output. On the other hand, for slow-start units, the power output follows a predefined power trajectory when the unit is starting up or shutting down. The startup and shutdown power trajectories for quick-start units are defined by the startup and shutdown capabilities, see Figure 3.

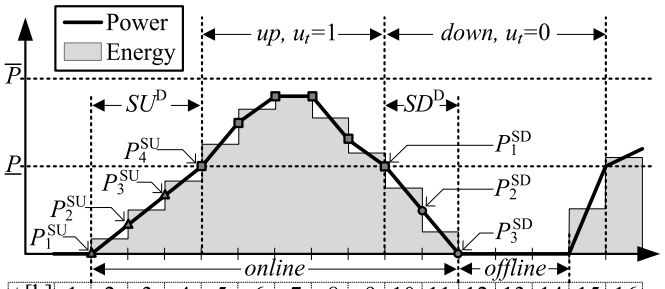

t [h]	1	2	3	4	5	6	7	8	9	10	11	12	13	14	15	16
u_t	0	0	0	0	1	1	1	1	1	0	0	0	0	0	0	1
v_t	0	0	0	0	1	0	0	0	0	0	0	0	0	0	0	1
w_t	0	0	0	0	0	0	0	0	0	1	0	0	0	0	0	0

Figure 2: Operating states including start-up and shut-down power trajectories for slow-start units

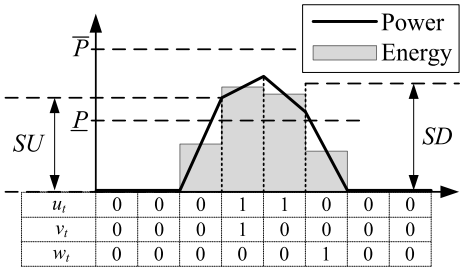

u_t	0	0	0	1	1	0	0	0
v_t	0	0	0	1	0	0	0	0
w_t	0	0	0	0	0	1	0	0

Figure 3: Startup and shutdown capabilities for quick-start units

This section first presents the basic operating constraints that applies for both slow- and quick-start units. However, the total unit's production output is different for each of them. Section 3.2 and Section 3.3 show how to obtain the total production, power and energy, for slow- and quick-start generating units, respectively.

3.1 Basic Operating Constraints

The unit's generation limits taking into account startup SU and shutdown SD capabilities, which are $SU, SD \geq \underline{P}$ by definition, are set as follows, see Figure 3:

$$\begin{aligned} p_t \leq & \left(\overline{P} - \underline{P}\right) u_t - \left(\overline{P} - SD\right) w_{t+1} \\ & + \left(SU - \underline{P}\right) v_{t+1} \qquad t \in [1, T-1] \end{aligned} \tag{1}$$

$$p_T \leq \left(\overline{P} - \underline{P}\right) u_T \tag{2}$$

$$p_t \geq 0 \qquad \forall t \tag{3}$$

and the logical relationship between the decision variables u_t, v_t and w_t; and the minimum uptime TU and downtime TD limits are ensured with

$$u_t - u_{t-1} = v_t - w_t \qquad \forall t \in [2, T] \tag{4}$$

$$\sum_{i=t-TU+1}^{t} v_i \leq u_t \qquad \forall t \in [TU+1, T] \tag{5}$$

$$\sum_{i=t-TD+1}^{t} w_i \leq 1 - u_t \qquad \forall t \in [TD+1, T] \tag{6}$$

$$0 \leq u_t \leq 1 \qquad \forall t \tag{7}$$

$$0 \leq v_t \leq 1, \quad 0 \leq w_t \leq 1 \qquad \forall t \in [2, T] \tag{8}$$

where (4)-(6) describe the convex hull formulation of the minimum-up and -down time constraints proposed in [13].

3.2 Slow-Start Units

The slow-start units are assumed to produce $\underline{P}$ at the beginning and at the end of the up state, see Figure 2. At those points the startup and shutdown power trajectories are as shown in Figure 2. Consequently, constraints (1)-(8) describe the operation of slow-start units during the up state when $SU, SD = \underline{P}$.

Be aware that the minimum down time TD is function of the minimum offline time, i.e., TD is equal the startup and shutdown duration processes ($SU^{\mathrm{D}} + SD^{\mathrm{D}}$) plus the minimum offline time of the unit. This then avoids the possible overlapping between the startup and shutdown trajectories. That is, constraint (6) ensures that the unit is down ($u_t = 0$) for enough time to fit the unit's startup and shutdown power trajectories.

As presented in [10], the total power output including the startup and shutdown power trajectories for slow-start units is obtained with

$$\widehat{p}_t = \underbrace{\sum_{i=1}^{SU^{\mathrm{D}}} P_i^{\mathrm{SU}} v_{t-i+SU^{\mathrm{D}}+2}}_{\text{(iii) SU trajectory}} + \underbrace{\sum_{i=2}^{SD^{\mathrm{D}}+1} P_i^{\mathrm{SD}} w_{t-i+2}}_{\text{(ii) SD trajectory}} + \underbrace{\underline{P}\,(u_t + v_{t+1}) + p_t}_{\text{(i) Output when being } up} \qquad \forall t \tag{9}$$

For a better understanding of (9), we can analyse how the power trajectory example in Figure 2 is obtained from the three different parts in (9):

1. Output when the unit is *up*: Although the unit is *up* for five consecutive hours, there are six total power values that are greater than or equal to $\underline{P}$, from $\widehat{p}_4$ to $\widehat{p}_9$ (see the squares in Figure 2). When $t{=}4$, the term v_{t+1} in (i) becomes v_5 ensuring (the first) $\underline{P}$ at the beginning of the *up* period, and the term u_t adds (the remaining five) $\underline{P}$ for $t = 5 \dots 9$. In addition, p_t adds the power production above $\underline{P}$.
2. Shutdown power trajectory: This process lasts for two hours, $SD^{\mathrm{D}}{=}2$; then, the summation term (ii) becomes $P_2^{\mathrm{SD}} w_t + P_3^{\mathrm{SD}} w_{t-1}$, which is equal to P_2^{SD} for $t{=}10$ and P_3^{SD} for $t{=}11$, being zero otherwise. This provides the shutdown power trajectory (see the circles in Figure 2).
3. Startup power trajectory: the startup power trajectory can be obtained using a procedure similar to that used in 2) (see the triangles in Figure 2).

Similarly to (9), the total energy production for slow-start units is given by

$$e_t = \underline{P} \cdot u_t + \frac{p_t + p_{t-1}}{2} + \sum_{i=1}^{SD^{\mathrm{D}}} \frac{P_{i+1}^{\mathrm{SD}} + P_i^{\mathrm{SD}}}{2} w_{t-i+1} + \sum_{i=1}^{SU^{\mathrm{D}}} \frac{P_{i+1}^{\mathrm{SU}} + P_i^{\mathrm{SU}}}{2} v_{t-i+SU^{\mathrm{D}}+1} \qquad \forall t \tag{10}$$

3.3 Quick-Start Units

The total power for a quick-start unit is given by

$$\widehat{p}_t = \underline{P}\,(u_t + v_{t+1}) + p_t \qquad \forall t \tag{11}$$

and the total energy production is

$$e_t = \frac{\underline{P}\,(2u_t + v_{t+1} + w_t) + p_{t-1} + p_t}{2} \qquad \forall t \tag{12}$$

It is interesting to note that even though $SU, SD \geq \underline{P}$ (by definition), the resulting energy from (12) may take values below $\underline{P}$ during the startup and shutdown processes, see Figure 3.

The energy for slow- and quick-start units can also be obtained in function of the total power output $\widehat{p}_t$, $e_t = \frac{\widehat{p}_t + \widehat{p}_{t-1}}{2}$ for all t. Bear in mind however that sometimes only the total power, (9) and (11), or the total energy, (10) and (12), production is needed as a function of p, u, v, w.

Notice that (9)-(12) are defined for all t and they use variables that are outside the scheduling horizon $[1, T]$. Those variables are considered to be equal to zero when their subindex is $t < 1$ or $t > T$.

In summary, constraints (1)-(8), when $SU, SD = \underline{P}$, together with (9) and (10) describe the technical operation of slow-start units. Constraints (1)-(8) together with (11) and (12) describe the technical operation of quick-start units.

3.4 Total Unit Operation Cost

The objective function of any UC problem involves the total unit operation costs of each generating unit c_t, which is defined as follows

$$c_t = C^{\mathrm{NL}} u_t + C^{\mathrm{LV}} e_t + C^{\mathrm{SU}'} v_t + C^{\mathrm{SD}'} w_t \tag{13}$$

Note that the no-load cost (C^{NL}) considered in (13) ignores the startup and shutdown periods. This is because the C^{NL} only multiplies the commitment during the up state u_t. In order to consider the no-load cost during the startup & shutdown periods, $C^{\mathrm{SU}'}$ and $C^{\mathrm{SD}'}$ are introduced in (13) and defined as:

$$C^{\mathrm{SU}'} = C^{\mathrm{SU}} + C^{\mathrm{NL}} SU^{\mathrm{D}} \tag{13a}$$

$$C^{\mathrm{SD}'} = C^{\mathrm{SD}} + C^{\mathrm{NL}} SD^{\mathrm{D}} \tag{13b}$$

where $SU^{\mathrm{D}}, SD^{\mathrm{D}} = 1$ for quick-start units, see Figure 3.

4 Convex Hull Proof

In this section we first prove that inequalities (1)-(3) are facet defining and then that inequalities (1)-(8) define an integral polytope. Finally, we also prove that inequalities describing the operation of slow-start units, (1)-(8) together with equalities (9)-(10), define an integral polytope. Similarly, inequalities describing the operation of quick-start units, (1)-(8) together with equalities (11)-(12), also define an integral polytope.

Note that the variables w_t are completely determined in terms of u_t and v_t using (4). Therefore, in the following we eliminate variables w_t and assume that constraints (1), (6), and (8) are reformulated accordingly.

Definition 1 Let $\overline{D}_T\left(TU, TD, \overline{P}, \underline{P}, SU, SD\right) = \left\{(u, v, p) \in \mathbb{R}_+^{3T-1} | \, (u, v, p) \text{ satisfy (1)-(8)}\right\}$. Let $\overline{C}_T\left(TU, TD, \overline{P}, \underline{P}, SU, SD\right)$ be the convex hull of the points in $\overline{D}_T\left(TU, TD, \overline{P}, \underline{P}, SU, SD\right)$ such that $u \in \{0,1\}^T$, $v \in \{0,1\}^{T-1}$.

For short, we denote $\overline{C}_T\left(TU, TD, \overline{P}, \underline{P}, SU, SD\right)$ by $\overline{C}_T$ and $\overline{D}_T\left(TU, TD, \overline{P}, \underline{P}, SU, SD\right)$ by $\overline{D}_T$.

For easy exposition, we introduce the points $x^i, y^i, z^i \in \overline{C}_T$, as shown in Figure 4. We also introduce the parameters U, D and P which are equivalent to $U = SU - \underline{P}$, $D = SD - \underline{P}$ and $P = \overline{P} - \underline{P}$, respectively.

Proposition 1 $\overline{C}_T$ is full-dimensional in terms of u, v and p.

Proof From Figure 4, it can be easily shown that the $3T$ points x^i, y^i and z^i for $i \in [1, T]$ are affinely independent when $g_t, g^T = 0$, $g_t^y = P$ and $g_t^z = U$. Note that in case $D = 0$ the point $y^{(1)}$ must be removed and the point $y^{(T+1)}$ added, thus keeping the $3T$ affinely independent points. This applies for all the following proofs; but for the sake of brevity, we assume from now on that $D \neq 0$. □

Theorem 1 *The inequalities in* (1) *describe facets of the polytope* $\overline{C}_T$.

Proof We show that (1) describe facets of $\overline{C}_T$ by the direct method [15]. We do so by presenting $3T - 1$ affinely independent points in $\overline{C}_T$ that are tight (satisfy as an equality) for the given inequality. Note in Figure 4 that the point z^T (the origin) satisfies (1)-(3) as equality. Therefore, to get $3T - 1$ affinely independent points, we need only $3T - 2$ other linearly independent points.

The following $3T - 2$ points are linearly independent and tight for (1) when $g^T = 0$, $g_t, g_t^y = P$ and $g_t^z = U$: $T - 1$ points x^i for $i \in [1, t-1] \cup [t+1, T]$, T points y^i for $i \in [1, T]$, and $T - 1$ points z^i for $i \in [1, T-1]$. □

Theorem 2 *The inequality* (2) *describe a facet of the polytope* $\overline{C}_T$.

	u_1	u_2	$\cdots$	u_{t-1}	u_t	u_{t+1}	$\cdots$	u_{T-1}	u_T	p_1	p_2	$\cdots$	p_{t-1}	p_t	p_{t+1}	$\cdots$	p_{T-1}	p_T	v_2	$\cdots$	v_{t-1}	v_t	v_{t+1}	$\cdots$	v_{T-1}	v_T	w_2	$\cdots$	w_{t-1}	w_t	w_{t+1}	$\cdots$	w_{T-1}	w_T
$x^{(1)}$	(1	0	$\cdots$	0	0	0	$\cdots$	0	0)	0	0	$\cdots$	0	0	0	$\cdots$	0	0)	0	$\cdots$	0	0	0	$\cdots$	0	0)	1	$\cdots$	0	0	0	$\cdots$	0	0)
$x^{(2)}$	(1	1	$\cdots$	0	0	0	$\cdots$	0	0)	0	0	$\cdots$	0	0	0	$\cdots$	0	0)	0	$\cdots$	0	0	0	$\cdots$	0	0)	0	$\cdots$	0	0	0	$\cdots$	0	0)
$\vdots$	$\vdots$	$\vdots$	$\ddots$	$\vdots$	$\vdots$	$\vdots$	$\ddots$	$\vdots$	$\vdots$	$\vdots$	$\vdots$	$\ddots$	$\vdots$	$\vdots$	$\vdots$	$\ddots$	$\vdots$	$\vdots$	$\vdots$	$\ddots$	$\vdots$	$\vdots$	$\vdots$	$\ddots$	$\vdots$	$\vdots$	$\vdots$	$\ddots$	$\vdots$	$\vdots$	$\vdots$	$\ddots$	$\vdots$	$\vdots$
$x^{(t-1)}$	(1	1	$\cdots$	1	0	0	$\cdots$	0	0)	0	0	$\cdots$	0	0	0	$\cdots$	0	0)	0	$\cdots$	0	0	0	$\cdots$	0	0)	0	$\cdots$	0	1	0	$\cdots$	0	0)
$x^{(t)}$	(1	1	$\cdots$	1	1	0	$\cdots$	0	0)	0	0	$\cdots$	0	0	0	$\cdots$	0	0)	0	$\cdots$	0	0	0	$\cdots$	0	0)	0	$\cdots$	0	0	1	$\cdots$	0	0)
$x^{(t+1)}$	(1	1	$\cdots$	1	1	1	$\cdots$	0	0)	0	0	$\cdots$	0	g_t	0	$\cdots$	0	0)	0	$\cdots$	0	0	0	$\cdots$	0	0)	0	$\cdots$	0	0	0	$\cdots$	0	0)
$\vdots$	$\vdots$	$\vdots$	$\ddots$	$\vdots$	$\vdots$	$\vdots$	$\ddots$	$\vdots$	$\vdots$	$\vdots$	$\vdots$	$\ddots$	$\vdots$	$\vdots$	$\vdots$	$\ddots$	$\vdots$	$\vdots$	$\vdots$	$\ddots$	$\vdots$	$\vdots$	$\vdots$	$\ddots$	$\vdots$	$\vdots$	$\vdots$	$\ddots$	$\vdots$	$\vdots$	$\vdots$	$\ddots$	$\vdots$	$\vdots$
$x^{(T-1)}$	(1	1	$\cdots$	1	1	1	$\cdots$	1	0)	0	0	$\cdots$	0	g_t	0	$\cdots$	0	0)	0	$\cdots$	0	0	0	$\cdots$	0	0)	0	$\cdots$	0	0	0	$\cdots$	0	1)
$x^{(T)}$	(1	1	$\cdots$	1	1	1	$\cdots$	1	1)	0	0	$\cdots$	0	g_t	0	$\cdots$	0	g^T	0	$\cdots$	0	0	0	$\cdots$	0	0)	0	$\cdots$	0	0	0	$\cdots$	0	0)
$y^{(1)}$	(1	0	$\cdots$	0	0	0	$\cdots$	0	0)	D	0	$\cdots$	0	0	0	$\cdots$	0	0)	0	$\cdots$	0	0	0	$\cdots$	0	0)	1	$\cdots$	0	0	0	$\cdots$	0	0)
$y^{(2)}$	(1	1	$\cdots$	0	0	0	$\cdots$	0	0)	P	D	$\cdots$	0	0	0	$\cdots$	0	0)	0	$\cdots$	0	0	0	$\cdots$	0	0)	0	$\cdots$	0	0	0	$\cdots$	0	0)
$\vdots$	$\vdots$	$\vdots$	$\ddots$	$\vdots$	$\vdots$	$\vdots$	$\ddots$	$\vdots$	$\vdots$	$\vdots$	$\vdots$	$\ddots$	$\vdots$	$\vdots$	$\vdots$	$\ddots$	$\vdots$	$\vdots$	$\vdots$	$\ddots$	$\vdots$	$\vdots$	$\vdots$	$\ddots$	$\vdots$	$\vdots$	$\vdots$	$\ddots$	$\vdots$	$\vdots$	$\vdots$	$\ddots$	$\vdots$	$\vdots$
$y^{(t-1)}$	(1	1	$\cdots$	1	0	0	$\cdots$	0	0)	P	P	$\cdots$	D	0	0	$\cdots$	0	0)	0	$\cdots$	0	0	0	$\cdots$	0	0)	0	$\cdots$	0	1	0	$\cdots$	0	0)
$y^{(t)}$	(1	1	$\cdots$	1	1	0	$\cdots$	0	0)	P	P	$\cdots$	P	D	0	$\cdots$	0	0)	0	$\cdots$	0	0	0	$\cdots$	0	0)	0	$\cdots$	0	0	1	$\cdots$	0	0)
$y^{(t+1)}$	(1	1	$\cdots$	1	1	1	$\cdots$	0	0)	P	P	$\cdots$	P	g_t^y	D	$\cdots$	0	0)	0	$\cdots$	0	0	0	$\cdots$	0	0)	0	$\cdots$	0	0	0	$\cdots$	0	0)
$\vdots$	$\vdots$	$\vdots$	$\ddots$	$\vdots$	$\vdots$	$\vdots$	$\ddots$	$\vdots$	$\vdots$	$\vdots$	$\vdots$	$\ddots$	$\vdots$	$\vdots$	$\vdots$	$\ddots$	$\vdots$	$\vdots$	$\vdots$	$\ddots$	$\vdots$	$\vdots$	$\vdots$	$\ddots$	$\vdots$	$\vdots$	$\vdots$	$\ddots$	$\vdots$	$\vdots$	$\vdots$	$\ddots$	$\vdots$	$\vdots$
$y^{(T-1)}$	(1	1	$\cdots$	1	1	1	$\cdots$	1	0)	P	P	$\cdots$	P	g_t^y	P	$\cdots$	D	0)	0	$\cdots$	0	0	0	$\cdots$	0	0)	0	$\cdots$	0	0	0	$\cdots$	0	1)
$y^{(T)}$	(1	1	$\cdots$	1	1	1	$\cdots$	1	1)	P	P	$\cdots$	P	g_t^y	P	$\cdots$	P	P	0	$\cdots$	0	0	0	$\cdots$	0	0)	0	$\cdots$	0	0	0	$\cdots$	0	0)
$z^{(1)}$	(0	1	$\cdots$	1	1	1	$\cdots$	1	1)	U	0	$\cdots$	0	g_t	0	$\cdots$	0	g^T	1	$\cdots$	0	0	0	$\cdots$	0	0)	0	$\cdots$	0	0	0	$\cdots$	0	0)
$z^{(2)}$	(0	0	$\cdots$	1	1	1	$\cdots$	1	1)	0	U	$\cdots$	0	g_t	0	$\cdots$	0	g^T	0	$\cdots$	0	0	0	$\cdots$	0	0)	0	$\cdots$	0	0	0	$\cdots$	0	0)
$\vdots$	$\vdots$	$\vdots$	$\ddots$	$\vdots$	$\vdots$	$\vdots$	$\ddots$	$\vdots$	$\vdots$	$\vdots$	$\vdots$	$\ddots$	$\vdots$	$\vdots$	$\vdots$	$\ddots$	$\vdots$	$\vdots$	$\vdots$	$\ddots$	$\vdots$	$\vdots$	$\vdots$	$\ddots$	$\vdots$	$\vdots$	$\vdots$	$\ddots$	$\vdots$	$\vdots$	$\vdots$	$\ddots$	$\vdots$	$\vdots$
$z^{(t-2)}$	(0	0	$\cdots$	0	1	1	$\cdots$	1	1)	0	0	$\cdots$	U	g_t	0	$\cdots$	0	g^T	0	$\cdots$	0	1	0	$\cdots$	0	0)	0	$\cdots$	0	0	0	$\cdots$	0	0)
$z^{(t-1)}$	(0	0	$\cdots$	0	0	1	$\cdots$	1	1)	0	0	$\cdots$	0	g_t^z	0	$\cdots$	0	g^T	0	$\cdots$	0	0	1	$\cdots$	0	0)	0	$\cdots$	0	0	0	$\cdots$	0	0)
$z^{(t)}$	(0	0	$\cdots$	0	0	0	$\cdots$	1	1)	0	0	$\cdots$	0	0	U	$\cdots$	0	g^T	0	$\cdots$	0	0	0	$\cdots$	0	0)	0	$\cdots$	0	0	0	$\cdots$	0	0)
$\vdots$	$\vdots$	$\vdots$	$\ddots$	$\vdots$	$\vdots$	$\vdots$	$\ddots$	$\vdots$	$\vdots$	$\vdots$	$\vdots$	$\ddots$	$\vdots$	$\vdots$	$\vdots$	$\ddots$	$\vdots$	$\vdots$	$\vdots$	$\ddots$	$\vdots$	$\vdots$	$\vdots$	$\ddots$	$\vdots$	$\vdots$	$\vdots$	$\ddots$	$\vdots$	$\vdots$	$\vdots$	$\ddots$	$\vdots$	$\vdots$
$z^{(T-1)}$	(0	0	$\cdots$	0	0	0	$\ldots$	0	1)	0	0	$\cdots$	0	0	0	$\ldots$	U	g^T	0	$\cdots$	0	0	0	$\ldots$	0	1)	0	$\ldots$	0	0	0	$\ldots$	0	0)
$z^{(T)}$	(0	0	$\cdots$	0	0	0	$\ldots$	0	0)	0	0	$\cdots$	0	0	0	$\ldots$	0	0)	0	$\cdots$	0	0	0	$\ldots$	0	0)	0	$\ldots$	0	0	0	$\ldots$	0	0)
$y^{(T+1)}$	(1	1	$\cdots$	1	1	1	$\cdots$	1	1)	P	P	$\cdots$	P	g_t^y	P	$\cdots$	P	0)	0	$\cdots$	0	0	0	$\cdots$	0	0)	0	$\cdots$	0	0	0	$\cdots$	0	0)

Figure 4: $3T$ Affinely independent points for $g_t, g^T = 0$, $g_t^y = P$ and $g_t^z = U$, where $U = SU - \underline{P}$, $D = SD - \underline{P}$ and $P = \overline{P} - \underline{P}$.

Proof As mentioned before, it suffices to show $3T-2$ linearly independent points that are tight for (2). The following $3T-2$ points are linearly independent and tight for (2) when $g_t = 0$, $g^T, g_t^y = P$ and $g_t^z = U$: T points x^i for $i \in [1,T]$, $T-1$ points y^i for $i \in [1,T-1]$, and $T-1$ points z^i for $i \in [1,T-1]$. □

Theorem 3 *The inequalities in* (3) *describe facets of the polytope* $\overline{C}_T$.

Proof The following $3T-2$ points are linearly independent and tight for (4) when $g_t, g_t^y, g_t^z, , g^T = 0$: T points x^i for $i \in [1,T]$, $T-1$ points y^i for $i \in [1,t-1] \cup [t+1,T]$, and $T-1$ points z^i for $i \in [1,T-1]$. □

We may conclude that (1)-(3) describe facets of $\overline{C}_T$.

Now, we prove that the inequalities (1)-(8) are sufficient to describe the convex hull of the feasible solutions.

We need a preliminary lemma.

Lemma 1 *Let* $P = \{x \in \mathbb{R}^n | Ax \leq b\}$ *be an integral polyhedron, i.e,* $P = conv(P \cap \mathbb{Z}^n)$. *Define* $Q = \{(x,y) \in \mathbb{R}^n \times \mathbb{R}^m | x \in P, 0 \leq y_i \leq c_i x, i = 1,\ldots,k,\ y_i = d_i x, i = k+1,\ldots,m\}$, *where* $1 \leq k \leq m$, $c_i, d_i \in \mathbb{R}^n$, *and* $c_i x \geq 0$, $d_i x \geq 0$ *for* $i = 1,\ldots,m$ *and for each* $x \in P$. *Then every vertex* $(\tilde{x},\tilde{y})$ *of* Q *has the property that* $\tilde{x}$ *is integral.*

Proof Suppose by contradiction that there exists a vertex $(\tilde{x},\tilde{y})$ of Q such that $\tilde{x}$ is not integral. Then $\tilde{x}$ is not a vertex of P and therefore there exist $\bar{x}^1, \bar{x}^2 \in P$ such that $\tilde{x} = \frac{1}{2}\bar{x}^1 + \frac{1}{2}\bar{x}^2$. Moreover, $\tilde{y}_i = c_i\tilde{x}$ for $i = 1,\ldots,k$, indeed if there exists r, $1 \leq r \leq k$, such that $0 \leq \tilde{y}_r < c_r\tilde{x}$, then $(\tilde{x},\tilde{y})$ is a convex combination of the point $(\tilde{x},\hat{y})$ and the point $(\tilde{x},\check{y})$, where $\hat{y}_r = c_r\tilde{x}$, $\check{y}_r = 0$, and $\hat{y}_i = \check{y}_i = \tilde{y}_i$ for $1 \leq i \leq m$, $i \neq r$.

For $j = 1,2$, let $\bar{y}_i^j = c_i\bar{x}^j$ for $i = 1,\ldots,k$ and $\bar{y}_i^j = d_i\bar{x}^j$ for $i = k+1,\ldots,m$. Then $(\tilde{x},\tilde{y}) = \frac{1}{2}(\bar{x}^1,\bar{y}^1) + \frac{1}{2}(\bar{x}^2,\bar{y}^2)$, i.e., $(\tilde{x},\tilde{y})$ is a convex combination of $(\bar{x}^1,\bar{y}^1)$ and $(\bar{x}^2,\bar{y}^2)$. Contradiction. □

Theorem 4 *The polytope* $\overline{C}_T$ *and* $\overline{D}_T$ *are equal.*

Proof The thesis can be proved by showing that $\overline{D}_T$ defines an integral polytope. This easily follows by applying Lemma 1, considering P as the integer polytope defined by inequalities (5)-(8) (see [13]), p_t as the additional variables and (1)-(3) as the new inequalities. □

Finally, we prove that inequalities describing the operation of slow- and quick-start units define integral polytopes.

Table 1: Generator Data for Quick-start Units

Gen	Technical Information							Cost Coefficients†			
	$\overline{P}$ [MW]	$\underline{P}$ [MW]	$TU\&TD$ [h]	SU [MW]	SD [MW]	p_0* [MW]	$\text{Ste}_0^\diamond$ [h]	C^{NL} [$/h]	C^{LV} [$/MWh]	C^{SU} [$]	C^{SD} [$]
1	455	150	8	252	303	150	8	1000	16.19	9000	0
2	455	150	8	252	303	150	8	970	17.26	10000	0
3	130	20	5	57	75	20	5	700	16.60	1100	0
4	130	20	5	57	75	20	5	680	16.50	1120	0
5	162	25	6	71	94	25	6	450	19.70	1800	0
6	80	20	3	40	50	20	3	370	22.26	340	0
7	85	25	3	45	55	25	3	480	27.74	520	0
8	55	10	1	25	33	10	1	660	25.92	60	0
9	55	10	1	25	33	10	1	665	27.74	60	0
10	55	10	1	25	33	10	1	670	27.79	60	0

* p_0 is the unit's initial production prior to the first period of the time span.
$\diamond$ Ste_0: hours that the unit has been online prior to the first period of the time span.

Table 2: Energy Price ($/MWh)

$t = 1 \dots 12 \rightarrow$	13.0	7.2	4.6	3.3	3.9	5.9	9.8	15.0	22.1	31.3	33.2	24.8
$t = 13 \dots 24 \rightarrow$	19.5	16.3	14.3	13.7	15.0	17.6	20.2	29.3	49.5	53.4	30.0	20.2

Definition 2 Let the polytope that describes the operation of slow-start units be $\overline{S}_T\left(TU, TD, \overline{P}, \underline{P}, SU^{\text{D}}, SD^{\text{D}}, P_i^{\text{SU}}, P_i^{\text{SD}}\right) = \left\{(u, v, p, \widehat{p}, e) \in \mathbb{R}_+^{5T-1} | \, (u, v, p) \text{ satisfy inequalities (1)-(10) for } SU, SD = \underline{P}\right\}$, for short denoted as $\overline{S}_T$. Let the polytope that describes the operation of quick-start units be $\overline{Q}_T\left(TU, TD, \overline{P}, \underline{P}, SU, SD,\right) = \left\{(u, v, p, \widehat{p}, e) \in \mathbb{R}_+^{5T-1} | \, (u, v, p) \text{ satisfy inequalities (1)-(8) and (11)-(12)}\right\}$, for short denoted as $\overline{Q}_T$.

Theorem 5 *The polytopes $\overline{S}_T$ and $\overline{Q}_T$ define integer polytopes on variables u, v.*

Proof This easily follows by applying Lemma 1. For the polytope describing the operation of slow-start units $\overline{S}_T$, P is the integer polytope $\overline{D}_T$ (see Theorem 4), $\widehat{p}_t, e_t$ are the additional variables, and (9)-(10) the new equalities. Similarly, for the polytope describing the operation of quick-start units $\overline{Q}_T$, P is the integer polytope $\overline{D}_T$, $\widehat{p}_t, e_t$ are the additional variables, and (11)-(12) the new equalities. □

In conclusion, the constraints describing the technical operation of both slow- and quick-start units are convex hulls. These constraints are (1)-(8), when $SU, SD = \underline{P}$, together with (9) and (10) for slow-startup units; and (1)-(8) together with (11) and (12) for quick-start units.

5 Numerical Results

To illustrate the computational performance of the formulation proposed in this paper, a self-UC problem for a price-taker producer is solved for different time spans. The goal is then to optimally schedule the generating units to maximize profits (difference between the revenue and the total operating cost [2,10]) during the planning horizon:

$$\max \sum_{t=1}^{N} \sum_{g=1}^{G} \left[\pi_t e_{gt} - c_{gt}\left(u_{gt}, v_{gt}, w_{gt}, e_{gt}\right)\right] \tag{14}$$

where subindex g stands for generating units and G is the total quantity of units; π_t refers to the energy prices, which for these case studies are shown in Table 2; and c_{gt} is the total operating cost per unit g and period t, which is defined in (13) for the proposed power-based UC formulation. The self-UC problem also arises when solving UC with decomposition methods such as Lagrangian Relaxation [3].

Two different 10-unit system data are considered, one containing only quick-start units and another containing both quick- and slow-start units. The 10-unit system data for quick-start units is presented in Table 1. The power system data are based on information presented in [1,9]. The computational performance of the power-based formulation for quick-start units (see Section 3), labelled as *PwQ*, is compared with those in [1] and [12], labelled as *1bin* and *3bin*, respectively.

The other 10-unit system data including slow-start units is created in order to observe the computational performance of the formulation for slow-start units. We create this new case study by replacing the first

Table 3: Generator Data For Slow-start Units

Gen	Technical Information								
	$\overline{P}$ [MW]	$\underline{P}$ [MW]	$TU\&TD$ [h]	SU [MW]	SD [MW]	SU^{D} [h]	SD^{D} [h]	p_0 [MW]	Ste_0 [h]
1	455	150	8	150	150	3	2	150	8
2	455	150	8	150	150	3	2	150	8
3	130	20	5	20	20	2	2	20	5
4	130	20	5	20	20	2	2	20	5
5	162	25	6	25	25	2	2	25	6
6	80	20	3	20	20	1	1	20	3
7	85	25	3	25	25	1	1	25	3

Table 4: Computational Performance of The UC Formulations for Different Time Spans (in days)

	IntGap (%)			LP time (s)				MIP time (s)*		Nodes		
days	*Pw*$^{\diamond}$	*3bin*	*1bin*	*PwQ*†	*PwSQ*†	*3bin*	*1bin*	*3bin*	*1bin*	*Pw*$^{\diamond}$	*3bin*	*1bin*
64	0	0.88	2.57	0.42	0.47	0.80	0.95	12.01	13.79	0	496	487
128	0	0.87	2.57	1.03	1.22	2.06	2.60	45.54	(3.33E-4)	0	528	603915
256	0	0.87	2.57	2.62	3.15	5.38	6.88	199.18	(5.21E-4)	0	533	229035
512	0	0.87	2.57	6.96	8.55	14.29	18.83	734.03	(5.35E-4)	0	488	136128

* $(\cdot)$ shows the final optimality tolerance if the time limit is reached

$\diamond$ *PwQ* is equal to *PwSQ* for these cases

† For these formulations, the LP and MIP times are equal

seven quick-start units from Table 1 by slow-start units. The data for these seven slow-star units is provided in Table 3. For these slow-start units, the power outputs for the startup (shutdown) power trajectories are obtained as an hourly linear change from 0 ($\underline{P}$) to $\underline{P}$ (0) for a duration of SU^{D} (SD^{D}) hours. Be aware that *1bin* and *3bin* are modelled only for quick-start units because: 1) those traditional UC formulations ignore the units' startup and shutdown power trajectories and including these trajectories will considerably increase the models' computing complexity [10]; and 2) the main purpose of these case studies is to compare the computational performance of the proposed formulations with the traditional UC formulations (which ignore the startup and shutdown trajectories).

In short, two different case studies are considered, the first case study models 10 quick-start units (see Table 1) for formulations *3bin*, *1bin* and *PwQ*. The second case study models also 10 units, seven slow-start (see Table 3) and three quick-start units (units 8 to 10 in Table 1) and this case study is solved using the proposed formulation for both slow- and quick-start units, which is labelled as *PwSQ*.

All tests were carried out using CPLEX 12.5 on an Intel-i7 3.4-GHz personal computer with 8 GB of RAM memory. The problems are solved until they hit the time limit of 10000 seconds or until they reach optimality (more precisely to 10^{-6} of relative optimality tolerance).

Table 4 shows the computational performance of the self-UC problem (14) subject to the different UC formulations for different time spans (up to 512 days to consider large case studies). The tightness of each formulation is measured with the Integrality Gap (IntGap), defined as the relative distance between their MIP and LP optimums [14,9]. Note that the MIP optimums of *PwQ* and *PwSQ* were achieved by just solving the LP problem, IntGap$=0$, hence solving the MIP problems in LP time. On the other hand, as usual, the branch-and-cut method was needed to solve the MIP for *3bin* and *1bin*. Table 4 also shows the MIP time and nodes explored for the different formulations.

Table 5 shows the dimensions for all formulations for the different time spans. Note that *PwQ* and *PwSQ* are more compact, in terms of quantity of constraints, than *3bin* and *1bin*. The formulations *PwQ* and *PwSQ* presents the same quantity of binary variables of *3bin*, but twice continuous variables. This is because *PwQ* and *PwSQ* model power and energy as two different variables. The formulation *1bin* presents a third of binary variables in comparison with the other formulations, but it is the formulation presenting the largest quantity of continuous variables, constraints and nonzero elements in the constraint matrix. This is the result of reformulating the MIP model to avoid the startup and shutdown binary variables. The work in [1] claims that this would reduce the node enumeration in the branch-and-bound process. Note however that this reformulation is the least tight, see IntGap in Table 4, and it is also the largest, hence presenting the worst computational performance, similar results are obtained in [12,9].

In conclusion, the proposed formulation presents a dramatic improvement in computation in comparison with *3bin* and *1bin* due to its tightness (speedups above 85x and 8200x, respectively); and it also presents a lower LP burden due to its compactness, see Table 5.

Table 5: Problem Size Comparison of The UC Formulations for Different Time Spans (in days)

	# constraints			# nonzero elements				# real var			# binary var	
days	*Pw**	*3bin*	*1bin*	*PwQ*	*PwSQ*	*3bin*	*1bin*	*Pw**	*3bin*	*1bin*	*Pw*†	*1bin*
64	76749	107459	138225	432673	440339	417313	469719	30720	15360	46080	46080	15360
128	153549	214979	276465	865825	881171	835105	939735	61440	30720	92160	92160	30720
256	307149	430019	552945	1732129	1762835	1670689	1879767	122880	61440	184320	184320	61440
512	614349	860099	1105905	3464737	3526163	3341857	3759831	245760	12288	368640	368640	122880

* *PwQ* is equal to *PwSQ* for these cases

† *PwQ*, *PwSQ* and *3bin* are equal for this case

6 Conclusion

This paper presented the convex hull description of the basic constraints of slow- and quick-start generating units for power-based unit commitment (UC) problems. These constraints are: generation limits, and minimum up and down times, startup and shutdown power trajectories for slow-start units, and startup and shutdown capabilities for quick-start units. Although the model does not include some crucial constraints, such as ramping, it can be used as the core of any UC formulation and thus helping to tighten the final UC model. Finally, different case studies for a self-UC were carried out, where the proposed formulation solved the MIP problem as an LP. Consequently, solving the self-UC problem significantly faster when compared with two other traditional UC formulations.

Acknowledgements

The authors thank Laurence Wolsey, Santanu Dey, and Paolo Ventura for useful discussion about the proof of the Lemma 1.

References

1. Carrion, M., Arroyo, J.: A computationally efficient mixed-integer linear formulation for the thermal unit commitment problem. IEEE Transactions on Power Systems **21**(3), 1371–1378 (2006). DOI 10.1109/TPWRS.2006.876672
2. Frangioni, A., Gentile, C.: Solving nonlinear single-unit commitment problems with ramping constraints. Operations Research **54**(4), 767–775 (2006). DOI 10.1287/opre.1060.0309
3. Frangioni, A., Gentile, C., Lacalandra, F.: Solving unit commitment problems with general ramp constraints. International Journal of Electrical Power & Energy Systems **30**(5), 316–326 (2008). DOI 10.1016/j.ijepes.2007.10.003
4. Frangioni, A., Gentile, C., Lacalandra, F.: Tighter approximated MILP formulations for unit commitment problems. IEEE Transactions on Power Systems **24**(1), 105–113 (2009). DOI 10.1109/TPWRS.2008.2004744
5. Gentile, C., Morales-Espana, G., Ramos, A.: A tight MIP formulation of the unit commitment problem with start-up and shut-down constraints. Technical Report IIT-14-040A (2014). URL `http://www.iit.upcomillas.es/aramos/papers/LP-based_UC.pdf`
6. Guan, X., Gao, F., Svoboda, A.: Energy delivery capacity and generation scheduling in the deregulated electric power market. IEEE Transactions on Power Systems **15**(4), 1275–1280 (2000). DOI 10.1109/59.898101
7. Lee, J., Leung, J., Margot, F.: Min-up/min-down polytopes. Discrete Optimization **1**(1), 77–85 (2004). DOI 16/j.disopt.2003.12.001
8. Morales-Espana, G., Garcia-Gonzalez, J., Ramos, A.: Impact on reserves and energy delivery of current UC-based market-clearing formulations. In: European Energy Market (EEM), 2012 9th International Conference on the, pp. 1–7. Florence, Italy (2012). DOI 10.1109/EEM.2012.6254749
9. Morales-Espana, G., Latorre, J.M., Ramos, A.: Tight and compact MILP formulation for the thermal unit commitment problem. IEEE Transactions on Power Systems **28**(4), 4897–4908 (2013). DOI 10.1109/TPWRS.2013.2251373
10. Morales-Espana, G., Latorre, J.M., Ramos, A.: Tight and compact MILP formulation of start-up and shut-down ramping in unit commitment. IEEE Transactions on Power Systems **28**(2), 1288–1296 (2013). DOI 10.1109/TPWRS.2012.2222938
11. Morales-Espana, G., Ramos, A., Garcia-Gonzalez, J.: An MIP formulation for joint market-clearing of energy and reserves based on ramp scheduling. IEEE Transactions on Power Systems **29**(1), 476–488 (2014). DOI 10.1109/TPWRS.2013.2259601
12. Ostrowski, J., Anjos, M.F., Vannelli, A.: Tight mixed integer linear programming formulations for the unit commitment problem. IEEE Transactions on Power Systems **27**(1), 39–46 (2012). DOI 10.1109/TPWRS.2011.2162008
13. Rajan, D., Takriti, S.: Minimum Up/Down polytopes of the unit commitment problem with start-up costs. Research Report RC23628, IBM (2005). URL `http://domino.research.ibm.com/library/cyberdig.nsf/1e4115aea78b6e7c85256b360066f0d4/cdcb02a7c809d89e8525702300502ac0?OpenDocument`
14. Williams, H.P.: Model Building in Mathematical Programming, 5th edition edn. John Wiley & Sons Inc (2013)
15. Wolsey, L.: Integer Programming. Wiley-Interscience (1998)

Article VI

G. Morales-Espana, R. Baldick, J. García-González, and A. Ramos, "Robustified Reserve Modelling for Wind Power Integration in Ramp-Based Unit Commitment," *IEEE Transactions on Power Systems*, 2014, paper under review. JCR 2012 data: impact factor 2.921 and 5-year impact factor 3.601.

Robustified Reserve Modelling for Wind Power Integration in Ramp-Based Unit Commitment

Germán Morales-España, *Student Member, IEEE,* Ross Baldick, *Fellow, IEEE,*
Javier García-González, *Member, IEEE,* and Andres Ramos

***Abstract*—This paper proposes a "robustified" network-constrained Unit Commitment (UC) formulation as an alternative to the robust and stochastic UC formulations under wind generation uncertainty. The formulation draws a clear distinction between power-capacity and ramp-capability reserves to deal with wind production uncertainty. These power and ramp requirements can be obtained from wind forecast information. The model is formulated under the ramp-based scheduling approach, which schedules power-trajectories instead of the traditional energy-blocks and takes into account the inherent startup and shutdown power trajectories of thermal units. These characteristics allow a correct representation of unit's ramp schedule which define their ramp availability for reserves. The proposed formulation significantly decreases operation costs if compared to traditional deterministic and stochastic UC formulations while simultaneously lowering the computational burden. The operation cost comparison is made through 5-min economic dispatch simulation under hundreds of out-of-sample wind generation scenarios.**

***Index Terms*—Mixed-integer programming, operating reserves, ramp scheduling, robustified formulation, unit commitment.**

NOMENCLATURE

A. Indexes and Sets

$g \in \mathcal{G}$	Generating units, running from 1 to G.
$b \in \mathcal{B}$	Buses, running from 1 to B.
$l \in \mathcal{L}$	Transmission lines, running from 1 to L.
$t \in \mathcal{T}$	Hourly periods, running from 1 to T hours.

B. Parameters

D_{bt}	Power demand on bus b at the end of hour t [MW].
Γ_{lb}	Shift factor for line l associated with bus b [p.u.].
Γ^{P}_{lg}	Shift factor for line l associated with unit g [p.u.].
$\overline{F}_l$	Flow limit on transmission line l [MW].
$\overline{P}_g$	Maximum power output [MW].
$\underline{P}_g$	Minimum power output [MW].
RD_g	Ramp-down capability [MW/h].
RU_g	Ramp-up capability [MW/h].
SD_g	Startup ramping capability [MW/h].
SU_g	Shutdown ramping capability [MW/h].
W_{bt}	Nominal forecasted wind power at end of hour t [MW].
$\overline{W}_{bt}$	Upper bound of the forecasted wind power at the end of hour t [MW].
$\underline{W}_{bt}$	Lower bound of the forecasted wind power at the end of hour t [MW].
$W^{\mathrm{R}-}_{bt}$	Ramp-down forecasted wind requirement for the whole hour t [MW/h].
$W^{\mathrm{R}+}_{bt}$	Ramp-up forecasted wind requirement for the whole hour t [MW/h].

C. First-stage Variables

r^{-}_{gt}	Down power-capacity reserve scheduled [MW].
r^{+}_{gt}	Up power-capacity reserve scheduled [MW].
$r^{\mathrm{R}-}_{gt}$	Down ramp-capability reserve scheduled [MW/h].
$r^{\mathrm{R}+}_{gt}$	Up ramp-capability reserve scheduled [MW/h].
u_{gt}	Binary variable which is equal to 1 if the unit is producing above $\underline{P}_g$ and 0 otherwise.
v_{gt}	Binary variable which takes the value of 1 if the unit starts up and 0 otherwise.
z_{gt}	Binary variable which takes the value of 1 if the unit shuts down and 0 otherwise.

D. Second-stage Variables

p_{gt}	Power output above minimum output at the end of hour t [MW].
$\widehat{p}_{gt}$	Total power output at the end of hour t, including startup and shutdown trajectories [MW].
$\overline{r}_{gt}$	Reserve deployment to provide the upper-wind dispatch $\overline{w}_{bt}$ [MW].
$\underline{r}_{gt}$	Reserve deployment to provide the lower-wind dispatch $\underline{w}_{bt}$ [MW].
w_{bt}	Wind dispatch for the nominal wind case W_{bt} [MW].
$\overline{w}_{bt}$	Wind dispatch for the upper bound wind $\overline{W}_{bt}$ [MW].
$\underline{w}_{bt}$	Wind dispatch for the lower bound wind $\underline{W}_{bt}$ [MW].

E. Functions

$c^{\mathrm{F}}_{gt}(\cdot)$	Fixed production cost [$].
$c^{\mathrm{V}}_{gt}(\cdot)$	Variable production cost [$].

I. INTRODUCTION

IN recent years, high penetration of variable generating sources, such as wind power, has challenged independent system operators (ISO) in keeping a reliable power system operation. The deviation between expected and real wind production must be absorbed by the power system resources (reserves), which must be available and ready to be deployed in real time. To guarantee this availability, the system resources must be committed in advance, usually day-ahead, by solving the so-called unit commitment (UC) problem.

A. Literature Review

1) Dealing with Uncertainty in UC: Stochastic and robust optimization have gained substantial popularity for UC optimization under parameter uncertainty. In the stochastic optimization approach, the stochasticity can be represented through an explicit description of scenarios and their associated probability [1], [2]. This approach presents however some practical limitations: 1) it may be difficult to obtain an accurate probability distribution of the uncertainty; and 2) a large number of scenario samples is required to obtain robust

solutions, which results in a computationally intensive problem (often intractable).

The robust optimization approach partly overcomes these disadvantages 1) by requiring moderate information about the underlying uncertainty, such as the mean and the range of the uncertain data; and 2) by immunizing the solution against all realizations of the data within the uncertainty range. However, it may be too conservative, since the objective function is to minimize the worst-case cost scenario, which may never be realized in practice. To deal with overconservatism, 1) a parameter commonly called budget-of-uncertainty is introduced in the optimization problem to control the conservatism of the robust solution [3], [4]; and 2) more recently, [4] proposes an unified stochastic and robust UC model that takes advantage of both stochastic and robust optimization approaches, where the objective is to achieve a low expected total cost while ensuring the system robustness.

Although the computational burden of adaptive robust UC does not depend on the number of scenarios, it requires solving a mixed integer programming (MIP) problem together with a bilinear program to obtain the worst-case scenario. This problem is considerably more complex to solve than a pure MIP, requires ad-hoc solving strategies [3], [4], and only local optimum is guaranteed, in contrast with the boundedly close to global optimum guaranteed by the MIP.

2) Power-Capacity and Ramp-Capability Reserves: In order to solve the day-ahead UC it is necessary to take into account that wind generation is subject to uncertainty. As the wind power forecasting error can be significant 24 hours in advance, the range of possible values of wind power for each hour of the following day can be very broad. As a consequence, ISOs need to schedule some power-capacity reserve to guarantee that committed system resources will be able to cope with any value of wind generation that can be realised within that range.

When getting closer to the real time, for instance one hour in advance, the range of possible values for the next hour is smaller. However, even within such short time interval, wind generation can increase or decrease its value at a rate that will require that conventional generators adapt their output to follow that ramp to keep the demand-supply balance. Therefore, apart from the day-ahead power-capacity reserve, it will be necessary to ensure that for any hour, the committed system resources will be able to cope with the expected maximum ramp of variation of the wind generation. Thus, a ramp-capability reserve is also needed.

To illustrate the need of a clear differentiation between power-capacity and ramp-capability reserves, consider the following example. Figs. 1a and 1b show two different set of wind scenarios which present the same power-capacity uncertainty ranges, but completely different ramp uncertainty ranges. Dealing with the scenarios in Fig. 1b requires higher ramp-capability, although both set of scenarios demand the same power-capacity requirements. In fact, some power systems have experienced short-term scarcity events caused by resources with sufficient power capacity but insufficient ramp capability [5]. In response, ISOs are developing market-based ramping products, thus making a clear difference between

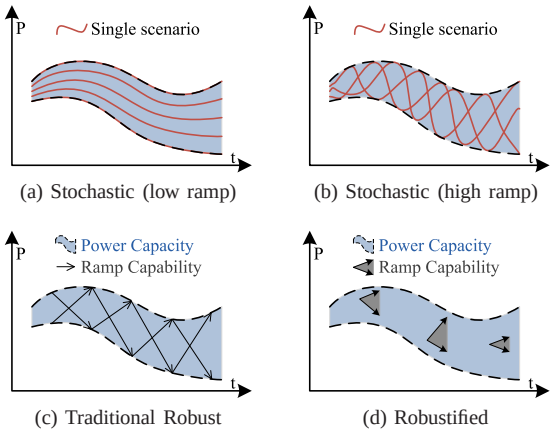

(a) Stochastic (low ramp) (b) Stochastic (high ramp)

(c) Traditional Robust (d) Robustified

Fig. 1: Different approaches to deal with wind uncertainty

power-capacity and ramp-capability requirements [5], [6].

The stochastic UC implicitly captures both reserve requirements through scenarios, e.g. see Figs. 1a and 1b. However, to correctly represent these reserve requirements, a large number of scenarios may be needed, resulting in a high computational cost. On the other hand, to the best of our knowledge, there is no reported work on modelling ramp uncertainty (or power temporal correlation) in robust UC. The traditional robust optimization approach assumes that changes from maximum to minimum day-ahead expected wind production is possible in real time, see Fig. 1c. This results in a too conservative solution, as such profiles that shift from the maximum to the minimum bounds established 24 hours in advance are very unlikely to occur. Including temporal correlation in the uncertainty representation into robust optimization problems may considerably increase its computational complexity [7], which is already a bilinear MIP for the simplest uncertainty representation in UC problems [3].

3) Ramp-based UC: Conventional day-ahead UC formulations fail to deal with ramp capabilities appropriately. Inefficient ramp management arises from applying ramp-constraints to energy levels or (hourly) averaged generation levels; consequently, energy schedules may not be feasible [8]. In addition, traditional UC models assume that units start/end their production at their minimum output. That is, the intrinsic startup and shutdown power trajectories of units are ignored. As a consequence, there may be a high amount of energy that is not allocated by UC but it is inherently present in real time, thus affecting the total load balance and causing a negative economic impact [9]. For further details of the drawbacks of conventional UC scheduling approaches, the reader is referred to [10], [11] and references therein.

To overcome these drawbacks, [11] proposes the ramp-based UC scheduling approach. This approach uses piecewise linear power trajectories for both generating units and demand instead of the commonly established staircase profile for energy blocks. The use of an instantaneous power profile allows the model to efficiently schedule reserves and ramping resources. In comparison with conventional UC models, the ramp-based UC approach guarantees that, first, energy schedules can be delivered and, second, that operating reserves can be deployed respecting the ramping and capacity limits of

generating units. In addition, the model takes into account the normally neglected power trajectories that occur during the startup and shutdown processes, thus optimally scheduling them to provide energy and ramp, which help to satisfy the power demand.

B. Robustified Ramp-Based UC Formulation: An Overview

This paper proposes a ramp-based network-constrained UC formulation as an alternative to the robust and stochastic UC formulations to deal with wind generation uncertainty. Similarly to the stochastic and robust approaches, the proposed "robustified" formulation seeks to provide commitment (first-stage) decisions that give flexibility (adaptability) to the power system to face wind uncertainty. This flexibility is provided by units and wind dispatch (second-stage). Wind dispatch flexibility is modelled by considering curtailment in the UC formulation. Curtailment may appear due to either economic reasons or technical reasons, e.g., insufficient network capacity. This flexibility helps to reduce the reserve requirements since part of the uncertainty can be faced by curtailment, as practiced in ERCOT and MISO. Introducing other renewable energy sources to the formulation is straightforward if they can be curtailed.

The proposed formulation draws a clear distinction between power-capacity and ramp-capability reserve requirements to face wind uncertainty, see Fig. 1d. Allowing a different value for the ramp requirements results in a more realistic setting, as discussed above. To adequately manage ramping resources, the model is formulated under the ramp-based scheduling approach. The formulation is represented as a mixed integer programming (MIP) problem, which has become the leading approach in the electricity sector due to significant improvements on MIP solvers. The core of the proposed MIP formulation is built upon the convex-hull and the tight-and-compact formulations presented in [12] and [9], respectively, thus taking advantage of their mathematical properties. These formulations reinforce the convergence speed by reducing the search space (tightness) and at the same time by increasing the searching speed with which solvers explore that reduced space (compactness).

We present an extensive numerical study on the IEEE 118-bus test system, where we compare the robustified formulation with the stochastic and with the deterministic approaches. To perform comparisons and to obtain an accurate estimate of the performance of each UC policy, the hourly commitment obtained from each UC approach is evaluated through a 5-min economic dispatch for 200 out-of-sample scenarios.

C. Contributions and Paper Organization

The principal contributions of this paper are as follows:

1) We formulate a robustified network-constrained UC to deal with wind generation uncertainty under the ramp-based scheduling approach. Given a pre-specified nodal power-capacity and ramp-capability reserve requirements, the robustified UC seeks commitment (first-stage) decisions that guarantee that enough resources (reserves) are ready to adapt to any realization of wind generation uncertainty. The level of conservatism of the solution is controlled by the reserve parameters and curtailment flexibility. That is, once the reserve requirements are fixed, the robustified UC reshape these requirements by considering curtailment.
2) We develop a practical compact MIP formulation to deal with wind uncertainty. The formulation remains compact since it only needs two reserve requirements, unlike the stochastic approach where problem size depends on the number of considered scenarios. The proposed formulation is a linear MIP problem, rather than a bilinear MIP problem resulting from robust UC, thus avoiding the computational and non-linear complexity that arises from bilinear problems.
3) The proposed robustified UC approach can be used by ISOs to ensure that enough power-capacity and ramp-capability resources are available to deal with wind uncertainty in real-time operation. ISOs can also adjust the level of conservatism of the solution by adjusting the reserve requirements, based on their preferences and on their available information of wind uncertainty.

The remainder of this paper is organized as follows. Section II details the mathematical formulation of the different operating reserves and their links with the ramp schedules. Section III presents some numerical examples as well as a comparison with the deterministic and stochastic UC approaches. Finally, concluding remarks are made in Section IV.

II. Mathematical Formulation

This section presents the proposed mathematical formulation of the robustified ramp-based UC. This section first discusses the relationship between the wind uncertainty range and the power system reserve requirements. The next part is devoted to modelling the reserve constraints for generating units and the network constraints. Finally, the objective function is defined.

A. Wind Uncertainty Range and Power System Requirements

The first step to build the robustified model is to define the uncertainty range. In this paper, the uncertain parameters are the power-capacity and ramp-capability ranges of wind production, see Fig. 1d. The wind power-capacity uncertainty range of node b at time t is defined by the upper and lower bounds $\left[\overline{W}_{bt}, \underline{W}_{bt}\right]$. The wind ramp uncertainty range of node b at time t is defined by $\left[W_{bt}^{\mathrm{R}-}, W_{bt}^{\mathrm{R}+}\right]$. The nominal value of wind ramp is defined by the trajectory of the nominal wind power production W_{bt}.

In this paper, we consider the nominal value of wind production W_{bt} as the middle value of the uncertainty range, i.e., $\left(\overline{W}_{bt} + \underline{W}_{bt}\right)/2$. The proposed formulation is general, so ISOs could define any other nominal wind value, e.g., the most expected wind production. The only limitation is that the nominal value of wind production must be defined within the wind uncertainty range.

The flexibility that brings the fact that wind generation can be curtailed is taken into account. Thus, the possible dispatched wind range that results from the UC may (shrink) be different than the forecasted range, as shown in Fig. 2.

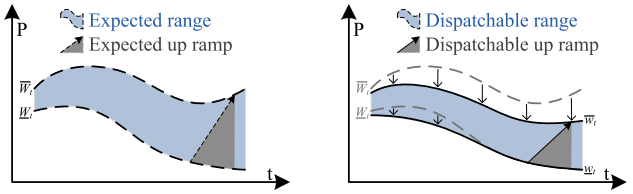

(a) Forecasted range (b) Dispatchable range

Fig. 2: Forecasted and dispatchable wind uncertainty ranges

To allow curtailment in the formulation, the wind-dispatch variables are bounded by their associated wind forecast bounds:

$$0 \leq \underline{w}_{bt} \leq \underline{W}_{bt},\ 0 \leq w_{bt} \leq W_{bt},\ 0 \leq \overline{w}_{bt} \leq \overline{W}_{bt} \quad \forall b,t \quad (1)$$

and we define the variables $w_{bt}^{\mathrm{R}+}$ and $w_{bt}^{\mathrm{R}-}$ as the maximum ramp up and down range, exceeding wind nominal values, that can fit within the dispatchable uncertainty range, respectively:

$$w_{bt}^{\mathrm{R}+} = (\overline{w}_{bt} - w_{bt}) + \left(w_{b,t-1} - \underline{w}_{b,t-1}\right) \quad \forall b,t \quad (2)$$

$$w_{bt}^{\mathrm{R}-} = (\overline{w}_{b,t-1} - w_{b,t-1}) + (w_{bt} - \underline{w}_{bt}) \quad \forall b,t. \quad (3)$$

Once the wind uncertainty ranges are defined, the power system must supply demand and reserves for these ranges:

$$\sum_{g\in\mathcal{G}} \widehat{p}_{gt} = \sum_{b\in\mathcal{B}} (D_{bt} - w_{bt}) \quad \forall t \quad (4)$$

$$\sum_{g\in\mathcal{G}} r_{gt}^{+} \geq \sum_{b\in\mathcal{B}} (w_{bt} - \underline{w}_{bt}) \quad \forall t \quad (5)$$

$$\sum_{g\in\mathcal{G}} r_{gt}^{-} \geq \sum_{b\in\mathcal{B}} (\overline{w}_{bt} - w_{bt}) \quad \forall t \quad (6)$$

$$\sum_{g\in\mathcal{G}} r_{gt}^{\mathrm{R}+} \geq \sum_{b\in\mathcal{B}} \inf\left(\tilde{W}_{bt}^{\mathrm{R}-}, w_{bt}^{\mathrm{R}-}\right) \quad \forall t \quad (7)$$

$$\sum_{g\in\mathcal{G}} r_{gt}^{\mathrm{R}-} \geq \sum_{b\in\mathcal{B}} \inf\left(\tilde{W}_{bt}^{\mathrm{R}+}, w_{bt}^{\mathrm{R}+}\right) \quad \forall t. \quad (8)$$

where (4) is a power balance at the end of hour t. Be aware that the energy balance for the whole hour is automatically achieved by satisfying the power demand at the beginning and end of each hour, and by considering a piecewise-linear power profile for demand and generation [11].

Equality (4) ensures that the system provides the power and ramp requirements for the wind nominal case. Constraints (5)-(6) and (7)-(8) guarantee that the system can provide the maximum power and ramp deviations from the nominal case, respectively. Parameters $\tilde{W}_{bt}^{\mathrm{R}+}$ and $\tilde{\mathrm{W}}_{bt}^{R-}$ are the maximum up and down ramp deviations from the nominal ramp, respectively, and are obtained as follows:

$$\tilde{W}_{bt}^{\mathrm{R}+} = W_{bt}^{\mathrm{R}+} - (W_{bt} - W_{b,t-1}) \quad \forall b,t \quad (9)$$

$$\tilde{W}_{bt}^{\mathrm{R}-} = W_{bt}^{\mathrm{R}-} - (W_{b,t-1} - W_{bt}) \quad \forall b,t \quad (10)$$

The infimum functions in (7) and (8) guarantee that the ramp requirement do not exceed the scheduled wind range by choosing the minimum value between the forecasted ramp requirement and the maximum possible ramp within the scheduled wind range. An MIP equivalent formulation for the infimum function in (7) and (8) is provided in [13].

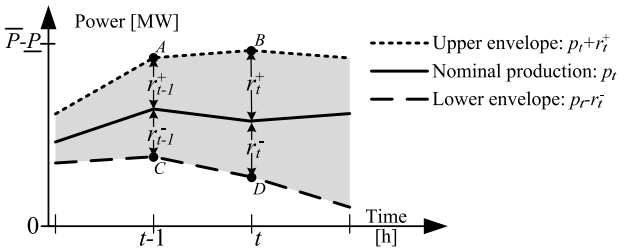

Fig. 3: Unit's operating range

B. Individual Unit's Constraints

This section presents a set of constraints that guarantee that a unit can provide any power trajectory within its scheduled ramp-capability $r_{gt}^{\mathrm{R}+}, r_{gt}^{\mathrm{R}-}$ and power-capacity r_{gt}^{+}, r_{gt}^{-} reserve ranges. Fig. 3 shows how the nominal case and the power-capacity reserves define upper and lower envelopes for units' operation.

1) Commitment Logic: The relation between the commitment, startup and shutdown variables is given by:

$$u_{gt} - u_{g,t-1} = v_{gt} - z_{gt} \quad \forall g,t. \quad (11)$$

Constraints imposing the minimum up/down times and different startup types are also included, see [11].

2) Total Power Output for The Nominal Production: The proposed formulation considers slow- and quick-start units. For the sake of brevity, we present the set of constraints for quick-start units, which can startup within one hour:

$$\widehat{p}_{gt} = \underline{P}_g \left(u_{gt} + v_{g,t+1}\right) + p_{gt} \quad \forall g,t. \quad (12)$$

The slow-start units are included into the formulation by only modifying (12), thus including shutdown and different-startup power trajectories that take longer than one hour. The reader is refereed to [9], [11], [12] for further details.

3) Power-Capacity Reserves: The upper and lower envelopes must be within the unit's capacity limits, see Fig. 3:

$$p_{gt} + r_{gt}^{+} \leq \left(\overline{P}_g - \underline{P}_g\right) u_{gt} - \left(\overline{P}_g - SD_g\right) z_{g,t+1} + \left(SU_g - \underline{P}_g\right) v_{g,t+1} \quad \forall g,t \quad (13)$$

$$p_{gt} - r_{gt}^{-} \geq 0 \quad \forall g,t \quad (14)$$

4) Ramp-Capability Reserves: The unit's nominal production defines the ramp-capability that is available in every period:

$$p_{gt} - p_{g,t-1} + r_{gt}^{\mathrm{R}+} \leq RU_g u_{gt} + \left(SU_g - \underline{P}_g\right) v_{g,t+1} \quad \forall g,t \quad (15)$$

$$-p_{gt} + p_{g,t-1} + r_{gt}^{\mathrm{R}-} \leq RD_g u_{gt} + \left(SD_g - \underline{P}_g\right) z_{gt} \quad \forall g,t \quad (16)$$

5) Relationship Between Power-Capacity and Ramp-Capability Reserves: The following constraints ensure that the unit operate within the ramp limits on either the upper or lower envelopes, respectively:

$$-r_{gt}^{\mathrm{R}-} \leq r_{gt}^{+} - r_{g,t-1}^{+} \leq r_{gt}^{\mathrm{R}+} \quad \forall g,t \quad (17)$$

$$-r_{gt}^{\mathrm{R}-} \leq r_{gt}^{-} - r_{g,t-1}^{-} \leq r_{gt}^{\mathrm{R}+} \quad \forall g,t \quad (18)$$

where (17) and (18) can be obtained from Fig. 3, see Appendix A for further details.

The available up (down) ramp-capability $r_{gt}^{\mathrm{R}+}$ ($r_{gt}^{\mathrm{R}-}$) is bounded by the maximum upwards (downwards) power change that is possible within power-capacity operating range, $C{\rightarrow}B$ ($A{\rightarrow}D$) in Fig. 3:

$$r_{gt}^{\mathrm{R}+} \leq r_{g,t-1}^{-} + r_{gt}^{+} \quad \forall g,t \tag{19}$$

$$r_{gt}^{\mathrm{R}-} \leq r_{g,t-1}^{+} + r_{gt}^{-} \quad \forall g,t. \tag{20}$$

Constraints (19) and (20) guarantee that once the unit is scheduled to provide ramp-capability reserve, there is a scheduled power-capacity range that can allow this ramp-capability deployment.

Finally, all these reserve variables are defined as positive:

$$r_{gt}^{+}, r_{gt}^{-}, r_{gt}^{\mathrm{R}+}, r_{gt}^{\mathrm{R}-} \geq 0 \quad \forall g,t. \tag{21}$$

In summary, constraints (13)-(21) guarantee that the unit can provide any power trajectory within its scheduled ramp-capability and power-capacity reserve ranges.

C. Including Network Constraints

By finding a feasible dispatch for the lowest expected wind bound $\underline{w}_{bt}$, all other possible wind realizations within the uncertainty range are feasible. That is, all scenarios can become $\underline{w}_{bt}$ by curtailment. Consequently, all scenarios can be dispatched and, in the worst case, the maximum quantity of wind that can be dispatched for any scenario would be $\underline{w}_{bt}$. Now, by ensuring a feasible dispatch for the upper expected wind bound $\overline{w}_{bt}$, we guarantee that wind scenarios up to $\overline{w}_{bt}$ can also be dispatched.

Now, we need to find the units' reserve deployments $\overline{r}_{gt}$ and $\underline{r}_{gt}$ for the upper and lower expected wind bounds, respectively. These reserve deployments must be within the scheduled power capacity limits:

$$-r_{gt}^{-} \leq \overline{r}_{gt}, \underline{r}_{gt} \leq r_{gt}^{+} \quad \forall g,t \tag{22}$$

and they must also satisfy ramp limit constraints:

$$-r_{gt}^{\mathrm{R}-} \leq \overline{r}_{gt} - \overline{r}_{g,t-1} \leq r_{gt}^{\mathrm{R}+} \quad \forall g,t \tag{23}$$

$$-r_{gt}^{\mathrm{R}-} \leq \underline{r}_{gt} - \underline{r}_{g,t-1} \leq r_{gt}^{\mathrm{R}+} \quad \forall g,t. \tag{24}$$

Finally the transmission capacity constraints are enforced for both the upper and lower expected wind bounds:

$$-\overline{F}_l \leq \sum_{g\in\mathcal{G}} \Gamma_{lg}^{\mathrm{P}} \left(\widehat{p}_{gt} + \overline{r}_{gt}\right) + \sum_{b\in\mathcal{B}} \Gamma_{lb} \left(\overline{w}_{bt} - D_{bt}\right) \leq \overline{F}_l \quad \forall l,t \tag{25}$$

$$-\overline{F}_l \leq \sum_{g\in\mathcal{G}} \Gamma_{lg}^{\mathrm{P}} \left(\widehat{p}_{gt} + \underline{r}_{gt}\right) + \sum_{b\in\mathcal{B}} \Gamma_{lb} \left(\underline{w}_{bt} - D_{bt}\right) \leq \overline{F}_l \quad \forall l,t \tag{26}$$

The demand balances for these scenarios are guaranteed by (4) together with:

$$\sum_{g\in\mathcal{G}} \overline{r}_{gt} = \sum_{b\in\mathcal{B}} \left(w_{bt} - \overline{w}_{bt}\right) \quad \forall t \tag{27}$$

$$\sum_{g\in\mathcal{G}} \underline{r}_{gt} = \sum_{b\in\mathcal{B}} \left(w_{bt} - \underline{w}_{bt}\right) \quad \forall t \tag{28}$$

and the nominal wind production must be within its upper and lower wind dispatches:

$$\underline{w}_{bt} \leq w_{bt} \leq \overline{w}_{bt} \quad \forall b,t. \tag{29}$$

Notice that total reserve deployment for the upper wind dispatch (27) is negative, this means that the power system must decrease its overall generation when wind production is above the nominal value. Notice in (27) and (28) that the power-capacity reserve requirements are provided by $\overline{r}_{gt}, \underline{r}_{gt}$ then these variables provide the limits on r_{gt}^{-}, r_{gt}^{+}. In other words, variables $\overline{r}_{gt}, \underline{r}_{gt}$ will be equal to either r_{gt}^{-} or r_{gt}^{+}. Therefore, (23) and (24) are more constrained and dominate (17) and (18), that is, (17) and (18) are then redundant.

Although (5) and (6) ensure that the units can provide the required power-capacity reserves, they do not guarantee that there is transmission capacity available to deploy them. However, constraints (25)-(29) guarantee that these power-capacity reserves can be deployed.

D. Objective Function

The proposed UC formulation optimizes over a nominal value of wind production and some weight can be given to the upper and lower wind bounds:

$$\min \sum_{t\in\mathcal{T}} \sum_{g\in\mathcal{G}} \Bigg[\underbrace{c_{gt}^{\mathrm{F}}\left(u_{gt}, v_{gt}, z_{gt}\right)}_{\text{First stage}} + \underbrace{\alpha_1 c_{gt}^{\mathrm{V}}\left(\widehat{p}_{gt}\right) + \alpha_2 c_{gt}^{\mathrm{V}}\left(\widehat{p}_{gt} + \overline{r}_{gt}\right) + \alpha_3 c_{gt}^{\mathrm{V}}\left(\widehat{p}_{gt} + \underline{r}_{gt}\right)}_{\text{Second stage}} \Bigg] \tag{30}$$

where $\alpha_1 + \alpha_2 + \alpha_3 = 1$. Henceforth, we set $\alpha_2 = \alpha_3 = \frac{\alpha}{2}$, hence $\alpha_1 = (1-\alpha)$. The weight α gives the flexibility to ISOs to give importance to the limits of the uncertainty range.

Similarly to the robust and stochastic approaches, the first-stage counts the fixed production cost $c_{gt}^{\mathrm{F}}(\cdot)$ which is composed by the no-load, shutdown and different startup costs, depending on how long the unit has been offline [11]. The second stage counts the variable production cost $c_{gt}^{\mathrm{V}}(\cdot)$ that is calculated based on the units' energy production, which can be easily obtained from $\widehat{p}_{gt}$ [11].

III. Numerical Results

The performance of our proposed approach is evaluated using the modified IEEE 118-bus test system, available online at www.iit.upcomillas.es/aramos/IEEE118_SUSD-Ramps.xls, for a time span of 24 hours. The system has 118 buses, 186 transmission lines, 91 loads, 54 thermal units and three wind units. The power system data are based on that in [2] and it was adapted to consider startup and shutdown power trajectories. All tests were carried out using CPLEX 12.6 [14] on an Intel-i7 3.4-GHz personal computer with 16 GB of RAM memory. The problems are solved until they hit a time limit of 7200 seconds or until they reach an optimality tolerance of 0.05%.

In this section, we first show the procedure used to evaluate the performance of the UC solutions. Then, we perform sensitivity analysis of the proposed formulation in terms of the

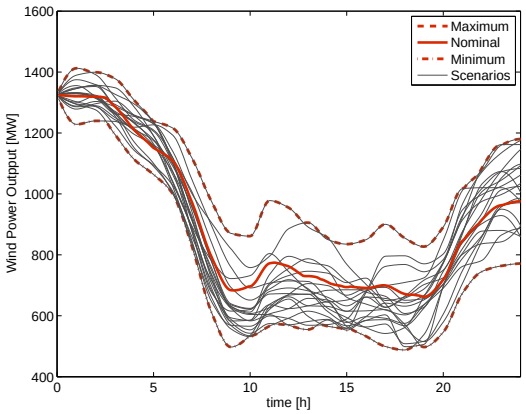

Fig. 4: Representation of wind uncertainty over time, scenarios and bounds

Table I: SENSITIVITY OF OBJECTIVE WEIGHT α

α	Scheduling Hourly		Validation: 5-min Economic Dispatch					
			Dispatch Costs [k$]			Violations		
	UC [k$]	# SU	Average	Std	Worst	# Sc	# Tot	MWh
0	52.026	14	771.115	14.351	814.471	2	2	0.038
0.1	51.986	14	770.823	14.365	814.223	2	2	0.038
0.2	51.949	14	770.970	14.348	814.087	2	2	0.048
0.3	51.986	14	770.806	14.364	814.206	2	2	0.038
0.4	51.961	14	770.928	14.392	814.201	2	2	0.038
0.5	51.351	13	771.642	14.361	814.667	2	2	0.038
0.6	51.259	13	771.822	14.408	815.037	0	0	0.000
0.7	50.446	14	772.659	14.325	815.602	1	1	0.004
0.8	50.623	14	772.657	14.378	816.045	5	5	0.108
0.9	50.435	14	772.725	14.327	815.951	5	5	0.108
1.0	49.824	13	773.503	14.355	816.718	5	5	0.108

objective weight and uncertainty range. Finally, we compare the performance of the proposed approach with the deterministic and stochastic approaches.

A. Evaluating Approach

The uncertainty model: we use latin hypercube sampling (LHS) to generate scenarios for the uncertain wind production. We assume that the wind production follows a multivariate normal distribution with predicted value W and volatility matrix Σ. The idea in applying LHS is to optimally distribute the samples to explore the whole area in the experimental region, avoiding the creation of scenarios that are too similar (clusters) [15].

To compare the performance of the different UC approaches, we make a clear difference between the scheduling stage and the validation stage. The computational experiments proceed as follows.

1) Scheduling stage: solve the different UC models and obtain the hourly commitment solutions, using 20 wind scenarios for each of the three wind units. Fig. 4 shows the aggregated wind production of these wind scenarios.
2) Out-of-sample validation stage: for each fixed UC solution, solve a 5-min economic dispatch problem repetitively for a set of 200 new wind scenarios. Notice that around the 20% of these out-of-sample scenarios fall outside the uncertainty bounds shown in Fig. 4.

In the 5-min economic dispatch, we introduce penalty costs for the violation of some constraints to mimic the high costs due to corrective actions in real time operations. The penalty costs are set to 10000 and 5000 $/MWh for demand-balance and transmission-limits violations, respectively, as suggested in [16] (similarly to [3], [4]). These penalty costs represent the expensive real-time corrective actions that an ISO needs to take in the event that the actual system condition significantly deviates from the expected condition, such as dispatching fast-start units, voltage reduction or load shedding.

We show the performance of the UC strategies in eight aspects, two related with the scheduling stage and six with the validation stage. These aspects, presented in Tables I to III, are described ass follows. Scheduling stage: 1) the fixed production costs described in Section II-D (UC [k$]), and 2) the number of startups (# SU). These two aspects indicate the commitment decisions that were needed by each approach to prepare the system to deal with the given wind uncertainty. Validation stage: 3) the average dispatch costs (Average), indicates the economic efficiency of the UC decision; 4) the volatility of these costs (Std), represented by the standard deviation of dispatch costs, which indicates the reliability of the real-time dispatch operation under the UC decision; 5) the dispatch cost of the worst-case scenario (Worst), indicates how robust the UC decision is against the worst-case scenario (from the 200 out-of-sample scenarios); 6) number of scenarios where there were violations in either demand-balance or transmission-limits constraints (# Sc); 7) total number of these violations (# Tot); and 8) total accumulated energy that could not be accommodated, demand-balance violations (MWh). The last three aspects also indicate how robust the UC decision is against different wind scenarios.

B. Sensitivity Analysis

1) Changes of Objective Weight α: We test the performance of the proposed approach under different α and the results are shown in Table I. Notice that the performance does not change considerably. The maximum values of the Average, Std and Worst-case dispatch cost are 0.6% above the minimum values. These small changes are because the model guarantee feasibility through a set of hard constraints; however, the results may change considerably if we relax some constraints and introduce penalty-cost violations. Henceforth, we set $\alpha = 0.1$.

2) Changes of Uncertainty Range: Table II shows the results in the scheduling and validation stage for different values of the uncertainty range, from 0 to 100%. The 100% uncertainty range is defined by the bounds shown in Fig. 4, and the 0% is equivalent to a deterministic UC using only the nominal wind case. These ranges were equally changed to the power-capacity and ramp-capability ranges. It can be clearly observed that the larger the considered uncertainty range, the UC costs and number of startups increase because the UC solutions become more conservative. Consequently, the dispatch costs and violations decreases.

Through different uncertainty ranges, there is a significant reduction in the Average and Std dispatch costs. This significant reduction is closely related to the violations reduction and its associated costs, which represent the expensive emergency actions that the ISO has to take to maintain system reliability.

Table II: SENSITIVITY OF UNCERTAINTY RANGE

%	Scheduling Hourly		Validation: 5-min Economic Dispatch					
			Dispatch Costs [k$]			Violations		
	UC [k$]	# SU	Average	Std	Worst	# Sc	# Tot	MWh
0	46.705	10	1067.017	575.205	5479.411	103	1744	5884.536
10	46.906	10	1018.959	505.127	5017.905	101	1492	4928.511
20	46.725	10	966.994	461.833	4797.448	87	1259	3883.190
30	47.443	11	877.291	337.356	3905.236	53	759	2102.645
40	47.941	12	825.176	228.394	3130.061	31	308	1052.421
50	47.973	12	795.862	134.644	2317.292	16	145	460.961
60	48.691	13	780.770	67.952	1617.704	11	77	165.247
70	51.583	13	772.493	26.906	1039.311	6	39	43.814
80	51.442	13	770.863	14.830	831.475	4	12	3.647
85	51.930	14	770.535	14.522	814.291	3	6	2.008
90	51.911	14	770.562	14.384	814.089	2	2	0.038
95	51.934	14	770.740	14.382	814.246	2	2	0.038
100	51.986	14	770.823	14.365	814.223	2	2	0.038

Table III: COMPARISON BETWEEN THE PROPOSED ROBUSTIFIED, STOCHASTIC AND DETERMINISTIC APPROACHES UNDER THE 200 OUT-OF-SAMPLE WIND SCENARIOS

	Scheduling Hourly		Validation: 5-min Economic Dispatch					
			Dispatch Costs [k$]			Violations		
	UC [k$]	# SU	Average	Std	Worst	# Sc	# Tot	MWh
RobRes	51.986	14	770.823	14.365	814.223	2	2	0.038
StchOpt	54.765	12	808.971	200.096	2903.841	28	259	611.473
DetRes	55.492	16	857.199	279.813	3254.877	55	611	1793.881

Notice that the uncertainty range of 85% presents the lowest average dispatch costs. This indicates that the uncertainty range can be slightly reduced without sacrificing the efficiency and robustness of the UC solution. We can observe in the ranges (85% and above) presenting few violations that considering lower uncertainty levels leads to better economic benefit, but worse risk performance, which is represented by the standard deviation of the dispatch cost. Using this information, a proper tradeoff can be made by decision makers.

Henceforth, we set the uncertainty range to 100%.

C. Comparing the Proposed Robustified Approach with the Deterministic and Stochastic Approaches

The performance of the proposed robustified reserve modelling approach, RobRes, is compared with the deterministic-reserve modelling, DetRes, and the stochastic, StchOpt, approaches. All three models are based on the ramp scheduling approach proposed in [11].

To obtain the commitment strategies of all UC approaches, we use the 20 wind scenarios shown in Fig. 4, as described in the scheduled stage in Section III-A. We assume these scenarios to be the only information available for the scheduling stage. Therefore, we use these data to describe the different wind uncertainty representation required by the different UC approaches. The robustified approach RobRes uses the nominal wind production together with minimum and maximum bounds of power-capacity and ramp-capability, which are obtained from this set of scenarios. The stochastic approach StchOpt uses all 20 scenarios. Finally, the deterministic approach DetRes uses the nominal wind production and two hourly reserves, upwards and downwards which are defined as $\sum_b \left(W_{bt} - \underline{W}_{bt}\right)$ and $\sum_b \left(\overline{W}_{bt} - W_{bt}\right)$, respectively.

1) Reliability of Dispatch Operation: Table III compares the performance of the different UC approaches. From the scheduling stage, we can observe that DetRes commits the largest quantity of resources, because this is the only approach that cannot readjust (optimize) the given level of reserves by considering wind curtailment. That is, the reserve requirements for the deterministic approach results in a larger quantity of committed resources. RobRes presents lower UC costs than StchOpt, but RobRes started two more units. This indicates that the uncertainty information acquired by these two approaches leads to very different commitment strategies, where the RobRes solution seeks to guarantee feasibility to the given uncertainty ranges, and StchOpt seeks to minimize the expected costs of the given scenarios.

From the validation stage in Table III, we can observe the following:

1) The Average and Std dispatch costs of StchOpt are around 6% and 40% lower than DetRes, respectively. This clearly shows the advantages of the stochastic strategy over the deterministic one, as expected.
2) Although DetRes committed the largest quantity of resources, it is the least robust. This is mainly because the deterministic approach only models the network constraints for the nominal case and it cannot guarantee that the committed reserves can be deployed. This is in contrast to RobRes and StchOpt, where generating units are committed taking into account that power must be delivered to specific places in the network where the uncertainty appears.
3) The Average dispatch cost of StchOpt is around 5% higher than RobRes, and the Std for StchOpt is more than an order of magnitude higher (13.9 times). Similarly, the total quantity of violations and the energy unbalance of StchOpt is more than two (130 times) and four (16k times) orders of magnitude higher than RobRes, respectively.

In short, the robustified approach RobRes presents a better economic-benefit and risk performance than the deterministic and stochastic approaches for this study case. Consequently, RobRes offers more robust commitment decisions which lead to a better system reliability.

Although we use LHS to represent the space of scenarios adequately, the performance of StchOpt may be improved by introducing a larger quantity of scenarios in the scheduling stage or by a better scenario sampling. To observe the performance of RobRes and DetRes compared with a "perfect" stochastic approach, we carried out the economic dispatch validation using the same scenarios used by StchOpt in the scheduling stage. Table III shows the performance of the different UC approaches under the 20 scheduling scenarios. For this case, StchOpt presented the lowest Average dispatch cost, around 0.3% lower than RobRes, but the Std and the Worst-case are higher than RobRes. Notice that StchOpt presented constraint violations in two scenarios even though these scenarios were used in the scheduling stage. This is because the scheduling stage considers a simplified hourly piece-wise linear approximation of the 5-min smooth power profile of the set of scenarios shown in Fig. 4.

2) Computational Performance: Table V shows a comparison of problem size and computational burden between the

Table IV: COMPARISON BETWEEN THE PROPOSED ROBUSTIFIED, STOCHASTIC AND DETERMINISTIC APPROACHES UNDER THE 20 SCHEDULING WIND SCENARIOS

	5-min Economic Dispatch Simulation					
	Dispatch Costs [k$]			Violations		
	Average	Std	Worst	# Sc	# Tot	MWh
RobRes	770.863	12.360	795.588	1	1	0.002
StchOpt	768.793	21.888	848.723	2	12	5.729
DetRes	803.457	119.146	1263.678	3	36	71.670

Table V: PROBLEM SIZE AND COMPUTATIONAL BURDEN OF THE DIFFERENT APPROACHES

	Problem Size [#]				Computational Burden	
	Constraints	Nonzero elements	Continuous variables	Binary variables	CPU Time [s]	Nodes explored
RobRes	36141	1074712	21096	6520	90.45	250
StchOpt	225141	5600307	169776	6376	867.88	819
DetRes	18093	315424	11016	6376	8.75	29

different approaches. Notice that all three formulations have almost the same quantity of binary variables, but RobRes has around 2.2% more than the others. This is due to the modelling of the infimum function that RobRes requires, see Section II-A.

When comparing the number of constraints, nonzero elements and continuous variables, RobRes is around twice the size of DetRes, and StchOpt is more than 12 and 6 times larger than DetRes and RobRes, respectively. On the other hand, the CPU time of RobRes is around an order of magnitude higher than that of DetRes, and one lower than that of StchOpt. Finally, unlike DetRes and RobRes, the problem size and computational burden of StchOpt highly depends on the quantity of scenarios that it considers.

IV. CONCLUSIONS

In this paper, we proposed a robustified network-constrained unit commitment formulation as an alternative to the robust and stochastic UC under wind generation uncertainty. The formulation draws a clear distinction between power-capacity and ramp-capability reserves to deal with wind production uncertainty. The model is formulated under the ramp-based scheduling approach, which schedules power-trajectories instead of the traditional energy-blocks and takes into account the inherent startup and shutdown power trajectories of thermal units. The formulation is compact since only needs two reserve requirements, unlike the stochastic approach which problem size depends on the quantity of scenarios. If compared with the robust approach, which requires to solve a bilinear mixed integer programming (MIP) problem, the proposed formulation only requires to solve a linear MIP problem, thus avoiding the computational and non-linear complexity that arises from bilinear problems. Study cases showed that the proposed formulation significantly decreases operation costs compared to traditional deterministic and stochastic UC formulations while simultaneously lowering the computational burden. The operation cost comparison was made through 5-min economic dispatch simulation under hundreds of out-of-sample wind generation scenarios. As future studies, the performance of the proposed formulation must be compared with the traditional stepwise energy-block formulations under both stochastic and robust approaches for different power systems.

APPENDIX

The ramp-up and -down constraints on the upper envelope, $A \rightarrow B$ in Fig. 3, are ensured with

$$\left(p_{gt} + r^{+}_{gt}\right) - \left(p_{g,t-1} + r^{+}_{g,t-1}\right) \leq RU_{gt} \quad \forall g,t \qquad (31)$$

$$-\left(p_{gt} + r^{+}_{gt}\right) + \left(p_{g,t-1} + r^{+}_{g,t-1}\right) \leq RD_{gt} \quad \forall g,t. \qquad (32)$$

On the other hand, (33) is obtained by reorganizing the ramp-up constraints given in (15) and (17), and (34) by reorganizing (16) and (17):

$$r^{+}_{gt} - r^{+}_{g,t-1} \leq r^{\mathrm{R}+}_{gt} \leq RU_g - p_{gt} + p_{g,t-1} \quad \forall g,t \qquad (33)$$

$$-r^{+}_{gt} + r^{+}_{g,t-1} \leq r^{\mathrm{R}-}_{gt} \leq RD_g + p_{gt} - p_{g,t-1} \quad \forall g,t \qquad (34)$$

where these two constraints are equivalent to (31) and (32), respectively. Similarly, (15) and (16) together with (18) guarantee the ramp-up and -down constraints on the lower envelope scenario, $C \rightarrow D$ in Fig. 3.

REFERENCES

[1] A. Papavasiliou, S. S. Oren, and R. P. O'Neill, "Reserve requirements for wind power integration: A scenario-based stochastic programming framework," *IEEE Trans. Power Syst.*, vol. 26, no. 4, pp. 2197–2206, Nov. 2011.

[2] C. Sahin, M. Shahidehpour, and I. Erkmen, "Allocation of hourly reserve versus demand response for security-constrained scheduling of stochastic wind energy," *IEEE Trans. Sustain. Energy*, vol. 4, no. 1, pp. 219–228, 2013.

[3] D. Bertsimas, E. Litvinov, X. A. Sun, J. Zhao, and T. Zheng, "Adaptive robust optimization for the security constrained unit commitment problem," *IEEE Trans. Power Syst.*, vol. 28, no. 1, pp. 52–63, Feb. 2013.

[4] C. Zhao and Y. Guan, "Unified stochastic and robust unit commitment," *IEEE Trans. Power Syst.*, vol. 28, no. 3, pp. 3353–3361, Aug. 2013.

[5] MISO, "Ramp capability product design for MISO markets," Tech. Rep., Jul. 2013.

[6] CAISO, "Flexible ramping products: Second revised draft final proposal," California Independent System Operator, USA, Tech. Rep., Oct. 2012. [Online]. Available: http://www.caiso.com/Documents/SecondRevisedDraftFinalProposal-FlexibleRampingProduct.pdf

[7] A. Ben-Tal, L. E. Ghaoui, and A. Nemirovski, *Robust Optimization*. Princeton University Press, Aug. 2009.

[8] X. Guan, F. Gao, and A. Svoboda, "Energy delivery capacity and generation scheduling in the deregulated electric power market," *IEEE Trans. Power Syst.*, vol. 15, no. 4, pp. 1275–1280, Nov. 2000.

[9] G. Morales-Espana, J. M. Latorre, and A. Ramos, "Tight and compact MILP formulation of start-up and shut-down ramping in unit commitment," *IEEE Trans. Power Syst.*, vol. 28, no. 2, pp. 1288–1296, 2013.

[10] G. Morales-Espana, J. Garcia-Gonzalez, and A. Ramos, "Impact on reserves and energy delivery of current UC-based market-clearing formulations," in *European Energy Market (EEM), 2012 9th International Conference on the*, Florence, Italy, May 2012, pp. 1–7.

[11] G. Morales-Espana, A. Ramos, and J. Garcia-Gonzalez, "An MIP formulation for joint market-clearing of energy and reserves based on ramp scheduling," *IEEE Trans. Power Syst.*, vol. 29, no. 1, pp. 476–488, 2014.

[12] G. Morales-Espana, C. Gentile, and A. Ramos, "Tight MIP formulations of the power-based unit commitment problem," *Optimization Letters*, 2014, under Review. [Online]. Available: http://www.iit.upcomillas.es/aramos/papers/Power-UC_ConvexHull.pdf

[13] G. Morales España, "Unit commitment: Computational performance, system representation and wind uncertainty management," Ph.D. dissertation, Pontifical Comillas University, KTH Royal Institute of Technology, and Delft University of Technology, Spain, Sep. 2014.

[14] "CPLEX 12," IBM ILOG CPLEX, User's Manual, 2013. [Online]. Available: http://gams.com/dd/docs/solvers/cplex.pdf

[15] P. Glasserman, *Monte Carlo methods in financial engineering*. New York: Springer, 2003.

[16] FERC, "RTO unit commitment test system," Federal Energy and Regulatory Commission, Washington DC, USA, Tech. Rep., Jul. 2012.

For KTH Royal Institute of Technology:
DOCTORAL THESIS IN ELECTRICAL ENGINEERING
TRITA-EE 2014:041
www.kth.se

ISSN 1653-5146
ISBN 978-84-697-1230-6